FTD-HC-23-721-71

FOREIGN TECHNOLOGY DIVISION

CHARACTERISTICS OF SEISMIC WAVES IN NUCLEAR EXPLOSIONS AND EARTHQUAKES

by

I. P. Pasechnik

Security Classification

DOCUMENT CONTROL DATA - R & D

(Security classification of title, body of abstract and indexing annotation must be entered when the overall report is classified)

1. ORIGINATING ACTIVITY (Corporate author)	2a. REPORT SECURITY CLASSIFICATION
Foreign Technology Division Air Force Systems Command U. S. Air Force	UNCLASSIFIED
	2b. GROUP

3. REPORT TITLE

CHARACTERISTICS OF SEISMIC WAVES IN NUCLEAR EXPLOSIONS AND EARTHQUAKES

4. DESCRIPTIVE NOTES (Type of report and inclusive dates)

Translation

5. AUTHOR(S) (First name, middle initial, last name)

Pasechnik, I. P.

6. REPORT DATE	7a. TOTAL NO. OF PAGES	7b. NO. OF REFS
1970	318	360

8a. CONTRACT OR GRANT NO.	9a. ORIGINATOR'S REPORT NUMBER(S)
F33657-71-D-0057	
b. PROJECT NO. 1256	FTD-HC-23-721-71
c.	9b. OTHER REPORT NO(S) (Any other numbers that may be assigned this report)
d.	

10. DISTRIBUTION STATEMENT

Approved for public release; distribution unlimited.

11. SUPPLEMENTARY NOTES	12. SPONSORING MILITARY ACTIVITY
	Foreign Technology Division Wright-Patterson AFB, Ohio

13. ABSTRACT

Examined are the kinetic and dynamic characteristics of volume and surface seismic waves excited by nuclear explosions in various media. Investigated is the level and spectral compositions of microseisms in various seismogeological regions; discussed is also the question concerning the choice of optimum parameters of seismic equipment. Shown are possibilities of using the data obtained at explosions for the study of the internal structure of the earth. [AM0129345]

DD FORM 1 NOV 65 1473

UNCLASSIFIED
Security Classification

14. KEY WORDS	LINK A		LINK B		LINK C	
	ROLE	WT	ROLE	WT	ROLE	WT
Seismic Wave Earthquake Nuclear Explosion						

EDITED TRANSLATION

CHARACTERISTICS OF SEISMIC WAVES IN NUCLEAR EXPLOSIONS AND EARTHQUAKES

By: I. P. Pasechnik

English pages: 318

Source: Kharakteristiki Seysmicheskikh Voln pri Yadernykh Vzryvakh i Zemletryaseniyakh 1970, pp. 1-191

Translated under: F33657-71-D-0057

PREPARED BY:

TRANSLATION DIVISION
FOREIGN TECHNOLOGY DIVISION
WP-AFB, OHIO.

TABLE OF CONTENTS

UDK 550.34

Characteristics of Seismic Waves in Nuclear Explosions and Earthquakes. Pasechnik, I.P. Izdatel'stvo Nauka, 1970, 193 pages.

The monograph examines the kinematic and dynamic characteristics of body and surface seismic waves produced by nuclear explosions in various media. The similarity of the kinematic characteristics of explosion waves and earthquakes is noted, as well as the differences of their dynamic characteristics. The monograph elucidates the distinctive features of waves which can be applied as criteria for identifying the seismic records of explosions and earthquakes.

The level and spectral composition of microseisms in various seismogeological areas are studied, and light is also shed on the question of selecting the optimum parameters for seismic equipment.

The monograph demonstrates the possibilities of using data obtained during explosions for studying the internal structure of the Earth.

The book is intended for seismologists and geophysicists.
46 tables. 76 illustrations. 360 entries in the bibliography.

Editor, candidate of physico-mathematical sciences
S. D. Kogan

INTRODUCTION

The seismic method of detecting and identifying nuclear explosions has won universal recognition as one of the basic methods of detecting all types of nuclear explosions, except those carried out in outer space and in the air at great altitudes (higher than several tens of kilometers).

The seismic method is applicable for the detection of nuclear explosions both at small and at great epicentral distances amounting to as much as 16,000 - 17,000 km. This method is particularly effective in the detection and identification of underground and underwater nuclear explosions. As of now, it is the only known method for detecting and identifying underground explosions which are fully camouflaged.

In this book, the term "detection" is understood to mean establishing by seismic data the fact and the time of occurrence of a seismic phenomenon, the coordinates of its epicenter, and the determination of its energy (or magnitude).

The term "identification" is understood to mean establishing, on the basis of the total characteristics of the seismic waves registered, the type of phenomenon: earthquake, or an underground, underwater, contact, or atmospheric nuclear explosion.

Until the banning of testing in three media (in the water, in the air, and in outer space) in 1963, the seismic method was applied widely with great success in many countries (the USSR, the United States, Japan, France, England, Sweden, and others) for the purposes of detecting and identifying underwater, contact, and atmospheric explosions. In these cases, it supplemented a complex of other geophysical and geochemical methods, including the recording of infrasonic and

hydroacoustic waves, the recording of electromagnetic radiation of radio signals, the gathering of radioactive products in the air and in the water, and some others.

Seismic data from a properly adjusted and automated monitoring system for nuclear explosions, in principle, enable one to establish 20 - 30 minutes later the fact that an explosion has been carried out far away, to determine the coordinates of its epicenter, and to estimate approximately its TNT equivalent.

At the present time the seismic method is being applied very effectively in a number of countries for the detection and identification of numerous underground nuclear explosions which are carried out in various parts of the globe. Data pertaining to records of seismic waves caused by explosions are published in the bulletins of the seismic services of the United States, Sweden, and other countries, and also in a world-wide seismological bulletin [167].

The importance and the timeliness of further developing the seismic method, particularly criteria for the identification of underground nuclear explosions, are universally recognized. The difficulties encountered by this method in a number of cases in identifying underground explosions by national agencies are utilized by the western countries as a pretext against the conclusion of an agreement to ban underground nuclear explosions, which has been advocated by the Soviet Union since 1958. As is known, the western countries insist on carrying out international inspections at the locations of unidentified seismic phenomena [341, 343], which is not necessary at the present level of detection methods. In this connection, one must refer to the report of the conference (Sweden, 1968) of a seismic scientific group [326] of leading seismologists of ten countries, including those from four nuclear countries — the United States, the USSR, England, and France — who unanimously recognized the possibility of identifying underground explosions by criteria of magnitude (M, m_b).

In connection with talks on banning nuclear explosions in 1958, and with the banning of testing in three media in 1963, the seismic method developed greatly, both here in our country, and also abroad, particularly in the United States, England, France, Sweden, and in other countries.

As for the further elaboration of the seismic method of detection and identification of nuclear explosions, scientists of the Soviet Union have put forward and developed a number of ideas, which contributed in large measure to reaching agreements concerning the banning of nuclear testing in three media. For instance, it was substantiated that national agencies can, without international inspections, monitor explosions. These ideas were discussed widely at the Geneva talks on banning tests of nuclear weapons during the period 1958 - 1961. They gave the impetus to carrying out far-reaching experimental and theoretical research on the dynamic and kinematic characteristics of seismic waves caused by explosions and earthquakes, to the development of equipment, including that for digital magnetic recording of seismic oscillations, to the perfection of methods and techniques of observation, and to the elaboration of interpretation methods by means of electronic computers [1-3, 52-57, 60-77, 81-86, 89-90, 92-106, 109-111, 128-130]. Theoretical and computer seismology developed further. Recording data of seismic waves from explosions were utilized widely for increasing the precision of the hodographs of the basic seismic waves, for obtaining new information about the structure of the crust, the mantle, and the core of the Earth, and also in a number of other fields of seismology [63, 65, 66, 170, 207, 220, 221, 248, 249].

The works of Soviet scholars in the above-mentioned directions are widely known, not only here in our country, but also abroad. These works were reported systematically at international symposiums and were widely publicized in the USSR and abroad.

In the United States, considerable means were allocated by the government for developing the method carried out in accordance with

programs coordinated at the governmental level, such as the "Vela Uniform", "Vela hotel", and "Cowboy" [247 and others (1)] (programs for developing methods of detecting and identifying nuclear explosions and of carrying them out secretly) as well as the Plowshare [137, 153, 265, 307, 308] (a program for using nuclear explosions for peaceful purposes, etc.). Participating in the above-mentioned programs were the most prominent physicists, seismologists, geophysicists and engineers of many scientific institutions and companies of the United States and a number of western countries, as well as various agencies of the ministry of defense, the Atomic Energy Commission, and other departments of the United States government. Research on various programs is coordinated by a single government center, the ARPA [142, 143, 151-156, 210, 235, 266, 268, 271-278, 281, 293, 299, 302-316, 320-324, 351, 356, etc.].

Work is being carried out widely to elaborate the latest types of seismic equipment, methods of increasing its effective sensitivity, criteria for distinguishing the seismic recordings of underground nuclear explosions, methods of on-the-spot inspection of unidentified seismic phenomena, and also to elaborate the theoretical foundations of seismology and questions of the excitation and propagation of seismic waves from nuclear explosions.

The United States has established its world-wide network consisting of 125 detecting stations, 65 of which are located near the borders of the USSR and other socialist countries [267].

Concerning the massive upsurge of research in the detection and identification of nuclear explosions, one can also form an idea from the number of published works, which exceeded 2,000 in the period from 1958 to 1965. The published works deal chiefly with questions connected with the detection and identification of underground nuclear explosions. The number of works devoted to questions

---

Footnote (1) appears on page 9

of detecting atmospheric and contact nuclear explosions is relatively small.

Considerable research has been carried out by scholars of England, France, Sweden, and other countries [145, 146, 183, 245, 262, 292, 309, 335, 336, 344, etc.].

The detection and identification of underground nuclear explosions is the most complex question in the detection of nuclear explosions by the seismic method.

Unlike other types of nuclear explosions, in fully hidden — camouflaged — underground explosions at great epicentral distances, indisputable proofs of a nuclear explosion cannot be obtained — that is, radioactive products cannot be detected. Under these conditions, the seismic method is at the present time the only detection and identification method. Identification relies on seismic recordings, and is based on the differences in the dynamic characteristics of the recordings between seismic waves of explosions and those of earthquakes. These differences, i.e., criteria, are connected with the different sources of seismic oscillations during explosions and during earthquakes [97, 195, 252, 269, 343, 353, 355].

From the short survey of the research carried out on the seismic method, it is obvious that large groups of scholars, both in our country and abroad, took part in its creation.

In the present work, generalized conclusions are drawn from the research results of the author on the development of the seismic method for detecting and identifying nuclear explosions. In drawing the generalized conclusions, the published works of other authors were also utilized. The following basic problems are investigated in the work.

The work explains what types of seismic waves can be recorded and traced for various types of explosions at a considerable range

of epicentral distances (up to 16,000 - 17,000 km). The work studies the spectral composition of the waves caused by explosions and earthquakes, and also the spectral composition of microseismic interference. On the basis of the analysis of these data, the question of selecting the optimum parameters for seismic equipment is discussed: the pass band, the magnification band, and the dynamic range. Ways of increasing its effective sensitivity are examined. Groundwork is provided for the principles of selecting the most favorable regions for recording explosion waves and for the location of seismic stations. The work analyzes the kinematic and dynamic characteristics of the most steadily recorded waves and their dependence on a number of factors: the epicentral distance, the magnitude of the phenomenon, the focal depth, the properties of the rocks enclosing the explosions, and the differences in the seismogeological structure on the propagation path of the waves and in the region where the detecting station is located. The characteristics of explosion waves are contrasted with the corresponding characteristics of earthquake waves. Which characteristics differ most pronouncedly for both types of sources and can be used as criteria for the identification of explosions is established.

The solution of the tasks just enumerated is based on a study of the wave field in all types of explosions. Use is made of experimental material, chiefly that obtained by the Institute of Earth Physics of the USSR Academy of Sciences, but also works published in the domestic and foreign literature. The material in the book is arranged in the following order.

Chapter I gives the parameters of the equipment used in recording nuclear explosions, the recordings of which serve as the experimental basis for the present work.

Chapter II examines methodological problems of spectral analysis of seismic waves of explosions and earthquakes, and also of microseismic interference.

Chapter III discusses several questions concerned with increasing the effective sensitivity of the equipment.

Chapters IV - VI analyze the dynamic and kinematic characteristics of body and surface waves of explosions.

Chapter VII gives an estimation of the share of the energy of an explosion which goes into the formation of seismic waves in atmospheric as well as for contact, underground and underwater explosions.

In the conclusions, the basic results of the work and the directions of future research are briefly formulated.

The author expresses gratitude to S. D. Kogan for his valuable advice, and to A. M. Polikarpov for his assistance in the work.

FOOTNOTE

Footnote (1) on page 5 See works cited in [319, 321, 356].

CHAPTER I

SEISMIC EQUIPMENT USED IN RECORDING SEISMIC WAVES FROM EXPLOSIONS

The information introduced in the present work concerning the characteristics of seismic waves caused by nuclear explosions was obtained from the records of galvanometric recording instruments.

Many years of experience have established the usefulness of galvanometric recording instruments, which are widely used for observing earthquakes, for the reliable determination of the kinematic and dynamic characteristics of seismic waves, including those of displacements or the velocities of oscillating motion of the soil in seismic waves caused by nuclear explosions. A great advantage of the galvanometric method of recording is the highly stable functioning of the receiving channel in a wide range of periods, from hundredths of a second to several tens of seconds. Other advantages are its high sensitivity, the invariability of the parameters in time, and the simplicity of the apparatus and of its operation. When the equipment is tuned to a narrow passband (range of periods from 0.1 to 1.5 seconds), the amplification of the equipment can be increased to values on the order of 10^6, and when groups of seismographs are used — to 10^7 or more. In this case, it is possible to record extremely

small displacements of the soil, amounting to only a few angstroms, in seismic waves. Due to these qualities, galvanometric recording equipment has already been widely used for more than 50 years in seismic observations of earthquakes, and in recent years also in those of explosions.

However, galvanometric recording equipment also has some shortcomings. One is the relatively small dynamic range (on the order of 35 - 40 dB). Another drawback connected with this is the necessity of using several seismographs to obtain records with different amplifications and filtrations. It is also difficult to mechanize the data processing. Practice shows that a dynamic range of the equipment on the order of 100 dB is necessary in recording seismic waves caused by explosions.

Magnetic recording equipment is free of the shortcomings mentioned above ([3, 92] etc.). An ever increasing number of seismic stations are at the present time equipped with magnetic recording devices, both of the digital [3, 92, 325, 329] and of the analog [183, 335, 338] types.

Brief data are given below about the parameters and the filtering and distorting properties of the equipment, chiefly galvanometric recording equipment, used for recording seismic waves caused by nuclear explosions. Descriptions of this equipment are given in [6-9, 12, 20-22, 59 etc.].

§ 1. Kinematic Elements of Soil Motion in Seismic Waves Recorded During Explosions

To record the seismic waves caused by nuclear explosions in a wide range of epicentral distances from several kilometers to 16,000 - 17,000 km, the equipment is ordinarily adjusted so as to record displacements of the soil both for body and for surface waves. Specifically, in the seismic stations of the USSR, wide-band equipment with

type SVK (vertical seismograph designed by Kirnon) and SGK (horizontal seismograph designed by Kirnon) seismographs adjusted to the standard characteristics [93, 112] (see Table 1, item 3) records displacements of the soil in body and surface waves of near explosions and earthquakes (with epicentral distances up to 1,000 - 2,000 km), and in body waves of distant explosions and earthquakes (Δ > 2,000 km) (see Chapter VII). Displacements of the soil in surface waves of distant explosions and earthquakes are recorded by long-period equipment adjusted to the parameters shown in item 1 of Table 1.

It is advisable to record the displacement velocity in a number of cases, especially when recording the body waves of atmospheric, underground, and underwater explosions, so that the useful signal can be better distinguished against the background interference.

As for equipment used to record velocities or functions close to them in dilatational waves caused by contact or atmospheric explosions, there are seismographs of types SKM and USF [12], as well as others with a narrow passband, adjusted to the parameters shown in items 5 - 7 of Table 1.

As recording equipment, the following have been in use in the USSR: type RS-II and OSB-VI recorders developed at the IPE*; oscillographs of type POB-12, N-700, OMS, and others with their corresponding galvanometers, types of which are shown in Table 1 [20, 35, 112, etc.].

Examples of the amplitude-frequency characteristics of the galvanometric recording equipment used at seismic stations of the USSR are shown in Figure 1. Examples of those used in the stations of the world-wide network of the United States are shown in Figure 2 [237].

Table 2 gives the parameters of the equipment most frequently used in the seismic stations world-wide network of the United

*Translator's Note: IPE designates the Institute of Physics of the Earth.

TABLE 1. PARAMETERS OF EQUIPMENT INSTALLED IN SEISMIC STATIONS OF THE USSR, RECORDINGS OF WHICH WERE USED IN THE PRESENT WORK.

	Type of instrument	Type of galvanometer	Period of seismometer pendulum T_1, sec	Period of frame of galvanometer T_2, sec	Damping of seismometer pendulum D_1	Damping of galvanometer D_2	Coupling coefficient σ^2	Maximum amplification of channel V_{max}	Period, or range of periods, at which the channel has the maximum amplification T_{max}, sec	Absolute pass band, taken at the level of 0.7 from the maximum amplification of the channel T_{left} - T_{right}, sec	Relative pass band $\frac{T_{left}-T_{right}}{T_{max}}$, %
1	Three-component installation of long-period seismographs of type SKD	M 17/12	20	18	1,0	1,0	0,3	2—3·10⁸	20	5—30	120
2	Three-component installation of long-period seismographs of type SKD with rejection filters	M 17/12	20	18	1,0	1,0	0,3	4—5·10⁸	20	0,2—25	
3	Three-component installation of wide-band seismographs of type SK with standard constants	GK-VII	12,5	1,2	0,5	5,5	0,3	1—2·10⁸	0,3—12	0,2—15	

TABLE 1. PARAMETERS OF EQUIPMENT INSTALLED IN SEISMIC STATIONS OF THE USSR, RECORDINGS OF WHICH WERE USED IN THE PRESENT WORK.

	Type of instrument	Type of galvanometer	Period of seismometer pendulum T_1, sec	Period of frame of galvanometer T_2, sec	Damping of seismometer pendulum D_1	Damping of galvanometer D_2	Coupling coefficient σ^2	Maximum amplification of channel V_{max}	Period, or range of periods, at which the channel has the maximum amplification T_{max}, sec	Absolute pass band, taken at the level of 0.7 from the maximum amplification of the channel T_{left} - T_{right}, sec	Relative pass band $\frac{T_{left}-T_{right}}{T_{max}}$, %
4	Three-component installation of wide-band seismographs of type SKD with lengthened characteristics	GK-VII	25	1,2	0,5	8,0	0,25	10^9	0,5—20	0,5—20	
5	Three-component installation of seismographs of type SKM with narrow passband	GK-VII	2,5	0,4	0,5	4,5	0,3	$(3-10)\cdot10^9$	0,9	{ 0,1—1,0; 0,1—2,5	320
6	Three-component installation of short-period seismographs of type USF	GK-VII	1,2	0,4	1,0	4,0	0,3	$4\cdot10^9$	0,5	0,06—1,5	320

TABLE 1. PARAMETERS OF EQUIPMENT INSTALLED IN SEISMIC STATIONS OF THE USSR, RECORDINGS OF WHICH WERE USED IN THE PRESENT WORK.

	Type of instrument	Type of galvanometer	Period of seismometer pendulum T_1, sec	Period of frame of galvanometer T_2, sec	Damping of seismometer pendulum D_1	Damping of galvanometer D_2	Coupling coefficient σ^2	Maximum amplification of channel V_{max}	Period, or range of periods, at which the channel has the maximum amplification T_{max}, sec	Absolute pass band taken at the level of 0.7 from the maximum amplification of the channel $T_{left} - T_{right}$, sec	Relative pass band $\frac{T_{left} - T_{right}}{T_{max}}$, %
7	FSSS Equipment (Frequency selecting seismic station) with SVKM seismometer, amplifier, and filter	GB-IV	2,5	0,1	0,5	5,0	0	$3 \cdot 10^3$ 10^4 10^5 $7 \cdot 10^4$ $1,2 \cdot 10^5$	0,1—10 0,85 0,45 0,22 0,095	0,1—10 0,6—1,3 0,36—0,7 0,14—0,29 0,07—0,12	w. b.* 80 75 70 55

*w.b. — uniform (wide) passband in the range of periods of 0.1 - 10 sec.

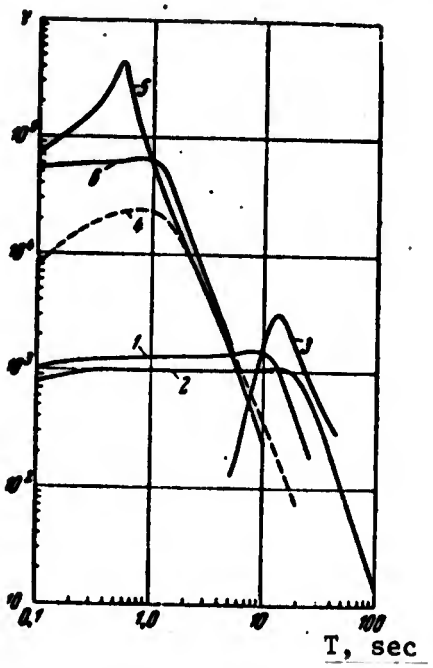

Figure 1. Amplification curves of seismographs installed in several seismic stations of the USSR.

1 - SK seismographs with standard constants; 2 - the same, with M17/12 galvanometer; 3 - the same, with M17/12 galvanometer with rejection filter; 4, 6 - SKM seismographs; 5 - USF-ZM seismographs.

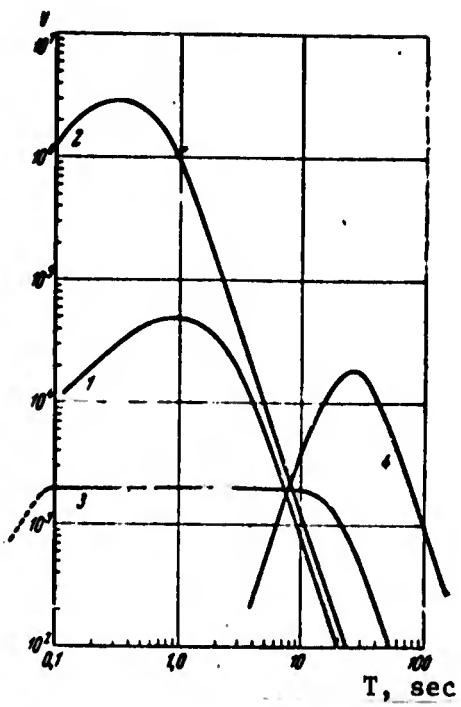

Figure 2. Amplification curves of seismic equipment with the parameters recommended by the Geneva conference of experts of 1958 [131]. Equipment installed in stations for detecting nuclear explosions of the United States and other countries.

1 - short-period seismographs with narrow passband; 2 - group of ten short-period seismographs;
3 - wide-band seismographs;
4 - long-period seismographs.

Table 2 gives the parameters of the equipment most frequently used in the seismic stations of the world-wide network of the United States and in other countries [169, 267, 343 etc.].

§ 2. On the Necessity of Using Filtering Equipment

In the overwhelming majority of explosions, the intensity of the resulting seismic oscillations is small in comparison with the intensity of the microseismic interference of the first order. In connection with this, useful oscillations from explosions can be recorded on wide-band equipment at considerable epicentral distances only if the explosions have a relatively great intensity (of megaton caliber).

Therefore, to record explosions of a small or medium intensity(from several to hundreds of kilotons), it is necessary to use selective filtering equipment, that is, to knowingly introduce the equipment distortions into the records of the explosions. Unless this is done, in the overwhelming number of cases it would be impossible to distinguish the signals from smaller explosions, especially underground or underwater ones, on the seismograms against the background interference.

It turned out to be possible to apply filtration of oscillations based on frequency selection,due to the differences in the amplitude spectra between microseismic interference and the seismic waves caused by explosions. These questions are dealt with in detail in Chapter III.

Table 3 gives information on the dominant periods of body and surface waves in records obtained with wide-band equipment during explosions. These values are usually close to the periods of the maximum values of the amplitude spectra.

The maximum of the frequency spectrum of intensive microseisms of the first order lies within the range of the passband of the wide-band channel. In connection with this fact, at periods on the order of 3.5 - 6.0 seconds, the working amplification V of this channel

TABLE 2. PARAMETERS OF EQUIPMENT APPLIED IN SEISMIC STATIONS OF THE UNITED STATES [343] AND OTHER COUNTRIES*

Type of seismograph	Period of seismometer pendulum T_1, sec	Period of galvanometer frame T_2, sec	Damping of seismometer pendulum D_1	Damping of galvanometer D_2	Coupling coefficient σ^2	Maximum amplification V_{max}	Period at maximum amplification T_{max}, sec
Short-period Benioff	1.0 1.0	0.2 1.0	1.0 1.0	1.0 1.0	0 0	10^6 10^6	0.3 1.0
Anderson-Wood	1.0	-	0.8	-	-	$2.8 \cdot 10^3$	1.0
Sprengneser H, H-D	4-20	1.5-20	1.0	1.0	0.4	10^4	1-10
Long-period Benioff	25	90	1.0	1.0	-	$2 \cdot 10^4$	25
Long-period Press-Ewing	30	100	1.0	1.0	-	$(0.1\text{-}2) \cdot 10^4$	40

*At the present time, new types of seismographs are being applied in the seismic stations of the United States and other countries.

TABLE 3. VALUES OF THE PREDOMINANT OR MAXIMUM PERIODS IN BODY AND SURFACE WAVES CAUSED BY EXPLOSIONS CARRIED OUT IN VARIOUS MEDIA IN THE RECORDINGS OF WIDE-BAND AND NARROW-BAND SEISMOGRAPHS

Types of explosions	Type of seismograph	Epicentral distance Δ, km	Period (sec) for waves:		
			P, PP, PKP, PcP	*S, SS, SKS*	L_R
Underground	Short-period, Benioff	200—10 000	0,5—1,2	1,0—1,5	
	SK, SKM	200—1000	0,5—0,8	0,6—1,0	5—8
	SKM, SK	200—10 000	0,7—2,0	1,0—3,5	10—20
	SKD	2000—10 000	3,5	5—6	20—30
	SKM	to 17 000	1,2—1,6		
Underwater	Short-period, Benioff	6000—10 000	1,0—1,1	1,0—1,5	
	SK, SKM	200—1000	0,5—1,0	4—6	20
	SK, SKM	1000—10 000	1,5—3	4—6	
	SK	to 16 000	2,5—3		
Contact	Short-period Benioff	10 000	1,2—1,4		
	SK	200—1000	2—3	3—4	6—8
	SK, SKD	4000—10000	4—6	8—10	20—40
	SKM	4000—10000	1,5—2,5		
Atmospheric	Short-period Benioff	300—2000	0,5—0,9		
		7000—10 000	0,7—1,2		
	Press-Ewing	5000—10 000	8—12	15—20	20—70
	SK	200—1000	2,0—10	4—8	6—12
	SKM	200—1000	0,6—1,5	5—6	4—10
	SK	1000—10 000	6,0—12	8—15	20—40
	SKM	1000—10 000	1,5—2,5		8—15
	SKD	2000—10 000	10—14	10—18	20—60

usually cannot be increased to more than 1,000 - 2,000. Naturally, this particular equipment cannot record low-intensity seismic oscillations from smaller explosions at such a low amplification. Further on we will characterize the intensity of seismic phenomena caused by explosions either in terms of seismic magnitude M, determined according to surface waves, or in terms of m, determined according to the body waves [24, 217-227]. In this case, the recording range of body and surface waves by the wide-band channel, in explosions of a given intensity carried out in various media, can be determined for phenomena with definite magnitudes.

Table 4 gives information about the approximate recording range by a wide-band channel of waves of different types of underground, underwater, contact, and atmospheric explosions. As is clear from Table 4, the recording range of dilatational and surface waves for atmospheric and contact explosions by type SK and SKD seismographs at M magnitudes on the order of 3.5 - 4.5 amounts to 3,000 - 5,000 km. At M magnitudes of 4.5 - 5.5, it amounts to 10,000 - 12,000 km. For underwater and underground explosions, at m magnitudes greater than 5, the recording range of dilatational waves amounts to 10,000 - 12,000 km.

In order to increase the effective amplification of the receiving channel in recording relatively low-intensity body seismic waves with periods on the order of 1 - 2 seconds, chiefly those caused by underground and underwater nuclear explosions, it was necessary to narrow down the passband, limiting it on the longer-period side by values of $T \gtrsim 1.5 - 2.0$ seconds. Such seismographs were called short-period seismographs or seismographs with a narrow passband.

In order to increase the effective amplification of the seismic receiving channel in the period range higher than 10 - 12 seconds — which is necessary in recording surface waves from distant atmospheric, contact, and underground explosions — it was necessary to widen the passband to periods $T \gg 10 - 15$ seconds, and at the same time to lower the amplification of the channel in the range of

TABLE 4. ACTUAL RECORDING RANGES OF BASIC PHASES OF BODY AND SURFACES WAVES, RECORDED IN A QUIET AREA BY GALVANOMETRIC RECORDING EQUIPMENT, DURING EXPLOSIONS CARRIED OUT IN VARIOUS MEDIA (THE DATA FOR BODY WAVES ARE DERIVED FROM RECORDS OF SHORT-PERIOD SEISMOGRAPHS; THOSE FOR SURFACE WAVES — FROM RECORDS OF WIDE-BAND AND LONG-PERIOD SEISMOGRAPHS).

Types of explosions	Magnitudes		Power kt	Recording range (in thousands of km) for waves:					Literature
	m	M		P	S (or L_g), PS	PKP	SKS	L_R	
Underground ($h > 100$ m)									
in salt, granite or other crystalline rocks	4,8—5,0	3,0	1—2	5—10	2,0—2,5	17,0	—	2	
	6,1	3,8	80	12	5,0—6,0	17—18	—	5—10	
in tuff	5,0	4,0	5	8	2,0—2,5			2	
	6,2	4,5	200	10—12	3—4	16,5		10	
in alluvium	4,7	3,0	1—2	10	1,5			1	
	5,2	4,0	20	10—11	2—3	16,5		4	
Underwater $h < 150$ m	5,0		5	10—11	2—3	16		3	
	5,5		20	11	2—3	16		3—4	
$h > 150$ m	5,5		4	11	4—5	16		4	
	6,5		30	11—12	10	17	14	12	
Contact	4,4	3,0	20	0,7—1,0	1,0			2	
	4,7	3,5	100	1,0; 2—3	2—3			2,5—3	
	5,3	4,2	1000	4—5	3—4	15—16	15	5—8	
	6,2	5,0	15000	10—12	11	16	15	12	[103, 289]
Atmospheric $h > 1$ km		2,8	20	1—2	1—1,5			2,0—3	
		3,0	100	3,0	2,0—2,5			3—4	
		3,8	1000	4—6	2—3			4—5	
		4,5	10000	10—11	10			13—13,5	
$h = 30$—70 km		2,0	2,0	0,3	0,3			0,5	[309]
		3,5	500	0,7	1,5			2	
		4,0	1000	5—7	5			10	[289]

T < 10 seconds. Among such seismographs are included the SKD, Benioff, Press-Ewing long-period seismographs and others [149, 256].

Application of rejection filters. In a number of cases when using short-period or long-period seismographs with the necessary passband, one cannot attenuate the microseisms of the first order enough. In such cases, electromechanical rejection filters are often applied [47, 294 etc.].

The rejection filters which are applied in practice consist of auxiliary galvanometers with little attenuation, with the periods of natural oscillations coinciding with or close to the period of the microseisms. These galvanometers are connected in series in the circuit of the working coil of the seismograph and of the working galvanometer.

In the stations of the USSR, galvanometers of type M 17/6 with a natural oscillation period of six seconds are used as rejection filters, both for long-period and for short-period channels [36].

In long-period channels seismographs of type SKD are used, adjusted to a natural oscillation period on the order of 20 - 25 seconds, and galvanometers of type M 17/12 with a natural oscillation period of 18 seconds [36] (see Figure 1). Galvanometers of type M 17/6 and others are used as filters.

In a short-period channel, a seismograph of type USF is used with a galvanometer of type GK-VII with a period of 0.4 seconds (with light-weight frame). A galvanometer of type M 17/6 is used as the filter.

Rejection filters make it possible to sharply attenuate (by 10 - 20 times or more) the amplification of the channel in a narrow range of periods of intense five-second microseisms with only a slight decrease of the amplification in the range of periods higher than 10 seconds (see characteristic 2 in Figure 1).

Ordinarily signals of short-period and long-period seismographs are recorded either on separate channels of the same recorder, or more frequently, on separate recorders. This creates definite difficulties in processing and operating the equipment.

At the Institute of Physics of the Earth of the USSR Academy of Science, N. Ye. Fedoseyenko proposed a scheme of photo-optical or photo-electric mixing of oscillations which would be picked up simultaneously by seismographs adjusted at different passbands, while they would be recorded at the actual time on a single track (see Figure 3).

The use of such schemes of mixing oscillations is particularly effective when the oscillations are recorded by short-period and long-period channels with rejection filters. In this case, one can on a single track record dilatational, transverse, and surface waves with the following amplifications: on the order of 10^6 in periods of 15 - 24 seconds; on the order of 10^4 in periods of 15 - 40 seconds; and on the order of 10^3 in periods of 3 - 10 seconds (see Figure 3). If there are no rejection filters, the recordings obtained under analogous conditions are complicated by microseisms (see Figure 4).

§ 3. Influence of Equipment Parameters on the Form of Seismic Oscillation Recordings

The recordings of body waves during explosions are short trains of oscillations, ordinarily consisting of 3 - 4 extrema on seismograms of wide-band channels or of 4 - 8 extrema on seismograms with channels with a narrow passband. The dilatational waves as a rule arrive with a steep front. Surface waves on the seismograms look like dispersing trains of quasi-sinusoidal oscillations, in some cases with no sharp leading fronts (see Figures 3 - 5).

Considerable distortions in the form of the recordings are connected with the pulsed character of the body waves, especially their initial

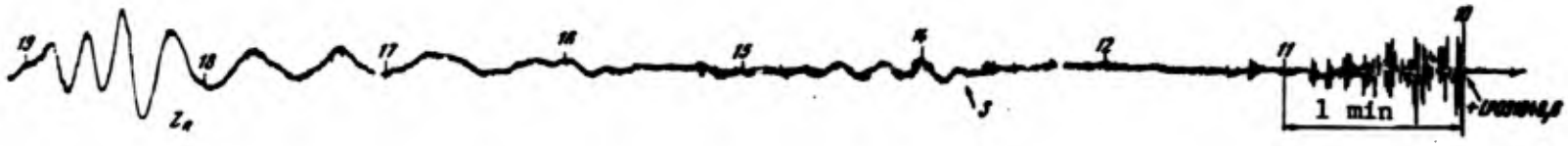

Figure 3. Recording of body and surface waves of an atmospheric explosion, taken by equipment with photoelectric mixing. Recording obtained at an epicentral distance of 2,100 km by type CKVD and USF seismographs with rejection filters (galvanometers M 16/3).

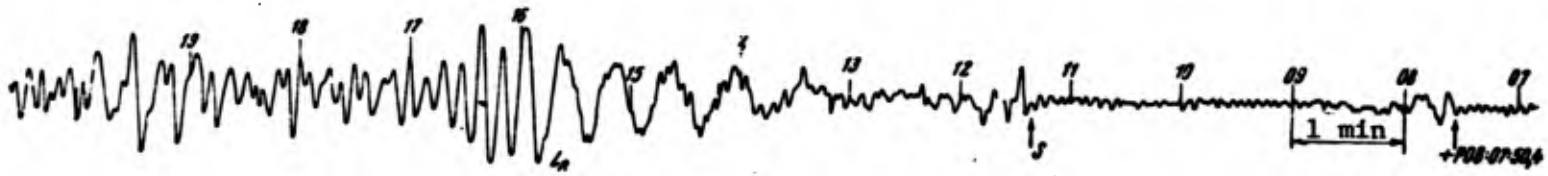

Figure 4. Recording of body and surface waves of an atmospheric explosion, taken by SVKD seismograph without rejection filter at epicentral distance of 2,100 km. Recording complicated by microseisms of the first kind.

sections. The biggest distortions in recordings of body waves are observed in seismograms of short-period instruments with narrow passbands. At the same time, the recordings of dilatational waves are of great significance for detecting and identifying nuclear explosions: recognition of explosions depends on their shapes, while the seismic magnitude of the phenomenon is determined from the ratio of the amplitude to the period. The intensity of the explosion is also estimated in the same way.

This section examines the distortions introduced into the seismic recordings by SK seismographs adjusted to standard constants, by SKM seismographs with narrow passbands, by short-period USF seismographs, etc. The character of the distortions for suddenly beginning stationary sinusoidal oscillations and Berlage type pulses is examined for the seismographs mentioned. The distortions of the experimental recordings obtained on equipment with different filtering properties are also examined.

1. Distortion of the form of recordings by SK seismographs, adjusted to standard constants. The distortions of the initial part of the recording of seismic waves made by type SK seismographs, operating with type GK-VII galvanometers, which are widely used in seismic stations of the USSR, are examined in [60] for cases when the displacement of the soil $X(t)$ has the appearance of a suddenly beginning sinusoidal oscillation:

$$\left.\begin{aligned} X &= X_{max}\sin\frac{2\pi t}{T} \text{ at } t>0,\\ X &= 0 \qquad\qquad \text{at } t<0. \end{aligned}\right\} \tag{1}$$

It is shown that in the range of periods $T_1 > T_\omega > T_2$, the amplitude of the first oscillation on the recording in this case can be minimized considerably (up to 30%) in comparison with the amplitude of the stabilized oscillation, and the first half-period can be minimized up to 10% or somewhat more in comparison with the actual value. The

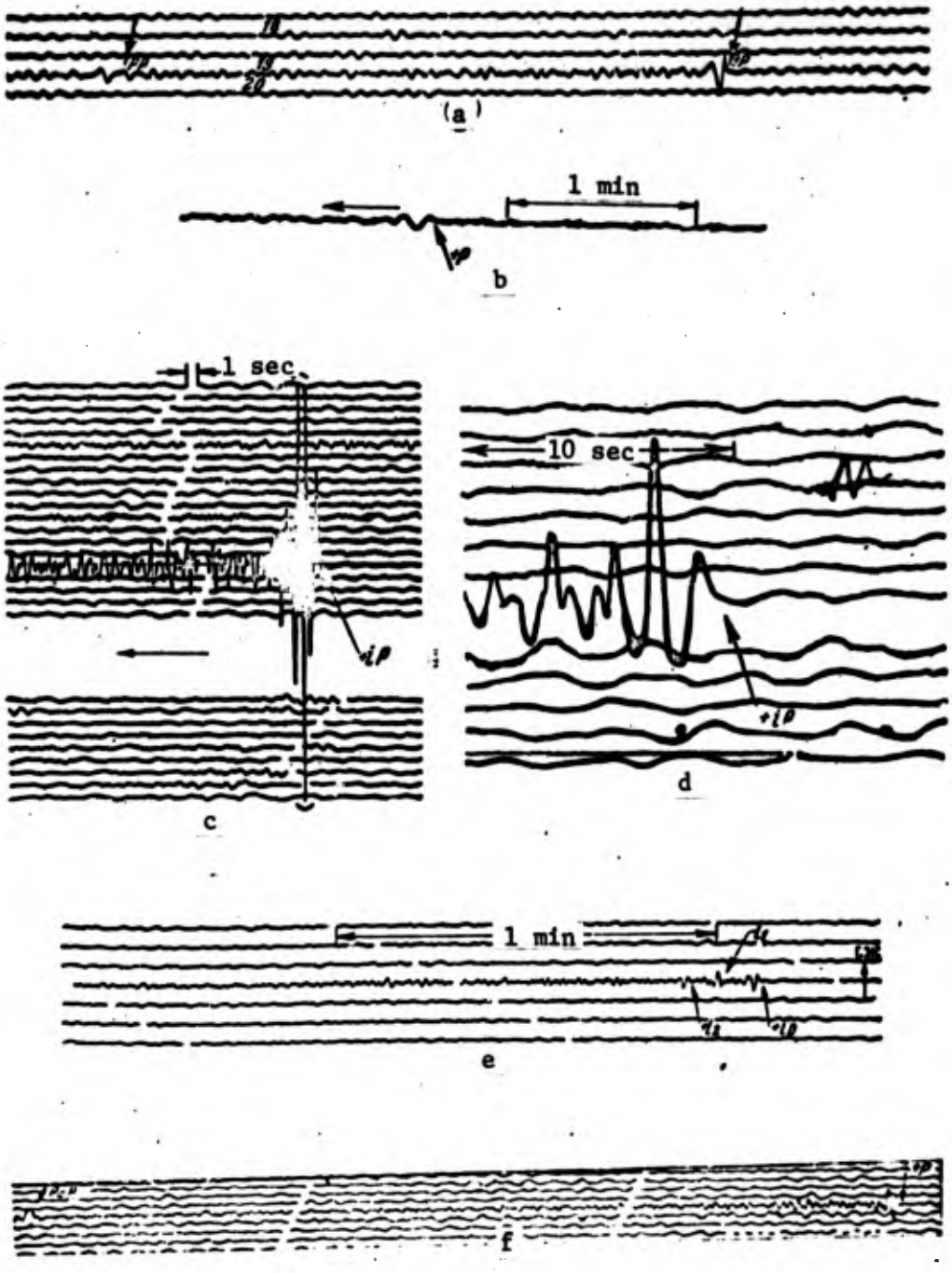

Figure 5. Recordings of P waves taken by equipment with various frequency characteristics.

Wide-band SVK seismographs: a - contact explosion in the Marshall Islands (Δ = 9,400 km); b - atmospheric explosion at Christmas Island (Δ = 8,800 km); SVKM seismographs with narrow passband: c - underground explosion in Nevada (Δ = 9,900 km); d - atmospheric explosion (Δ = 2,900 km); e - underwater explosion off the coast of California (Δ = = 7,910 km); f - underground explosion (Δ = 3,700 km; P and PcP waves).

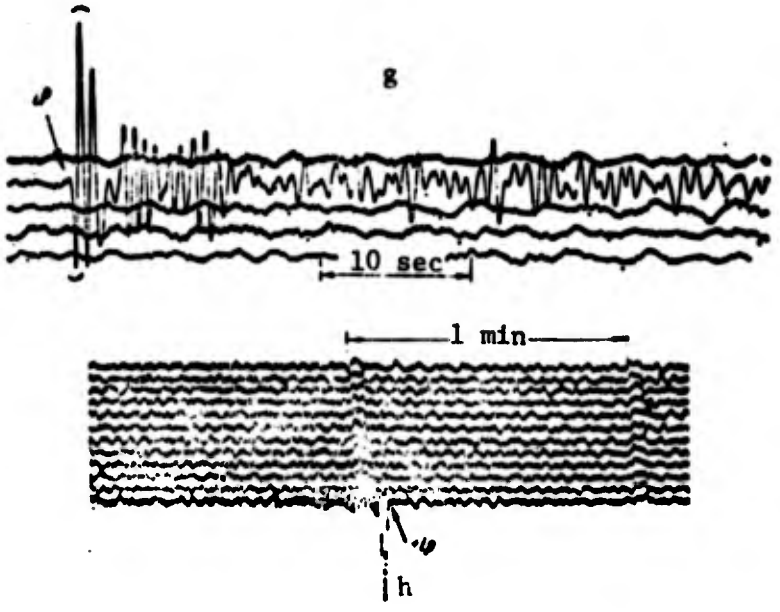

Figure 5. (continued)

Vertical Benioff seismographs: g - contact explosion in the Marshall Islands (Δ = 9,000 km); h - underground explosion in salt (Gnome), New Mexico (Δ = 4,500 km), according to data in [190].

amplitudes and periods of the subsequent oscillations are only slightly distorted, and in practice their distortions can be omitted from consideration.

In [60] graphic methods are developed for introducing corrections into the values of the amplitudes and periods of the initial oscillations in cases when suddenly beginning stationary oscillations act on a type SK seismograph. These methods were used in the present work in calculating the true displacements and periods in the first motion of body waves of atmospheric, contact, and powerful underground explosions recorded by type SK seismographs. These corrections were not introduced into the recordings of surface waves since they were negligible. In the interpretation of surface waves, attention was given chiefly to the maximal oscillations in the train, which are usually not confined to the initial part of the train.

2. Distortion of shape of records when using seismographs with narrow passbands. In this case, there are significant distortions of the initial portions of the records of dilatational waves P_n and P, which are of important significance for purposes of detecting and identifying nuclear explosions. Therefore, when calculating the distortions, it is advisable to consider the excitation function as a pulse of finite duration. Besides this, in oscillations caused by explosions, the first derivative of displacement is usually continuous, while the second derivative or a derivative of a higher order undergoes a discontinuity. In this connection, the excitation function was presented, not as a suddenly beginning stationary sinusoidal oscillation, but as a Berlage type pulse:

$$\left.\begin{aligned} X &= X_{max}\, te^{-pt} \sin\frac{2\pi t}{T} \text{ at } t>0, \\ X &= 0 \qquad\qquad\qquad \text{at } t<0. \end{aligned}\right\} \tag{2}$$

For the special case when the Berlage pulse is $X = te^{-pt} \sin 2\pi t$, that is when $X_{max} = 1$, $p = \pi$, and $T = 1$ second, calculations were carried out for the distortions of the shape of the pulse in question by seismic receiving channels with narrow passbands (see Figure 6).

Calculations were carried out for the following parameters of the receiving channel:

For SVKM seismographs: $T_1 = 2.5$ sec, $T_2 = 1.1$ sec, $D_1 = 1.5$, $D_2 = 3$, $\sigma^2 = 0.3$;

For Benioff seismographs: $T_1 = 1$ sec, $T_2 = 0.2$ sec, $D_1 = D_2 = 1$, $\sigma^2 = 0$.

Curves 1, 2 and 3 in Figure 6 show that, when Berlage pulses are recorded by type SVKB seismographs and Benioff seismographs, considerable distortions are introduced. In this case, for SVKM seismographs a reduction of the amplitude of the first extremum by about 25% occurs in comparison with the amplitude of the second extremum. Also, a reduction in the time of the first half-oscillation of 20% occurs in

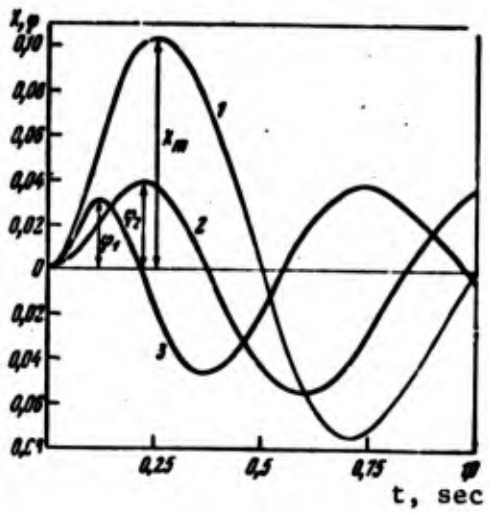

Figure 6. Example of calculating distortions in the shape of Berlage pulse recordings (1)

$$X = te^{-\pi t} \sin^2 \frac{\pi t}{T},$$

at T = 1 sec, with SVKM seismograph (2) and Benioff seismograph (3)

m = amplitude of first extremum of reference pulse

$\phi_{1,2}$ = amplitudes of distorted pulses.

comparison with the half-period of the forced oscillation in the Berlage pulse. The distortions introduced into the recording by the Benioff seismograph, which has a narrower band and shorter period, are somewhat larger than the distortions introduced by the type SVKM seismograph, which has a wider band and a longer period. For example, the time of the first half-oscillation was reduced by more than 50% in comparison with the half-period of the same half-oscillation in the forced Berlage pulse.

The above-mentioned distortions in recordings of dilatational P waves by seismographs with different absolute passbands are calculated for Berlage type pulses and agree with the observed data given below [99].

3. Experimental data on distortions in the form of dilatational wave recordings. From the practical point of view, it is most interesting to study the distortions in the form of recordings during underground explosions, inasmuch as the seismic method is the only method for the detection and identification of this type of explosion. The form of the train of oscillations in the P wave plays an important role in the identification of explosions and earthquakes. In the identification of explosions, the shape of the rounded train in the P waves is used as the criterion. The form is characterized by the correspondence of

the amplitudes of the first and the subsequent oscillations, by the direction of the first motion, and by a number of other peculiarities of the records. For this reason, it is essential that during the recording of the P waves during explosions the receiving equipment should not excessively reduce the amplitudes of the first oscillations, particularly of the first motion, and also should not substantially distort the shape of the recording of the entire train of oscillations in the P wave. Experience shows that the reliability of identifying recordings of explosions, especially of underground ones, depends to a considerable degree on how correctly the parameters of the recording equipment have been selected.

One can form an idea about the accuracy of recording the first motion by equipment with different parameters by determining the relationship of the amplitude of the first motion to the amplitude of the second and maximum oscillations in the train of the dilatational wave, recorded by the equipment with different parameters.

Let us examine the relationships just mentioned, calculated from records obtained in the same station with equipment with different parameters for a number of underground nuclear explosions at three substantially different epicentral distances (Δ = 2,800 km, Δ = = 4,500 km, Δ = 9,900 km) (Table 5).

Recordings for dilatational waves during the underground explosions in question were not received on the long-period and wide-band channels. The first dilatational waves were recorded only by equipment with a narrow passband.

It is clear from an analysis of the data given in Table 5 that the shape of the oscillations, the accuracy of the recordings of the first motion, and also its amplitude depend on two parameters of the receiving channel: the width of the passband and the maximum period of the frequency characteristic. By the absolute width of the passband in this case is understood a band taken within the range of the values of the boundary periods on a level of 0.5 from the maximum of

TABLE 5. RELATIONSHIP OF THE AMPLITUDE OF FIRST MOTION TO THE AMPLITUDE OF THE SECOND AND MAXIMUM OSCILLATIONS IN DILATATIONAL P WAVES ON RECORDINGS OF UNDERGROUND EXPLOSIONS OBTAINED AT THE SAME STATION BY EQUIPMENT WITH VARIOUS PARAMETERS

Types of seismographs	Period at the maximum amplification T_{max}, sec	Absolute width of the passband, sec	Relative width of the passband, %	Relationship of the amplitude A_1 of first motion to the amplitude of the second A_2 and of the maximum oscillation A_{max}							
				Δ = 2,800 km m = 5.3		Explosion in crystalline rocks (Sahara) May 1, 1962 Δ = 4,350 km m = 5.3		Explosion in tuff (Nevada) May 12, 1962 Δ = 9,900 km m = 5.4		Explosion in Nevada Sep. 13,1962 Δ = 9,900 km m = 6.4	
				A_1/A_2	A_1/A_{max}	A_1/A_2	A_1/A_{max}	A_1/A_2	A_1/A_{max}	A_1/A_2	A_1/A_{max}
SVKM	0.9	0.1 - 2.5	320	0.8	0.53	0.3	0.25	0.75	0.6	0.75	0.63
USF	0.6	0.06 - 1.5	320	0.7	0.48	0.1	0.1	0.75	0.6	0.75	0.45
SVKM (with amplifier, without filter)	1.8	0.75 - 2.55	85	0.29	0.20	0.4	0.2	0.63	0.5	not registered	

TABLE 5. RELATIONSHIP OF THE AMPLITUDE OF FIRST MOTION TO THE AMPLITUDE OF THE SECOND AND MAXIMUM OSCILLATIONS IN DILATATIONAL P WAVES ON RECORDINGS OF UNDERGROUND EXPLOSIONS OBTAINED AT THE SAME STATION BY EQUIPMENT WITH VARIOUS PARAMETERS

(continued)

Types of seismographs	Period at the maximum amplification T_{max}, sec	Absolute width of the passband, sec	Relative width of the passband, %	Relationship of the amplitude A_1 of first motion to the amplitude of the second A_2 and of the maximum oscillation A_{max}							
				Δ = 2,800 km m = 5.3		Explosion in crystalline rocks (Sahara) May 1, 1962 Δ = 4,350 km m = 5.3		Explosion in tuff (Nevada) May 12, 1962 Δ = 9,900 km m = 5.4		Explosion in Nevada Sep. 13,1962 Δ = 9,900 km m = 6.4	
				A_1/A_2	A_1/A_{max}	A_1/A_2	A_1/A_{max}	A_1/A_2	A_1/A_{max}	A_1/A_2	A_1/A_{max}
SVKM (with amplifier and with filter)	1.75	1.3 - 2.2	55	0.65	0.52	0.5	0.1	0.5	0.5	0.8	0.53
	0.85	0.6 - 1.3	80	0.36	0.31	0.1	0.1	0.66	0.2	0.83	0.18
	0.45	0.36 - 0.7	75	0.15	0.1	not registered		not registered		0.98	0.98
	0.22	0.14 - 0.29	70	there was no recording						0.8	0.66
	0.095	0.07 - 0.12	55	0.1	—	"	"	"	"	not registered	

the frequency characteristic, as is the custom in seismology. The relative width of the passband designates the ratio of the absolute passband width to the maximum period of the frequency characteristic, expressed in percent.

The direction of the first motion was recorded most accurately by equipment with a uniform amplification in periods ranging from 0.1 to 1.0 - 1.2 second. Adequate results were given also by equipment having an amplification maximum located at periods on the order of 1.0 - 1.8 second. The equipment has a passband with a relative width on the order of 100% or more. The ratio of the amplitude of the first motion to the maximum in this case amounts to approximately 0.5. The accuracy of recording the first motion is influenced substantially by widening the passband in the direction of the longer periods, which, however, is limited by the increase of the interference level. When the band is narrowed and shifted towards the shorter periods — for instance if the passband is 0.3 - 0.7 seconds — the amplitude of the first oscillation decreases sharply. The amplitude maximum in this case shifts into the region of subsequent oscillations (the fifth or sixth extremum). No records at all were obtained on equipment when the passband was moved towards shorter periods (see below, Figure 10).

Thus, when using equipment with a narrow passband, whose amplification maximum is moved towards the shorter periods and whose amplification can be increased under ordinary conditions up to 10^6 or more, either the first motion does not show up clearly in the recordings of distant underground explosions, or the oscillations excited by such explosions are not recorded at all. When the passband of the equipment is narrowed, the distortions of the true shape of the signal increase.

When calculating displacements of the soil, appropriate corrections calculated for the prescribed type of pulses are introduced, for example, pulses of the Berlage type or other types [60, 18].

When selecting the parameters of the equipment, one applies some of their optimum values, in each case taking into consideration the concrete conditions of interference at the detecting point and the spectral composition of the useful oscillations.

However, this practice will soon become obsolete and will be replaced by the practice of recording seismic waves with wide-band equipment with magnetic recordings having a large dynamic range, followed by analysis of the oscillations on electronic computers. The pertinent filtrations, corrections, etc., will be introduced automatically.

§ 4. Differences in Magnitude Values in Records from Instruments with Different Frequency Characteristics

It has been established experimentally that the values of the m or M seismic magnitude for the same explosion from the records of seismographs which are located at the same point but which have different frequency characteristics do not as a rule coincide [103 etc.]. Ordinarily, the largest values of m or M are from records of seismographs with the widest bands. This is explained by the fact that, when wide-band seismographs are used, the spectrum of the recorded waves usually is located within the range of the passband of the receiving equipment. When equipment with a narrow passband is used, only a certain limited portion of the wave spectrum comes within the range of this band. There may possibly be cases when the spectral band of the waves does not coincide with the narrow passband of the equipment. In such cases, the intensity of the recording, as was shown in the preceding section, will be considerably reduced and, accordingly, the magnitude to be determined will be underestimated.

Table 6 gives the divergences in the magnitudes of m and M, as determined from recordings of wide-band SK seismographs and of SKM and USF seismographs with narrow passbands, when recording seismic waves excited by contact, atmospheric, and underground explosions.

TABLE 6. DIFFERENCES IN THE VALUES OF m AND M, DERIVED FROM RECORDS OF WIDE-BAND SEISMOGRAPHS OF TYPE SK AND SEISMOGRAPHS CF TYPE SKM AND USF WITH NARROW PASSBAND (FOR VALUES OF m ON THE ORDER OF 5.5)

Types of explosions	Range of Δ, km	Values of Δm			Values of Δm	
		$m_{SK}-m_{SKM}$	$m_{SK}-m_{B}$	$m_{SK}-m_{USF}$	$M_{SK}-M_{SKM}$	$M_{SK}-M_{USF}$
Contact	5150-9000	0.4	0.3	–	0.3	0.3
Atmospheric	500-5000	0.3	0.3	0.3	0.3	0.3
Under-ground	6000-9900	0.3	0.4	0.3	0.3	0.3
Mean value		0.3	0.3	0.3	0.3	0.3

As is clear from Table 6, when waves excited by contact, atmospheric, and underground explosions are recorded, the magnitudes from data of SK seismographs adjusted to standard constants are greater by 0.3 units of magnitude than the same values from the records of type SKM and USF seismographs adjusted to the constants shown in Table 1 [103].

When waves caused by underground and underwater explosions are recorded, the m magnitude in the records of type SKM instruments is larger by approximately 0.1 - 0.2 units of magnitude than the values from the records of type USF seismographs which have even narrower bands (see Figure 1).

The values of M determined from records of long-period seismographs with rejection filters also are reduced in comparison with the values determined from the records of wide-band seismographs.

The above-mentioned phenomenon of the dependence of the m and M values on the frequency characteristics of the receiving equipment

must be taken into consideration in establishing the dependences of m and M for seismic phenomena on the magnitude of the TNT equivalent of the explosions. The correlations in question should be established separately for the readings of wide-band and narrow-band seismographs. In the present work, as a rule, the values of M were determined solely by the records of wide-band and long-period seismographs.

In the future, it will be necessary to establish both experimentally and by calculations the values of the pertinent corrections for the most widely applied types of instruments and for pulses close to the real ones.

Recently, the dependence of m on the magnitude has been revealed. When the values of m are increased ≥ 6, the value of Δm decreases to 0.15 - 0.1. When m is decreased to 4.5, an increase of Δm to 0.4 - 0.5 units of magnitude is noted.

§ 5. Optimum Parameters of the Equipment Recommended in [131] for Stations Detecting Nuclear Explosions

For purposes of detecting and identifying nuclear explosions carried out in various media, it is necessary to record waves of different types — dilatational, transverse, and surface, whose periods of oscillations are different for the same explosion. Besides this, the periods of the same types of waves and the corresponding correlations of intensities in body and surface waves differ considerably for different types of explosions. Therefore, for the same explosion, especially one of a small intensity, at epicentral distances greater than 1,000 km one cannot always obtain sufficiently intensive records of the body and surface waves with only one set of seismic receiving equipment. This is connected with the small dynamic range of galvanometric recording equipment and with the presence of intense microseisms, some of which may be microseisms of the first order.

Therefore, stations for detecting nuclear explosions must be equipped with several sets of equipment, each one of which is adjusted

to the optimum parameters for obtaining the most satisfactory records either for body waves or for surface waves. In addition, recording must be performed at different levels of amplification, usually at two.

At the present time, the stations are each equipped with three sets of seismic equipment, each consisting of three components. They have approximately the following characteristics: 1) a short-period set with narrow passband from 0.1 to 1.5 - 2.0 sec with amplification on the order of 10^5 - 10^6; 2) a wide-band set with a passband of from 0.2 to 10 - 12 sec and amplification on the order of 10^3; 3) a long-period set with a passband of from 8 - 10 to 60 - 80 sec, with an amplification on the order of $(2 - 3)\cdot 10^4$ in periods of 20 - 25 sec, and with a drop of the left slope of the characteristics on the order of 60 - 80 dB.

A number of stations are equipped with from 20 to 100 or more short-period vertical seismometers with periods of 1 sec with a total amplification of 10^6 or more [91, 131, 169, 212, 335, 343].

As examples, Figure 2 shows amplification curves of equipment installed in modern seismic stations for detecting nuclear explosions of the United States and other countries [169, 191, 211, 212, 335, 343]. They have the parameters recommended by the Geneva conference of experts of 1958 [131].

In the future, it is expected that equipment with magnetic digital recording — for instance, that of type KOD, designed by the IPE of the USSR Academy of Sciences [92] — will go into use. This equipment possesses a great dynamic range (on the order of 60 dB, but up to 120 dB when there are two levels of sensitivity). When this equipment is put into use, it will no longer be necessary to install a large number of sets of selective equipment in the same station.

In this way, as equipment with galvanometric recording instruments — previously used for recording earthquake waves — came to be used for recording explosions, the equipment was perfected. This improvement of the equipment was directed mainly towards endowing it with a greater sensitivity in a restricted range of periods. In the USSR, the short-period SKM and USF seismographs, and galvanometers with light-weight frames were devised for these purposes. This made possible an increase of the effective amplification of the equipment by a factor of 60 - 500 in periods on the order of 1 sec in comparison with seismographs of type SK. Long-period seismographs of type SKD were devised. When galvanometers of type M 17/12 and rejection filters were used, they made it possible to increase the amplification in periods on the order of 10 - 25 sec up to $(1 - 1.5) \cdot 10^4$. There have been designed recording instruments of type OSB-VI, OMS, and others with photographic recording, as well as those with visible recording on graph, electrographic, and thermal paper.

Special equipment with magnetic analog and digital recording has also been designed in the USSR and in other countries.

CHAPTER II

THE APPLICATION OF FREQUENCY ANALYSIS OF SEISMIC OSCILLATIONS FOR THE STUDY OF THE DYNAMIC CHARACTERISTICS OF SEISMIC WAVES

The amplitude spectra of the body and surface waves (hereinafter referred to simply as the wave spectra) are used in the present work in comparing some of the dynamic characteristics of seismic waves caused by explosions carried out in various media with those caused by earthquakes. Examination of the spectra of seismic waves caused by explosions and by earthquakes makes it possible in a number of cases to bring out clearly some auxiliary dynamic differences in the character of the records — differences which are indistinguishable in a comparison of the records themselves. This is connected with the fact that divergences in the spectra of pulse oscillations which are close to each other in shape often appear more sharply than divergences in shape of the reference pulses themselves. For the purposes mentioned above, it is possible to use amplitude or energy spectra both of separate waves and of the whole record of seismic oscillations on the seismogram.

This chapter briefly examines the tasks, connected with a study of the dynamic characteristics of seismic waves, which are to be

solved chiefly by research on the amplitude spectra of seismic waves. The means of obtaining the spectra are also described, and several examples are adduced, illustrating principally the methodological aspect of the question. The comparison of the spectra of waves caused by explosions and those caused by earthquakes is to be found in Chapters V and VI of this work.

§ 1. Areas in which Spectra are Applied

The spectra of seismic waves contain information by which one can identify the character of the source, as can be done using other parameters of the record. For instance, one can distinguish the records of both near and distant underground, underwater, and atmospheric nuclear explosions from the records of most earthquakes and near industrial explosions. However, in cases when the wave spectra of explosions and earthquakes do not differ sharply, it is difficult to use them for the purposes mentioned above. The fact is that the character of a spectrum depends on a number of causes: on the geological structure at the source area, at the station, and along the entire path of propagation of the waves; on the depth, height, and power of the source; on the attenuation of the waves with the epicentral distance, and others.

By using the relationships of the wave spectra of different seismic phenomena, for example, of underground nuclear explosions and earthquakes, propagated along the same or close paths, and recorded in the same stations, one can exclude the influence of the medium, including even the effects of attenuation to a certain degree. Naturally the spectral differences in waves of explosions and earthquakes must be used in an identification, in combination with other kinematic and dynamic characteristics of the recordings.

For example, the following tasks can be solved by means of spectral analysis.

1. Study of the spectral composition of the useful signals (seismic waves and interference) of microseisms. By knowing the spectra of the useful signal and the interference, one can improve the conditions of recording the useful waves in the following manner: a) one can select the optimum parameters of the equipment for obtaining the greatest ratio of the amplitude of the useful signal to the amplitude of the interference, or in some cases, for practically total suppression of interference; b) one can select the optimum parameters of the group of seismographs for the purpose of selecting the oscillations, both according to frequency and also according to direction, or according to their velocity characteristics. Spectral methods are used to select the means of suppressing interference in a single station equipped with a three-component installation of seismographs and in a number of other cases.

2. Determining the basic parameters of the spectra of the useful signal — the period of the maximum for the P wave, which practically coincides with the dominant period of not-too-short quasi-sinusoidal seismic pulses; the width of the spectral band and the steepness of the drop of its slopes; and the ratios of amplitudes of different spectral components, the so-called spectral coefficients. It is necessary to determine these parameters of the spectra, for instance, in selecting the useful signals at the point of detection according to their spectral characteristics, and in several other cases.

3. Determining the spectra of simple waves composing the interference oscillation, according to the spectrum of the interference wave, when there are differences in the predominant periods of the simple wave spectra.

4. Determining the spectra of the useful signals recorded by wave-band equipment on a background of intense interference, mainly of microseisms of the first order. This is possible when there are differences in the predominant periods between the useful signal and

the interference. In this case, the spectra of the useful signal and those of the interference are divided up into two or more isolated sections, in which amplitude increases can be seen in the area of the spectra maxima, which are distinguished from each other by their periods.

5. Identifying seismic waves of different types — dilatational, transverse, surface — by their spectra.

6. Using spectra recordings to distinguish explosions from those of certain earthquakes which are similar to them, which occur in the same area, and which are recorded by a network of the same stations. Among other things, the ratios of the spectra of dilatational, transverse, and surface waves, or the spectra of the entire oscillation recording are used for this purpose. This is based on the difference in the mechanism of the forces at the source, including the different duration of the source, and the dimensions of the latter. The method of determining the forces at the source by the spectra of the body and surface waves, chiefly Rayleigh waves, which are recorded at distant stations, is described, for example, in the works [55, 56, 345, 347, etc.].

7. Study of the spectra of the basic shock of an earthquake and the subsequent aftershocks for the purpose of identifying them.

8. Evaluation of the absorptive properties of the medium in a certain range of periods, and also determining the dependence of the absorption coefficient on the frequency. Knowledge of these relationships enables one to evaluate the amplitudes of oscillations in the waves in records of equipment which filters according to frequency. In addition, the determination of the absorption coefficients of seismic oscillations in the waves, and also their dependence on the frequency, is of independent significance, basically for studying the properties of the Earth's crust, mantle, and core.

9. Plotting of spectral calibration curves for classifying earthquakes and explosions in terms of energy.

In addition to the tasks enumerated above, spectral methods can also be used for solving many other general seismological and special problems, for example, for determining the relative intensities of explosions, etc.

Phase spectra are not used in this work due to the fact that the methods of their quantitative interpretation with reference to the seismology problems being examined here are as yet relatively undeveloped, even though when spectra are calculated on computers both the amplitude spectra and the phase spectra are calculated simultaneously.

Among the problems which may possibly be solved by simultaneously using amplitude spectra and phase spectra are problems such as determining the forces in action at the source, studying the dispersion of the seismic waves, building models of the media, and others.

In the following sections, the methods of obtaining amplitude spectra are described briefly, and examples of solving some of the above-mentioned problems are given. Some of the problems enumerated above are touched upon also in the following chapters.

§ 2. Methods of Obtaining Spectra

The possibility of making the transition from analysis of the shape of the pulse in the seismogram x(t) to analysis of its complex spectrum $\bar{S}(\omega)$, as is well known, is based on the following Fourier transformation

$$\bar{S}(\omega)=\int_{-\infty}^{+\infty}x(t)\,e^{i\omega t}\,dt=\int_{-\infty}^{+\infty}x(t)\cos\omega t\,dt+i\int_{-\infty}^{+\infty}x(t)\sin\omega t\,dt=J_1(\omega)+iJ_2(\omega), \qquad (3)$$

where the pulse x(t) is defined by the following expression:

$$x(t)=\frac{1}{2\pi}\int_{-\infty}^{+\infty}\bar{S}(\omega)e^{-i\omega t}\,dt. \qquad (4)$$

The modulus of spectrum (3)

$$|\bar{S}(\omega)|=\sqrt{J_1^2(\omega)+J_2^2(\omega)} \qquad (5)$$

is an amplitude spectrum, and the argument

$$\Phi(\omega)=\operatorname{arc\,tg}\frac{J_2(\omega)}{J_1(\omega)} \qquad (6)$$

is its phase spectrum [135].

In this work, amplitude spectra are presented graphically in terms of the relationship of $|\bar{S}(T)|$ to T, where T is the period in seconds. In certain cases, they are presented in terms of the relationship of $|\bar{S}f(t)|$ to the frequency f = 1/T in hertz, or the relationship of $|S(\omega)^{-}|$ to the circular frequency (ω), expressed in rad/sec.

In this work, the spectra were determined by two methods: from the records of the FSSS* designed by K. K. Zapol'skiy [49, 50], and by the method of parabolic interpolation on an electronic computer [86]. The raw material in both methods consisted of the seismograms obtained in seismic stations by equipment with galvanometric recording on photographic paper.

Determination of spectra on electronic computers. In order to determine the spectra by means of calculations, the part of the oscillographic record which is analyzed is converted into numerical data. These numerical data must then be transferred onto cards,

*FSSS (chastotno-izbiratel'naya seismicheskaya stantsiya) Frequency Selecting Seismic Station.

by means of which the information is introduced into the computer. When the data are being converted into numerical form, the duration section Δt is indicated on the oscillograph record. This section contains all the oscillations having a relation, in the opinion of the interpreter, to the train of the wave being analyzed. The amplitude of oscillations on the record is measured at equal time intervals, for instance, in the case of P waves of underground explosions, at 20 points in each one-second interval in the record of oscillations. The semi-automatic devices described in [15, 75] were utilized in converting the data to numerical form.

In order to obtain an approximate spectrum with an accuracy on the order of 5-10%, it is necessary, as was shown in [14], to measure 10-15 values of the ordinates for one period of the oscillation being analyzed. As the number of measured points in the period of oscillation is increased, there will be an increased accuracy of calculation of the spectra by the method of parabolic interpolation. In this work, no less than 20 values of the amplitude in one period of oscillation were measured when the records were converted to numerical data; therefore, the spectra given in this work, as a rule, have an accuracy not less than $\pm$ 5%.

Evidence has been introduced in the literature for amplitude values in $|\bar{S}(\omega)|$ and $\Phi(\omega)$ ranging from hundreds to several tenths of one ω. The number of $|\bar{S}(\omega)|$ and $\Phi(\omega)$ values mentioned in the literature have been on the order of 50 per 1 hertz.

The examples of spectra given in Figure 7 a) and b) were calculated on electronic computers for dilatational waves P_n and P of an underground nuclear explosion. They were recorded at different epicentral distances.

In the spectra calculated on electronic computers for portions of the records containing 5-10 oscillations, there is a scatter of the adjacent values of the amplitudes of the spectral components.

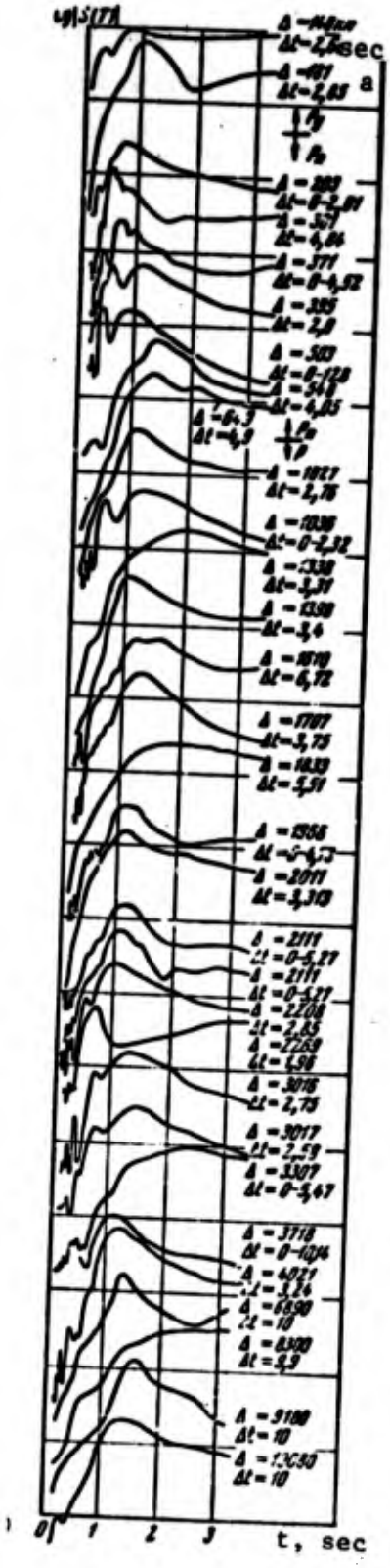

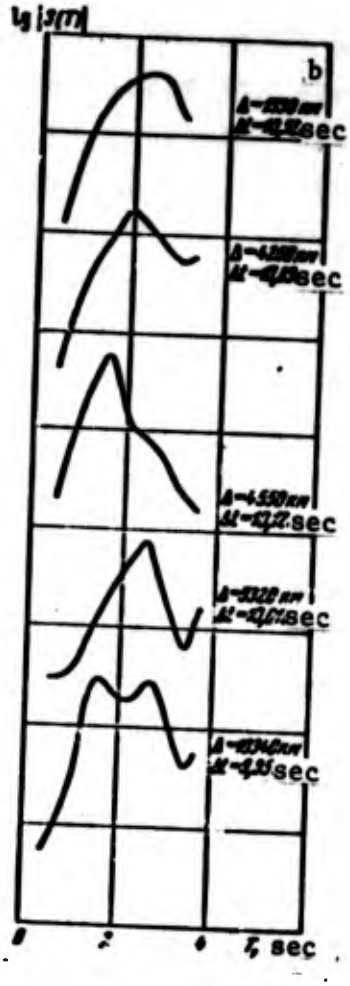

Figure 7. Amplitude spectra of dilational waves. a) P_n and P waves recorded for the identical underground explosion at a range of Δ of 140 to 10,080 km by single-type equipment. b) P waves recorded by wide-band SK seismographs during underground explosions. The relative distribution of the spectra is given on an arbitrary scale.

This is what is called brokenness of the spectra. It may evidently be connected with the interference character of the oscillations, with errors in converting the raw records to numerical data, or with a number of other causes. The phenomenon of brokenness of the spectra is not observed as a rule in spectra of waves containing 2-3 oscillations. Therefore, when plotting graphically the broken spectra, they were smoothed out in advance by averaging five or nine successive values of the amplitudes of adjacent spectral components. Hereafter this method is called the method of averaging at five or nine points without overlapping. Another method which was also used was that of averaging over five or nine succesive values, in which case the averaging interval shifted successively to a single value. This method is named the method of averaging with overlapping. In both methods, the averaged value was around the middle of the averaged interval — for instance, at the third point when five points were being averaged, etc.

In most cases the method of averaging at five points with overlapping was used. When 50 values of the amplitude spectral component per one hertz were recorded, good results were obtained with the method of averaging five successive values of the amplitudes of the spectral components without overlapping.

Examples of the spectra of one P wave from an underground nuclear explosion are shown in Figure 8. The spectra were plotted without averaging (1), by averaged values at nine points without overlapping (3), and at five points with overlapping (4). It must be noted that visual averaging of the amplitude spectrum (curve 2 in Figure 8) also gives satisfactory results.

An examination of the spectra in Figure 8 reveals clearly that averaging of adjacent amplitude values makes it possible to give them a smooth shape, removing the brokenness of the spectra, that is, to smooth out individual anomalous overshoots, evidently connected with the interference character of the oscillations, with accidental errors,

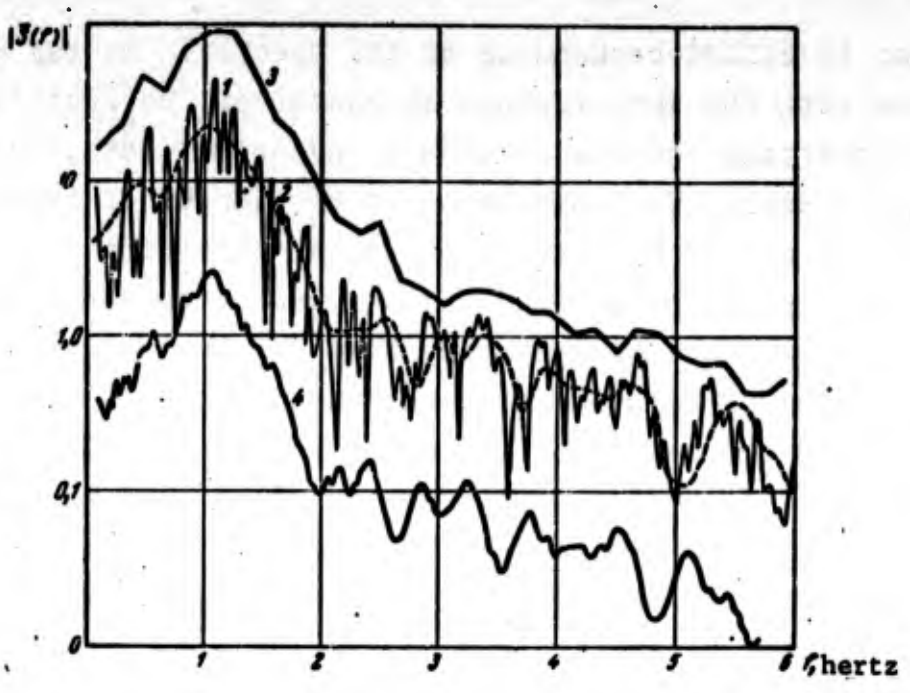

Figure 8. Examples of different means of averaging broken-up spectra for prolonged sections of a recording of P waves of an underground explosion. 1 - Spectrum before being averaged. 2 - Visual averaging. 3 - Averaging over nine successive points without overlapping. 4 - Averaging over five successive points with overlapping.

for instance, those occurring when converting data to numerical form, etc.

In order to carry out an experimental evaluation of the errors introduced into the spectra when the records are converted to numerical form by various computers, pertinent calculations were made of the spectra of waves recorded during underground nuclear explosions and earthquakes. Errors occurring during repeated computations, both on single-type machines and on hybrid machines, ordinarily fall within the range of about $\pm$ 5%, that is, within the range of errors of calculations of spectra by the parabolic interpolation method [14, 86]. Exclusion of the steady component is also specified in the program for calculating the spectra.

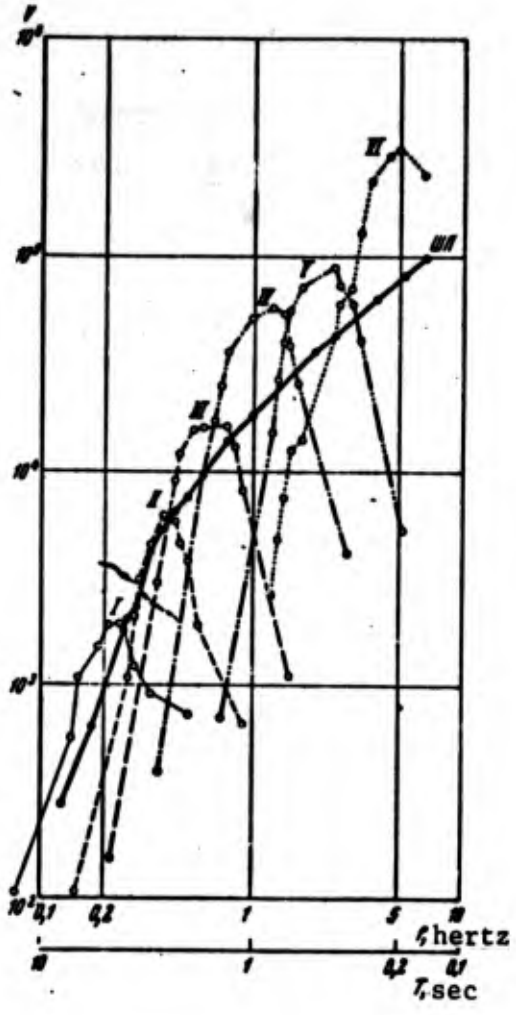

Figure 9. Amplitude-frequency characteristics of seven-channel FSSS station. I-VI are various filtrations.

Plotting spectra from records of FSSS station [49, 50]. In this case the spectra are calculated from seismogram records by separate channels with octave filters of the spectral components of oscillations of the soil in the given seismic wave. The lines of oscillations in the records of each channel, pertaining to the given wave, characterize its energy in the period interval corresponding to the pass-bands of the channels of the FSSS station.

Figure 9 gives an example of the amplitude-frequency characteristics of a seven-channel FSSS station, the records of which are analyzed in this work. The station is calibrated according to the displacement velocity in the seismic waves. This makes it possible to calculate the absolute values of the displacement velocities. To maintain control over the operation of the seismic receiving channels in each seismogram, a standard electric signal from the constant amplitude generator is entered on all tracks at the same time. This electric signal maintains a constant voltage at all frequencies [42]. A signal with an amplitude of 1 μV at frequencies from 0.1 to 20-30 hertz is usually impressed at the channel inputs.

The process of obtaining raw records for calculating the spectra is carried out in the following way. The electric signal from the seismometer recording the velocities of soil oscillations is simultaneously introduced into 6-8 or more recording devices, each one of

which consists of a separate amplifier, filter, and short-period galvanometer with f = 10 - 100 hertz. Recording also takes place simultaneously by the channel with the wide passband (WB).

Figure 10 gives examples of recordings made by an FSSS station of the P wave from a distant (Δ = 9,900 km) underground nuclear explosion carried out by the USA in Nevada, and also of recordings of near (Δ = 40 and 60 km) industrial explosions carried out in limestone quarries. The same seismogram also shows records of signals from the constant amplitude generator with a voltage amounting to 1 μV in the range of periods from 0.1 to 30 hertz.

The amplitude spectra of the waves can be plotted according to the records of the FSSS station. The methods of plotting them are described in [49, 50[a], 133]. However, in this work the records of the FSSS equipment were used only for relative comparison of some of the conventional spectral characteristics — the "conventional FSSS-spectra," plotted for underground explosions and earthquakes. To plot the conventional FSSS-spectra, the maximum values of the voltage at the channel outputs were plotted on the ordinate axis in microvolts. The magnitudes of these values were proportional to the displacement velocities in the waves.

Figure 11 gives examples of conventional FSSS-spectra of velocities for the dilatational P waves of underground nuclear explosions, near industrial explosions, and also earthquakes.

Table 7 gives the mean values of the maximum amplitudes in the velocity spectra of explosions and earthquakes in the records of six channels of the FSSS station. The mean values were normalized on the third channel. Also, Table 7 gives data concerning the underground nuclear and industrial explosions, and also about earthquakes. When examining Table 7 it should be taken into account that the mean values of the maximum components pertain to the period of maximum amplification of the channels, which in a number of cases did not

---

Footnote (1) appears on page 78.

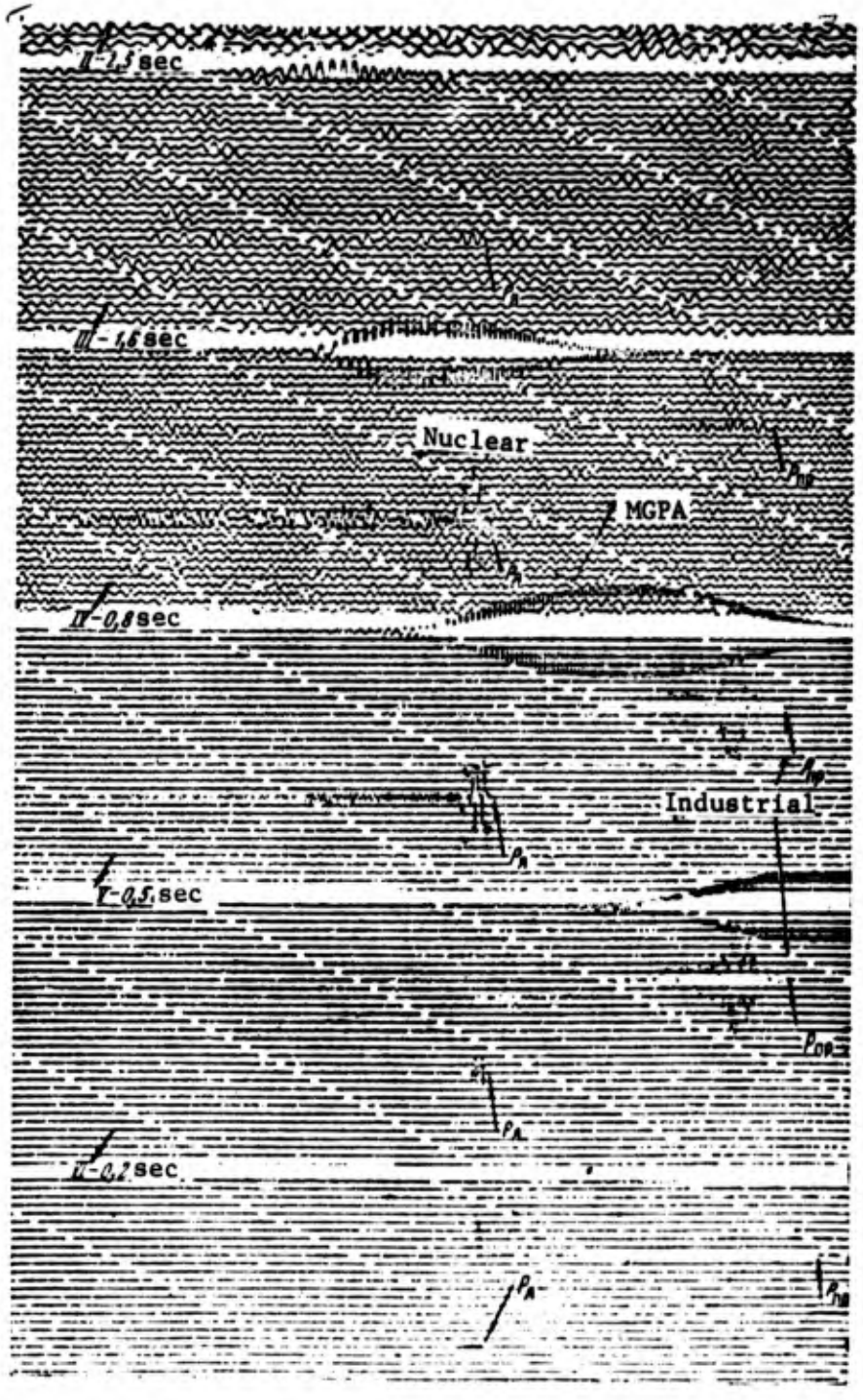

Figure 10. Examples of recording, by five channels of a FSSS station, of P_{nuc} waves of an underground nuclear explosion in Nevada (Δ = 9,900 km), of body waves P and and S, of surface waves of a near (Δ = 60 km) industrial explosion. In the upper tracks of each channel are shown the calibration signals of the MGPA; filtrations II-VI correspond to the characteristics of Figure 9.

TABLE 7. EXAMPLES OF ARBITRARY FSSS-SPECTRA OF VELOCITIES FOR P WAVES OF UNDERGROUND NUCLEAR EXPLOSIONS, NEAR INDUSTRIAL EXPLOSIONS, AND EARTHQUAKES, RECORDED BY THE SAME STATION.

Character of phenomenon	Date and region of epicenter	Magnitude		Epicentral Distance Δ, km	Depth of focus, km	Number of Channels					
		M	m			6	5	4	3	2	1
						Periods at maximum amplification, sec					
						0.2	0.5	0.8	1.6	2.5	5.0
						Relative maximum amplitudes					
Earthquake	Averaged spectrum of 100 earthquakes	4,5÷6,5	5,5÷6,6	1200÷10 000	30÷300	0,31	0,61	0,99	1,0	0,62	0,37
	Sep 6, 63, 0600 hrs	7		7040	100	0,1	0,39	0,50	1,0	1,43	0,87
	Sep 21, 63, 2300 hrs	7		7250	100	0,12	0,23	0,30	1,0	0,80	1,02
	Dec 16, 63, 1300 hrs	~6		2410	50÷100	0,1	0,25	0,88	1,0	2,21	1,70
Underground nuclear explosions	Nevada, Sep 13, 63		5,5÷6,2	9900	0,4÷0,7	0,01	0,18	0,55	1,0	0,56	0,08
	Platform region		5,3÷5,8	2700		0,24	0,52	0,88	1,0	0,15	0,01
Industrial explosions	Lime quarry	~1,0		40÷60	0,003	2,70	4,35	4,0	1,0	0,1	0,05

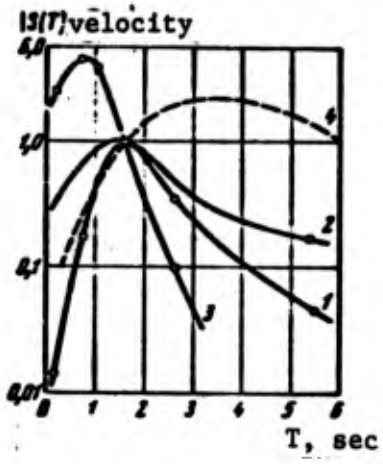

Figure 11. Examples of arbitrary FSSS-spectra of velocities of particles of the medium in P waves of explosions and earthquakes. 1 - Underground nuclear explosion in Nevada (Δ = 9,900 km). 2 - Averaged spectrum of 100 earthquakes (Δ = 1,200 - 10,000 km). 3 - Industrial explosion in a quarry (Δ = 60 km). 4 - P waves of a distant earthquake on Sept. 21, 1963 (Δ = 7,250 km). The dots represent experimental data.

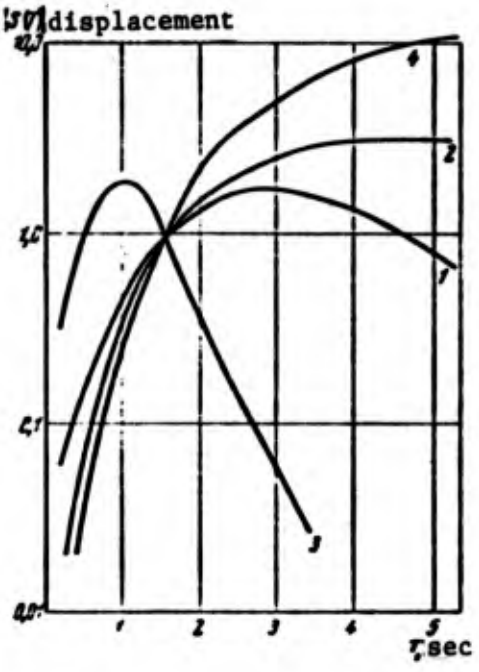

Figure 12. Examples of the FSSS-spectra of displacements of particles of the medium in the P waves of explosions and earthquakes, converted from the spectra of velocities shown in Figure 11. 1 - For an underground explosion (Δ = 9,900 km). 2 - Averaged spectrum of 100 earthquakes (Δ = 1,200 - 10,000 km). 3 - Near industrial explosions in a quarry (Δ = 60 km).

coincide with the period of the maximum oscillation. The amplitude values themselves were calculated for the period measured in the record. The standard deviation from the mean value for earthquakes amounts to about ± 10% from the measured values.

In this work, the amplitude spectra for displacements in the waves were mainly calculated on electronic computers. Therefore, it was of considerable interest to make the transition from the "conventional FSSS-spectra" to displacement spectra in the waves as calculated on electronic computers. It was established that for such a transition it is necessary to multiply the amplitudes of the spectral components by the corresponding values of the periods, that is, the "conventional

FSSS-spectra" which are close to the spectra of velocities in the waves.

Figure 12 shows the FSSS-spectra of displacements for the P waves of explosions and of earthquakes.

A strict check of the identity of the FSSS-spectra and the spectra calculated on electronic computers was carried out in the work of M. A. Gostev.

Let us note that the FSSS-spectra characterize the spectral distribution for 6-8 definite discrete values of the periods, while the spectra calculated on the electronic computers make possible considerably greater detail. However, an 18-channel FSSS equipment with a range of recordable frequencies from 0.1 to 75-100 sec has recently been designed and put into use.

The equipment and methods elaborated in [61, 62, etc.] can be used for determining the spectra.

Introducing corrections into the spectra for irregular equipment characteristics. The spectra are distorted when there is unequal amplification of the equipment, and corresponding corrections must be introduced to remove these distortions. Corrections are introduced by dividing the spectral component values by amplification of the equipment at the corresponding period. When introducing corrections for the distorting action of the receiving equipment, it is advisable in practice to do so within the range of the channel passband, taken at a level of 0.5 of its maximum amplification. Attempts to introduce corrections far beyond the range of the passband may in many cases lead to considerable errors.

However, in [115] the possibility is shown of introducing corrections into spectra for an irregular amplification of the equipment, and consequently, the possibility of obtaining true spectra even

beyond the range of the indicated passband of the receiving channel.

Corrections for equipment distortions are introduced into the spectra in cases when it is essential to know the true spectra of waves of different types — for example, when studying the influence of seismic waves on edifices and in a number of other cases. However, in cases when one is performing a comparative study of the spectra of records of waves from explosions and from earthquakes, obtained on single-type distortion equipment to identify the source, usually corrections are not introduced into the spectrum for irregular channel amplification.

The spectral frequency range used in solving various problems. Even though spectra are determined in a frequency range from several hundredths of one second to several tens of seconds, in order to obtain reliable conclusions it is necessary to use only those sections in which the amplitudes of the spectral components amount to no less than 5% of the amplitude of the maximum of the spectrum.

Thus, for example, well-founded quantitative conclusions on the spectra of body waves P and P_n of underground nuclear explosions and earthquakes, recorded by short-period seismographs, can be made only in the range of periods from 0.2 to 2.5 sec, even though spectra have been obtained in a range of frequencies from one hundredth to 10 sec.

The fact is that in the above-mentioned case, the spectrum in the range of periods greater than 2.5-3 sec is very distorted by the short-period equipment, while in the range of shorter periods ($T < 0.2$ sec), substantial errors are introduced when converting the recordings into numerical data. Therefore, the introduction of the corresponding correction beyond the bounds of the above-mentioned range of periods may lead to significant mistakes.

When records obtained from type SK and type SKD seismographs are used, the boundaries within which the quantitative characteristics

of the spectra can be studied are expanded considerably into the region of larger values of T (up to 40 - 60 sec).

Below we shall examine some quantitative characteristics of the amplitude spectra which are used in this work. Examples are given of their determination for body waves P_n and P of nuclear explosions and of earthquakes. The spectra of surface waves are examined in Chapter VI.

§ 3. Quantitative Comparisons of Differences in Spectra of Waves of Explosions and Those of Earthquakes

In comparing the spectra of different waves, or the spectra of the same waves caused by explosions and by earthquakes, in some cases it is advisable to give a quantitative characterization of the wave spectra in a definite range of periods.

In this work, the following quantitative characteristics of spectra are examined: 1) the periods T_{sp} of the maxima of the spectra; 2) the boundary frequencies T_{left} and T_{right}, i.e., the absolute width of the spectra ΔT_{sp}, determined on the level of 0.5 from the amplitude of the maximum of the spectrum; 3) the steepness of the drop of the amplitude on the slopes of the spectra γ_{left} and γ_{right}; 4) the relationships of the spectral components — the spectral coefficients.

Determining the dominant oscillation periods in the waves by the period of their spectra maximum. In several works [4, 14, 55, 56, 64, 80, 90, 99, etc.] and in chapters II - VI of this work, a comparative study of the periods of body and surface waves, recorded during explosions and earthquakes, has been carried out. The periods were measured directly by seismograms. In these works, the periods T_{dom} of the oscillations with the maximum amplitudes in the given wave (hereafter called the dominant periods) were measured for thousands of records of earthquakes and hundreds of records of explosions. The maximum periods T_{max} visible on the records were also measured.

The comparison made it possible to bring out clearly the differences in the periods of dilatational, transverse, and some other types of waves in records of explosions and earthquakes. It was established that the dominant periods in P and PKP waves in the records of underground and underwater explosions with magnitudes $m \leq 6$ obtained by means of type SK, SKM, and USF seismographs, within the range of areas where waves are present, occur within the range of 0.5 to 2.0 sec. At magnitudes $m \geq 6.1$ in records of type SK and SKD seismographs, the dominant periods reach 3 - 4 sec.

In the records of approximately 60% of all the distant earthquakes, the dominant periods are greater than the values mentioned above, while the extreme values of T for P waves of explosions and earthquakes overlap each other (see below, Figure 43, and also [90, 226]) beginning with $\Delta > 3{,}000$ km.

The difference discovered in the periods can be used as a criterion for distinguishing records of explosions among the records of most (approximately 60%) earthquakes.

The process of measuring the dominant periods in seismograms is linked with a number of difficulties, and demands a certain practice and intuition in the interpreter. It would seem that this process would be difficult to automate. It is much simpler to make measurements of the maximum period of the amplitude spectrum of T_{sp}, which practically coincides, as will be shown below, with the value of the dominant period in the P waves in the record in the case of quasi-sinusoidal oscillations, the duration of which is not less than 2 - 3 T_{dom}. Measurements by the spectra of T_{sp} can be carried out also for those oscillations differing in shape from the quasi-sinusoidal shape.

The determination of T_{sp} is a less accessible operation than measurement of T_{dom} in the seismograms, inasmuch as — in order to find T_{sp} — it is necessary to transform the oscillograph records — for

instance, by converting them into numerical data — and then to carry out the subsequent calculations on electronic computers.

In [51] it was shown that the divergence between T and T_{sp} for a single-period sinusoidal pulse amounts to 15%; for a pulse consisting of two periods, it amounts to 4%. For one consisting of three, it amounts to only 0.1%. Therefore, for records of dilatational and transverse waves of an explosion, the pulses of which usually consist of two or more oscillations, the values of the dominant periods measured by the seismograms ought to coincide in practice with the periods of the spectra maxima. The estimation, made in work [51], of the divergences between T_{dom} and T_{sp} were verified experimentally using records of quasi-sinusoidal oscillations with frequencies on the order of 100 hertz, which are the oscillations usually recorded in seismic prospecting.

It was interesting to carry out an analogous comparison for the records of waves recorded during underground nuclear explosions and during earthquakes. For this purpose, more than 200 records of P waves of explosions and about 100 records of P waves of earthquakes were subjected to analysis.

Table 8 gives the values of the mean relative errors in determining the values of $(T_{dom} - T_{sp})/T_{sp}$ in percent for a number of underground nuclear explosions, as well as the values of the standard deviations. The same table also shows the range of epicentral distances and the number of stations where the spectra of P waves were determined at each explosion.

As is obvious from the data given in Table 8, the standard deviations for determining the periods in the P waves recorded during underground nuclear explosions did not exceed 5%; this value was somewhat greater for earthquakes. In this manner, in a mass determination of wave periods in seismograms, one can with equal justification make use of direct measurements of the dominant periods

TABLE 8. VALUES OF RELATIVE ERROR IN DETERMINING DOMINANT PERIODS OF P WAVES FROM MEASUREMENTS ON SEISMOGRAMS OF T_{dom} AND FROM THE MAXIMUM OF THE SPECTRUM T_{sp} FOR UNDERGROUND EXPLOSIONS

Region and conditions of the explosion	m	Range of Δ, km	Type of seismographs	Number of stations	Mean relative error $\frac{T_{dom} - T_{sp}}{T_{sp}}$, %	Standard deviation %
Nevada, tuff	5.2	200-4000	Benioff	15	±5	1.6
Continent	5.3	1400-4400	USF, SKM	18	±10	3.8
Sahara	5.4	2400-6600	"	15	±12	4.7
Nevada	6.3	6500-9800	"	10	±8	3.0

TABLE 9. VALUES OF PERIODS T_{sp} OF MAXIMA AND OF BOUNDARY PERIODS T_{left}, T_{right} AT A LEVEL OF 0.5 OF A_{max}, DETERMINED BY THE SPECTRA OF P_n AND P WAVES OF UNDERGROUND NUCLEAR EXPLOSIONS

Type of wave	Range of Δ, km	m	Short-period seismographs			Wide-band seismographs SK		
			T_{sp}, sec	T_{left}, sec	T_{right}, sec	T_{sp}, sec	T_{left}, sec	T_{right}, sec
P_n	200-800	5.2-5.5	0.58±0.10	0.35±0.10	1.2±0.10	0.60	0.30	1.3
P	1100-10100	5.2-6.3	1.20±0.20	0.70±0.17	1.6±0.15	2.2±0.15	1.3±0.3	2.6±0.10

in the seismograms, as well as determination of the periods by the maximum of the amplitude spectrum for the given wave train.

Determining the width of the spectra. Table 9 gives the values of the width of the spectrum $\Delta T = T_{dom} - T_{left}$ for P_n and P waves recorded during underground explosions by means of short-period and wide-band seismographs (see Figure 7a, b). The maxima of the spectra of P_n waves (beginning with an epicentral distance from 200 to 800 km)

during underground explosions with a value of $m \leq 6.0$ fall in periods of approximately 0.6 ± 0.10 sec. However, in a number of cases still another extreme at a period of about one second is observed. This extreme is evidently attributable to the superposition of oscillations of later phases which pertain to different waves. The maxima in the spectra of P waves at epicentral distances of 1,100 - 4,000 km occur in the records of short-period seismographs at periods of approximately 1.0 - 1.6 sec. Subsequently, at greater epicentral distances they shift into the region of somewhat larger periods, on the order of 1.2 - 2.0 sec. The periods T_{left} and T_{dom} for P_n waves fluctuate from 0.3 - 0.4 sec to 1.1 - 2.2 sec, and for P waves from 0.9 - 1.2 to 1.8 - 2.8 sec.

In records of wide-band seismographs, the periods T_{sp}, T_{left}, and T_{dom} are somewhat greater than in records of short-period seismographs.

The data given above (see Figure 7 and Table 9) indicate that during underground explosions, T_{sp}, T_{left}, and T_{dom} in the spectra of the P_n and P waves change very little when Δ increases in the entire region where they are present and where they are being tracked.

Determining the steepness of the decrease in the spectra slopes. To a certain degree, the steepness of the spectra slopes at a level from 0.5 to their maximum amplitude is determined by the width of the spectral band. However, in this case the steepness of the spectra slopes is undetermined beyond the bounds of the spectrum width. At the same time, it may be necessary to know the above mentioned characteristics of the spectrum — for instance, when selecting the filtration and in a number of other cases.

The steepness of the spectrum slopes in any of its sections, in practical calculations, may be approximately characterized by exponent γ in the following expression:

$$\frac{A_m}{A_i} = \left(\frac{T_m}{T_i}\right)^{\gamma}. \qquad (7)$$

where A_m and A_i are the amplitude components of the spectrum, and T_m and T_i are the periods corresponding to them at two points of the section of the slope of the spectrum being studied. One of the components, A_m, is located near the maximum of the spectrum, and the other, A_i, is located on the slope of the spectrum.

An analogous characteristic of the spectrum was applied in [333] for spectra of dilatational and transverse waves of underground nuclear explosions carried out in Nevada in alluvium on December 3, 1961 and January 18, 1962. The dilatational and transverse waves were recorded at the Tinemakh station (Δ = 185 km) by short-period Benioff seismographs.

The values of γ were calculated at a section of the spectrum from its maximum from periods of one second to 0.5 sec. During this, corrections were not introduced into the spectra for the irregularity of the amplification of the equipment. It was established that the amplitude of the components of the spectrum of the dilatational and transverse waves, recorded at a distance of Δ = 180 km in the range of periods from one to 0.5 sec, falls off proportionally to the square of the period.

In this work, the values of γ, both for the left slope γ_{left} and for the right slope γ_{right} of the spectrum, were calculated for P_n and P waves of underground nuclear explosions, including those carried out in Nevada.

Table 10 gives the values of exponents γ_{left} and γ_{right} in formula (7) for the spectra of P_n and P waves. Since the periods of the maxima of the spectra of P_n and P waves, recorded during the given underground nuclear explosion within the range of the entire region where these waves are present, undergo very few changes as the value of Δ increases, it is possible to average the entire aggregate of data concerning γ_{left} and γ_{right} obtained in a specific range of epicentral distances.

TABLE 10. MEAN VALUES OF EXPONENT γ IN FORMULA (7), DETERMINED FROM THE SPECTRA OF UNDERGROUND NUCLEAR EXPLOSIONS CARRIED OUT IN VOLCANIC TUFFS (BY A NETWORK OF STATIONS) AND IN CRYSTALLINE ROCKS

Power of the explosion	Range of epicentral distances, km	Type of seismograph and passband of channel, sec	Type of wave	γ_{left} (T from 0.2 to 1 sec)			γ_{right} (T from 1 to 2 sec)		
				Not taking into account the frequency characteristics	Taking into account the frequency characteristics	Number of observations	Not taking into account the frequency characteristics	Taking into account the frequency characteristics	Number of observations
5-19 kt m=5.0-5.2	200-700	SVKM, Benioff, 0.1-0.7	P_n	1.53±0.16	2.2±0.16	19	1.3±0.23	-1.0±0.23	6
	1010-4000 6890-10080	SVKM, 0.1-2.5	P	1.83±0.10	2.53±0.10	22	1.16±0.12	-1.14±0.12	13
Sep 13, 1963 (200 kt) m=6.2	6500-9900	SVK, 0.2-10	P	—	2.16±0.1	7	—	-1.0±0.1	7
		SVKM, 0.1-2.5	P	—	2.28±0.15	13	—	-1.21±0.17	13

Table 10 gives the mean values of γ_{left} and γ_{right} of underground nuclear explosions carried out in Nevada, both those which have been corrected and those which have not been corrected for the irregular amplification of the equipment. For the P_n waves, the values were calculated in a range of periods from 0.2 to 1.0 sec, and γ_{right} in a range from one to two sec.

As is obvious from the data given in Table 10, the amplitude of the components of the spectrum of P waves recorded at epicentral

distances from 1,100 to 10,080 km in the range of periods from one to two sec, drops off proportionally to the period at a rate of -1.1 ± 0.12, and in the range of periods from one to 0.2 sec, proportional to the period at a rate on the order of 2.4 ± 0.10.

Somewhat smaller values of γ_{left} and γ_{right} — 1.8 ± 0.10 and 1.0 ± 0.1, respectively — were obtained for the P waves recorded at a more powerful explosion (Q = 200 kt) on September 13, 1963 on wide-band type SVK equipment with a regular amplification in the range of periods from 0.2 to 10 sec. On the other hand, this can be attributed to the fact that the spectra of waves recorded by wide-band seismographs of type SK were used in determining γ_{left} and γ_{right} during the explosion of September 13, 1963, and also to the fact that this particular explosion was considerably more powerful than the other explosions.

For P_n waves recorded in the range from 200 to 700 km, the values were $\gamma_{left} = 2.2\pm0.16$ and $\gamma_{right} = -1.3\pm0.23$. That is, they were practically the same as the corresponding values for the P waves.

Steepness of the decrease in the spectra slopes for P waves of earthquakes. Analogous calculations of γ_{left} and γ_{right} were also carried out for the P waves of more than 100 earthquakes recorded at USSR seismic stations at distances of $\Delta \geq 1{,}200$ to 10,000 km by SKM and SK seismographs. The M magnitude for most of the earthquakes amounts to 5.5 to 6.5.

The steepness of only the left slope was basically studied for P waves recorded on wide-band SK seismographs. These waves differ sharply in the nature of their records from the same waves occurring during underground and underwater nuclear explosions (considerably greater periods of oscillations, greater duration of train). At this time, the periods of the maxima of the spectra, according to which the values of γ_{left} were determined, differed somewhat for different earthquakes.

As a result of studies of more than 100 spectra of P waves from distant earthquakes, it was established that the value of γ_{left} in the range of T from 0.5 to 5-6 sec falls within the range of 2.2 to 2.5. In order to determine γ_{right} in the spectra of waves from earthquakes, it is necessary to use records of long-period seismographs of type SVKD and others.

Both γ_{left} and γ_{right} were studied for P waves of earthquakes recorded by type SKM seismographs. These waves are similar in the shape of their oscillations to P waves of underground and underwater nuclear explosions, recorded on the same seismographs. Their values are shown in Table 11.

As is clear from the data given in Table 11, for P waves of distant earthquakes, the value of γ_{left} is approximately 2.5 in the range of periods from 0.5 sec to T_{max} (approximately 2 - 2.5 sec), and the value of γ_{right} is -1.5 - 1.6 in the range from T_{max} to T = 4 sec.

Thus, the steepness of the spectra of P waves from distant earthquakes, recorded with type SKM seismographs with a narrow passband, does not differ significantly from the steepness of the slopes of the spectra of the corresponding waves from distant underground and underwater nuclear explosions.

Spectral coefficients. The differences in spectra of the same waves from explosions and from earthquakes can be characterized by the magnitude of the ratio between the amplitudes of the spectral components of different periods and the amplitude of the spectral component with the given period. This ratio corresponds with the following expression:

$$K_{im} = \lg \frac{|\bar{S}(T_i)|}{|\bar{S}(T_m)|}.$$

Here T_m is the constant value of the period, and T_i may be different. Ordinarily the values of T_m are selected close to the region of the

TABLE 11. VALUES OF γ_{left} AND γ_{right} FOR SPECTRA OF P WAVES OF DISTANT (Δ > 4,000 km), THE RECORDS OF WHICH ARE SIMILAR TO THE RECORDS OF P WAVES OF DISTANT UNDERGROUND AND UNDERWATER NUCLEAR EXPLOSIONS (SKM SEISMOGRAPHS)

Type of phenomenon	Area of epicenter and Δ, km	Stations	From T_{max} to T = 0.5 sec γ_{left}	Number of observations	From T_{max} to T = 4 sec γ_{right}	Number of observations
Earthquakes	Asia and Pacific Ocean (Δ = 4,000-10,000 km)	ESSS* and temporary	2.47±0.2 3.36±0.07	16 10	-1.64±0.2 -1.75±0.05	16 10
Underground and underwater nuclear explosions	Nevada, Pacific Ocean (Δ = 7,000 km)	"	2.14±0.2 2.80±0.34 2.65±0.16 1.67 2.67±0.01	5 5 3 5 5	-1.49±0.2 - -1.13±0.08 -1.27±0.01 -1.67±0	5 - 3 5 5
	Mean value	—	2.33±0.08	23	-1.39±0.14	18

*Translator's Note: This designates Unified Seismic Service of the USSR.

maximum of the spectrum, and those of T_i are selected in the interval from the maximum to the limiting values of the periods of the spectrum. Hereafter we shall call the values of K_{im} the "spectral coefficients." It is convenient to make use of the spectral coefficients when comparing the FSSS-spectra of the same waves recorded during explosions and during earthquakes. In cases when only the discrete values of the spectral components are determined, it is convenient to use the relationship in (8) also when comparing the spectra calculated on electronic computers.

As an example of comparing the FSSS-spectra of the dilatational waves of underground nuclear explosions and of earthquakes, recorded at the same station, Table 12 gives the values of eight of their spectral coefficients. Here, T_m = 1.6 sec is the period of the maximum of the frequency spectrum of the underground nuclear explosion, and T_i = 0.2; 0.3; 0.5; 1.6; 2.0; 2.5; 4.0; and 5.4 sec.

As is obvious from Table 12, the spectral coefficients of the P waves for explosions in the Nevada region are different from the corresponding mean values for 102 earthquakes, the foci of which were located in various regions of the world. They also differ from the spectral coefficients of near (Δ = 40 - 60 km) industrial explosions.

Special study was devoted to the possibility of dividing, by their spectral coefficients, the P waves of underground and underwater nuclear explosions and those of distant earthquakes with $m \gtrsim 5 - 5.5$, recorded by SKM seismographs with a narrow passband. The records of waves in these cases were similar to each other in the shape of their trains, and did not differ in their period of oscillations.

It is obvious from the analysis of their spectral coefficients that in this case a certain difference in the values of K_{im}, on the order of about 0.5 of the logarithmic unit in the periods of $T_i \geq 2$ sec is observed, while the root-mean-square deviation of the unit value from the mean value for the explosions and earthquakes amounted to σ = 0.15.

TABLE 12. MEAN VALUES OF SPECTRAL COEFFICIENTS K_{im}, CALCULATED FROM THE P WAVES OF SPECTRA OF DISPLACEMENTS OF DISTANT UNDERGROUND NUCLEAR EXPLOSIONS, NEAR INDUSTRIAL EXPLOSIONS, AND EARTHQUAKES.

Type of phenomenon and date	Area of epicenter	m	M	Number of phenomena	Station, Δ, km	Type of seismographs	$K_{im} = \lg \frac{\lvert \bar{S}(T) \rvert_i}{\lvert \bar{S}(T) \rvert_m}$; $T_m = 1,6$ sec							
							T_i, sec							
							0,2	0,3	0,5	1,6	2,0	2,5	4,0	5,4
Underground explosions, 1963	Nevada	5,4—6,2	—	7	ESSN*, 6500—10000	SVK	—0,60	—0,46	—0,22	0,00	+0,04	0,08	—0,22	—0,5
Earthquakes September, October, 1963	Europe Asia Africa	5,4—6,6	4,5—6,5	102	Temporary, 1300—10000	FSSS	—1,7	—1,3	0,16	0,00	0,09	0,36	0,56	0,56
Industrial explosions	Lime quarries	—	~1	20	Temporary, 60—80	FSSS	—0,8	—0,48	+0,1	0,00	—0,7	—0,1	0,01	—

*Translator's Note: This designates Unified System of Seismic Observations.

When recording the P waves of explosions and earthquakes on equipment with wider bands than the SKM equipment, the values of K_{im} can be determined for greater periods than is possible in SKM instruments. In such cases, the values of K_{im} for earthquakes would be determined quite reliably at $T_i >> 5$ sec, and it would be possible to use them for distinguishing between the records of explosions and those of earthquakes.

§ 4. Determining the Absorption Coefficient of Dilatational Seismic Waves P_n and P and Their Frequency Dependence

Thus far the absorption coefficients of dilatational seismic waves P_n and P, propagated in the Earth's mantle, have in most cases been estimated from an analysis of changes in the amplitudes of the maximum oscillations in the given waves with changes of the epicentral distance [185, 227]. This method in its contemporary form does not permit us to study with sufficient accuracy the dependence of the absorption coefficient on frequency. In [105] an attempt was made to estimate the absorption amplitude coefficients and their dependence on frequency. This attempt used methods based on a study of the changes in the amplitude spectra of the P_n and P waves recorded during underground nuclear explosions which occur as the epicentral distance Δ changes. The solution of these questions is of general geophysical and applied significance — for instance, when assessing the possibility of recording the short-period components of the P_n and P waves caused by underground nuclear explosions.

The following assumptions were taken for granted in the calculations:

1 - Attenuation of the P_n and P waves due to the absorption phenomenon is described by the factor $e^{-\alpha L}$ where α is the absorption amplitude coefficient, depending on the frequency f, and L is the distance along the seismic ray.

2 - The characteristics for which the seismograph is adjusted (the soil and the structure of the Earth's crust at all points of detection at different Δ) are assumed to be identical, and changes of the oscillation amplitudes in the P_n and P waves due to the heterogeneous structure of the upper mantle and crust are considered not to be dependent on the frequency.

3 - Absorption in the lower mantle can be characterized by a certain approximate mean value of the absorption coefficient α. This mean value does not depend on the depth. In actual fact, α is a function of the depth. However, it is not possible in this work to establish the character of this dependence due to the limited experimental data.

Under the above-mentioned assumptions, the absorption coefficient of the waves and its dependence on frequency may be determined according to the changes in wave spectra accompanying changes of the epicentral distance by the method described in [18]. This same method is applicable for determining the absorption boundary coefficient and its dependence on frequency in P_n waves.

Data used. In calculating the amplitude spectra of the P_n and P waves, use was made of seismic records of underground nuclear explosions with a power from 5 to 200 kt, carried out in the USA in Nevada, and in other areas. Only records of P_n and P waves obtained by means of vertical seismographs were used. The records of the P_n waves were obtained only by means of a single profile. For this reason, in this work the assumption was made that the horizontal Mohorovicic discontinuity occurs along the line of observations.

Determining α_{P_n} and α_P. The ratios of the amplitudes of the spectral components $A(f_k)/A(f_i)$ were determined according to the amplitude spectra of the P_n waves, observed during explosions within the range of Δ = 200 - 740 km carried out under identical conditions, and also according to the spectra of the P waves observed in the range

of Δ = 1,968 - 9,500 km. For explosions of a power up to 40 kt, the value f_k = 1 hertz was adopted; for explosions with a power of 200 kt, a value of 0.62 hertz was adopted. The following values of f_i were adopted: 3.3, 2.5, 1.67, 1.25, 0.83, 0.71, 0.62, 0.55, 0.50, 0.40, and 0.33 hertz.

The angular coefficients of the lines approximating these experimental relationships were determined according to the dependence of $\ln[A(f_k)/A(f_i)]$ on L (examples of them are shown in Figures 13 and 14) in the above-mentioned ranges of Δ by the least square method.

The angular coefficients of these lines represent the differences in the absorption coefficients $\Delta\alpha_{P_n}$ and $\Delta\alpha_P$ for the two frequencies f_k and f_i. Their values are shown in Figure 13 and 14 by small circles. The values of $\Delta\alpha_{P_n}$ and $\Delta\alpha_P$, in their turn, were approximated by the least square method by means of lines (the broken lines in Figures 15 and 16); the angular coefficients of these lines characterize the dependence of the difference in the absorption coefficients $\Delta\alpha(f)$ on frequency. The dependence on frequency of the absorption coefficients themselves $\alpha_{P_n}(f)$ and $\alpha_P(f)$ was obtained by transposing the lines $\Delta\alpha(f)$ to the coordinate origin (shown in Figures 15 and 16 by the solid lines). The dependence of $\Delta\alpha$ on f for the explosion of September 13, 1963, is shown in Figure 17.

The equations of the approximating lines have the following characteristics: for P_n waves of explosions $\alpha_{P_n} = (1.9\pm0.12)\cdot10^{-3}$ f km^{-1}; for P waves $\alpha_P = (2.8\pm0.27) \times 10^{-4}$ f km^{-1}; and for the explosion of September 13,1963, $\alpha_P = 1.84\cdot10^{-4}$ f km^{-1}.

Here the root-mean-square deviations of the coefficients α are given by the $\pm$ sign.

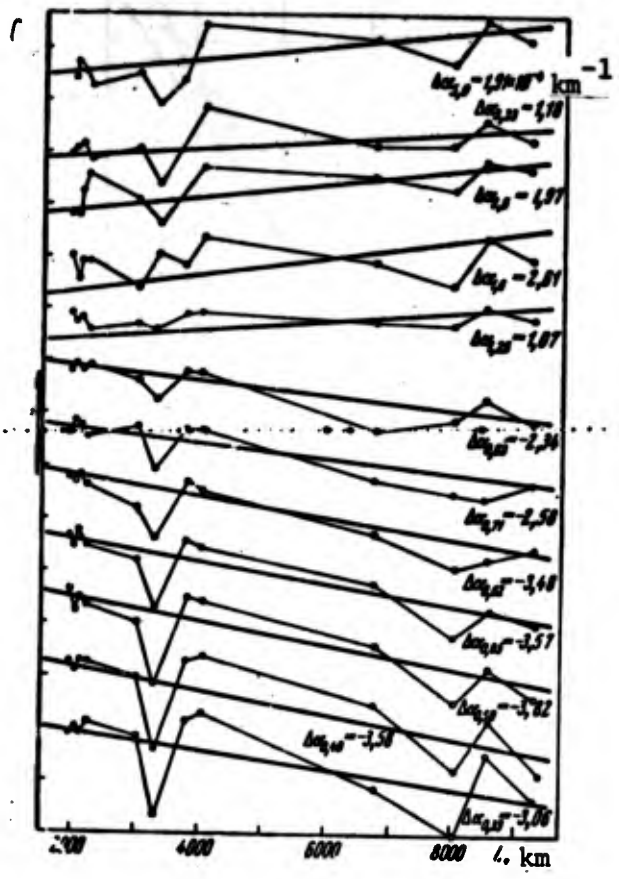

Figure 13. Relationship of the ratio $\ln[A(f_{0.62})/A(f_i)]$ to L in the spectra of P waves of an underground explosion. The inclinations of the lines, approximating the observed values, characterize the differences of the absorption coefficients at frequencies of f = 0.62 hertz and f_i.

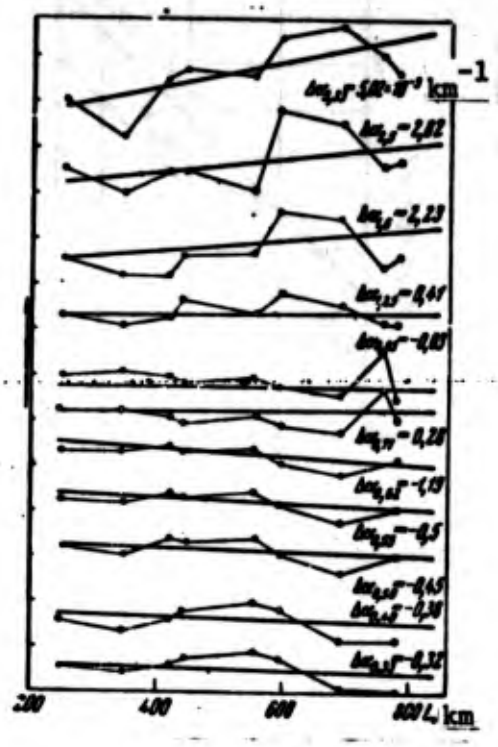

Figure 14. Relationship of the ratio $\ln[A(f_{0.62})/A(f_i)]$ to L in the spectra of P_n waves of an underground explosion.

Discussion of the results. Figure 18 shows the values of the absorption coefficients α_{P_n} and α_P found in this work by spectral methods. This same figure contains the absorption coefficients of dilatational waves for various crystalline and metamorphic rocks occuring in the Earth's crust. These values were determined by amplitude methods in the range of frequencies from 1 to 50-60 hertz. The data were obtained from [18]. As is clear from Figure 18, line I in a wide range of frequencies, from 0.1 to 50-60 hertz, approximates well enough the corresponding experimental values of the absorption coefficients in the rocks of the Earth's crust and of the upper mantle. Line II proceeds parallel to

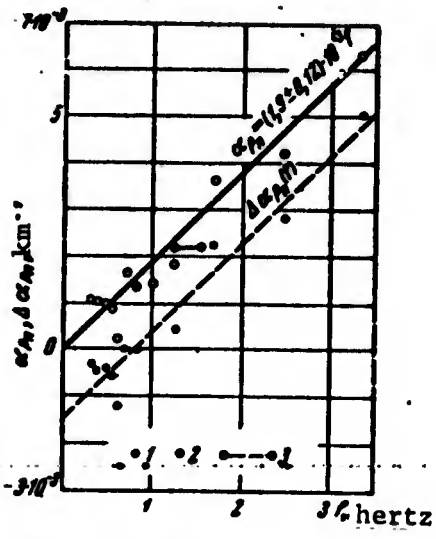

Figure 15. Frequency-dependence of the difference in the absorption coefficients $\Delta\alpha_{P_n}$ and the absorption coefficients α_{P_n} of P_n waves of underground explosions. 1 - experimental relationships of $\Delta\alpha_{P_n}$; 2 - experimental relationships of α_{P_n}; 3 - boundaries of α_{P_n} values determined from the amplitude curves in work [100].

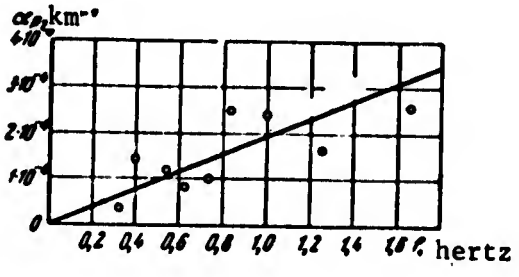

Figure 17. Frequency-dependence of absorption coefficient α_P of P waves recorded in a range of Δ from 2,745 to 9,500 km, during a powerful underground explosion in Nevada. The experimental values of α_P are indicated by dots.

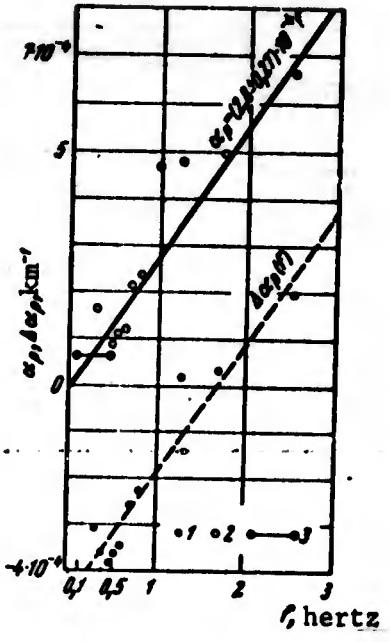

Figure 16. Frequency-dependence of the difference in the absorption coefficients $\Delta\alpha_P$ and the absorption coefficients α_P of P waves recorded in the range of Δ from 1,970 to 10,080 km during an underground explosion 1 - experimental relationships of $\Delta\alpha_P$; 2 - experimental values of α_P; 3 - boundaries of T_P values, for which $\alpha_P = 6 \cdot 10^{-5}$ km^{-1}, according to data in [45]

I, but approximately one order of magnitude below it. This is connected with the smaller values of the absorption coefficients in the lower mantle.

Thus, the dependence of the experimental values of α_{P_n} and α_P on frequency — found both by studying the changes in the ratios of the spectral components in the spectra of the P_n and P waves

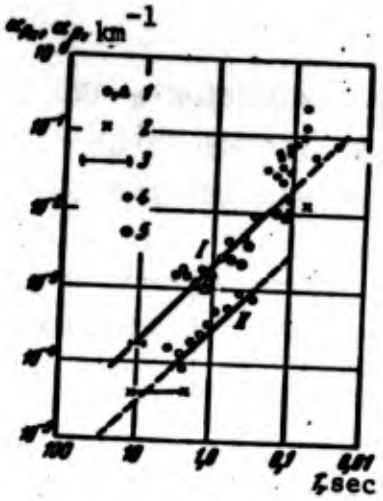

Figure 18. Consolidated data concerning the frequency-dependence of the absorption coefficients of dilatational waves, propagated: I. in the Earth's crust and the upper mantle; II. in the lower mantle. Experimental data are plotted: 1. according to the author's data; 2. according to [100]; 3. according to [84]; 4. according to [16]; 5. according to [45].

accompanying changes in the epicentral distance, and also by amplitude methods — can, in a definite range of periods, more or less approximate the above-mentioned linear relationships.

The fourth column in Table 13 gives the absorption decrement θ, found in this work by spectral methods, while the sixth column gives its values determined according tc the decrease in amplitudes, together with the epicentral distance. The latter values were taken from the data in works [45, 100, 132]. The records used in [100] for determining θ for explosions were the same as those used in this work. The fifth and seventh columns give the corresponding values of the Q-factor, $Q = \pi/\theta$, where θ is the absorption decrement.

It is obvious from a comparison of θ for the P_n waves, determined by various methods from records obtained on single-type equipment, that these values are close to each other for the same regions of the mantle; the values of Q are also correspondingly close to each other. In works [243, 244, 326] smaller values of θ, and correspondingly greater values of Q for P_n waves, were obtained when equipment with higher frequencies was used.

It should be emphasized that the values of θ and Q, found with the P_n waves, characterize the absorbing properties of a comparatively small layer of the mantle close to its upper boundary.

TABLE 13. VALUES OF PARAMETERS OF ABSORPTION δ AND Q FOR ROCKS IN THE EARTH'S CRUST AND IN THE UPPER AND LOWER MANTLE, DETERMINED BY SPECTRAL AND AMPLITUDE METHODS.

Regions of the Earth	Type of wave	Period, sec	Values of the decrements obtained in this work		Values of the decrements determined by other means		Literature
			δ	Q	δ	Q	
Earth's crust	P	0,3	—	—	0,010	200	[327]
	P	0,1—1,0	—	—	0,017	185	[132]
	P^*	0,5—0,8	—	—	0,11	286	[99]
	S^*	1,5—1,8	—	—	0,012—0,014	260—224	[99]
Upper mantle (at M boundary)	P_n	0,3	0,015	210	0,0055	570	[304]
	P_n	0,6—0,8	0,015	210	0,012	260	[99, 100]
	P_n	0,3—3,0	0,015	210	—	—	
Upper mantle to depths of about 600 km	$sScS$	25	—	—	0,017—0,02	185—151	[139, 140]
	P	8—12	—	—	0,012	260	[84, 134]
Lower mantle to depths of about 2,700 km	P	1,0	0,0029	1100			
	P	2,0	0,0029	1100	0,0013	2600	[45, 227]
	P	4,0	0,0029	1100	0,0023	1300	[45, 227]
	P	12,0	0,0029	1100	0,0080	400	[45, 227]
For depth intervals of 1,450-2,870 km	P	1,6	0,0022	1650			
To a depth of 2,900 km	ScS	25	—	—	0,0022	1430	[139]

When examining the absorption coefficients and decrements δ of the P waves propagated in various regions of the mantle, one must keep in mind the following circumstances. As the velocities undergo changes in the mantle together with increasing depth, the P waves, with the increase of Δ, proceed through successively deeper and deeper parts of the mantle. Thus, for example, when observing P waves at an epicentral distance of 20°, the wave attains depths of about 350 km. That is, the path of the wave proceeds entirely within the upper mantle, in which the mean velocity of the P waves amounts to about 8.5 km/sec. At Δ = 90° the P wave penetrates to depths of about 2,700 km, and the mean velocity along its path amounts to about 10.5 km/sec.

The absorbing properties in the mantle, as follows from the data in Table 13, decrease with increase in depth — that is, with the increase in velocity. This is indicated, among other things, by the different values of the coefficients and decrements of absorption for the P_n, P_a, and P waves, and also by the differences in Q when it is determined according to observations only in the range of L from 6,841 to 9,500 km. Therefore, the values found in this work of the absorption coefficients for the P waves ought to be regarded as somewhat approximate, average values. In order to estimate the absorption coefficients in definite ranges of depths of the mantle, it is necessary to use simultaneously the spectra of waves of various types: P, PP, PcP, PKP, and others.

CONCLUSIONS

1. The method of calculating, on digital electronic computers, the amplitude spectra of seismic waves caused by explosions and earthquakes was tested on an immense amount of material.

2. It was shown that the error in calculating the spectra in this case, when the records were converted into numerical data at different times and by means of different computers, does not exceed $\pm 5\%$.

3. It was established that, when the spectra are calculated on electronic computers, it is necessary to print out about 40 - 50 values of the amplitude for one hertz.

4. If the spectra are plotted immediately from the data supplied by the computer, they may be broken up by numerous supplementary extremes, evidently as a result of the interference character of the record, of mistakes when converting the records into numerical data, and for a number of other causes. This makes it difficult to analyze the data and to carry out quantitative calculations. It is also difficult to compare the spectra both of the same waves observed

at different epicentral distances and those of different waves, observed at a definite epicentral distance.

5. To eliminate this brokenness of the spectra, methods of smoothing them out were proposed, by averaging out 9, 5, and 3 successive values of amplitudes without overlapping, and at 9 and 5 points with overlapping.

The most satisfactory method of averaging the broken-up spectra is that of averaging five successive points with overlapping.

6. In order to compare the spectra of waves recorded by a single type of equipment, it is possible to use spectra which have not been corrected for irregular magnification of the receiving channel.

In order to compare the spectra of waves recorded on equipment with different characteristics, it is necessary either to reduce them to uniform characteristics, or to reduce them to the characteristics of a single type of equipment. However, if an attempt is made to introduce corrections for irregular frequency characteristics of the equipment far beyond the range of its passband, this may lead to considerable errors in determining the spectra.

7. It was shown that spectra obtained on FSSS equipment were practically identical with those calculated on electronic computers (within the range of the spectrum width).

8. When comparing the spectra of waves, when selecting the passband of the equipment, and in a number of other cases, it is advisable to use the basic parameters characterizing the spectrum: the period of the spectrum maximum, the steepness of the drop of its slopes, and the relationship of the spectra of separate waves or of the entire recording.

In a number of cases it is advisable also to characterize the spectrum by boundary frequencies taken on a level of 0.5 from the amplitude of the spectrum maximum, and also by the spectral coefficients.

9. From comparisons of the dominant periods T_{dom} of quasi-sinusoidal oscillations in the P waves recorded during underground nuclear explosions, and of the corresponding periods T_{sp} of the amplitude spectra maxima of these waves, it was established that the values of T_{dom} and T_{sp} were identical, within an accuracy of measurement errors amounting to about $\pm 10\%$. When determining mass numbers of periods in body P waves and in other types of waves, one may with equal justification use either the method of measuring the dominant periods on the seismogram, or that of determining the periods of the amplitude spectrum maximum of the train for P waves, P_n waves, or other waves.

10. It was shown that it is possible to determine, from the spectra of the P_n and P waves, the absorption coefficients α and their dependence on frequency in the Earth's mantle. The dependence relationships were shown for P_n waves as $\alpha_{P_n} = 1.9 \cdot 10^{-3} f\ km^{-1}$, and for P waves as $\alpha_P = 2.8 \cdot 10^{-4} f\ km^{-1}$.

11. A brief examination of the tasks to be solved by analyzing the spectra of seismic waves confirms the fact that it is possible to obtain quantitative information about the character of seismic oscillations from a study of the spectra. This indicates that the methods of spectral analysis must be used in elaborating and providing a basis for the seismic method of detecting and identifying nuclear explosions.

FOOTNOTES

Footnote (1) appears on page 50. See also: M.A. Gostev. Chastotno-vremennoy analiz seysmicheskikh kolebaniy apparaturoy CHISS (Time-and-frequency analysis of seismic oscillations by FSSS equipment). Candidates dissertation. IPE, USSR Academy of Sciences, 1965.

CHAPTER III

METHODS USED IN RECORDING NUCLEAR EXPLOSIONS TO INCREASE THE EFFECTIVE SENSITIVITY OF SEISMIC EQUIPMENT

Microseismic oscillations are always present in seismograms to one degree or another. They have an extremely wide spectrum, from hundredths of a second to tens or hundreds of seconds. However, their intensities are unevenly distributed in the spectrum. Depending on their period and intensity, microseisms usually are classified provisionally into three groups: (1) microseisms of the first order with periods on the order of 2-3 to 6-10 sec (in a number of works [26-30, 264 etc.] they are also called 4 - 6-second microseisms); (2) microseisms of the second order or long-period microseisms with T > 12 - 15 sec; (3) short-period microseisms with periods from hundredths of one second to 2 - 3 seconds.

In most cases, the sources of excitation of these types of microseisms are different. Specifically, microseisms of the first order are attributed to cyclonic activity over water areas. Microseisms of the second order and short-period ones can be caused by meteorological factors over continents and in the immediate area of

the detecting station, activity of industrial plants, and other factors.

Microseisms make it difficult, and in some cases impossible, to distinguish against their background useful seismic signals of low intensities, such as those of body waves with amplitudes of several millimicrons and surface waves with amplitudes of several tens of millimicrons, caused by explosions and earthquakes. The presence of microseisms complicates the application of criteria for distinguishing seismic phenomena.

The above-mentioned difficulties will remain even when wide-band magnetic recording is applied. The task is particularly complicated when the periods of the signal are close to those of the interference. Therefore, both in oscillographic and in magnetic recording efforts must be made in the very process of recording to lower the interference level and to raise the ratio of the amplitude of the useful signal to the amplitude of the interference — that is, to raise the effective sensitivity of the receiving equipment. This can usually be accomplished successfully, primarily by selecting the most favorable conditions for installing the seismographs, both in the sense of a low level of microseisms, and in the sense of the maximum amplitude of the useful signal.

The following measures which guarantee further suppression of interference amount to the application of instruments, or the combination of instruments with a methodical procedure: frequency selection, that is, filtration of oscillations, selection based on the direction of arrival of the oscillations by means of grouping, application of correlative and statistical methods of suppressing interference and of separating out the useful signal against the interference background, and a number of other methods.

If one is to select correctly the most favorable conditions for installing seismographs and for applying the appropriate means of

suppressing interference, it is necessary to know the spectral composition of the useful signal and of the interference, and also the relationship of the spectrum and the intensity of the interference with such factors as the character of the geological structure in the area of the station, the soil conditions at the point of detection, the geographical situation of the area, particularly how close it is to oceans, inland seas, and lakes, to industrial centers, to roads with heavy traffic, and other factors.

Many works have been devoted to the study of microseisms [26-30, 49, 112, 127, 157, 159, 201, 336 etc.]. However, in most cases, the microseisms were studied in regions where they had a considerable intensity. In fact, the microseisms which were studied were predominantly of the first order. Short-period microseisms have been studied only to a limited extent. Long-period microseisms with periods greater than 12 - 15 seconds have hardly been studied.

At the same time, periods of about 1 second and periods higher than 12 - 15 seconds are of the greatest interest in recording, respectively, dilatational waves of underground and underwater explosions, and surface waves for all types of explosions.

For purposes of detection and identification, the stations are located in regions with the minimum interference level (see §5 of this chapter). Unfortunately, microseisms have been studied incompletely for such regions, mainly because it is necessary to record them on special, highly sensitive equipment with a magnification from several tens of thousands — when recording microseisms of the first order — to several tens of millions when recording short-period microseisms. Let us recall that the magnification of wide-band and long-period equipment in the stations of the USSR usually does not exceed 1,000, and that of short-period equipment does not exceed 30 - 100 thousand (see Chapter II).

As attempts were being made for increasing the effective sensitivity of the equipment for recording seismic waves caused by

explosions, it became necessary to initiate supplementary research about microseisms. The purpose of this research was to study more thoroughly their spectral composition in a broad range of periods, from hundredths of one second to tens of seconds, and also the statistical characteristics of the spatial structure of the field of microseisms, including the energy characteristics of the process as a whole.

Below information is given on the spectral composition of interference and its level in the stations of the USSR. These stations are arbitrarily classified as quiet, medium, and noisy stations (see §2 of this chapter). The interference spectra are compared with the spectra of useful signals, and recommendations are given about selecting the most favorable station locations and the methods of installing seismographs. The measures for suppressing interference by instrumental and methodical means are also briefly examined.

The above-mentioned tasks are examined from the point of view of optimum recording of useful signals — that is, of obtaining the greatest ratio of the signal amplitude to the interference amplitude. The recommendations outlined below about interference suppression are applicable also in recording seismic waves caused by earthquakes.

The experimental data about the spectral composition and the spatial structure of the field of microseisms were obtained from numerous observations carried out in different regions of the USSR in the period from 1954 to 1967 [25-30, 101 etc.].

§ 1. General Characteristics of Microseisms

In the following, we briefly examine questions connected with the spectral composition and the intensity of microseisms in a broad range of periods, from hundredths of one second to several tens of seconds. Their intensity depends on the seismogeological structure of the area of detection and its geographical position. The statistical characteristics of the process are given for short-period microseisms and microseisms of the first order.

Microseisms of the first order. Microseisms of the first order constitute the basic interference in recording seismic oscillations on wide-band equipment, for instance that of type SK, SKD, etc. B. B. Golitsyn [40] started these studies. These microseisms are most intensive during periods of elevated cyclonic activity over water areas (during microseismic storms), when their amplitudes reach tens of microns in coastal stations, and several microns in inland continental stations. They are trains of quasi-sinusoidal oscillations following each other uninterruptedly (see Figure 19). Because of the motion of particles from the medium in them and because of their propagation velocity, they were until quite recently related to surface waves, chiefly those of the Rayleigh type. The propagation of microseisms of the first order over very large distances is assumed to be connected with the presence of wave guides in the Earth's mantle and crust.

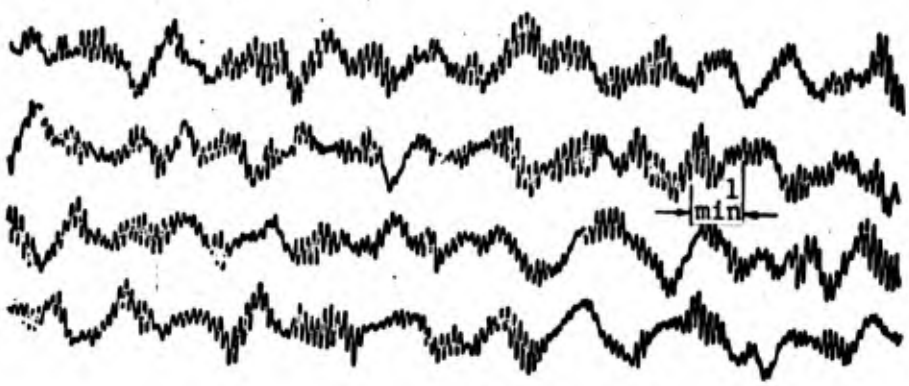

Figure 19. Example of a record by a SGKD seismograph of long-period microseisms with T ≈ 100 - 200 sec and of microseisms of the first order with T = 6 seconds. The seismograph was installed in metamorphic rocks (Kazakhstan) in a standard underground housing

The period of microseisms depends on the distance of the detecting stations from the sources of the microseisms. In coastal regions, the frequency spectrum maximum of microseisms falls in the interval of about 1.5 - 2.5 seconds, and in regions at a distance of 1,000 - 1,500 km or more from the coast — in the interval of 4 - 6 seconds.

In a number of areas, the periods of microseisms of the first order can reach 10 - 12 seconds. For example, the periods of

microseisms reached 10 - 12 seconds — depending on the distance of the area of the cyclonic activity — at the Mirnyy station in the Antarctic [127]. Recently, regular microseisms with periods of about 20 seconds, connected with cyclonic activity over the North Atlantic, have been noted.

The propagation phase velocity of microseisms of the first order depends on their periods, and also to a certain degree on the seismogeological structure along the propagation path and in the area of observations. Generally, it amounts to from 3 to 4 km/sec, according to data determined at three stations [112]. Records of 4 - 6-second microseisms were recently obtained in an inland continental area in a group of stations located along two intersecting contours, each with a length of about 50 km. The records of the microseisms were processed by correlation analysis methods [26]. It was established that the microseisms in a range of periods from several tenths of one second to 6 - 8 seconds can be regarded as a superposition of a regular wave component, propagated at great distances, and an irregular component, traced at short distances. The irregular component is apparently determined by short-period oscillations. The energy of the wave component amounts to up to 50% of the total energy of the process. The remaining part is assigned to the irregular background, the nature of which is not yet established. The composition of the microseisms, in addition to the wave component with a velocity of 3 - 4 km/sec, includes a vertical component with a velocity of 10 - 20 km/sec, that is, a component propagated with the velocity of dilatational waves through deep layers of the mantle. Its energy amounts to 0.1 to 0.4 of the total energy of the process.

Long-period microseisms. Little study has thus far been made of the long-period microseisms with periods from 10 - 15 to 200-300 seconds, which are present in the records of long-period seismographs, and sometimes in those of wide-band seismographs (Figures 19, 20).

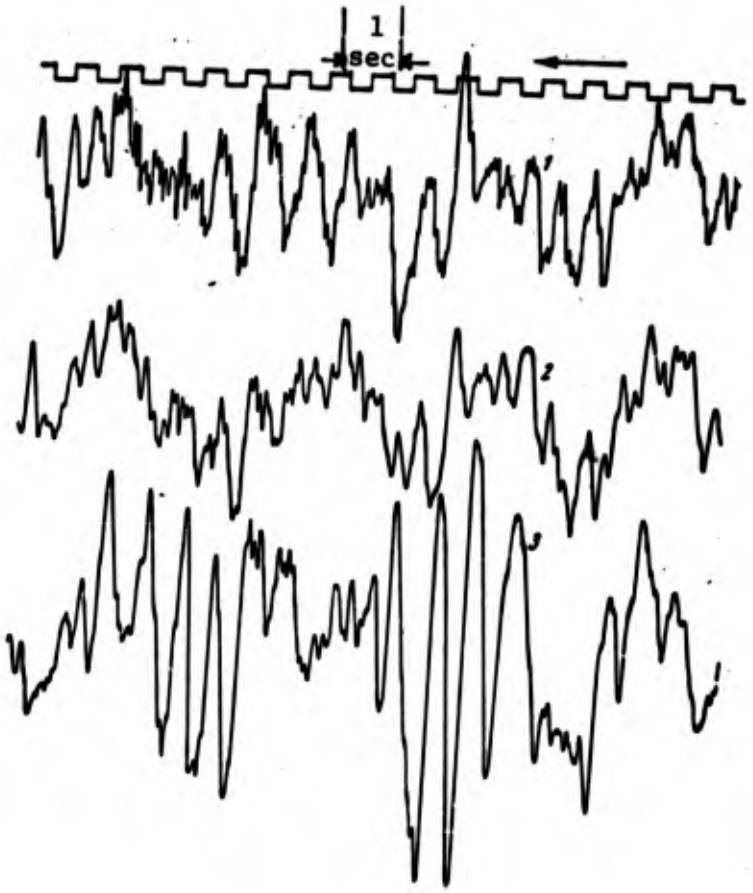

Figure 20. Example of a record of short-period microseisms and microseisms of the first order by vertical seismographs with amplification of about $3 \cdot 10^6$. The seismographs were installed in granite on a platform:

1 - in an adit; 2 - in a hole 50 meters deep;
3 - in a hole 1 meter deep.

Their appearance in the records of sensitive long-period seismographs is not noticeable when the seismographs have been installed under poor conditions, chiefly when the underground instruments have not been buried deep enough, or when the underground instruments have been located in porous sedimentary rock or in crumbling crystalline rock. In many cases, long-period interference is caused by design defects of the seismographs or the galvanometers. For example, because of unbalance of the seismometer pendulum on both sides of

its axis of rotation, a pendulum floating effect is observed when there are changes in the atmospheric pressure. Interference may be connected with temperature instability of the pendulum suspension springs, poor hermetic sealing of the instruments, absence of thermostatic control of the instruments, and a variety of other causes.

Interference predicated on design defects of the instruments can be eliminated or considerably reduced by introducing pertinent improvements in the design of the instruments themselves.

It is considerably more difficult to eliminate interference due to poor installation of long-period seismographs. The excitation mechanism of long-period interference is apparently connected with meteorological factors, such as changes in temperature, atmospheric pressure, and humidity of the environment, that is, factors which operate simultaneously over an immense area. Under their influence, the surface of the soil goes through slow seasonal inclinations or oscillatory motions [136], which are transmitted to the entire thick upper layer of rock. The slow motions which have been observed are complicated by faster oscillations, which appear in the records of long-period seismographs as quasi-sinusoidal oscillations with periods from 12-20 to 200-300 seconds or more.

The interference is strongest when the seismographs are installed in shallow instrument housings built in sedimentary rocks. In stations in the USSR, it is most intense in the winter and least intense in the summer. For instance, it has the shortest periods in the European part of the USSR during the winter, on the order of 15 - 20 seconds (Figure 20). During the summer it has the longest periods, on the order of 100 - 300 seconds or more. Besides, a marked dependence of the level of the microseisms on the time of day is observed in the winter.

The interference which is being examined is of low intensity when the seismographs are installed in relatively deep (with a depth of up to 20 m) underground housings sunk in solid bedrock of

crystalline and metamorphic rocks. This is demonstrated by the many years of experience in operation of long-period type SKD seismographs installed in shafts with a depth of 20 m, sunk in crystalline rock, and also by experience in work with seismographs installed in adits sunk at a considerable depth in crystalline rock.

The long-period microseisms connected with meteorological factors create great difficulties in recording seismic oscillations by long-period seismographs with a high amplification on the order of 10,000 - 20,000. Lowering the level of this interference is one of the important tasks in recording relatively low-intensity surface waves caused by nuclear explosions, including underground explosions.

Short-period microseisms. These microseisms can provisionally be divided into two groups: (1) microseisms with periods of 0.1 - 1.5 seconds, observed during calm, windless weather (Figure 21), and (2) sporadically appearing irregular microseismic oscillations with periods of 0.01 - 1.5 seconds, conditioned by the activity of local sources, such as wind (Figure 22), the movement of traffic, and other sources.

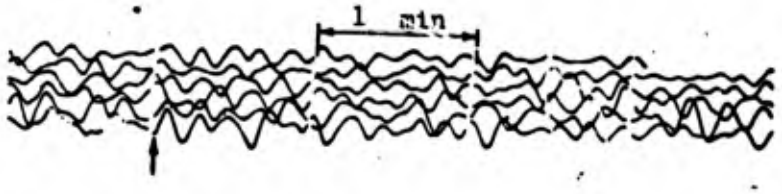

Figure 21. Example of a record of long-period microseisms made by an SVK seismograph installed on a concrete pedestal sunk to a depth of 1 meter into sedimentary rocks. The microseisms are connected with the temperature instability of the rocks. (Moscow region, March)

Special experiments, carried out in a number of areas composed of crystalline rocks (granites or basalts), showed that the microseisms with periods of about 0.5 - 1.5 seconds, observed during calm weather, consist of the superposition of regular, quasi-sinusoidal

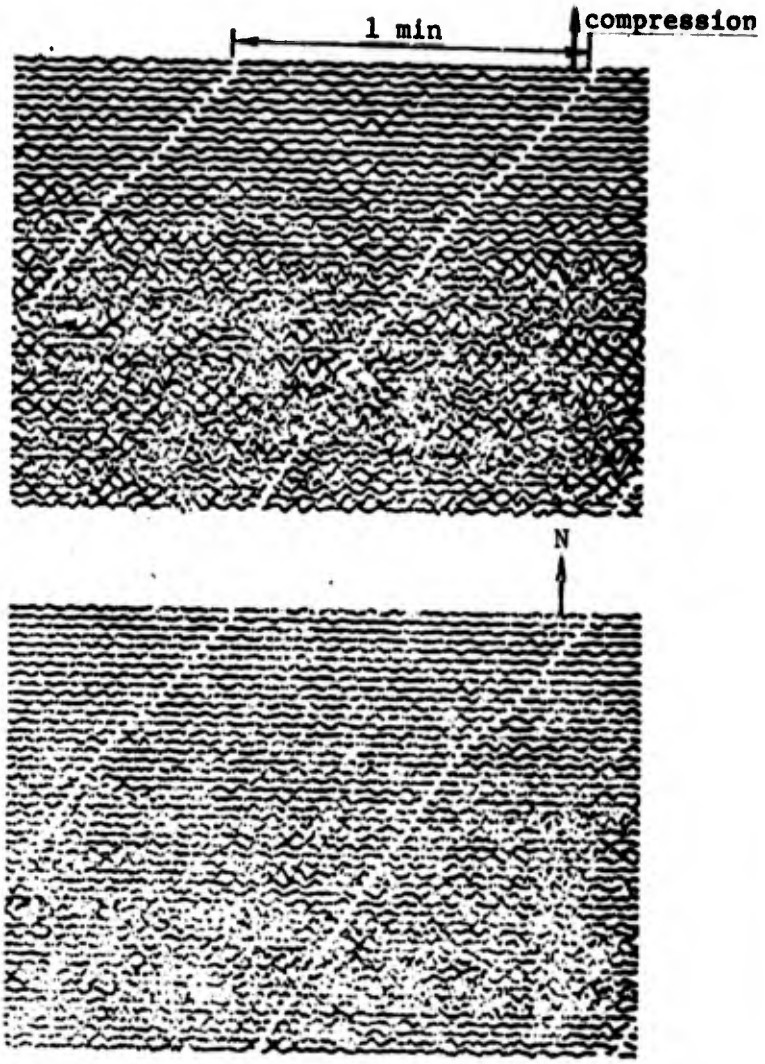

Figure 22. Example of a record of irregular short-period microseisms, caused by the influence of a stong wind at the observation point. SVK and SGK seismographs are installed in a shaft 20 meters deep sunk in granite (Khabarovsk region)

oscillations, evidently of Rayleigh and dilatational waves, and an irregular background. (In these observations, the microseisms with longer periods were filtered out during the recording process.) This indicates that the short-period microseisms evidently are produced both by distant sources (the regular wave component) and by local sources located nearby (the irregular component). The propagation velocity of the wave component in observations in crystalline

rocks was on the order of 2.5 - 4 km/sec. However, in this group of microseisms, a component propagated with the velocities of dilatational waves through the deep layers of the mantle was also distinguished. Up to 50% of all the energy of the process recorded under the above-mentioned conditions is ascribed to the above-mentioned wave components.

The correlation of the irregular microseisms with periods of about one second produced by local sources is disturbed at distances of about 600 - 1,000 m between the seismographs.

Microseisms with periods near one second constitute the basic interference in the detection and identification of seismic body waves caused by underground and underwater nuclear explosions, and also in the recording of dilatational waves in contact and atmospheric nuclear explosions. However, the intensity of short-period microseisms with periods of 0.5 - 1.0 sec is much less than the intensity of microseisms with periods of 4 - 6 seconds. In very quiet stations, located far away from the shores of open expanses of water, it can be as low as 0.1 - 0.5 millimicrons.

The recently obtained new data about the statistical properties and the spatial structure of the field of microseisms and their propagation velocities are extremely important when making use of methods for increasing the effective sensitivity of the seismic equipment, such as filtration, grouping of seismographs, correlation methods, including the method of accumulation, and others [31-35 etc.].

§ 2. Spectral Composition and Intensity of Microseisms

The averaged experimental values given in Table 14 (see also Figure 23) give an idea about the approximate average spectral composition and intensity of microseisms for the inland continental areas of the USSR with different geological structures, located a great distance from big lakes and inland seas. The data in Table 14

TABLE 14. LEVEL OF MICROSEISMIC INTERFERENCE FOR QUIET, MEDIUM, AND NOISY SEISMIC STATIONS IN THE TERRITORY OF THE USSR.

Period, sec	Displacement, millimicrons			A_{med}/A_{qu}	A_{noi}/A_{qu}
	Quiet station A_{qu}	Medium station A_{med}	Noisy station A_{noi}		
30-50	10(20)	50(100)	-	5	-
12-15	10	80	1000	8	100
5-6	30	300	2500	10	83
2	2	15	150	8	10
1	0.1-1.0	3.5	60	7	120
0.5	0.1	1.5	10	15	100
0.1	0.05	0.5	5	10	200

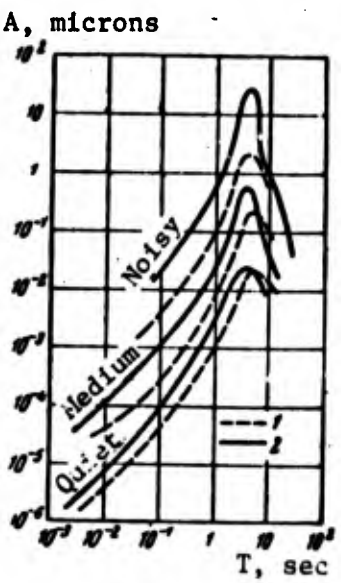

Figure 23. Level of microseismic noises in quiet, medium, and noisy stations of the USSR (1) and the USA (according to [337]) (2)

were obtained as a result of many years of seismic observations carried out in various areas of the USSR at more than 50 stations. Processing was carried out by direct measurement of the level of the microseisms in seismograms obtained by vertical instruments

adjusted to various periods [101].

It must be mentioned that the data given characterize the minimum amplitudes of the microseisms in the areas in question, inasmuch as in the observations, a choice was always made of the relatively quietest points and the most favorable conditions for installing the seismographs in shafts, adits, pits, wells, cellars, caves, and other natural shelters and man-made structures.

Depending on the level of the microseisms, stations and areas where stations are located can be classified as quiet, medium, and noisy. The demarcations are extremely provisional, and are based on the following three factors, which are connected to each other in many cases: the intensity of the microseisms, the geographic position of the area, and its geological structure.

Among the quiet areas we provisionally include those in which the level of microseisms with periods of one second amounts to about 0.1 - 1.0 millimicron. The medium areas are those where it amounts to several millimicrons, and the noisy areas are those where it amounts to several tens of millimicrons. The quiet areas are usually located inland on continents at least at a distance of 500 - 1,000 km from the open coasts of oceans and seas. They consist of crystalline or metamorphic rocks. Also, areas with permafrost are included among the quiet areas in the northeast of the USSR, including also the coastal areas lined with ice which goes out far away from the shore. Among the medium-noise areas are included the internal continental areas with outcroppings or near-surface deposits of solid bedrock of sedimentary or sedimentary-metamorphic rocks. The noisy areas include the open coastal regions with massive, thick layers of porous sedimentary deposits.

It is interesting to note that, in all three types of continental stations, the maximum interference level in the records of type SK seismographs appears at approximately the same periods: around 5 - 6 seconds.

The largest level of microseisms in the entire frequency range is observed when the seismographs are installed on the surface of porous sedimentary rocks. When the seismographs are installed on solid crystalline bedrocks, the level of microseismic interference usually is 50 - 100 times lower in comparison with that when they are installed on porous sedimentation in the same area (Figure 24).

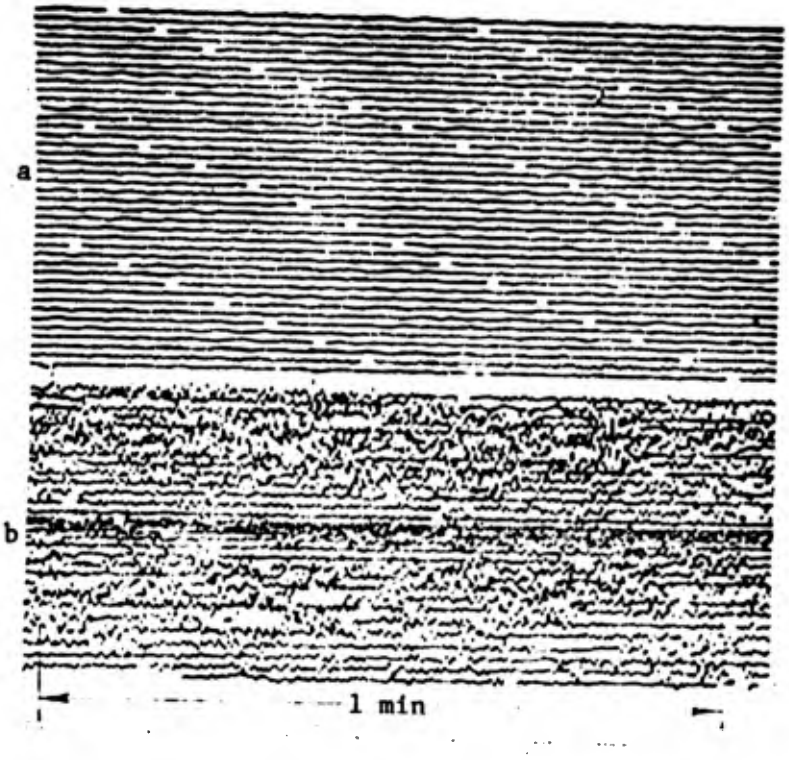

Figure 24. Examples of records of short-period microseisms by USF seismographs with amplification of 10^5, installed in the same place

a - in crystalline rocks; b - in a layer of alluvium

A low interference level is observed in the central part of the Eurasian continent, which is composed of crystalline or metamorphic rocks, and also in the permafrost regions on the northern coast of the Asiatic part of the USSR.

Thus, as follows from an analysis of the data given, the highest level is that of microseisms of the first order with periods of

4 - 6 seconds. In quiet stations, their amplitude amounts to tenths of microns, and in periods of microseismic storms, to several microns. As the period is decreased to 1 second, the amplitude of the microseisms declines regularly; with further decrease of the period, the decline proceeds more slowly than in the range of 4 - 1 second. In quiet stations, the amplitude of microseisms with periods ranging from 0.1 to 1 second amounts to about 0.01 - 1.0 millimicrons.

Results of computer calculations of microseism spectra. The amplitude spectra of microseisms in periods ranging from 1 to 14-15 seconds were studied from the records of wide-band seismographs of type SK, adjusted to the standard constants. In the overwhelming majority of cases, records of vertical seismographs were analyzed. However, special studies revealed that the amplitude spectra of microseisms were identical when calculated for the same time intervals from the records of both vertical and horizontal siesmographs having the same characteristics and installed at the same point.

Highly sensitive equipment with a narrow passband was used to study spectra in the range of periods less than 1 second. The length of the record section to be analyzed was selected so that the number of the oscillations to be analyzed would not be less than 10 - 20.

Figure 25, a shows examples of spectra of microseisms of the first order, recorded at the stations of Kulyab, Frunze, and Dushanbe with type SK seismographs.

Table 15 shows examples of information about the duration of the sections analyzed, the periods of the maxima of the spectra, and their boundary frequencies, taken at a level of 0.5 of the maximum amplitude.

Figure 25, b shows the average (in time) spectra of short-period microseisms calculated for periods ranging from 2 to 0.2 seconds for a station located on granite outcroppings, and for the quiet stations of the USSR.

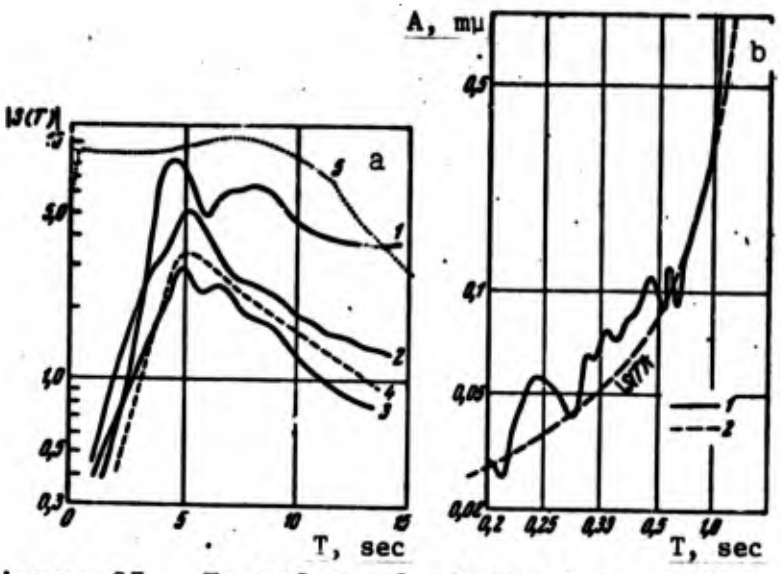

Figure 25. Examples of microseism spectra:

a - of the first order, recorded by SVK seismographs at stations in Central Asia at the same time; 1 - Kulyab; 2 - Frunze; 3 - Dushanbe; 4 - averaged spectrum for the quiet stations of the USSR; 5 - amplitude-frequency characteristics of the SVK seismograph; b - short-period microseisms; 1 - recorded in a station located on granite outcroppings; 2 - average spectrum for quiet stations of the USSR.

TABLE 15. CHARACTERISTICS OF THE AMPLITUDE SPECTRA OF MICROSEISMS FOR SEVERAL STATIONS OF THE USSR, OBTAINED FROM RECORDS OF WIDE-BAND TYPE SVK SEISMOGRAPHS.

Characteristics of the spectrum	Stations		
	Kulyab	Frunze	Dushanbe
Duration of the analyzed portion of the record, sec	60	114	122
Mean values of T, measured on the record, sec	5.8	5.0	5.0
Extreme values of T, measured on the record, sec	4-6	4-4.5	4-6
Period of spectrum maximum T_{sp}, sec	6	5.2	5.0
Boundary periods of T, sec, at a level 0.5 of the spectrum maximum amplitude	4.0-9.0	3.[illegible]-7.0	3.5-9.5

An examination of the spectra in Figure 25, a and b reveals that the shape of the microseism spectra recorded at different inland continental stations at periods ranging from 0.2 to 14-15 seconds is close to the shape of the line of the mean spectral distribution obtained by direct measurements in seismograms (see line 4 in Figure 25, a and line 2 in Figure 25, b).

It was established from the analysis of numerous data that the width of the spectral band, taken at the level of 0.5 from the value of the maximum, falls within the range of boundary frequencies from 3-4 to 7-9 seconds for the inland continental stations of the USSR. A sharper intensity decline is noted in the direction of the shorter periods than in the direction of the larger periods. The slopes of the microseism spectrum can be characterized approximately by the sharpness of their drop. The left slope in periods ranging from 0.01 to 4-5 seconds, and the right slope in periods ranging from 5-7 to 10-14 seconds, can be approximated by power curves of the following type:

$$\frac{A}{A_0}=\left(\frac{T}{T_0}\right)^{\gamma_{\text{пр}}} \quad \text{and} \quad \frac{A}{A_0}=\left(\frac{T}{T_0}\right)^{\gamma_{\text{лев}}}. \tag{9}$$

The mean value of γ in the ranges indicated are $\gamma_{left} \approx 1.5$ and $\gamma_{right} \approx -0.7 - 0.8$. The value, $\gamma_{left} = 1.5$, was found earlier by K. K. Zapol'skiy in observations of short-period microseisms in sedimentary rocks [49].

The above-mentioned character of the microseism spectrum is observed in practice in most of the quietest internal continental stations of the USSR. Approximately the same distribution of interference in the range from 0.01 to 60 seconds was obtained in the seismic stations of the USA [157, 159, 197, 201, 202, 337] (Figure 23).

The spectra of microseisms are similar in form over a wide range of periods in different stations in quiet internal continental stations. For surpressing microseisms, this makes it possible to

§ 3. Comparison of Microseism Spectra and of Useful Signals

From a comparison of the spectra of microseisms and those of the useful signals, it is possible to select the optimum parameters of the equipment guaranteeing that the most effective sensitivity — that is, the largest signal/interference ratio — will be obtained. It is also possible to estimate the minimum deviations in the dilatational P waves and in the surface L_R waves for various types of explosions.

Table 16 lists the approximate mean discrete values of the amplitudes of the spectral components of microseisms at quiet and medium stations of the USSR, and also those of the dilatational and surface waves during underground explosions with intensities of 1 and 10 kt, and also during contact with atmospheric explosions with intensities of 1 and 10 Mt. The values listed refer to the displacement spectra. The respective spectra, corrected for the irregular magnification of the equipment, are given in Figure 26.

In Table 16, the values of the amplitudes of the spectral components in the P and L_R waves are indicated for the two epicentral distances of 4,000 and 10,000 km. For an epicentral distance of 10,000 km, the values of A(T) in L_R waves for underground explosions with intensities of 1 and 10 kt are extrapolated according to the data of more powerful explosions, including the explosion of September 13, 1963 in Nevada, with an announced intensity of Q = 200 kt [241], for contact explosions with 1 Mt intensity according to the data for explosions in the Marshall Islands with announced intensities of Q = 10, 14, and 15 Mt [209], and for atmospheric explosions according to the data of explosions at Christmas Island with intensities of Q = 10 - 15 Mt [145].

L_R waves. The spectra of the L_R waves for contact and atmospheric explosions are similar in form when recorded on long-period equipment

TABLE 16. APPROXIMATE AMPLITUDES OF THE SPECTRAL COMPONENTS IN MILLIMICRONS (FOR DISPLACEMENTS) OF MICROSEISMS, AND ALSO OF DILATATIONAL P WAVES AND SURFACE L_R WAVES, RECORDED DURING VARIOUS KINDS OF EXPLOSIONS AT EPICENTRAL DISTANCES OF 4,000 AND 10,000 KM.

Period T, sec	Microseisms		Underground explosions				Contact explosions				Atmospheric explosions			
			P ($m = 5,1$)		L_R ($M = 4,0$)		P ($m = 5,3$)		L_R ($M = 4$)		P ($m = 3,8$)		L_R ($M = 3,5$)	
	Quiet Stations	Noisy Stations	$\Delta = 4000$ km	$\Delta = 10\,000$ km	$\Delta = 4000$ km	$\Delta = 10\,000$ km	$\Delta = 4000$ km	$\Delta = 10\,000$ km	$\Delta = 4000$ km	$\Delta = 10\,000$ km	$\Delta = 4000$ km	$\Delta = 10\,000$ km	$\Delta = 4000$ km	$\Delta = 10\,000$ km
30—40	(10)*	(50)	—	—	150	50	—	—	500	150	—	—	300	100
20—25	10	80	—	—	100	30	—	—	400	150	—	—	250	80
12—15	12	140	—	—	50	10	200	70	60	20	30	10	150	50
8—10	2,5	250	—	—	—	—	300	100	—	—	30	10	180	60
4—6	30	300	10	3	—	—	600	200	—	—	15	5	60	20
2—3	2	15	30	10	—	—	150	50	—	—	—	—	—	—
1,3—1,6	1,5	10	45	15	—	—	70	25	—	—	—	—	—	—
1,0	0,5	3,5	30	10	—	—	—	—	—	—	—	—	—	—
0,5	0,1	1,5	10	3	—	—	—	—	—	—	—	—	—	—
0,1	0,05	0,3	—	—	—	—	—	—	—	—	—	—	—	—

*Data which are insufficiently accurate are enclosed in parentheses.

at the epicentral distances being examined here. They are characterized by two maxima. One of them is at periods of about 15 - 20 seconds with a boundary frequency (taken at a level of 0.5 from the amplitude of the maximum) in the region of the shorter periods, 10 - 15 seconds. The second is at periods of 30 - 40 seconds with a boundary frequency in the region of longer periods, 40 - 50 seconds (Figure 26). The spectra maxima of the L_R waves during powerful underground explosions are slightly shifted in the direction of the shorter periods. However, in all cases, the region of the spectrum maximum of the L_R waves is shifted towards the larger periods, in comparison with the respective region of the spectrum of microseisms of the first order.

The amplitudes of the spectral components of L_R waves in the range of Δ = 4,000 - 10,000 km, in the ranges of the spectral band being examined here from 10 - 12 to 40 seconds, are 5 - 8 times greater than the corresponding values of the spectral components of microseisms at quiet stations for all types of explosions (both underground explosions with Q = 10 kt and contact or atmospheric explosions with Q = 10 Mt). They are commensurable with the amplitudes in medium-noise stations. In order to evaluate the correlations of the amplitudes of the useful signal $A_{u.s.}$ and of the interference A_{int} at other explosion intensities Q_1 carried out under comparable conditions for the given epicentral distance, one may calculate the signal level according to the experimentally established relationship:

$$A_1 = A_0(Q_1/Q_0)^{0.7 \div 0.8}. \qquad (10)$$

When m is known, the values of A/T in surface waves can be found from the correlation: M = (0.89 $\pm$ 0.21) m - (0.55 $\pm$ 0.12) [97, 326].

In this way, the passband of long-period equipment must be shifted towards the larger periods in order to increase the $A_{u.s.}/A_{int}$ ratio during recording at inland continental stations of the USSR

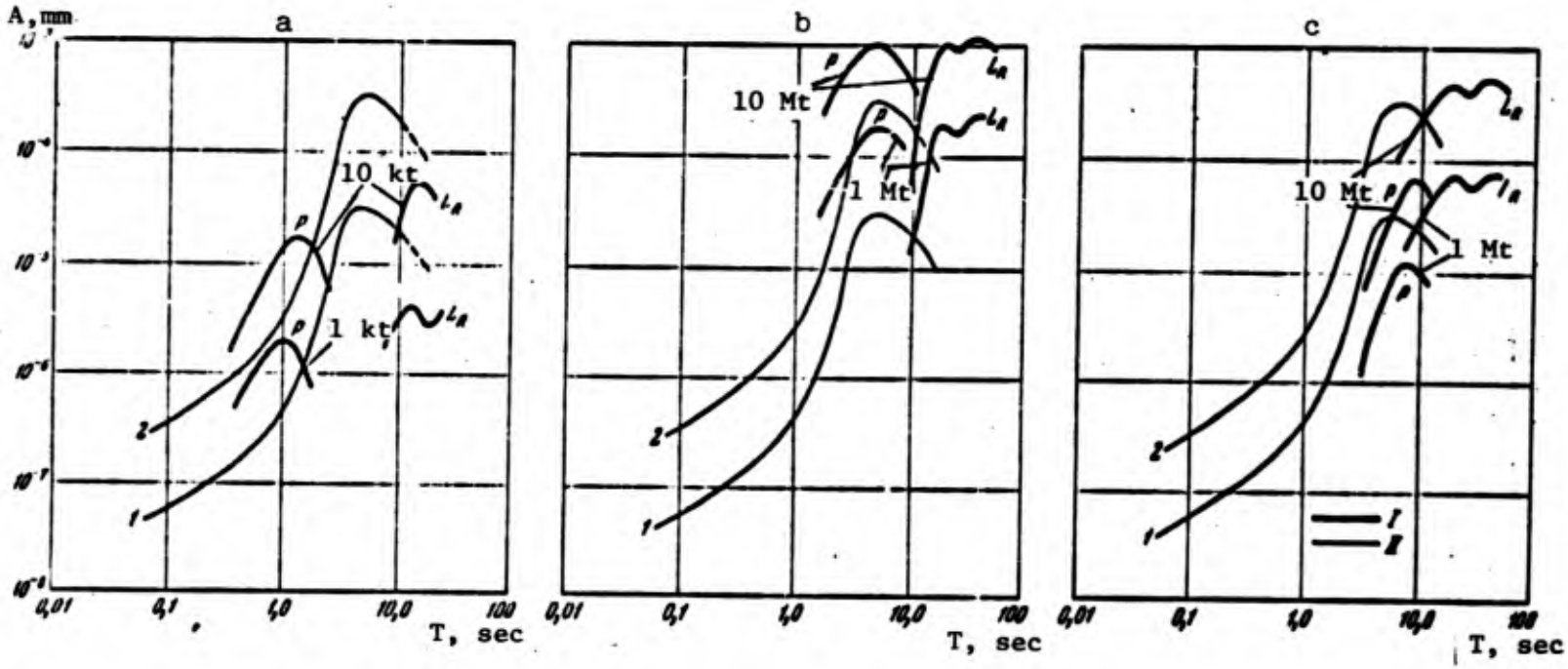

Figure 26. Comparative characteristics of the amplitudes of the microseisms in quiet and medium stations, and the amplitudes in dilatational P waves and surface L_R waves, recorded at Δ = 4,000 - 10,000 km during explosions in various media

a - underground explosions; b - contact explosions; c - atmospheric explosions; I - signals; II - interference; 1 - quiet stations; 2 - noisy stations.

for L_R waves caused by various kinds of explosions for Δ more than several thousand kilometers. A band with boundary periods from 12-15 to 40-50 seconds will be the optimum.

P Waves. For P waves, the spectra are not similar for different kinds of explosions. The periods of their maxima are all displaced towards each other, and their boundary periods also are different. Therefore, the question of the optimum conditions for recording P waves is examined separately for different types of explosions.

Underground and underwater explosions. For underground explosions with intensities from several kilotons to several hundred kilotons, the maximum of the spectrum in P waves is at periods from 1 to 2.0 seconds, and the band is in periods ranging from 0.5 to 2.0 - 2.5 seconds, i.e., the period of the maximum and the boundary periods are displaced with relation to the corresponding characteristics of the spectra of the microseisms of the first order into the region of smaller periods [203]. For an explosion with a power of 10 kt, the amplitudes of the spectral components, in the above-mentioned range of periods from 0.5 to 2.0 - 2.5 seconds, exceed by 5 - 6 times the corresponding values for microseisms in quiet stations. They are commensurate with the amplitudes in medium-noise stations. Approximately the same correlations are observed also during low-power underwater explosions in shallow water.

Consequently, in order to increase the $A_{u.s.}/A_{int}$ ratio, when recording P waves of underground and underwater nuclear explosions, the passband of the equipment must be shifted to the region of smaller periods in comparison with the band of the spectrum of microseisms of the first order. The optimum band will be one with boundary values of T on the order of 0.1 - 0.2 to 2.0 - 2.5 seconds with the maximum amplification at T on the order of 1 second. It is possible to raise the $A_{u.s.}/A_{int}$ ratio by 50 - 300 times or more in a number of cases by the above-mentioned means.

Contact explosions. The spectral bands of the P waves caused by contact explosions coincide with those of the microseisms. The amplitudes of the spectral components during an explosion with an intensity of 1 Mt, within the range of the spectrum band, exceed by approximately ten times the corresponding amplitudes of the microseisms in quiet stations, and by a somewhat lesser amount in medium-noise stations. However, in periods of about 1.5 - 2.5 seconds, the amplitudes of the spectral components in the P waves exceeded by 10 - 15 times the corresponding values of the A(T) of the microseisms. Therefore, when recording the P waves of distant contact explosions, it is advisable to shift the passband of the recording equipment in the direction of the shorter periods with reference to the spectrum band of the microseisms. The optimum band will be one with boundary periods from 0.2 - 0.3 to 2.0 - 3.0 seconds. In this case, it is possible to increase the $A_{u.s.}/A_{int}$ ratio by 30 - 50 times and more.

Atmospheric explosions. The spectral bands of the P waves and those of the microseisms overlap. However, the boundary periods in the spectrum of the P waves are shifted somewhat in the direction of the larger values of the periods ($T_{dom} \sim 12$ - 15 seconds). The amplitudes of the spectral components of the P waves within the range of the spectral band of the P waves of an atmospheric explosion with an intensity of Q = 1 Mt is about 2 - 3 times smaller than the corresponding values for microseisms. Therefore, P waves at a distance of $\Delta \sim 10{,}000$ km during an atmospheric explosion of 1 Mt can be recorded by a single seismograph only in especially favorable cases. In order to accomplish this, it is necessary to use a long-period equipment with a bandpass from 10 - 12 to 30 - 40 seconds and more, filtering out the microseisms of the first order. In this case, it is possible to increase the $A_{u.s.}/A_{int}$ ratio by several times (5-10 and more). The $A_{u.s.}/A_{int}$ ratio can also be substantially improved by the P waves derived from the displacement. Specifically, clear records of the P waves during atmospheric explosions were obtained by highly sensitive equipment with a band of 0.1 - 2.0 seconds (see

§ 1, Chapter I and Figure 3), which recorded the velocities in the P wave.

Thus, a comparison of the spectra of the useful signals and those of the microseisms leads to the conclusion that, by introducing filtration, one can considerably (from 5 - 10 to 200 - 300 times and more) increase the ratio of the useful signal amplitude to the interference amplitude. When it is necessary to increase this ratio by an even greater degree, it is necessary to apply the methodological procedures described in § 4 of this chapter.

§ 4. Measures for Increasing the Ratio of the Amplitude of the Useful Signal to the Amplitude of the Interference

A further increase of the ratio of the useful signal amplitude to the interference amplitude can be guaranteed by using several methodological procedures, particularly in combination with oscilation filtering. They include installing the seismographs in favorable areas, grouping the seismographs in arrays, using correlative statistical methods of lowering the interference level, based on using differences in velocities and in polarization of the interference and of the useful signal, and others.

The first two methodological procedures (installation of the seismographs in favorable areas, and grouping them in arrays) have been extensively tested during recording of numerous nuclear explosions in a number of stations located in different countries (USA, England, Canada). Several correlative and statistical procedures have been tested only in single stations for single explosions. General or theoretical considerations can be presented about the future prospects of several others.

1. The most widely adopted methodological procedures. Location of the stations in the most favorable areas for recording useful

signals (P waves). The experimental data accumulated at the present time show that the $A_{u.s.}/A_{int}$ ratio can be increased another 3 - 5 times if the seismographs are located in areas where the seismological conditions are favorable for recording seismic waves caused by explosions. Such areas include platform regions (for example, the European, Kazakh, Siberian, and other platforms), crystalline shields and massifs (for instance, the Baltic, Ukrainian, etc.), ancient mountain systems (for instance, the Urals, the area of the Taymyr peninsula, etc.), and also permafrost regions in the northeast USSR and regions with thick layers of precipitation and a low level of microseisms.

As an illustration, Table 17 gives data on the extent to which the magnitude Δm exceeded its mean value m_{mean} at temporary stations Nos. 1, 2 and 3, located on the Kazakh platform and in the Urals, during underground nuclear explosions, carried out in Nevada and the Sahara. The quantity m_{mean} was determined from a large (from 10 to 90) number of stations (the data of short-period seismographs were used). The excesses in question in the stations reached in some cases 0.7 unit of magnitude.

An analogous magnitude excess was noted in [103] and during recording at central Asian stations of the P waves of contact nuclear explosions carried out in the Marshall Islands (Table 18).

The relative location of the explosion epicenter and of the station also plays a certain role here. Thus, for example, in stations located on the Kazakh platform, the P waves are recorded with a relatively larger amplitude during explosions in Nevada, and in stations located in the Urals, the same is true for P waves during explosions in the Sahara. Similar results were obtained also in the USA [240]. Mountainous areas with a complex geological structure (the Pamirs, the Tien-Shan, the Altay, and others) are among those with the least favorable conditions for recording the P waves of underground and underwater explosions.

TABLE 17. EXCESS OF MAGNITUDE $\Delta m = m_{st} - m_{mean}$ AT TEMPORARY STATIONS NOS. 1, 2 AND 3 OVER ITS MEAN VALUE FOR FOUR UNDERGROUND NUCLEAR EXPLOSIONS CARRIED OUT IN NEVADA, USA.

Date	Area of epicenter	Mean values of magnitude m_{mean}	Number of stations	Stations No. 1, 2, located on Kazakh platform		Station No. 3, located in the Urals	
				Δm	Δ, km	Δm	Δ, km
May 1, 1962	Sahara	5.2	30	+0.20	5800	+0.30	6230
May 12, 1962	Nevada	5.24	20	+0.54	9800	+0.16	8210
July 6, 1962	Nevada	4.91	10	+0.21	9880	+0.13	8210
October 5, 1962	Nevada	5.25	28	+0.45	9880	+0.12	8210
September 13, 1963	Nevada	6.2	90	+0.50	9880		8210

Grouping of seismographs in arrays. The ratio of the amplitudes of the body P and S waves of explosions to the amplitudes of the interference (microseisms, reverberatory noises, noises caused by the signals themselves, and others) can be raised by using an array of seismographs at one station for simultaneous recording of the oscillations. When this is done, arrays consisting of several tens to several hundreds of seismographs are located either along intersecting lines, or at distances commensurate with the length of the signal wave [25-30, 147, 148, 158, 323, 359, 360]. An array of 525 seismographs (LASA) was set up in the USA [293].

The coherence of the signal and the incoherence of the interference, and the differences between their apparent velocities forms the basis of the principle of grouping in arrays.

The apparent velocity of the useful signals in P_n waves at distances of 200 to 1,000 km from the epicenter and of P waves at epicentral distances from 1,100 to 2,500 km amounts to about 8 km/sec. The apparent velocity of the P waves increases to 20 - 25 km/sec and more for further increases of the epicentral distance. Consequently, the apparent length of the λ^* waves of the useful signal exceeds 8 km. The apparent velocity of the irregular microseismic oscillations with periods of 1 second is usually not more than 2 - 4 km/sec, and consequently their apparent wavelength does not exceed 2 - 4 km. The difference in the propagation velocities of the signal and of the interference makes it possible to carry out not only frequency filtration when grouping seismographs in arrays, but also velocity filtration of the oscillations and filtration according to the signs of the directivity of the oscillations (that is, according to the azimuth of approach and the angle of departure). It is also possible to apply correlation methods of distinguishing the signal against the interference background, and a number of other procedures.

The most conspicuous increase of the effective sensitivity when seismographs are grouped in arrays — by $\sqrt{n}$ times and more, where n

TABLE 18. VALUES OF THE STATION CORRECTIONS OF THE MAGNITUDES $\Delta m = m_{st} - m_{mean}$ FOR SOME SEISMIC STATIONS OF THE USSR

Station	Abbrev. for the stations	Epicentral distance Δ, km	$\Delta m = m_{st} - m_{mean}$ Date & time of explosions				
			2/28/54 18.45.00	3/26/54 18.30.00	4/25/54 18.30.00	5/4/54 18.10.00	5/20/56 12.50.00
Kuril'	Kur	4070		−0,1			
Yuzhno-Sakhalin	YU-S	4450—4550	−0,4	−0,1		0,0	−0,2
Petropavlovsk-Kamchatskiy	Ptr.	4630—4650	−0,1	−0,2		−0,1	
Uglegorsk	Ugl.	4665	−0,1				
Vladivostok	Vld.	4730—4740	−0,5	−0,4	−0,6	−0,6	−0,5
Vremennaya 1	Vr. 1	5020—5130					−0,1
Magadan	Mgd	5450—5510			−0,1	+0,1	+0,3
Kyakhta	Kkht.	6600—6815	0,0	0,0		−0,1	
Kabansk	Kb.	6850—6860	0,0	+0,1	+0,2	−0,2	−0,4
Tiksi	Tks.	6920—7040					
Irkutsk	Irk.	7020—7030	+0,1	−0,1	+0,1	0,0	−0,2
Semipalatinsk	Smp.	8552—8650	−0,3	0,0	−0,1	0,0	
Vremennaya 2	Vr. 2	8680—8890					
Alma-Ata	Alm.	8710—8950	−0,1	+0,1	−0,3	−0,2	−0,1
Rybach'ye	Pbch.	8790—9120	−0,5	+0,1			
Alma-Ata 2	Alm.	9835—9170	+0,5	−0,1	0,0	0,0	−0,1
Namangan	Nmg.	9040					
Naryn	Nr.	9060—9580	−0,3	+0,3	+0,1	−0,1	
Frunze	Fr.	9170—9200	+0,4	+0,4	+0,3	+0,3	
Murgab	Mg.	9300—9700	−0,3	−0,1	−0,2	−0,2	
Chimkent	Chm.	9340					
Andizhan	An.	9390—9400	+0,5	+0,6	+0,6	+0,7	+,02
Fergana	Fg.	9445—9460	+0,3	+0,3	+0,3	+0,2	0,0
Khorog	Khrg.	9460—9560	−0,2				
Dzhergital	Dzh.	9550—9540	+0,4	+0,4	+0,5	+0,4	
Garm	Grm.	9600—9610	+0,3	−0,2	0,0	0,0	
Sverdlovsk	Svr.	9600—9775	0,0		−0,2		
Tashkent	Ts.	9620—9670	+0,3	+0,2	+0,1	+0,3	
Obi-Garm	O-Grm.	9660	+0,2				
Kulyab	Kub.	9665—9680	+0,3	+0,6	0,0	+0,4	
Dushanbe	Dnb.	9735—9770	+0,1	+0,3	+0,1	+0,4	
Samarkand	Smd.	9835—9850	+0,7				
Oazis-Bangera	O-B	10050					
Mirnyy	Mrn.	10390					
Ashkhabad	Ashkh.	10620	+0,4				
Mean values of magnitudes m_{mean}			6,2±0,3	6,0±0,2	6,0±0,2	6,0±0,2	5,8±0,2

(Table continued on next page)

TABLE 18. VALUES OF THE STATION CORRECTIONS OF THE MAGNITUDES $\Delta m = m_{st} - m_{mean}$ FOR SOME SEISMIC STATIONS OF THE USSR

Station	$\Delta m = m_{st} - m_{mean}$ Date & time of explosions 5/12/58 18.30.00	6/28/58 16.30.00	7/12/58 03.30.00	Mean values Δm_{mean}	Mean errors of determining Δm_{mean}	Type of seismograph	Rocks in the area of the station
Kuril'				−0,1		SK	Sedimentary
Yuzhno-Sakhalin				−0,18	±0,08	SK	Sedimentary
Petropavlovsk-Kamchatskiy				−0,13	0,04	SK	Sedimentary
Uglegorsk				−0,1		SK	Sedimentary
Vladivostok				−0,52	0,06	SK	Crystalline (quartzitic porphyres)
Vremennaya 1	−0,1	−0,1	−0,1	−0,1	0,00	SK	Crystalline (granite)
Magadan		+0,1		+0,1	0,05	SK	Sedimentary
Kyakhta	−0,1	−0,1	−0,3	−0,1	0,06	SK	Sedimentary
Kabansk	−0,2	−0,2	+0,2	−0,06	0,13	SK	Sedimentary
Tiksi		−0,3	−0,1	−0,2	0,10	SKM	Sedimentary, permafrost
Irkutsk		−0,1	0,0	−0,03	0,07	SK	Sedimentary (clays)
Semipalatinsk		−0,1		−0,1	0,08	SK	Sedimentary (sand-clay)
Vremennaya 2	−0,4	−0,4	−0,5	−0,43	0,04	SKM	Sedimentary, metamorphic, sedimentary (sand-clay deposits with gravel seam)
Alma-Ata	+0,2	0,0		−0,06	0,1	SK	same
Rybach'ye			−0,2	−0,2	0,13	SK	same
Alma-Ata 2		+0,1	+0,1	+0,07	0,10	SKM	Crystalline
Namangan	+0,2		+0,2	0,2	0,00	SK	Sedimentary
Naryn				0,0	0,20	SK	Sedimentary
Frunze		−0,2	+0,1	+0,25	0,10	SK	Sedimentary (gravel)
Murgab	+0,2			−0,12	0,07	SK	Sedimentary
Chimkent	+0,1			+0,1		SK	Loess
Andizhan	+0,2			+0,45	0,18	SK	Sedimentary (gravel)
Fergana				+0,22	0,1	SK	Sedimentary
Khorog				−0,2		SK	Crystalline
Dzhergital				+0,42	0,04	SK	Sedimentary
Garm				+0,12	0,12	SK	Crystalline
Sverdlovsk				−0,1	0,1	SK	Crystalline
Tashkent		+0,3	+0,3	+0,25	0,06	SK	Loess
Obi-Garm	+0,4			+0,3	0,10	SK	Crystalline (granite)
Kulyab		+0,2	+0,1	+0,26	0,15	SK	Loess
Dushanbe	0,0	+0,3	+0,3	+0,21	0,13	SK	Loess-like loam
Samarkand	+0,1			+0,4	0,30	SK	Loess
Oazis-Bangera			−0,3	−0,3		BEGIK-M	Crystalline
Mirnyy			+0,2	+0,2		SKM	Crystalline
Ashkhabad				+0,4		SK	Sedimentary (gravel)
mean values of magnitudes m_{mean}	5,8±0,2	6,0±0,2	6,0±0,2				

is the number os seismographs grouped in the array — is attained when separate channel-by-channel recording — for example, magnetic recording — is performed for each seismograph of the array, with subsequent automatic introduction of filtration and summation with the weight coefficients (by the maximum probability method) of the oscillations. There is regulated phase displacement between the separate channels. Such methods are used in stations of the USA, England, and Canada.

The use of electronic computers in grouping of arrays of seismographs makes it possible to carry out all the above-mentioned operations in real time. It is also possible to identify the records of underground and underwater explosions by the P waves. This is based on the differences in the correlograms of recordings of explosions and of earthquakes [91, 326, 336, 343, 344, etc.]. The effectiveness of different schemes of grouping is studied in [41, 91, etc.].

2. Methodological procedures tested out in single cases. The utilization of the different polarization characteristics of the useful signal and the microseisms. Utilization of differences in polarization between the useful signal and interference is one of the promising methods of overcoming interference, especially short-period accidental interference, in a station equipped with only a three-component set of seismographs (not grouped in arrays). In [327] it is proposed to make use of the differences in polarization by various methods, including that of plotting the trajectories of particles as a function of time. Such plotting makes it possible to distinguish the P and SV waves from accidentally polarized interference by means of rough estimates of the angle of departure of the linearly polarized P and SV body waves.

Chapters V and VI are devoted to the stability with which one can determine the polarization of P waves for different types of nuclear explosions at values of Δ ranging from several tens of km

to 10,000 km. Analogous studies were devoted to S waves recorded at epicentral distances of up to 800 - 1,200 km. The polarization has a very steady character for P waves in the range of the whole time interval when the waves are tracked. The angle of departure of the P waves is determined with a precision of about $\pm$ 5 - 7°. The polarization of the waves has a steady character only for the first one or two oscillations, and in the subsequent part of the record oscillations are observed which differ considerably depending on the angles of departure. Methods were also tested for determining the momentary values of the apparent angles of departure for the entire record of an earthquake. It was shown that it is possible to determine them in a statistically steady manner [327].

Statistical methods of separating the signal against the interference background. Methods of suppressing interference with the purpose of determining the direction of the first arrival on an unclear recording were worked out in the USSR and were tested in single records of underground explosions. The method is based on predictions of the character and level of the microseisms according to their character and level during the time period immediately preceding the moment of recording of the first motion [264]; the calculations were carried out on electronic computers. It is most advisable to apply this method when the data are simultaneously processed by a number of stations. During the processing, the criterion of the first motion can be used to identify the seismic phenomena.

3. Promising, but not yet tested methods. Method of accumulation. The method of accumulation [31-35] is one of the methods by which it is possible to separate the useful seismic signal against the background of interference when their amplitudes and periods are commensurable. This method is based on recording the mutual correlation function of seismic oscillations recorded by seismographs dispersed in an area or in space. The outermost seismographs of a group consisting of two, four or more seismographs are dispersed in

an area or in space. The outermost seismographs of a group consisting of two, four or more seismographs, are dispersed in this method at distances on the order of half the apparent wavelength of the useful signal. When recording the P waves caused by distant ($\Delta \geq 2{,}000$ - 10,000 km) underground and underwater explosions, the apparent wavelength in them amounts to about 8 - 30 km. Consequently, the outermost seismographs in the group in this method should be dispersed at distances of about 4 - 15 km, and in some cases at even greater distances.

The method of accumulation has been used thus far for seismic prospecting, including deep seismic soundings, where the periods of the oscillations in dilatational waves amount to less than 0.02 - 0.1 second. In this case, the automatic recording equipment in the field for the method of accumulation consists of a continuously operating electronic computing device which — during the process of recording or transcribing — performs the following operations on the signals recorded by the different seismographs in the group: a) summation with variable time shifts; b) remultiplication, and c) integration. Evidently the method of accumulation can be used for detection of underground, underwater, and also clear contact and atmospheric nuclear explosions under the condition that appropriate equipment has been provided which is suitable for the recording and subsequent transformation of the seismic oscillations with periods of about 1 - 2 seconds and more. The method of accumulation in principle makes it possible to determine the arrival moment and direction of a wave arriving against an interference background.

Method of suppressing (at a single station without arraying) microseisms of the first order when the direction towards their source is known. The method is based on the summation of the records of vertical and horizontal seismographs, one of which is in this case oriented towards the source, and the other in the perpendicular direction towards the first. Since in microseisms of the first order, the phase displacement in records of vertical and

horizontal seismographs are usually constant and equal to 90° (Rayleigh waves), it is possible, by summing the signal of these two seismographs, to considerably weaken the level of the microseisms.

It should be noted that during recording of nuclear explosions, tests were made of other means of increasing the effective sensitivity (grouping arrays of seismographs in deep holes, installing them on the bottom of seas and oceans, etc.) which have given satisfactory results [157, 197, 250].

Conclusions

Studies were made of the spectral composition of the useful signals — the body and surface waves of explosions — and of microseisms in stations located in areas with different geographical situations and geological structures. The following conclusions can be made on the basis of these studies.

1. In order to increase the effective sensitivity of the equipment installed at stations for detecting nuclear explosions, it is necessary to strive to lower the level of microseisms during the recording process. In order to accomplish this, it is necessary to locate the stations in quiet areas with a low microseism level, which must not exceed 0.5 - 1.0 millimicrons in a period of one second. The areas must be favorable for recording useful signals.

2. Quiet and favorable areas include platform regions and regions of some ancient mountain folds, and also permafrost areas.

3. It is advisable to install the seismographs at outcroppings of crystalline or metamorphic rocks, in housings sunk deep into the earth, on pedestals rigidly connected with the above-mentioned rocks, in housings with a stable ambient temperature, in holes, shafts, adits, and other underground structures.

4. The measures listed in points 1 - 3 make it possible to lower the microseism level in a wide range of periods up to 100 times and more in comparison with the background level in noisy regions which are unfavorable for recording the useful signals.

5. For further lowering the interference level in a limited range of periods, together with the above-mentioned methods, it is advisable to use filtration, grouping in arrays, and also correlation methods of recording and separating the waves.

6. In order to record the short-period body waves, primarily the dilatational ones, of underground and underwater explosions, it is essential to shift the maximum amplification of the equipment to the region of approximately 1-second periods, with the greatest possible lowering of the amplification in the region of larger periods. If filtration of the type mentioned is applied, it is possible to raise the amplification of individual seismographs at a period of 1 second to values on the order of 10^5 - 10^6 in a number of cases.

7. In order to distinguish signals with periods of 0.5 - 1.5 seconds at a ratio of their amplitude to the interference amplified with the same period, $A_{u.s.}/A_{int} = 2.0$, grouping of a large number ($n \geq 20$) of seismographs in an array is recommended. The seismographs should be dispersed around the area or along intersecting profiles. In this case, grouping in an array may improve the above-mentioned ratio up to $\sqrt{n}$ times, and also may guarantee a sufficient resolution of the signals in the recording and the possibility of better determining the characteristics of the seismic waves.

8. In order to record P waves with amplitudes on the order of 1 - 2 millimicrons in a period of 1 second within the territory of the USSR, it is possible to select quiet regions with a low interference background. In these cases it is possible to record the P waves in the entire region where they are present during underground and underwater explosions with a magnitude of $m \geq 4.5 - 4.8$.

9. In order to record surface waves and also some types of body waves, it is advisable to utilize long-period seismographs with a passband from 12 - 15 to 40 - 60 seconds with rejection filters at the periods of intense microseisms. This method of filtration assures that it will be possible in favorable cases to make use of an amplification on the order of $(2 - 3) \cdot 10^4$ within the range of the above-mentioned band. In this case, it will be possible to record the surface waves of phenomena with a magnitude of $M \approx 3 - 3.5$ (and, if long-period seismographs are grouped in arrays, a magnitude of $M \approx 2.0 - 2.5$) at distances of up to 10,000 - 11,000 km.

APPENDIX

Equipment Parameters Recommended by the Geneva Conference for Stations Detecting Nuclear Explosions

Equipment with the following parameters was recommended by the Geneva conference of experts [131] in 1958 for installation in stations on the ground for recording seismic oscillations during explosions carried out under different conditions.

1. A three-component set of seismographs with a maximum amplification on the order of 10^6 at a frequency of 1 hertz and with a passband adequate for reproducing the characteristic shape of the seismic signal. According to the author's own experience, this band has boundary frequencies between 0.1 - 0.2 and 2.0 - 2.5 seconds. The vertical component is recorded by a group of ten vertical seismographs dispersed at distances of 1.5 - 3.0 km and coupled with the recording instrument by cables. This installation should guarantee the best possible recording of dilatational waves.

The grouping of an array of horizontal seismographs was not specified, even though it can give the same effect as the grouping of an array of vertical seismographs.

2. A three-component set of seismographs with a narrow passband and an amplification on the order of $3 \cdot 10^4$ at periods of 2 - 2.5 seconds. This set guarantees that it will be possible to obtain good records of the dilatational, transverse, and surface waves of explosions and earthquakes with small distortions over a broad range of periods. This simplifies their identification to a considerable degree.

3. A three-component set of long-period seismographs with an amplification of $(1 - 2) \cdot 10^4$ at periods of about 25 seconds. This set is intended for the recording of surface waves of earthquakes and distant explosions.

4. A three-component set with a narrow passband from 1 to 10 seconds and an amplification of $(1 - 2) \cdot 10^3$. The curves of amplification of this equipment are given in Figure 2.

In 1959, at another conference of experts in Geneva, the parameters of the equipment destined for monitoring posts were somewhat improved by the working technical group No. 2[(1)]. Among other things, it was recommended that at each monitoring post 100, rather than ten, vertical seismographs should be installed in an array. Furthermore, the parameters of the equipment should be selected by taking into account the interference background at a given point. It was also recommended that long-period equipment be installed at all monitoring posts; the equipment should be provided with rejection filters for filtering out microseisms of the first order. It was also recommended that seismographs be installed in deep drilled holes.

At the present time, six stations with a full set of recommended equipment are in operation in the USA, and the number of seismographs grouped in arrays at one of the stations in Montana (the LASA system) amounts to 525 [212, 293, 323]. An array of long-period seismographs is in operation at this station. In England, two stations with array grouping have been built on English territory, as well as one each in Canada, India, and Australia. All in all, more than 20 stations with grouping in arrays are in operation in different countries [326]. Because of such a considerable number of highly sensitive stations, the USCGS service records and determines the parameters of distant seismic phenomena with magnitudes of $m \geq 4$ ($M \geq 3.2$) (see the seismological bulletins of the USCGS).

As magnetic recording equipment is improved and is applied successfully in seismic stations, including American and British stations with grouping in arrays, in the future it will no longer be necessary to install several sets of recording equipment simultaneously at one point. All the data received from several sets of recording

---

Footnote (1) appears on page 118.

equipment with the above-mentioned parameters can in principle be obtained with one or two sets of magnetic recording equipment having a large dynamic range.

According to the above-mentioned considerations, the question of the correct components for a set of equipment to be installed in stations for detecting and identifying nuclear explosions should be examined again after comprehensive testing of the new equipment, including the magnetic recording equipment.

However, there is no doubt that, even if magnetic recording is applied, it will still be necessary to install the equipment in places with a low background of interference. These places must have favorable seismological features for recording the oscillations caused by explosions. It will also still be necessary to use equipment grouped in arrays with separate recording of the readings of each separate seismograph and subsequent mixing of the oscillations, with the introduction of time lags, filtration, accumulation, etc., in the process of transcribing the magnetograms.

The effect of grouping in arrays can be enhanced somewhat if some of the seismographs comprising part of the array are located in a deep drilled hole at different depths, while some of the seismographs are also grouped in arrays on the surface.

FOOTNOTES

Footnote (1) on page 116 . See "Protocols of the Geneva Conference on Banning Nuclear Weapons Tests," 1959-1960, Funds of the United Nations.

CHAPTER IV

KINEMATIC AND DYNAMIC CHARACTERISTICS OF BODY WAVES RECORDED IN ZONE I

The regions in which body waves are tracked during explosions are provisionally divided into three zones: zone I with epicentral distances of up to 800 - 1,200 km; zone II, or the shadow zone, with epicentral distances from 1,200 to 2,000 - 2,500 km; zone III, with epicentral distances from 2,000 - 2,500 to 12,500 km; and zone IV, with epicentral distances from 12,000 to 18,000 - 20,000 km. In this book, zones II, III, and IV are treated together in Chapter V.

§ 1. Waves Recorded in Zone I

During powerful explosions carried out in various media — in the air, on the Earth, under the Earth, and under water — the same dilatational and transverse waves are recorded in zone I. These waves are connected with the layers in the Earth's crust, which are observed at the corresponding epicentral distances in the given area also during shallow-focus earthquakes. The following waves have been recorded during explosions in zone I: forward refracted waves P_0, S_0, propagated in sedimentary and sedimentary-metamorphic rocks; weakly

refracted broken waves $\overline{P}$, P*, P_n, $\overline{S}$, S*, S_n, propagated in the basic layers of the Earth's crust (granite, basalt), and also connected with the boundary of the upper Mantle, the Mohorovicic discontinuity.

Supercritical dilatational P_nP_n and transverse S_nS_n waves reflected from the M discontinuity have been clearly recorded. Supercritical waves reflected from the M discontinuity usually have a small intensity, and it is, as a rule, not possible to separate and track them in the recordings during point observations. Examples of the records of the waves observed in zone I are given in Figure 27.

During underground explosions, exchanged refracted waves of type $P_kP_lS_k$, $P_kS_lS_k$, and $S_kP_lS_k$, and apparently also reflected waves of type P_kS_k or S_kP_k, are generated and are present in the recordings. Here the letters k and l provisionally stand for the basic boundaries in the Earth's crust (between the sedimentary stratum and the granite layer, the granite and basalt layers, the foot of the basalt layer and the upper boundary of the mantle), and the intermediate boundaries in the above-mentioned layers and in the upper mantle. The clearest exchanged refracted waves of type $P_kP_lS_k$ were recorded for a sharp exchange boundary in the sedimentary stratum, for example salt — terrigenous rocks, etc. [328]. The kinematic and dynamic characteristics of the $\overline{P}$, P*, P_n, $\overline{S}$, S*, S_n, P_nP_n and S_nS_n waves have been relatively fully studied in zone I during powerful explosions.

A description of the characteristics of the body waves observed in zone I follows. Recordings obtained both during profile point observations and when the seismographs were distributed over the area were used. The description of the dynamic characteristics is based on the seismograms from wide-band seismographs of type SK with uniform characteristics in the range of periods from 0.1 to 10 seconds. Also well-resolved recordings obtained from type SKM and USF seismographs with a narrow, but uniform passband in the range of periods from 0.1 to 2.5 - 5 seconds were partially used.

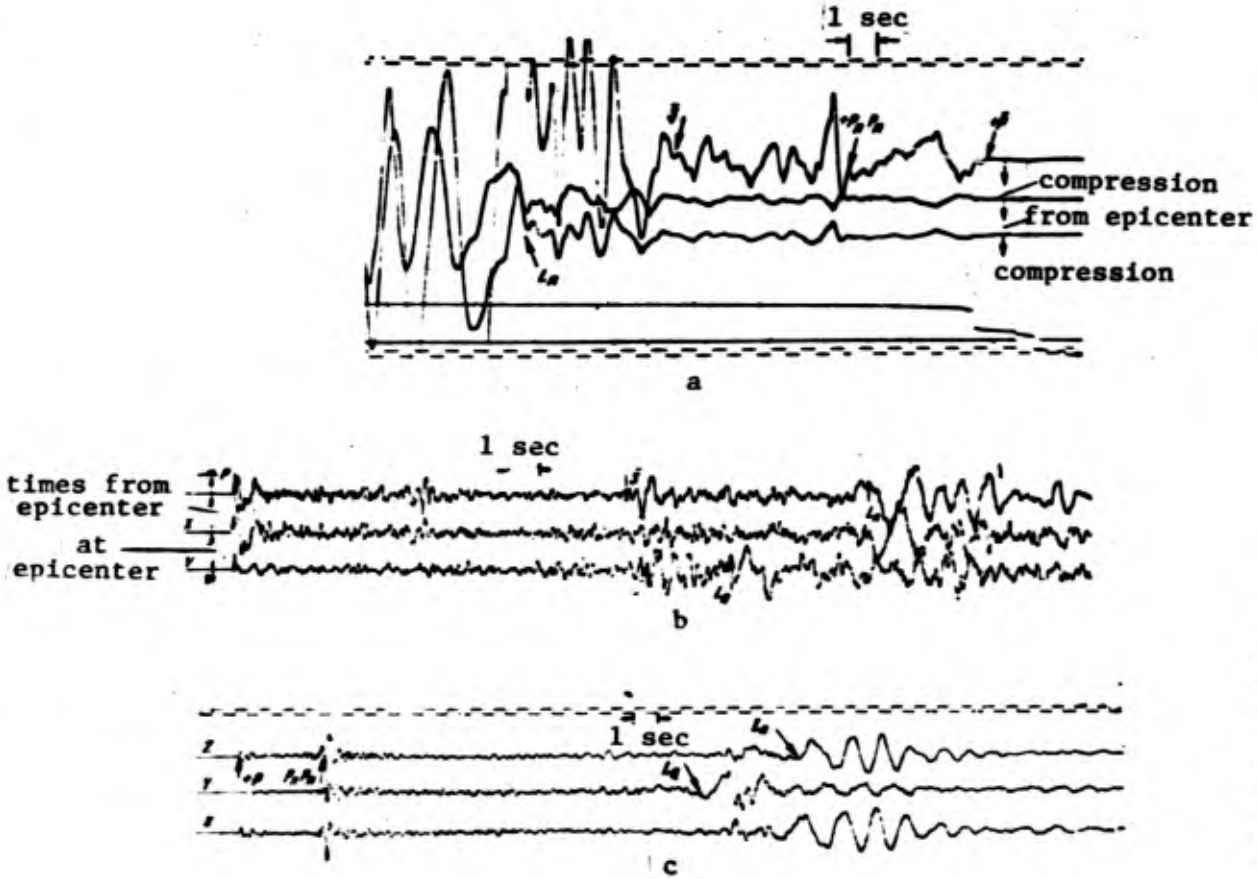

Figure 27. Examples of records of body and surface waves in zone I during various types of explosions:

During atmospheric nuclear explosions in the continental region:

a - Δ = 100 km, $\overline{P}$, P_n, $P_n \overline{S}$, L_R waves;

b - Δ = 480 km, P, S, L_g, L_Q L_R waves.

During underground explosions: c - Δ = 85 km, P, S, L_Q, L_R waves; d - Δ = 120 km, P, P_nP_n, L_Q, L_R waves. No S waves in the record. e - Δ = 200 km, P, P_nP_n, S S_nS_n waves.

(Figure continued on next page)

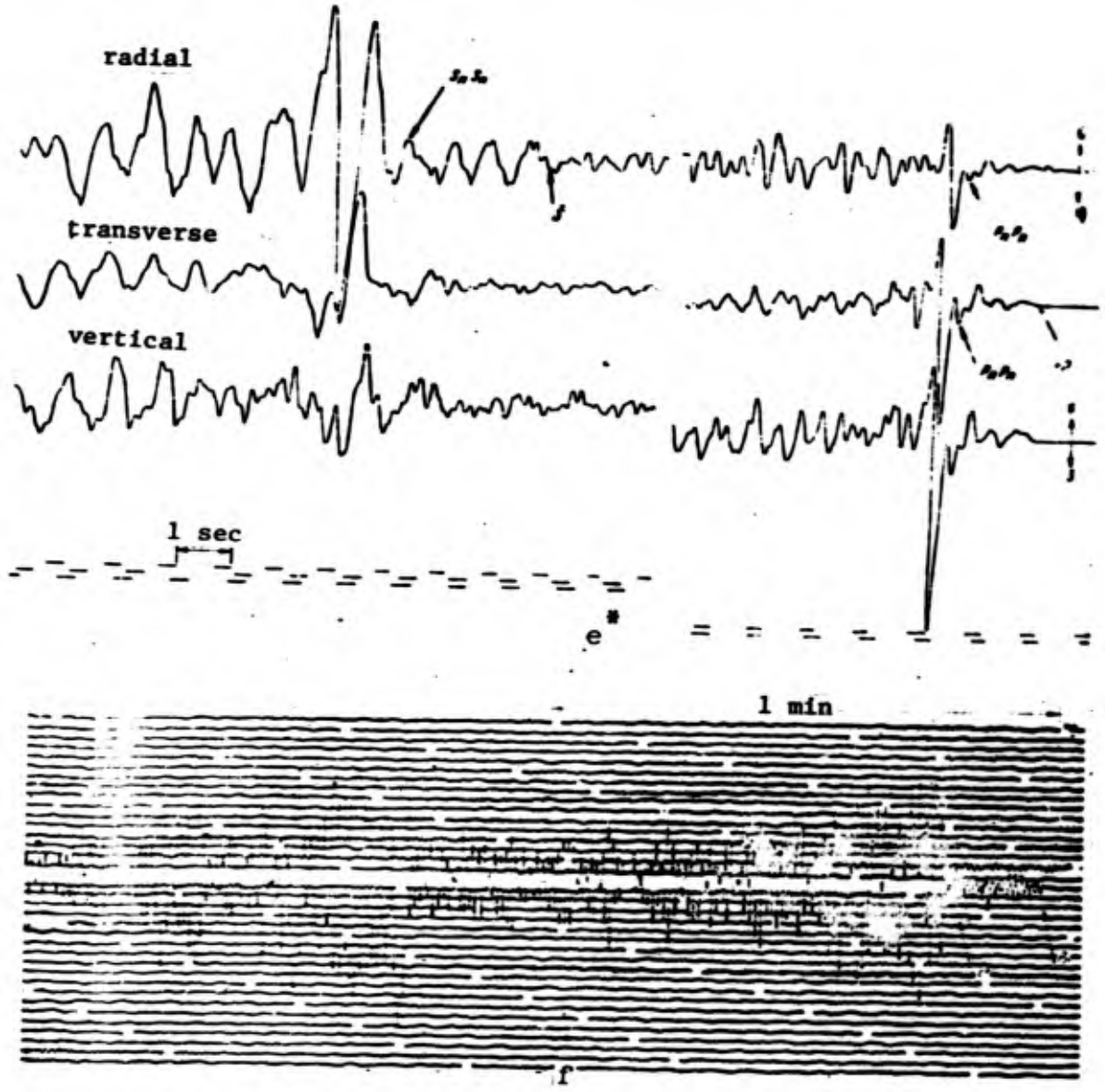

Figure 27

*Translator's Note: "d" is missing from foreign text.

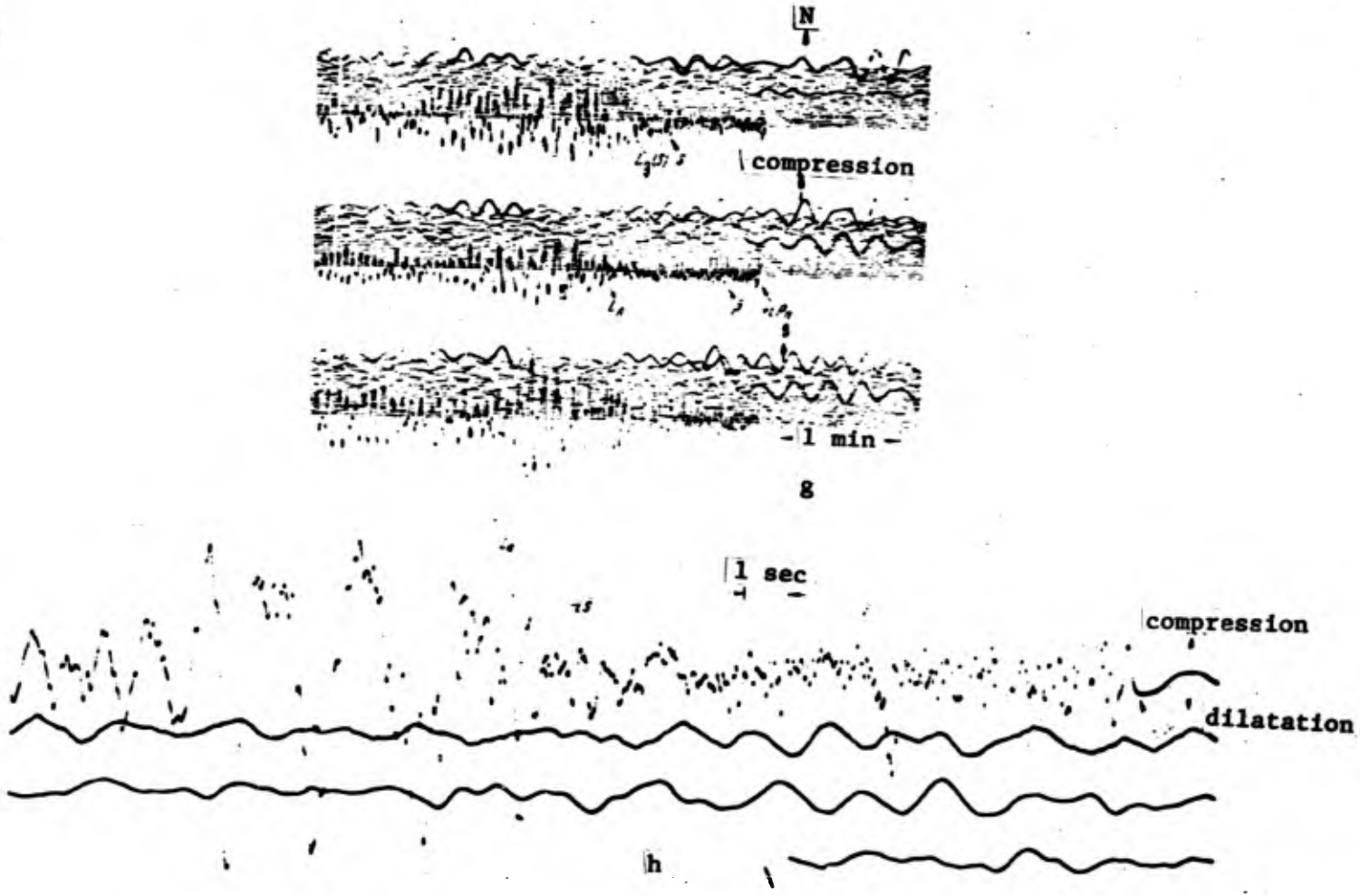

Figure 27. (continued)

f - Δ = 650 km, P_n, P* and other waves;

g - Δ = 410 km, P_n, P*, S, L_R and other waves.

During an underwater explosion:

h - Δ = 120 km, P, S, and L_R waves.

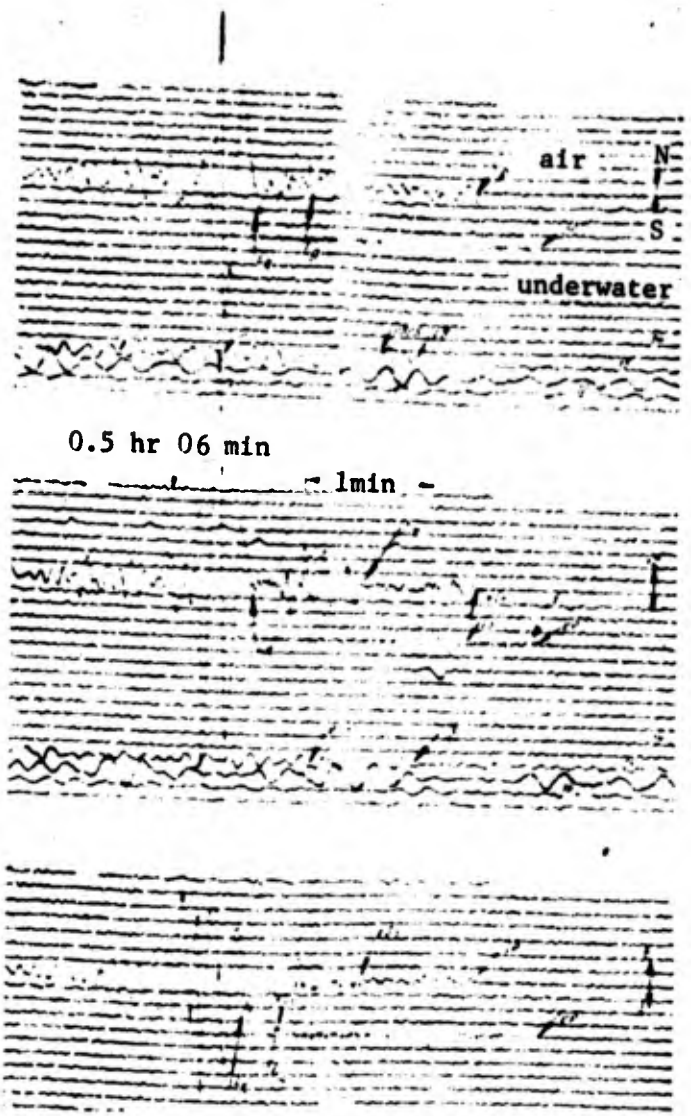

Figure 27 (continued)

In the works published thus far [99, 141, 170-174, 208, 317, 325 etc.] the characteristics of body waves in zone I are described basically according to the recordings of short-period filtering seismographs with selective characteristics. Most of them were of the Benioff type construction. The introduction of wide-band seismographs made it possible to analyze the dynamic characteristics of the waves.

The kinematic characteristics of the body waves — their travel time, hodographs, and the apparent velocities, as well as the trajectories of motion of particles in the waves — are practically the same for various types of explosions. Therefore, their description is given in a single section for all types of explosions. The dynamic characteristics of the waves, particularly the spectral composition of the oscillations, depend on the type of the explosions. Therefore, they are examined in Section 3 separately for each type of explosion. For the sake of comparison, data obtained during earthquakes are given, whose epicenters were located in the same area as the epicenters of explosions, or close to them.

§ 2. Hodographs of Waves Observed in Zone I

The travel time of the waves and their apparent velocities V^* vary somewhat, depending upon the seismogeological conditions of the area studied, the width and the character of the stratification of the basic layers of the Earth's crust, and the regions where the waves corresponding to different layers are traced. When the stratification of the boundaries is not horizontal, differences are observed in the travel times and the apparent velocities, even when the observations are carried out for the identical explosion in the same area in different directions. Therefore, for the waves traced in zone I, and also in the shadow zone, it is not possible to plot a single generalized hodograph for the entire globe. Attempts are made to plot, from the data for explosions, generalized regional hodographs of the dilatational waves — for instance, for the central part of the United States [168, 220, 221, 284, 296, 300, 332, 334].

Therefore, below in an examination of the regions of recording waves, their hodographs, and their apparent velocities, the range of values within which these characteristics of the wave fluctuate is given. These data are given in Table 19. For purposes of comparison, the average velocities of P_n and S_n waves, recalculated by Jeffreys for Europe, Central Asia, the northeast and northwest parts of North America, and Japan are given.

As is clear from the examination of the hodographs of the dilatational and transverse waves observed in zone I (Figures 28 - 30), exactly the same sequence of body waves is noted in atmospheric, contact, and underground explosions for different regions with a continental structure of the Earth's crust. In regions with a heavy stratum of sedimentary deposits, at distances of up to $\Delta \leq 10 - 15$ km, usually the first wave to appear on the seismogram is a P_0 wave. It is then replaced by a $\overline{P}$ wave, which is traced in the first arrival up to 90 - 110 km. The $\overline{P}$ wave is replaced by a P* wave, recorded in the first arrival in the range of $\Delta = 110 - 200$ km. At a distance of $\Delta \geq 200$ km, the first wave to be recorded is a P_n wave, which is traced in a number of regions up to 800 - 1,100 km and more. In the interval $\Delta = 80 - 100$ to 200 - 300 km, in the subsequent arrivals the most intense reflected dilatational and transverse P_nP_n and S_nS_n waves can be distinguished in the group of body waves.

The above-mentioned sequence of dilatational wave arrival is also observed for the corresponding transverse waves. The branches of the hodographs corresponding to the refracted $\overline{P}$, $\overline{S}$, P*, S*, P_n, and S_n waves, connected with the basic layers of the Earth's crust, can in most cases be approximated rather closely by segments of straight lines. It usually is not possible to establish weak refraction of the waves from the hodographs. In the ensuing arrivals, the P_n and S_n waves are observed up to $\Delta = 90°$ [297].

The equation of the hodographs for the waves being examined here can be represented as follows:

$$t_{P,S} = \frac{\Delta}{V_{P,S}} + t_{0P,S}.$$

Here, $V_{P,S}$ represents the velocities of the waves, and $t_{0P,S}$ is a segment cut off on the time axis by the given branch of the hodograph. It is the following [39]:

$$t_{0P,S} = \frac{2h\sqrt{V_2^2 - V_1^2}}{V_1 V_2}.$$

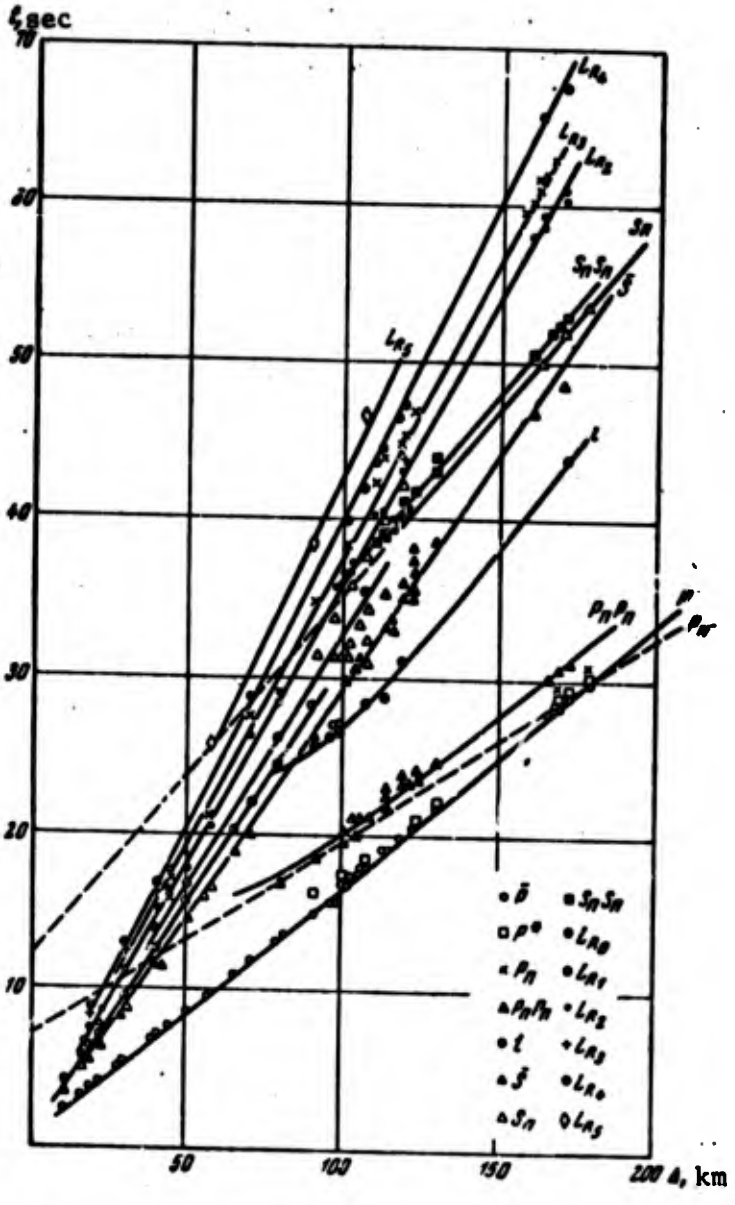

Figure 28. Hodographs of body and surface waves recorded during an underground nuclear explosion in the continental region in a range of Δ from 10 to 200 km

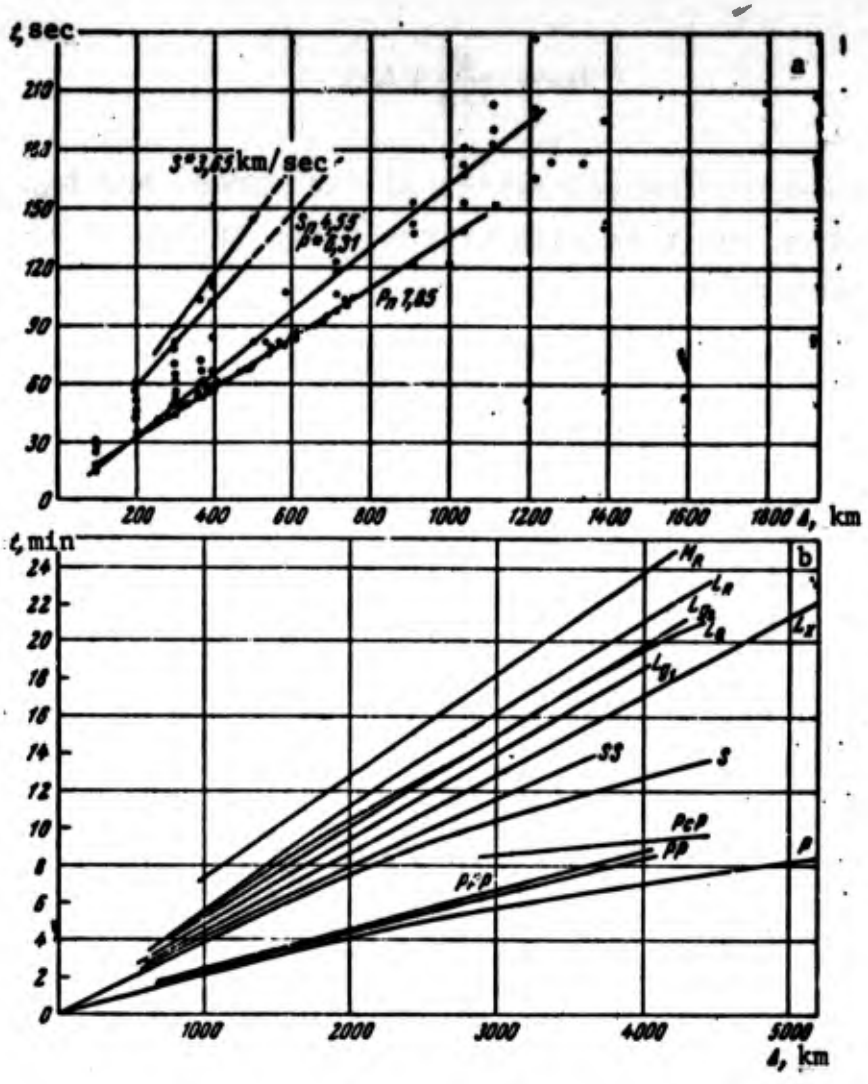

Figure 29. Hodographs of body waves recorded during underground explosions in the continental region

a - Δ = 100 - 1,200 km
b - Δ = 10 - 5,000 km

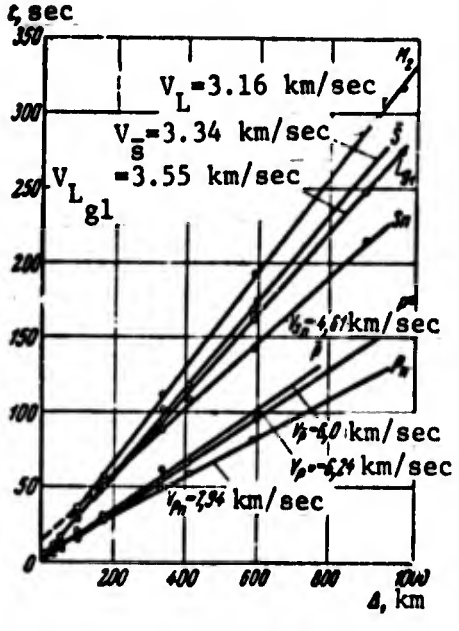

Figure 30. Hodographs of body and surface waves recorded during contact TNT explosion in zone I in the continental region

TABLE 19. VALUES OF THE APPARENT VELOCITIES OF DILATATIONAL AND TRANSVERSE WAVES IN ZONE I, CONNECTED WITH THE BASIC LAYERS IN THE EARTH'S CRUST, AS OBSERVED DURING EXPLOSIONS IN VARIOUS REGIONS

Character of structure of crust in region of observations	Type of source	Values of velocities of waves (in km/sec), epicentral distances (in km)										Literature
		P_0	S_0	$\bar{P}$	$\bar{S}$	P^*	P_nP_n	S^*	P_n	S_n	S_nS_n	
Platform, continental crust with thickness of 40-50 km	Underground explosion	5,5—6,0 (1—30)		6,01—6,15 (50—400)	3,30 (180—450)		7,75—7,10 (80—180)	3,60—3,65 (180—1000)	8,0—8,1 (200—1100)	4,52—4,55 (200—1000)	5,2—4,7 (100—200)	Auth
	Contact explosion			6,0—6,15 (10—600)	3,34 (20—900)	6,24 (200—1000)		3,60 (180—1000)	7,94—8,0 (200—600)			Auth
	Atmospheric explosion			6,00—6,10 (20—650)			7,75—7,10 (80—180)		8,0—8,1 (200—1000)	4,5±0,1 (200—1000)		Auth
Shield, thickness of crust about 40 km	Atmospheric explosion	5,5 (40—80)		5,5—6,0 (80—460)	3,3 (80—460)	6,2 (140—460)	7,75—7,70 (80—200)		7,9—8,1 (180—460) 8,140±0,41	4,57±0,028	5,2—4,6 (90—200)	[33]
Mountain country, thickness of crust about 45 km	Underground explosion	4,05 (10—30)	2,20 (10—50)	5,50 (10—550)	3,30 (200—350)	6,25 (180—750)		3,60 (10—1000)	7,8—8,05 (180—550)			Auth

TABLE 19. VALUES OF THE APPARENT VELOCITIES OF DILATATIONAL AND TRANSVERSE WAVES IN ZONE I, CONNECTED WITH THE BASIC LAYERS IN THE EARTH'S CRUST, AS OBSERVED DURING EXPLOSIONS IN VARIOUS REGIONS (continued)

Character of structure of crust in region of observation	Type of source	Values of velocities of waves (in km/sec), epicentral distances (in km)										Literature
		P_0	S_0	$\bar{P}$	$\bar{S}$	P^*	P_nP_n	S^*	P_n	S_n	S_nS_n	
Central Asia, thickness of crust about 45 km	Earthquakes			5,44—5,55 (100—560)		6,4—6,49 (200—900)			8,0—8,15 (200—900) 8,146±0,06	4,45—4,55 (200—500) 4,608±0,018		Autho. [38]
Nevada, USA, thickness of crust 30-35 km	Underground nuclear explosion			6,0 (30—130)		8,31 (100—1000)		3,65 (300—500)	7,85—8,1 (100—1100)	4,45 (200—500)		[141]
	Atmospheric nuclear explosion	6,0		6,0 (30—100)		6,5			7,66—8,1 7,996±0,0091			[170]
Southern California	Earthquakes			6,0		6,5		3,75	8,1—8,2	4,6		[45]
Nevada, USA	Earthquakes			5,2		5,8—6,15			7,01—8,1			[45]

TABLE 19. VALUES OF THE APPARENT VELOCITIES OF DILATATIONAL AND TRANSVERSE WAVES IN ZONE I, CONNECTED WITH THE BASIC LAYERS IN THE EARTH'S CRUST, AS OBSERVED DURING EXPLOSIONS IN VARIOUS REGIONS

Character of structure of crust in region of observation	Type of source	Values of velocities of waves (in km/sec), epicentral distances (in km)										Literature
		P_0	S_0	$\bar{P}$	$\bar{S}$	P^*	P_nP_n	S^*	P_n	S_n	S_nS_n	
New Mexico, USA	Underground nuclear explosion	6,0		6,0		6,45			8,176±0,060, 8,1	4,696±0,033		[322]
Australia, continental crust	Atmospheric explosion					6,12		3,56±0,03	8,23±0,02	4,75±0,02		[192]
	Underground TNT explosion					6,01±0,04		3,62±0,03	8,03±0,03			[193]
Pacific Ocean, oceanic crust	Contact nuclear explosion								8,19			[181]
Sahara, continental crust	Underground nuclear explosion			5,66 (100—200)			7,07—7,72 (100—200)		7,95 (180—450) 7,870±0,024	4,348±0,041		[280]

Note: Figures in parentheses indicate wave-tracking intervals in kilometers.

$t_{0P,S}$ varies in a considerable range depending on the structure of the crust in the given region, its thickness h, the thickness of the layers composing it h_i, and the velocities in the layers. Thus, for example, for P_n waves in the continental region where the thickness of the horizontal crust is about 40 - 45 km, t_{0P} amounts to 8 - 8.5 seconds, and t_{0S} for the S_n waves consequently amounts to 12 - 14 seconds (see the hodograph in Figure 28).

In regions with a small sedimentation thickness, the velocity of the P_0 wave does not differ noticeably from the velocity of the F wave, and the hodographs of these waves merge. In these cases, the wave which is being examined can be distinguished from the F wave by the fact that, when Δ increases, the amplitude of oscillations in it declines more rapidly than is characteristic for the F wave [325]. In regions with an oceanic structure of the crust, the F wave is absent, and the P* wave is traced as the first wave. In a number of continental platform regions, it is not possible to distinguish the P* wave as the first wave, and the hodograph of the F wave is immediately replaced by the hodograph of the P_n wave.

By comparing recordings of waves and their hodographs observed in identical regions during explosions and earthquakes, the identity of their kinematic characteristics was established (Figures 31, 32).

Special features of transverse wave recordings. The most clearly registered transverse waves were those recorded during atmospheric and contact explosions, in which the source can be regarded approximately as the percussive action of a concentrated vertical force on the surface of the Earth [116 - 119].

As has been established experimentally and theoretically [74, 306, 318], when the source is of this type, sufficiently intense transverse waves are excited. However, the ratio of the transverse wave intensity to the intensity of the corresponding dilatational waves during the explosions in a number of cases is somewhat less than during earthquakes with shallow foci (Figures 27, a, b).

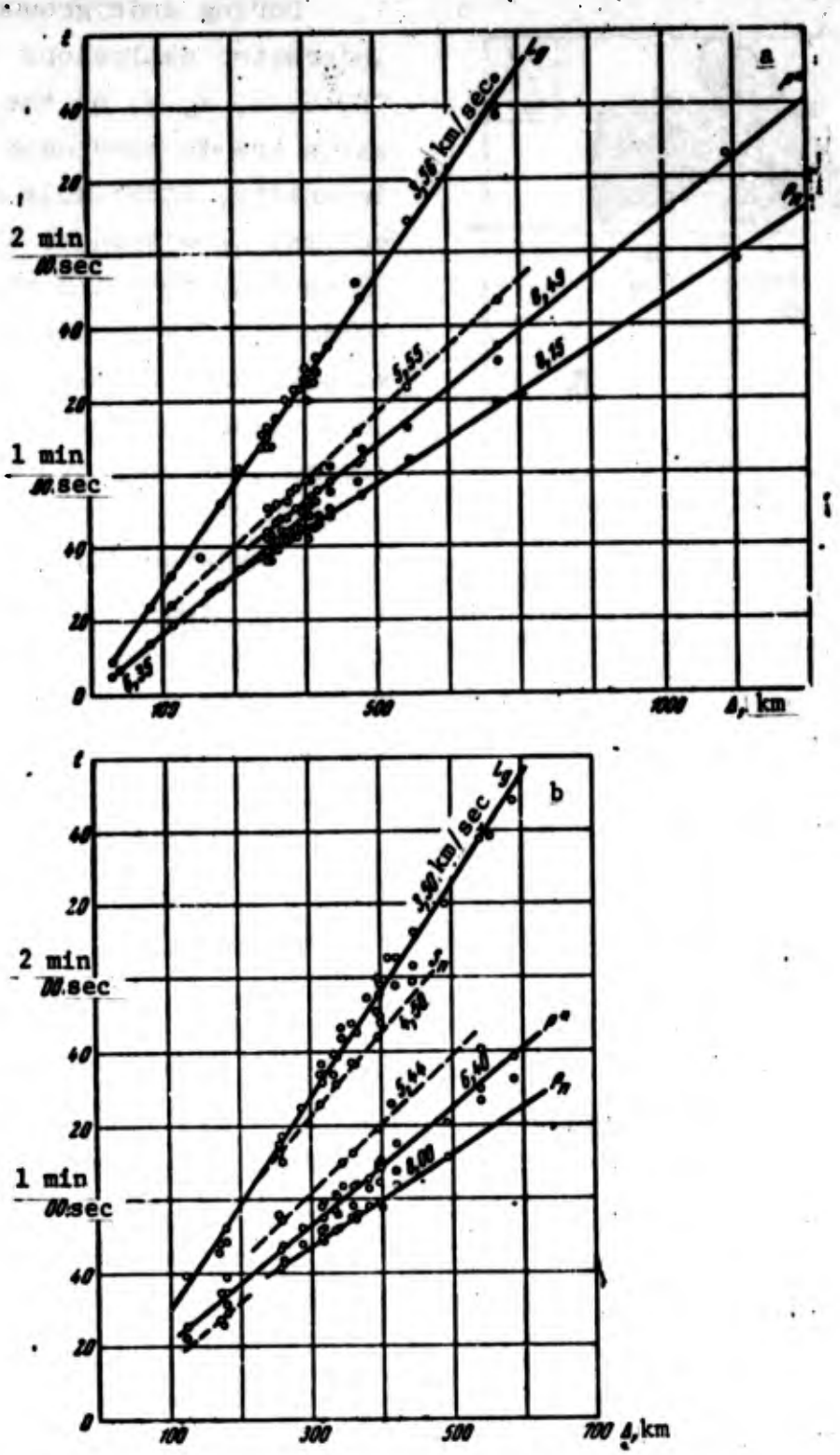

Figure 31. Examples of hodographs of body waves and L_g waves recorded in zone I during earthquakes with their foci in the Earth's crust

a - during earthquake No. 4;

b - during earthquake No. 2 (see the scheme in Figure 32).

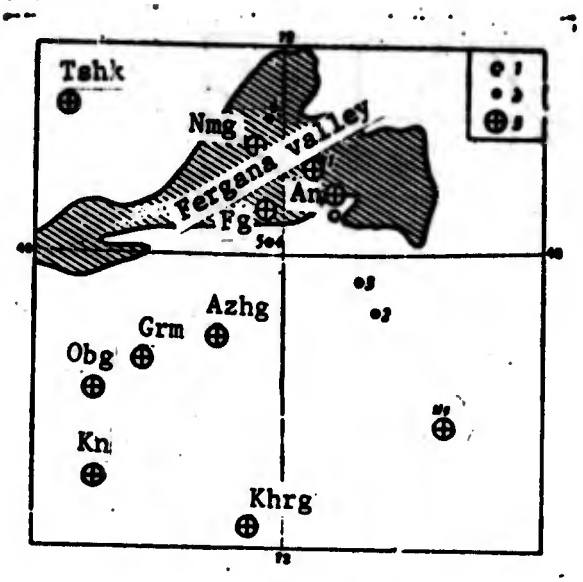

Figure 32. Scheme of distribution of epicenters of shallow-focus earthquakes (1), (2), the hodographs of which are shown in Figure 31, a, b, and the seismic stations (3).

During underground and underwater explosions (Figure 27, b, c, e, g, h) the transverse waves are in many cases of a low intensity, especially at close epicentral distances on the order of several tens and the first few hundreds of kilometers. In individual cases it may be difficult to distinguish them at all on the records, or they may be absent (Figure 27, f). Sometimes, however, during underground explosions of the same type in the same region, it is possible to distinguish clearly the transverse waves of the types mentioned above, and their amplitudes surpass by 2 - 3 factors the amplitudes of the P_n and P waves. In all types of explosions, the S wave in vertical seismographs usually appears in the opposite phase to that of the dilatational wave arrival (Figure 27, c, h).

In a number of works it is proposed that the transverse waves during some underground explosions originate due to the exchange of dilatational waves at nonuniform points in the structure of the Earth near the epicenter, such as fractures and other tectonic disturbances [189, 199, 255, 277, 301, 306, 318, 358]. However, the large ratio between the amplitudes of the limiting transverse waves and those of the dilatational waves indicates that transverse waves are generated at the focus of the explosion.

§ 3. Characteristics of the Wave Recordings

Atmospheric explosions. The records having the simplest appearance in zone I are those of waves in atmospheric explosions, carried

out in the atmospheric layer near the surface of the Earth. In these cases, the records of the dilatational and transverse waves obtained on seismographs of types SK, SKM, and others — within whose passbands the wave spectra occur — assume the appearance of short oscillation trains consisting of one to three oscillations with periods of 0.8 - 1.0 second, or less frequently up to 2.0 - 2.5 seconds (Figure 27, b). In recordings of these types of seismographs, the dilatational and transverse waves are divided by zones of relative amplitude damping. In these zones, the oscillation amplitudes in the recording are usually 3 - 5 times smaller than the maximum amplitudes of the dilatational and transverse wave oscillations.

In the recordings of seismographs with shorter periods, such as USF, adjusted to a narrow band from 0.1 to 1.5 - 2.0 seconds, or in those of short-period Benioff seismographs [99, etc.] and a number of others, the oscillation train in the waves contains a considerably larger number of oscillations — 3 to 6 or even more. The groups of oscillations in the waves in this case are not always divided in time by zones of relative oscillation damping, and some waves — appearing against a background of oscillations of other waves — can be distinguished by the increase in the recording amplitudes. The differences in the periods between the dilatational and the transverse waves are insignificant in these cases (Table 20). In recordings of low atmospheric explosions, the oscillations in the wave trains connected with basic boundaries in the Earth's crust, at distances of $\Delta < 200 - 300$ km, are modulated by oscillations with shorter periods on the order of 0.1 - 0.3 second.

The character of transverse wave recordings is somewhat different from that of the recordings of dilatational waves. At short distances of $\Delta < 200 - 300$ km, in the recordings of wide-band SK seismographs, the S waves appear in the form of a sharp pulse oscillation with a somewhat smaller period than the period in the P waves (Figure 27, b, etc.). At a distance of $\Delta > 400 - 500$ km the S waves are transformed into trains consisting of several oscillations with a period more or less the same as the periods in the dilatational waves.

TABLE 20. VALUES OF PERIODS IN BODY WAVES RECORDED IN ZONE I DURING VARIOUS TYPES OF EXPLOSIONS

Region	Range of Δ, km	Height, m	Power of explosion, kt	Number of explosions	Passband of equipment, sec	Wave	Mean period, T_{mean}, sec	Max. values of periods, T_{max}, sec	Wave	T_{mean}, sec	T_{max}, sec	Magnitude, m	Literature
Atmospheric explosions													
Continental	65—750				0,1—2,5	$\overline{P}$	0,7±0,06	0,63—0,82	$\overline{S}$	1,0±0,06	0,9—1,7	4,5—5,5	
					0,1—2,5	P^*	0,7	0,6—0,8	S^*				
					0,1—2,5	P_n	0,9	0,6—1,2	S_n	1,3±0,15	1,0—1,6		
					0,2—10	$\overline{P}$	1,5	1,3—1,7	S	1,1±0,1	0,7—1,7		
					0,2—10	P^*, P_n	1,5	1,4—1,6	S^*, S_n	0,8—2,0			
					0,2—10	P^*	1,0±1,0	8,0—1,1	S_n	8±1,0	7—9		
Nevada, USA	380—840	90—1800	1—20	50	0,1—0,8		0,9±0,1	0,7—1,0				2,8—5,0	[209, 322]
			1—20	50	0,1—0,8	P_n	0,8	0,5—1,0					
Contact explosions													
Continental	70—800				0,1—2,5	$\overline{P}$	0,4	0,3—0,4	$\overline{S}$	0,6			
					0,1—2,5	P^*	0,75	0,7—0,8	S^*	1,2	1,0—1,5		
					0,1—2,5	P_n	0,6	0,5—0,8	S_n	1,0	0,8—1,2		
					0,2—10	P_n	0,8	0,5—1,4	S_n	1,2	1,0—2,0		
Underwater explosions													
Continental	25—1000				0,1—2,5	$\overline{P}$	0,3	0,3—0,4	$\overline{S}$	0,3	0,2—0,6		[64, 99]
					0,1—2,5	P^*	0,6	0,5—0,8	S^*	1,0			
					0,1—2,5	P_n	0,6	0,5—0,8	S_n	0,8			
Nevada, USA	58,6—990	200—400	1—56	16	0,1—0,8	$\overline{P}$	0,3	0,25—0,8	S^*	1,0	0,6—1,4	4,7—5,6	
					0,1—0,8	P^*	0,5	0,23—0,9	S^*	1,3	1,2—1,5	4,7—5,6	
					0,1—0,8	P_n	0,5	0,25—0,8	S_n	0,8	0,6—1,1		
Underwater explosions													
Continental	100—1000				0,1—2,5	P^*	0,4	0,2—0,5	S^*	0,8			
					0,1—2,5	P_n	0,8	0,2—0,5	S_n	0,7			
					0,2—10	P_n	0,8	0,5—1,0	S^*	1,2			[205]

During the same atmospheric explosion, the transverse waves in the recordings of wide-band SK seismographs can, as a rule, be separated out and traced better than in the recordings of seismographs with a narrow passband. At the same time, the dilatational waves are separated out on instruments with a narrow passband much better than the transverse waves.

Contact explosions. In these explosions, the recordings of the body waves have a more complex character than in atmospheric explosions. In appearance they are similar to the recordings of atmospheric explosions carried out at low elevations over the Earth's surface. In contact explosions, just as in atmospheric explosions, it is possible to trace the transverse waves at greater distances Δ than is possible in underground explosions.

In contact explosions. the periods of the body waves in the recordings are approximately 1.5 times smaller than in atmospheric explosions. At distances $\Delta > 200 - 300$ km, the difference in the periods becomes insignificant. The oscillation trains in the dilatational and transverse waves are usually short and consist of 2 - 3 oscillations. They are modulated by short-period oscillations to a greater degree, especially at short distances of $\Delta < 300 - 500$ km, than are the oscillation trains in atmospheric explosions.

Underground explosions. The recordings of body waves in underground explosions in zone I differ considerably from the recordings of atmospheric or contact explosions. The basic differences are the following: a) the recording consists of a larger number of waves; b) the periods of the dilatational and transverse waves are considerably smaller than the periods of the waves in atmospheric and contact explosions. In recordings of wide-band seismographs, they amount to 0.3 - 0.4 second for dilatational waves, and to 0.6 - 0.8 second for transverse waves; c) the oscillation trains in the waves, as a rule, are not separated from each other by zones of relative amplitude decrease. Superposition of the oscillations of one train on another is observed, and the recording has an interference character (Figure 27, f).

The presence of a larger number of waves in the recordings of underground explosions is undoubtedly connected with the fact that the oscillations caused in this case have shorter periods. As a result, the occurrence of a larger number of waves is possible. The waves are refracted and reflected not only at the basic interfaces, but also at the intermediate interfaces in the Earth's crust [152, 320, 334, 340].

In the recordings of underground explosions, as was already mentioned above, the arrivals of transverse $\bar{S}$, S^*, and S_n waves cannot be distinguished positively in a number of cases. This may be connected with the low intensity of the transverse waves in cases when the source has near-spherical symmetry [43, 234]. In addition, the difficulties in distinguishing the transverse waves are connected with the fact that — during their recording — a surface channel wave of type L_{gl} occurs which is extremely intense in the recordings of all three components and which has a propagation velocity of 3.55 km/sec, which is close to the velocities of the $\bar{S}$ and S^* waves.

Underwater explosions. In underwater explosions carried out in shallow-water regions at shallow depths, or on the bottom of shallow-water basins, oscillations are caused with somewhat shorter periods than those recorded during underground explosions (Figure 27, b, h). The periods of the dilatational waves amount to 0.2 - 0.5 second. Immediately (0.5 - 1 second) after the first arrival, the sharp arrival of a relatively lengthy group of high-frequency oscillations is observed with periods of about 0.1 - 0.3 second (Figure 27, h). At At $\Delta \leq 300 - 400$ km, these oscillations complicate the recording, not only of the dilatational waves, but also of the transverse waves, and in some cases of the surface waves as well.

Another distinctive feature of the recording of shallow-water underwater explosions is the presence of an intense pulse which occurs right at the dilatation phase and which has a lance-shaped form at close distances of $\Delta \approx 110$ km, but at greater distances of $\Delta > 300$ km

is transformed into a group of short-period oscillations with periods of $T \approx 0.2 - 0.6$ second. In Figure 27, h, the arrival of the above-mentioned pulse is indicated by the letter i.

The occurrence of this pulse is apparently connected with the phenomenon in which the void formed as the result of an underwater explosion is quickly filled with water. This "collapse" of the void (a sort of repeated impact) has been noted during deep explosions [101, 102, 206].

The amplitude of the pulse i at a distance of $\Delta \approx 100 - 300$ km usually exceeds by 1.5 - 2 times the amplitude of the first dilatational wave. At even greater distances Δ, this ratio of amplitudes is even greater. The pulse i during shallow-water explosions is traced also in P waves as well. The time difference Δt_i for the arrival of pulse t_i and the dilatational wave t_p remains unchanged at all distances Δ. The value of Δt_i depends on the depth of the explosion and its intensity, and also, evidently, on the depth of the basin. For explosions carried out in shallow-water areas near the shores, Δt_i amounts to 4 to 7 seconds.

During the deep-water explosions carried out by the United States at depths of about 150 - 600 m in the deep-water regions of the Pacific Ocean, intense arrivals are observed 10 - 30 seconds after the arrival of the P waves. They are caused by pulsations of the gas bubbles [78]. We do not have data from observations in zone I during deep-water explosions carried out by the United States.

For underground and underwater explosions, the ratio between the maximum amplitudes in the transverse waves and the corresponding amplitudes in the dilatational waves A_S/A_P in the Δ range from 100 to 500 km falls within the range of 1 to 2.5. For earthquakes, $A_S/A_P > 2.5$ in about 90% of all cases. Approximately the same values of A_S/A_P for underwater explosions were obtained in [205, 352]. In [90], a complete study of the dependence of earthquake A_S/A_P on Δ for different seismoactive regions of the USSR was carried out. In the

range of Δ = 200 - 1,200 km, the average values of $A_S/A_P > 3.5$ according to the recordings of SKM instruments, in which T_{dom} = = 1.5 - 2.0 seconds.

Type PL, SL waves. Simultaneously with the arrival of dilatational waves, whose periods usually amount o 0.4 to 1.5 seconds in zone I — depending on the type of the explosion and the parameters of the recording equipment — arrivals of longer-period oscillations are also observed, which have been called PL and SL waves in the literature. The periods of these waves in all kinds of explosions are around 4 - 12 seconds — that is, are considerably greater than the oscillation periods in dilatational and transverse waves. The intensity of the PL and SL waves and their periods in the recordings depend on the intensity of the explosion and the properties of the receiving equipment. During powerful explosions, PL waves have been observed in the recordings of wide-band seismographs of type SK within the range of the entire zone I, and in zone III up to epicentral distances of about 5,000 and more. In these same zones analogous waves of type SL are observed in a number of cases. Waves of type PL and SL in zones II and III are observed chiefly during contact, atmospheric and powerful underground explosions.

Long-period PL waves have also been frequently observed during earthquakes as well. There has been no special study of the mechanism of the origin of long-period PL waves starting simultaneously with the arrival of the dilatational waves, and the available observations have not yet been systematically presented [295]. Study of the PL and SL waves is of great interest, since these waves evidently contain information about the source — such as information about its dimensions — and they may possibly be used in determining its parameters.

Supercritical P_nP_n and S_nS_n waves reflected from the M discontinuity P_nP_n waves were recorded clearly at distances of Δ = 80 - 200 km during atmospheric and underground explosions carried out in a number of platform regions (Figure 27, d, e).

Recordings of P_nP_n waves recorded during atmospheric explosions by means of vertical wide-band seismographs with a passband from 0.2 to 10 seconds represent oscillation trains occurring right at the compression phase. These trains consist of 3 - 4 extremes with an apparent period of oscillations on the order of 0.6 - 0.3 second. These waves are also recorded well by horizontal seismographs. The periods of the P_nP_n waves during underground and atmospheric explosions are approximately 1.2 - 1.3 times smaller than the periods of the $\bar{P}$, P*, and P_n waves recorded during these same explosions.

The maximum amplitude of oscillations in the P_nP_n waves in recordings of a vertical seismograph exceed by approximately 1.5 to 5 times or more the amplitudes of the $\bar{P}$, P*, and P_n waves recorded in the first and in the succeeding arrivals.

P_nP_n waves reflected from the M discontinuity were recorded during an underground nuclear explosion carried out by France in the Sahara on May 1, 1962, in the Akhaggar (sic) plateau region in the interval of Δ = 109 - 200 km; the apparent velocity of the P_nP_n waves amounted to 7.72 km/sec. The amplitude in the P_nP_n waves was approximately the same as the amplitudes of the $\bar{P}$ waves having an apparent velocity of 5.66 km/sec [260].

It must be observed that, both during explosions and during earthquakes, the P_nP_n and S_nS_n waves thus far have been recorded predominantly in regions with a continental structure of the Earth's crust.

The S_nS_n waves were recorded during underground explosions in the continental region in approximately the same range of epicentral distances as the P_nP_n waves (Figure 27, e and the hodograph in Figure 28). Their arrivals in the recordings are as clear as those of the P_nP_n waves. In the region of the hodograph minimum, they are not traced, just as in the case of the P_nP_n waves.

The S_nS_n waves are predominantly polarized in a horizontal plane perpendicular to the direction of propagation.

§ 4. Periods of Dilatational and Transverse Waves Recorded in Zone I

The periods of the dilatational and transverse waves recorded in zone I during various types of explosions were measured directly according to the seismograms, and also according to the maxima of their spectra. In those cases when the oscillation train in the wave consisted of only one oscillation, the duration of this oscillation was taken as the period. If the train consisted of several oscillations, the period of the oscillation with the maximum amplitude was measured. To measure $T_{P,S}$, recordings obtained by type SK, SKM, and USF seismographs were used.

The recordings of P waves during atmospheric explosions and also during some contact explosions recorded at a distance of $\Delta \leq 200$ km are complicated by PL waves. This is also true for powerful explosions at $\Delta \leq 500$ km. This made it difficult to measure the periods in the P waves. Data concerning T_P are not introduced in this work for P waves complicated by a superposition of PL waves.

Recordings of S waves in seismograms are usually not complicated by a superposition of SL waves, except for the recordings of the most powerful explosions. When the periods were being determined from the amplitude spectra calculated on electronic computers, the period of the amplitude spectrum maximum was in this case taken as the period T_{sp} of the oscillations in the train. Spectra of the P waves recorded at the same distance Δ during various types of explosions, illustrating the dependence of the maximum periods T_P on the type of explosions, are shown in Figure 33.

The comparison of T_{sp} and T_{dom} in the P_n and P waves, which was given in § 4 of Chapter II, showed that these values practically coincide.

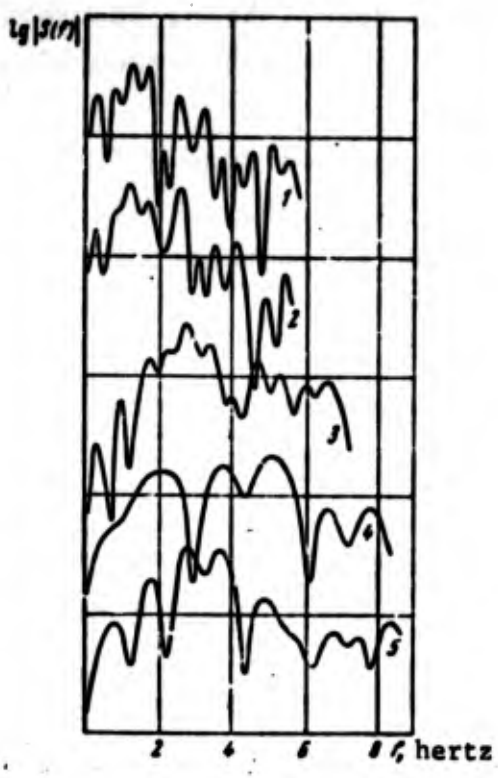

Figure 33. Spectra of P waves recorded by vertical USF seismographs with uniform amplification in a range of periods from 0.1 to 2.5 seconds at the same station (Δ = 70 - 75 km)

1 - 3 - during atmospheric explosions;
4 - during an underground nuclear explosion;
5 - during an underground TNT explosion.

The relative distribution of the spectra is given on an arbitrary scale.

Table 20 gives data on the periods of the dilatational and transverse waves obtained during explosions of various types in different regions, including Nevada.

Table 20 gives the average (T_{mean}) and extreme (T_{ext}) values of the periods of the dilatational $\bar{P}$, P*, and P_n waves and of the transverse $\bar{S}$, S*, and S_n waves. The periods measured from the recordings of horizontal instruments practically coincide with the measurement data in recordings of vertical seismographs.

The dependences of T_P and T_S on Δ are examined below, on the basis of the data given in Table 20.

Atmospheric explosions. During these explosions, the periods of the dilatational and transverse waves have somewhat larger values than during other types of explosions. In the range of powers and elevations of the explosions studied, the periods in the recordings of wide-band SK seismographs, and also in those of SKM and USF narrow-band seismographs, amount to 0.6 to 1.5 seconds for the dilatational waves within a range of Δ from 65 to 700 - 800 km. They amount to 0.7 to 1.7 seconds for the transverse waves. One exception is the data from those stations in which the P and S waves are complicated by PL and SL waves.

As Δ increases from 100 - 200 km to 700 - 800 km, the periods in recordings of narrow-band seismographs change very little, increasing somewhat with increasing Δ. The increase of T does not exceed 10 - 15%.

When the magnitude of the explosion M increases from 3.5 to 5.4 - 5.7, an increase of T_P and T_S by 10 - 20% is observed, as well as a weak increase in the periods of body waves and an increase of 2 - 4 times in the height of the explosion.

We will show that the data given above were obtained from a relatively large number of explosions (see Table 20).

Contact explosions. Approximately the same values of T_P and T_S were obtained for this type of explosions as were obtained for atmospheric explosions. However, the small number of observations makes this result less valid than the data obtained during atmospheric explosions.

Underground explosions. In underground explosions, somewhat smaller values of $T_{P,P*}$ and $T_{S,S*,S_n}$ were observed than during atmospheric and contact explosions. When Δ ranges from 100 to 200 - 300 km, the periods of the dilatational waves ordinarily fall within the range of 0.2 - 0.4 second, and those of the transverse waves — within the range of 0.5 - 0.6 second. In the range of Δ = 200 - 1,000 km, the values of T_P fall within the range of 0.5 - 0.8 second, and those of T_S — within the range of 0.8 - 1.0 second. When the explosion intensity increases by several hundred times, the periods of the dilatational and transverse waves in the range of Δ = 200 - 1,000 km increase slightly. No dependence of the wave periods on the epicentral distance was observed (Figures 34, 35).

This problem is examined in greater detail in § 3 of Chapter V. Approximately the same periods were observed also during underground explosions of chemical explosives with a power from 0.17 to 1 kt [89].

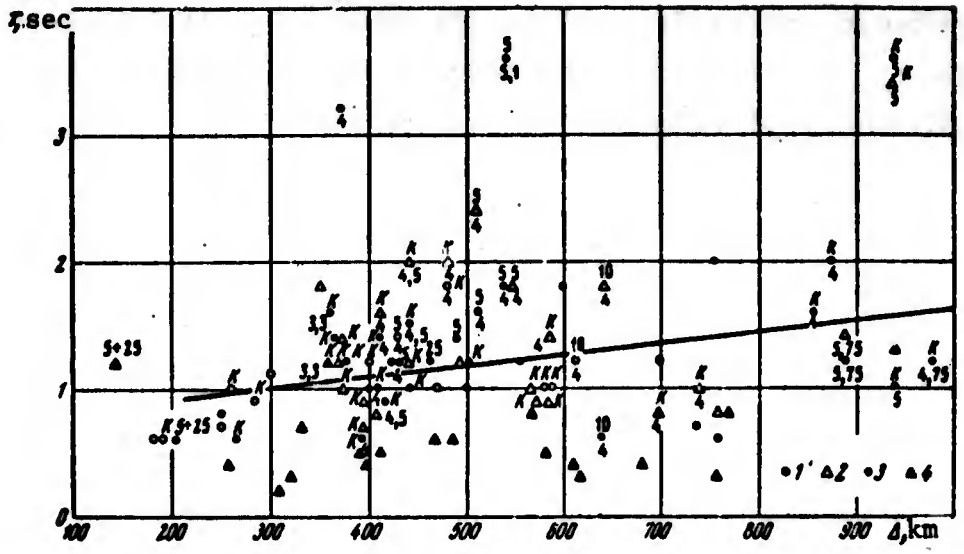

Figure 34. Dependence of the period of dilatational waves on the epicentral distance.

1 - 3 - for earthquakes with foci in the Earth's crust;
4 - for underground explosions.

Figures under the dots indicate the magnitudes M; figures over the dots indicate the depths of the foci, km.
K indicates a focus within the Earth's core.

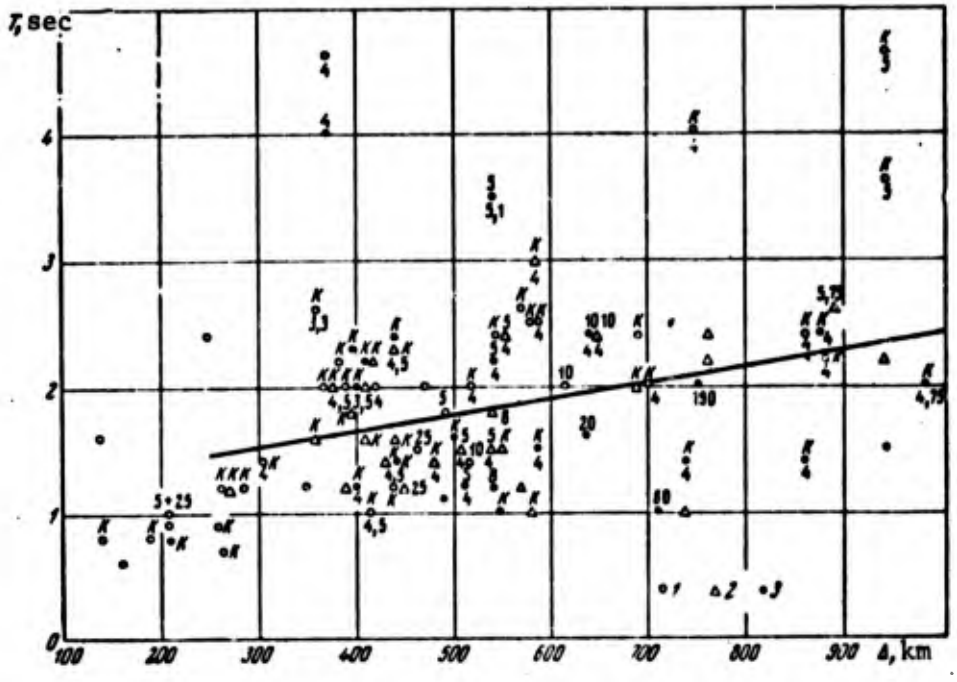

Figure 35. Dependence of the period of the transverse waves of earthquakes with their foci in the Earth's crust on the epicentral distance

1 - S wave; 2 - S* wave; 3 - S_n wave (the other symbols are the same as those in Figure 34)

During underground explosions accompanied by a discharge of soil onto the surface, in some cases the periods are 10 - 20% greater, in comparison with those of completely covered explosions (with no discharge).

A slight dependence of T_P and T_S on the properties of the rocks containing the explosion was also observed. They primarily depend on the acoustic stiffness in them ρv (ρ is the density, and v is the velocity of the P wave). The periods are 20 - 30% greater during explosions in dry, porous rocks such as alluvium, volcanic tuff, and others, in comparison with the corresponding values of ρv during explosions in dense crystalline (granites, basalts, etc.) and metamorphic (gneisses, etc.) rocks.

The values of T_P and T_S depend on the depth of the explosion. Thus, for instance, during explosions in deep holes, P and S waves were recorded with periods about one half of those obtained during explosions with charges of equal intensity carried out at depths of about 200 - 250 m.

Underwater explosions. The values of dilatational and transverse wave periods recorded in zone I were obtained during shallow-water explosions of a relatively small intensity. A characteristic feature of these explosions is that they have oscillations of the shortest periods for dilatational and transverse waves, in comparison with the oscillation periods in other types of explosions. For the P^* and P_n waves, the periods are about 0.2 - 0.8 second, and for S^* and S_n waves they are about 0.7 - 1.2 second.

Thus, the periods of the P and S waves recorded in zone I in a range of Δ = 200 - 1,00 km in all types of explosions, in recordings of instruments of type SK and others, fall within the following ranges: for dilatational waves, from 0.2 - 0.6 to 1.0 - 1.7 seconds, and for transverse waves, from 0.8 - 0.9 to 1.7 - 2.0 seconds.

§ 5. The Relationship T = T(Δ) of the Dilatational and Transverse Waves of Shallow-Focus Earthquakes, Propagated in the Earth's Crust

This relationship was studied in detail for a broad range of Δ in [90], including the regions of Central Asia and Western Siberia. However, the data given below were obtained in [99] by the same methods used in establishing analogous relationships for explosions. The relationships presented are close to those obtained in [90] for Central Asian earthquakes in the range of Δ = 200 - 1,000 km.

The changes of T = T(Δ) in the records of wide-band seismographs for the P, P*, P_n, $\bar{S}$, S*, and S_n waves in the range of Δ = 300 - 900 km for earthquakes with M = 4 - 5 with foci in the Earth's crust can be expressed by the following approximate linear dependences, which have been established experimentally [99]:

for $\bar{P}$, P*, and P_n waves:

$$T_{\bar{P},\,P^*,\,P_n} = (1{,}0 \pm 0{,}3) + 0{,}007\Delta, \tag{11}$$

for S, S*, and S_n waves:

$$T_{\bar{S},\,S^*,\,S_n} = (1{,}5 \pm 0{,}3) + 0{,}001\Delta. \tag{12}$$

Graphs illustrating the relationship T = T(Δ) for dilatational and transverse waves propagated in the Earth's crust are given in Figures 34 and 35.

The following conclusions can be drawn from a comparison of the relationship of $T_{P,S}(\Delta)$ observed in zone I during explosions and earthquakes, with comparable magnitudes: 1) during atmospheric and contact explosions, the periods of the P and S waves are approximately the same as those during the earthquakes which were examined; 2) during underground and underwater explosions, the periods of the P and S waves

are generally 20 - 30% less than the periods of the corresponding waves during earthquakes. The very highest values of T_P and T_S during explosions overlap with the corresponding lowest values during earthquakes.

§ 6. Character of Body Wave Polarization

The polarization of dilatational waves was studied by plotting the motion trajectories of soil particles in the given wave in a vertical plane on the basis of observations of two components: the vertical Z component and the horizontal-radial H component, oriented towards the epicenter.

For transverse waves, the trajectories were plotted both in the vertical and in the horizontal plane.

Polarization of the dilatational waves. Numerous trajectories plotted for dilatational $\bar{P}$, P*, and P_n waves, when recordings were not complicated by other oscillations, indicate that these waves have an almost linear polarization character in the vertical plane (see, for example, Figure 36). This applies to explosions carried out in various media — in the atmosphere, under the ground, and underwater. The trajectories plotted in the vertical plane passing through the epicenter and the station are inclined in the direction from the epicenter. In most cases, the trajectories of the dilatational waves have the form of ellipses. This may possibly be connected with the insufficiently exact identification of the magnification of the vertical and horizontal seismographs, and also with the heterogeneous structure of the upper part of the cross section.

The apparent angles e_0^* of departure of the seismic radiation in a given wave were determined from the inclinations of the trajectories with respect to the abscissa axis in cases when they were linear, or according to the inclinations of the major ellipse axes in cases when the trajectories were elliptical. The value of e_0^* was also determined according to the formula:

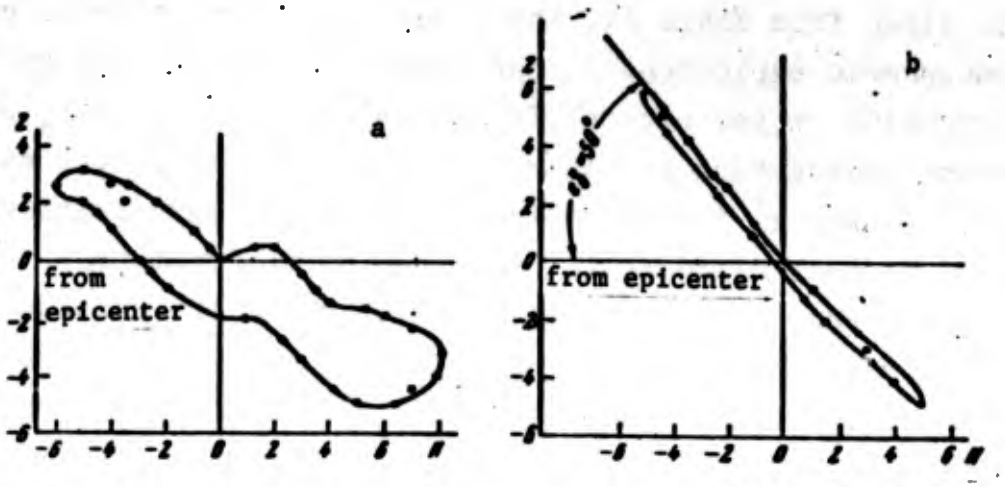

Figure 36. Trajectories of motion of particles of the medium in $\bar{P}$ and P_n waves recorded during air explosions

a - Δ = 100 km, P wave; b - Δ = 270 km, P_n wave. Between dots there is a time interval of 0.1 second.

$$\operatorname{tg} e_0^* = A_Z/A_R. \qquad (13)$$

Examples of e_0^* determined in this way for $\bar{P}$ and P_n waves excited by atmospheric and underground explosions in various regions are given in Table 21.

TABLE 21. VALUES OF APPARENT DEPARTURE ANGLES e_0^* FOR P* AND P_n WAVES, DETERMINED ACCORDING TO THE TRAJECTORIES OF MOTION OF PARTICLES OF THE MEDIUM

Epicentral distances Δ,,km	Type of wave	e_0^*, degree	Velocity v, km, sec	Epicentral distances Δ, km	Type of waves	e_0^*, degree	Velocity
80	$\bar{P}$	30.5	6.0	300	P_n	45	8.0
90	P*	35.5	6.4	360	P_n	50	8.0
100	P*	34.5	6.4	470	P_n	58	8.0
270	P*	34.5	6.4	620	P_n	62	8.0

As is clear from Table 21, the value of e_0^* for P* waves recorded during atmospheric explosions in the range of Δ = 90 - 270 km fluctuates (depending on the region) from 34.5 to 35.5°. For P_n waves traced during underground and atmospheric explosions in the range from 360 to 620 km, e_0^* increases from 45 to 62°. This scatter in the values of e_0^* at near distances Δ is caused by the fact that the observations were carried out in regions with different structures of the sedimentary and metamorphic rock strata, and, on the other hand, by the possibility of errors in identifying the amplification of the seismographs.

For P* and P_n waves, the e_0^* angles in the entire tracing interval are close to the values calculated by formulas for head waves, or they increase somewhat together with the increase of Δ. This indicates that they are weakly refracted waves. We will show that a similar increase of e_0^* together with the increase of Δ was observed earlier for the corresponding waves, both during explosions [259, 263] and during earthquakes [291].

As far as the polarization of dilatational P* and P_n waves is concerned, no differences were observed from the polarization of the same waves caused by TNT explosions and earthquakes.

Polarization of transverse waves. During atmospheric and underground explosions, intense S* and S_n waves are recorded which have a considerable amplitude in the SV component. This amplitude is commensurable with the amplitude of the SH component. The train in the S* and S_n waves consists of oscillations which appear to be attributable to the same wave. However, when a trajectory is plotted in the horizontal plane, it turns out that only one or two of the first oscillations are associated with transverse waves uncomplicated by other oscillations. The subsequent oscillations in the trains are interference oscillations. This is distinctly visible from the differences between the trajectories of the subsequent oscillations and those of the first oscillations (Figure 37). For the subsequent oscillations

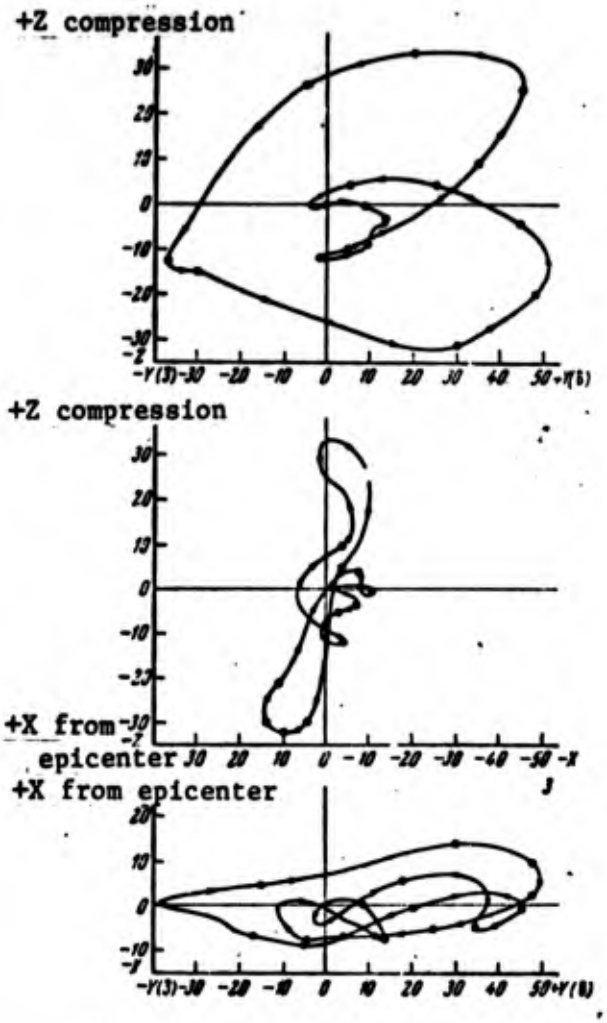

Figure 37. Trajectories of motion of particles of the medium in S wave recorded during an underground nuclear explosion at (Δ = 70 km)

1 and 2 - in vertical planes;
3 - in horizontal plane.

a change in the inclination of the trajectory and even a change in the direction of motion of the particles takes place.

The polarization in the initial part of the recording of oscillations of the transverse S* and S_n waves in the horizontal plane is nearly linear, although the trajectories in most cases have the appearance of elongated ellipses. In the subsequent part of the recording, the polarization has a complex character.

Particles of the medium in the S* and S_n waves in the vertical plane move away from the epicenter.

The angles of departure of seismic radiation, calculated according to the trajectories of motion of the particles for the transverse waves, are determined with less certainty than when they are calculated according to the dilatational wave trajectories. In general, however, they are close to the angles determined from the recordings of the corresponding dilatational waves.

Polarization in transverse waves during atmospheric, underground, and underwater explosions is the same as for the corresponding waves of earthquakes.

The above description of the wave pattern for dilatational and transverse waves in zone I, their hodographs (Figures 28 - 31), the wave velocities, the areas where they are traced (Table 19), and also the polarization (Table 21) indicates that the characteristics observed during explosions and during earthquakes with surface or shallow foci have similar values. This similarity is observed in explosions carried out in different media. This makes it possible to make use of the methods worked out in seismology for determining the seismic elements (the coordinates of the epicenters, the time at the focus, the angles of departure of the seismic radiation, etc.) in interpreting the recordings. At the same time, the possibility arises of making use of the regional hodographs obtained from a study of earthquakes for calculating the coordinates of the explosion epicenters, regardless of the medium in which these explosions occurred. The practical results obtained from applying the methods of interpretation worked out in seismology for determining the above-mentioned seismic elements in explosions confirm the correctness of the conclusions reached.

The following section gives a short description of some of the dynamic characteristics of the waves propagated in zone I.

§ 7. Character of the Drop in the A/T Ratio of Body Waves Together with the Increase of the Epicentral Distance in Zone I

Experimental seismic data obtained chiefly during underground nuclear explosions, and to a small extent during TNT explosions, are used to study the dependence of the A/T ratio of seismic waves on the epicentral distance Δ in zone I. Both these types of explosions produce similar recordings of the corresponding waves, and the behavior revealed in the recordings made it possible to also establish their quantitative agreement.

The dependence of A/T on Δ has been studied most thoroughly in zone I during underground nuclear explosions and TNT explosions.

The use of underground nuclear explosions for determining the dependence of A/T on Δ in body waves recorded in zone I was due to the following favorable factors:

1) The waves can be traced well during numerous explosions carried out in practically the same place;

2) During underground explosions, the energy of the body waves exceeds by 1,000 times or more the energy of the corresponding waves caused by contact and atmospheric explosions of the same intensity;

3) The oscillations in waves excited during underground explosions have a relatively shorter period composition ($T \approx 0.5 - 0.6$ second) than the corresponding spectral composition of oscillations in waves caused during atmospheric explosions ($T_p \approx 1.0 - 1.5$ seconds). This makes it possible to considerably increase the effective sensitivity of the receiving equipment. The amplification of the receiving equipment during recording of underground explosions can be raised to $10^5 - 10^6$, that is, by a factor of $10^2 - 10^3$ higher than the amplification of the wide-band equipment used in recording earthquakes and atmospheric explosions.

4) The epicenters of underground nuclear and TNT explosions are located inside the continents. Therefore, the body waves in zone I were traced at many stations (located in regions with a continental structure of the Earth's crust) both from the profiles oriented along different azimuths and from a network of stations distributed over the area [325].

Methods of studying the dependence of A/T on Δ. The dependence of A/T on Δ was studied in the following manner. Curves for $A/T = f(\Delta)$ were plotted in the system of coordinates $\lg(A/T)$; $\lg \Delta$. Then the amplitudes of the oscillations in the given wave were taken in millimicrons, the periods in seconds, and the epicentral distances in kilometers. Curves were plotted for the maximum oscillations for

the $\bar{P}$, P*, P_n, S*, V and S*H waves. In addition, analogous curves were plotted for the P_n waves for the first oscillation. The latter was of interest due to the possibility of identifying explosions from the direction of the first motion in the first dilatational wave.

Then the A/T curves plotted for each separate explosion were averaged graphically. The exponent n of the function of divergence and the amplitude absorption coefficient α in body waves propagated in the basic layers of the Earth's crust were determined according to the averaged curve [99, 100]. When several explosions were carried out from the same epicenter, the observed values of A/T were first reduced to a single level and entered in a single graph. The experimental values were then averaged graphically, and the values of n and α were determined according to the methods described in [18, 108].

Figure 38 gives examples of the curves discussed for the regions of Central Asia (chemical explosions) and for Nevada (nuclear explosions).

Decay of A/T with Δ. The law by which A/T of body waves, connected with the main boundaries in the Earth's crust, decreases with the distance in an ideally elastic medium may be expressed by the following relationship:

$$\frac{A}{T} = \frac{A_0/T}{(\Delta_i/\Delta_0)^q}, \qquad (14)$$

where A and A_0 are the amplitudes of the oscillations, respectively, at the point of observation and at a point closer to the epicenter. It is assumed that both points are located beyond the initial point of the wave, and Δ_i and Δ_0 are the corresponding epicentral distances.

In real media there is absorption. Therefore, if we approximate the observed curve by an exponential function of the type (14), and by a straight line in the selected system of coordinates (lg A/T, lgΔ), the factor q will be the effective divergence function which includes

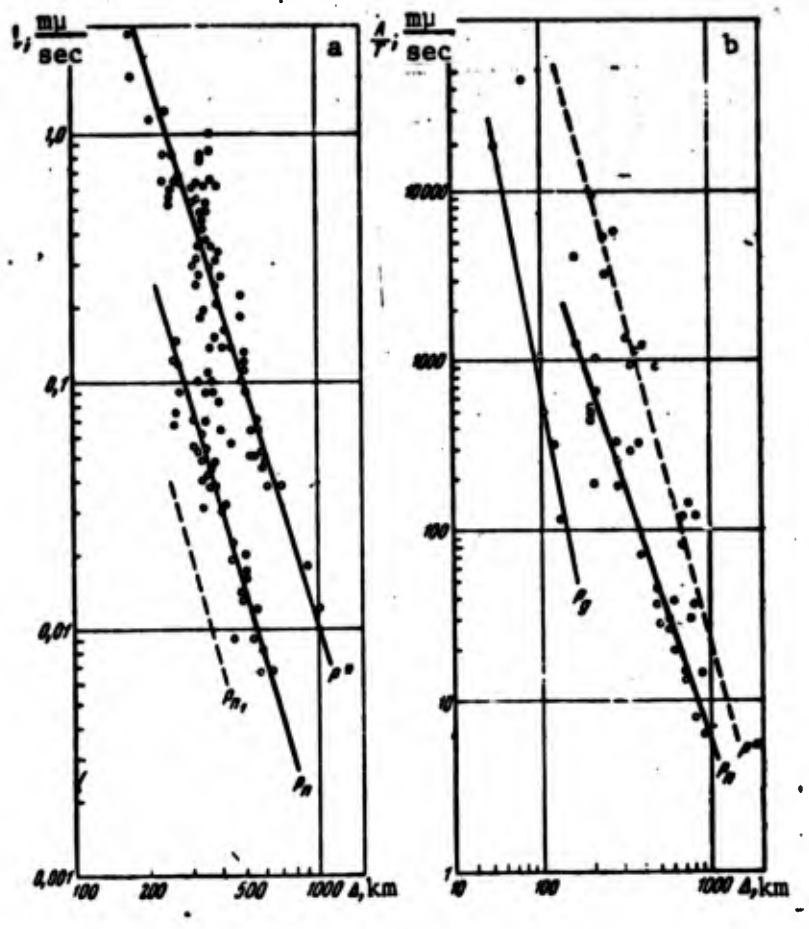

Figure 38. Amplitude graphs for P* and P_n waves observed during underground explosions in the continental region

a - for the Central Asia region;
b - for the Nevada region, according to data from [325].

Dots indicate experimental data

the decay of A/T together with the increase of distance Δ due to an increase of the wave front surface and due to absorption.

The average values of q for different waves observed in a number of regions during underground explosions and earthquakes found according to Formula (14) from the amplitude curves are given in Table 22.

TABLE 22. VALUES OF EXPONENT q IN FORMULA (14) FOR BODY WAVES OF VARIOUS CLASSES RECORDED IN ZONE I DURING EXPLOSIONS AND EARTHQUAKES

Region of epicenter	$\overline{P}$			P^*			P_n			S^*V, S^*H			S_nV			Literature
	range of Δ, km	T, sec	q	range of Δ, km	T, sec	q	range of Δ, km	T, sec	q	range of Δ, km	T, sec	q	range of Δ, km	T, sec	q	
Explosions																
Nevada	50—135	0,3—0,5	5,2	200—800	0,5—0,8	3,0	180—1100	0,5—0,8	3	200—500	1,1—1,2	2,8	200—500	1,1—1,2	2,8	
				160—800	0,3—0,5	3,2	160—950	0,3—0,5	3,06	200—2000						[317]
							180—1000	0,6—0,8	3,0		1,2—1,5	2,9—3,0				[325]
New Mexico			4,0						3,0							[322]
Earthquakes																
Central Asia	80—500	0,8—1,2	3	200—500	1,0—1,5	3	250—800	1,0—1,5	3,0	250—500	1,2—2,5	2,8				Author

As is clear from Table 22, the values of q for the P_n and S_nV waves with periods of 0.5 - 0.8 second are about 3.0; the same value of q has been established for S_nH waves.

The value of q found for the curve by averaging the amplitudes A_{P_n} of the first motion of the P_n wave is 3.2. This indicates that there is a stronger attenuation of A_{P_n} for the first motion than for the maximum oscillation amplitudes in this wave. The value of q in the P* wave is around 3.2, and for the S_n and S* waves the values of q are approximately 3. The standard deviation for the determination of q amounts to 0.1 to 0.15.

The fact that the values of A/T of P_n, P*, S_n and S* waves decrease inversely in proportion to Δ in the same degree leads to the conclusion that there is greater absorption of the transverse S_n and S* waves, since the oscillation periods in the transverse waves are approximately 1.5 - 2 times greater than those in the dilatational P_n and P* waves.

Out of all the waves examined, the most significant decrease in A/T together with the decrease of Δ was that observed for the P_0 waves. For the $\bar{P}$ waves, the value of q is close to the value of q for the P* and P_n waves.

An analysis of the amplitude curves plotted for the waves recorded during atmospheric explosions shows that the dependence of A/T on Δ is approximately the same as that established for waves recorded during underground explosions.

Determining the absorption coefficient of the waves and the exponent of the divergence function according to the amplitude curves. At the present time, amplitude curves have been obtained only for single profiles. Nevertheless, even from single amplitude profiles, the amplitude absorption coefficient α and the exponent of the

divergence function n for the $\bar{P}$, P*, P_n, S*, and S_n waves can be estimated by using methods developed in seismic prospecting [16, 18, 108].

It has been established theoretically and experimentally that the decrease in the oscillation amplitude of head waves, together with the decrease in Δ, can be expressed by an asymptotic relationship of the following type:

$$A = \frac{A_0 e^{-\alpha(\Delta_i - \Delta_0)}}{\left(\frac{\Delta_i}{\Delta_0}\right)^n}. \qquad (15)$$

Here, A_i and A_0 are the same values as in (14), and n and α are, respectively, the exponent of the divergence function and the amplitude absorption coefficient. For media with a constant velocities, the asymptotic value of n is 2 [18].

It must be noted that Formula (15) is, strictly speaking, inapplicable in the case of refracted waves. However, if the waves are weakly refracted and are observed at epicentral distances not exceeding 10 - 15 of the boundary depths, for approximate estimates it can be assumed that the waves glide along the refracting boundary.

In the numerous experimental determinations of n carried out in seismic prospecting in a thick-layer medium, the average values of n are close to 2, and the maximum values fluctuate within the range of 1.5 to 2.5 [16, 18].

In the present work, three methods were used to determine n and α: 1) The method of selecting a theoretical curve which best approximates the observed experimental amplitude curve; 2) the method of simultaneously determining n and α by a single curve [108]; 3) the spectral method [18].

Table 23 gives the values of the exponent of the divergence function and of the amplitude absorption coefficient α for the P_n,

TABLE 23. VALUES OF THE EXPONENT OF THE FUNCTION OF DIVERGENCE AND THE AMPLITUDE COEFFICIENT OF ABSORPTION FOR WAVES CONNECTED WITH THE BASIC BOUNDARIES IN THE EARTH'S CRUST, OBSERVED DURING UNDERGROUND EXPLOSIONS

Type of wave	Dominant period T, sec	By method of selection [16]		By method [108]		By amplitude spectra		Mean values	
		n	α, km^{-1}	n	α, km^{-1}	n	α, km^{-1}	n	α, km^{-1}
$\bar{P}$ maximum oscillations	0.4								0.017 [132] 0.0076 [325]
P_n first motion	0.3-0.4	1.9	0.004	2.2	0.0042	-		2	0.0035 ± 0.001
P_n maximum oscillations	0.6-0.8 0.3-0.5	2.0	0.002	2.0	0.0024	2 -	0.0023	2 -	0.0021 ± 0.0002 0.0022 [325]
S_nV maximum oscillations	1.0-1.5	2.0	0.002	1.4	0.0025			1.7	$0.0022 \pm\pm 0.0003$
S_nH maximum oscillations	1.0-1.5	2.0	0.002	1.4	0.003			1.7	0.0025 ± 0.0005

P* and S* waves found from recordings of underground explosions with single amplitude curves, and from their spectra by the above-mentioned methods. The values of the predominant periods of the waves in the recordings obtained by seismographs with a narrow passband are also given.

The values of α given in Table 23 for the first motion in the P wave is approximately twice as large as that for the maximum oscillations in the same wave. The values of α for the maximum oscillations in the P_n waves and in the S* waves are very close to each other.

The values of the absorption decrement for the P_n and S* waves are 0.012 - 0.014. This agrees with the values found earlier by different methods for certain crystalline rocks — granites and others (Table 24).

TABLE 24. VALUES OF ABSORPTION DECREMENTS θ AND VALUES OF $Q=\frac{\pi}{\theta}$ FOR EARTH'S CRUST FOR DILATATIONAL, TRANSVERSE, AND SURFACE WAVES

Region of epicenter	Type of wave	Recording range Δ, km	Range of T, sec	Accepted value of V, km/sec	Decrement $\theta=\frac{\pi}{QvT}$	$Q=\frac{\pi}{\theta}$	Method of determination	Literature
Explosions								
Central Asia (TNT explosions)	P^*	200—1000	0,8	6,4	0,021	150	Amplitude	Author
	P_n	200—800	0,6	8,4	0,024	130	»	»
	S^*	300—1200	1,2	3,7	0,012	260	»	»
	S_n	300—1000	0,8	4,3	0,012	260	»	»
	L_{g1}	150—1500	0,8	3,55	0,017	190	»	»
Nevada (nuclear explosions)	P_0	50—130	0,3	4,5	0,039	80	»	»
	P_n	180—450	0,3	5,5	0,016	200	»	»
	P_n	180—650	0,2—1,0	5,5	0,017	135	»	»
	P_n	200—1000	0,5—0,8	6,4	0,011	286	»	»
	P_n	200—750	0,6—0,8	8,0	0,013	241±30	Amplitude, spectral	»
	P_n	100—450	0,3	8,0	0,0055	570	Amplitude	[325]
	S^*	260—600	1,7	3,7	0,012	242±17	»	Author
	L_gL_{g1}		0,8	3,55	0,007	450±30	Spectral	[304]
	P_0		0,8	4,5	0,012	260±40	»	[304]
Earthquakes								
Central Asia	P_0	10—80°	0,025—1	4,8÷5,2	0,033	95	Spectral	[32]
	S_0	10—80	0,025—1	2,7÷2,9	0,025	126	»	[32]
	$\overline{P}$	15—100°	0,025—1	6,0÷6,1	0,017	184	»	[32]
	$\overline{S}$	15—100	0,025—1	3,5÷3,6	0,009	350	»	[32]
Kurile Islands	$\overline{S}$	50—160°	0,2—0,3	3,5	0,0035	90	Amplitude	[30]
	$\overline{S}$	80—200°	0,2—0,5	4,5	0,005	628	»	[30]
	$\overline{S}$	100—250°	0,2—0,5	4,5	0,015	293	»	[30]
USA	L_g		8—20	3,2	0,016	200	»	[45]

*Hypocentral distances are shown

It must be noted that the estimates of n and α given here are approximate, since they were made from single amplitude curves. However, the fact that the values of α are close to each other for different regions indicates that there is a relatively high degree of approximation.

Dependence of the absorption coefficient of P_n and S_n waves on frequency. The dependence of the absorption coefficient α_P on frequency f was studied by the spectral methods by the author for the P_n waves [105] (see § 5, Chapter II). Similar determinations were undertaken in [304] for P_g and L_g waves.

It was established in this work that, in the range of periods T = 0.3 - 2.5 second, α_P depends linearly on f in accordance with the following expression:

$$\alpha_{P_{nZ}} = 0{,}0019/\text{км}^{-1}. \qquad (16)$$

The linear dependence of the absorption coefficient on the frequency was also obtained for the S_g and L_g waves [304].

On the basis of the data obtained, the absorption decrements of waves propagated in the Earth's crust were determined, and the values of $Q = \pi/\theta$ were also calculated.

Table 24 gives composite data on the decrements θ and Q, obtained during explosions and earthquakes found in this work and obtained by a number of other authors.

The values of α calculated by Formula (16) for periods of $T_{P_{nZ}}$ = 0.8 sec oscillations in P_n waves, observed during underground explosions in various regions, coincide with the data given in Table 24 and with those obtained by other methods.

§ 8. Distribution of Nodal Lines for Dilatational Waves During Explosions and Earthquakes

The analysis of numerous experimental data obtained during nuclear explosions of various types, and also during underground and contact TNT explosions, has established without doubt that the dilatational waves always arrive in the compression phase, regardless of the azimuth in which the station is located with relation to the explosion epicenter [99]. This is caused by the symmetry of the explosion source. At the same time, during earthquakes, the first motion in the dilatational waves is, as a rule, observed in the compression phase by some stations and in the dilatation phase by others. A similar distribution of the directions of arrival for dilatational waves during earthquakes is connected with the shifting nature of the forces acting in the source.

The distribution of the signs in the first motions of dilatational waves recorded by a network of stations during explosions and earthquakes was analyzed with the methods used to study the mechanism of earthquakes [41]. In this analysis, the results of processing the recordings for each station were plotted on a Wulff net (Figures 39, 40); the "+" sign indicates arrivals in the compression phase, and the "-" sign indicates arrivals in the dilacation phase.

The distribution of signs for explosions in all cases studied makes it impossible to draw nodal lines (Figure 39), even when, in the recordings of individual stations, the wave arrived in the dilatation phase. The latter is connected, not with the source, but either with incorrect switching on of the equipment or with the impossibility of distinguishing the first arrivals because of their small amplitudes. This can usually be established easily by the phase correlation of the waves [99].

The distribution of signs during earthquakes makes it possible to draw nodal lines in the overwhelming majority of cases (Figure 40).

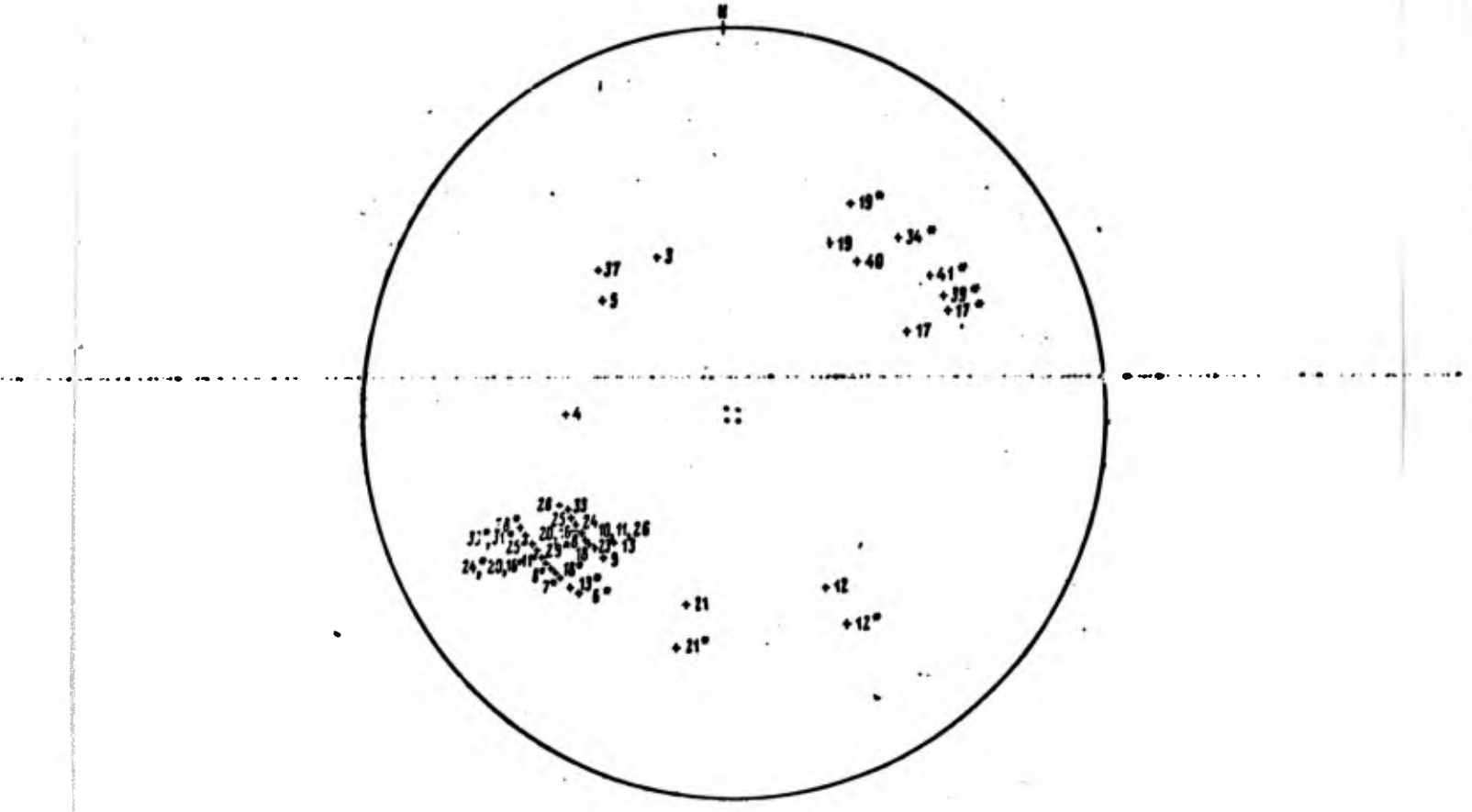

Figure 39. Distribution of directions of first motions in the first arrivals in dilatational waves recorded during an underground explosion

Figures are numbers of the stations

The differences in the distribution of signs of the first motions of dilatational waves during explosions and earthquakes may be used in identifying the recordings of explosions.

CONCLUSIONS

The following conclusions may be reached from the above comparison of the kinematic and dynamic characteristics of body waves propagated in zone I.

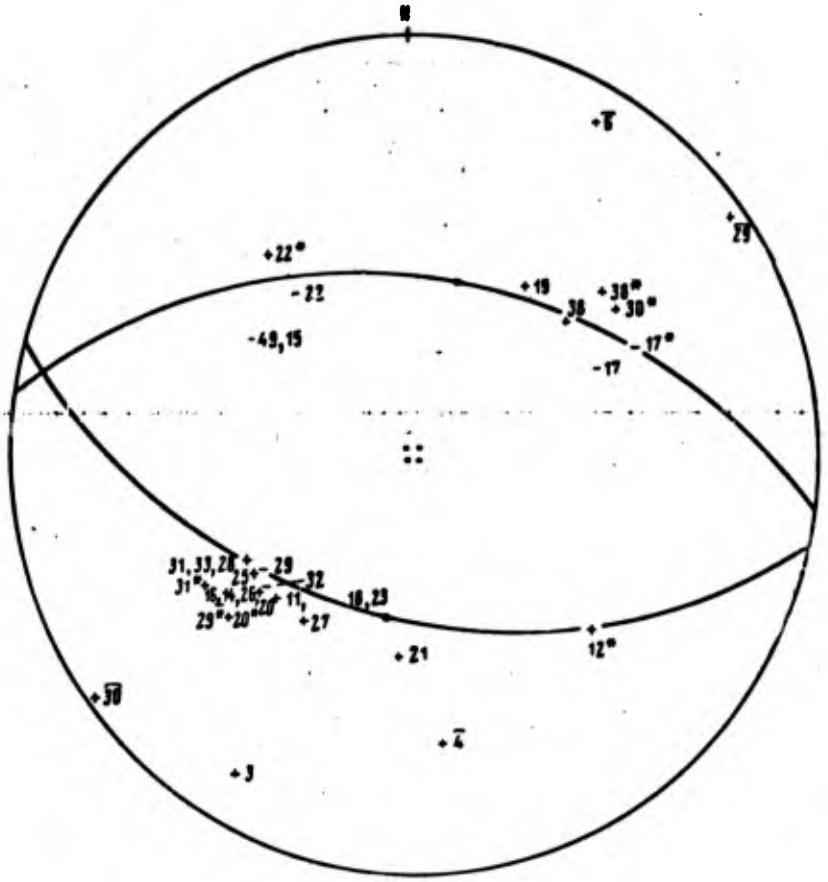

Figure 40. Distribution of directions of first motions in the dilatational waves recorded during an earthquake

Symbols are the same as in Figure 39

1. The wave pattern recorded in zone I during all types of nuclear explosions is analogous to the pattern observed during earthquakes.

2. The kinematic characteristics of the waves examined here — the hodographs, the propagation velocities, and the areas in which they are recorded in all types of explosions and in shallow-focus earthquakes (with their foci in the Earth's crust) — practically coincide. This makes it possible to use the methods of determining seismic elements, which were developed in seismology, in recording explosions.

3. It has also been established that there is a quantitative similarity, and even a qualitative similarity in some cases, for most of the dynamic characteristics of the waves examined here, which were excited by all types of explosions and earthquakes. This similarity is noted in the decay of the amplitudes of oscillations with the epicentral distance, in the ratio of the amplitudes to the period of the corresponding waves, in the values of the absorption coefficients and their dependence on frequency, in the motion trajectories of the particles of the medium, in the polarization, and also in the departure angles of the waves.

4. The following basic differences in the dynamic characteristics of the body waves of explosions and of earthquakes were established:

a) The periods of the body waves during underground and underwater explosions were 20 - 30% less than the periods of the corresponding waves of earthquakes with comparative magnitudes. The highest values of the periods during explosions overlap with the corresponding lowest values during earthquakes.

b) During underground and underwater explosions a comparatively smaller intensity of the oscillations is observed in the area of transverse waves than is the case for earthquakes. The ratio of the transverse wave amplitudes to the corresponding values of the dilatational wave amplitudes, A_S/A_P, is less than 2.5 for explosions, while for 90% of the earthquakes studied, $A_S/A_P > 2.5$.

c) During earthquakes a growth of the oscillation period is observed together with the increase of the epicentral distance. In explosions, this is almost never observed, or is observed to a smaller degree.

d) In explosions, in contrast to earthquakes, the dilatational waves usually arrive in the compression phase at all stations surrounding the epicenter.

CHAPTER V

CHARACTERISTICS OF BODY WAVES RECORDED IN ZONES II, III, AND IV

The fullest wave pattern in Zones II, III and IV is that observed during powerful atmospheric and contact explosions. The following body waves have been recorded during powerful explosions in the above-mentioned zones: P, PP, PPP, PPPP, PcP, PcS (ScP), PS(SP), PPS, PKP (PKP_1, PKP_2), PKPPKP, S, SS, SSS, SSSS, ScS, SKS and a number of others. During underground and underwater explosions, a less full wave pattern was observed. Specifically, forward and reflected transverse waves were recorded only in zone II, and in a few cases, in zone III, while exchanged reflected waves of type SP were not recorded at all [63, 99, 101, 145, 165-168, 180, etc.].

In most cases, P, PP, PcP, SP, PKP, and S waves were identified from a combination of a number of signs: travel times, the character of polarization, the decrease of the amplitude with the epicentral distance, etc. Other waves were identified only by travel times and the character of the polarization. In all cases, the times in the epicenter and the coordinates of the epicenters of the explosions were known exactly, either from the reports of the Atomic Energy Commission of the USA or from the seismic bulletins of the Coastal and Geodesic Service of the USA and other publications. Examples of seismograms

with records of body waves obtained during various types of explosions are given in Figures 3 - 5, 10, and 41. Examples of hodographs of the body waves recorded during atmospheric and underground explosions are shown in Figures 29 and 42.

Records of Soviet seismic stations, as well as data given in works [145, 146, 63, 309, etc.] and in the seismic bulletins of the USA, Sweden, and other countries were used mainly in plotting the hodographs.

The hodographs given are the most complete for the given types of explosions. The descriptions of the wave patterns in earlier works [63, 99, 101, 168] referred chiefly to dilatational waves, caused by contact and sometimes underground explosions; transverse waves are not examined in them.

Comparatively few works are devoted to studying the dynamic characteristics of body waves caused by explosions in the zones under discussion, and the dynamic characteristics of the PP and S waves, including those during atmospheric explosions, were hardly studied.

In this chapter, an attempt is made to analyze these characteristics chiefly on the basis of the experimental materials obtained in the seismic stations of the USSR during various types of explosions.

The data at our disposal made possible a relatively thorough study of the kinematic and dynamic characteristics of the P waves recorded during all types of explosions. These waves are most important for detection and identification of explosions. Other types of waves, such as the PKP waves, whose records were obtained mainly by foreign stations, are characterized less completely.

Records of the PKP waves during underground explosions were obtained in Soviet stations only by the Antarctic stations at Mirnyy and at Oazis Banger [99]. These stations were set up in 1956 [66, 67, 87]. Records of the PKP waves during the underwater Wigwam explosion

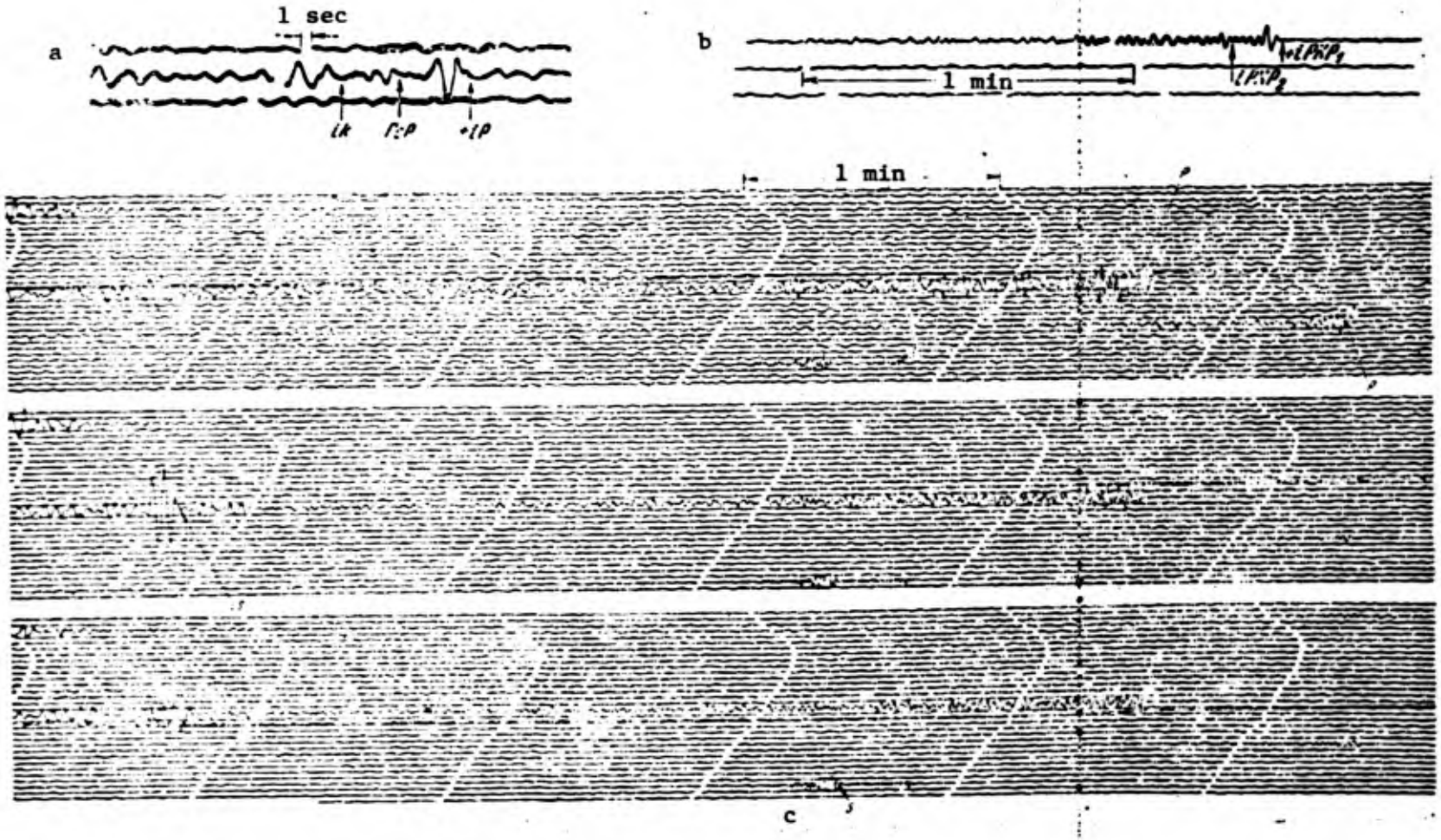

Figure 41. Examples of records of body waves of nuclear explosions carried out in various media. a: Δ = 9,000 km during a contact explosion in the Marshall Islands. b: PKP_1 and PKP_2 waves (Δ = 16,500 km). c: 1 - record of a deep-focus earthquake (Δ = 2,340 km); 2 - record of waves of a contact explosion (Δ = 5,150 km); 3 - record of a local earthquake (Δ = 136 km).

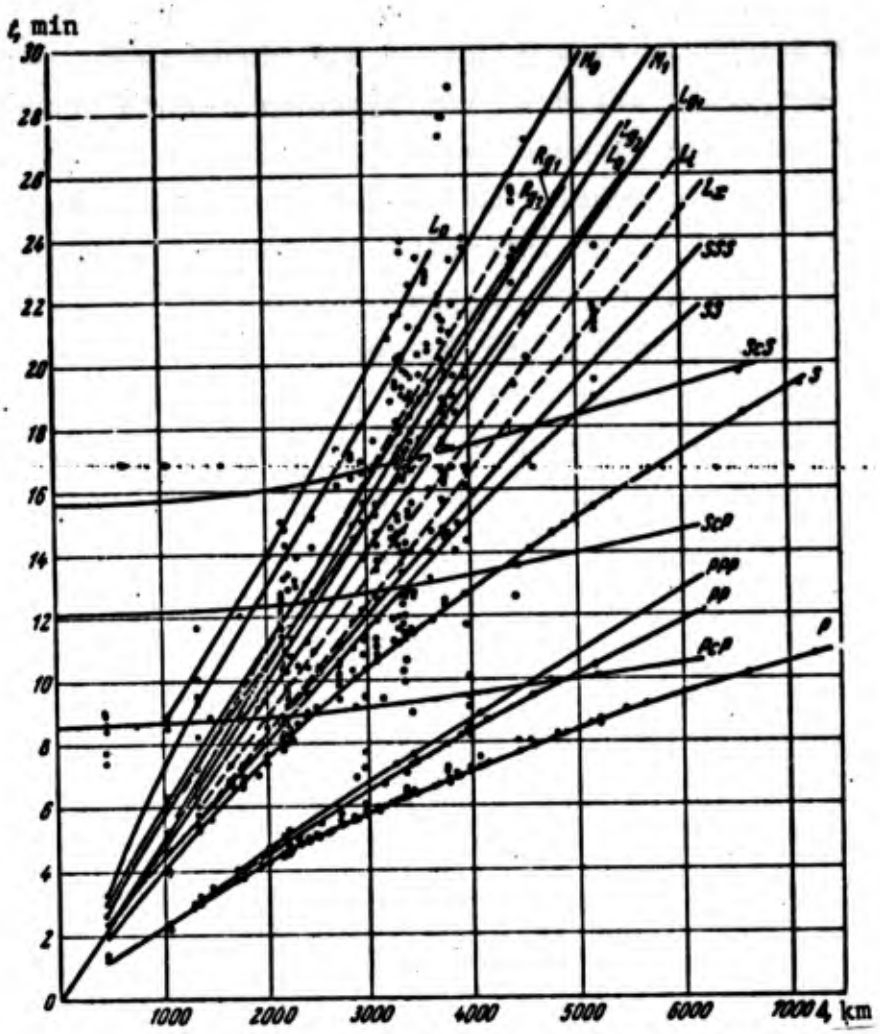

Figure 42. Composite hodographs of some body and surface waves recorded during atmospheric explosions. The experimental values of the travel times of the waves are indicated by dots. The Jeffreys-Bullen hodographs for the surface focus are indicated by solid lines for the body waves, and the observed averaged values for the surface and channel waves, are shown by broken (sic) lines.

were obtained in the USSR stations of the ESSN (Unified System of Seismic Observations) [23].

§ 1. Character of Oscillations in Body Waves Recorded During Various Types of Explosions

Noticeable differences in records of body waves are observed, depending on the type of explosion.

During atmospheric explosions in all three zones, body (dilatational and transverse) waves of the types mentioned above are recorded. Approximately the same types of waves are observed also in records of powerful contact explosions. During underground and shallow-water explosions with about 20 kt intensity, transverse waves are recorded only in zone II and in the beginning of zone III. At a distance of $\Delta > 5{,}000 - 6{,}000$ km, only P and PcP waves are observed, and also PP and PcS waves in some cases. In zone IV, only PKP (PKP_1 and PKP_2) waves are observed, and in some cases PKPPKP waves. During deep underwater explosions, the records have a somewhat different character. They are complicated by numerous groups of oscillations whose amplitude is commensurate with oscillations in the basic waves. The nature of these groups is not yet clear. Part of them are connected with repeated blasts, and part with reflections from the uneven ocean bottom. In observations along the continental channels, in zone II and in the beginning of zone III — in the area of arrival times of reflected PcP, PcS, ScS and other waves — the seismograms are complicated both by channel waves L_x, L_i, and L_g, and also by Rayleigh and Love surface waves. In observations along the oceanic channels, they are complicated only by surface waves: channel waves along the oceanic channels during explosions either are not observed or are of low intensity just as during earthquakes.

Depending on the type of explosion, changes are observed in the amplitude ratios of waves of different types, as well as differences in the apparent periods of waves and in the durations of the oscillation trains, and the appearance of some new groups of oscillations, particularly during underwater explosions. However, the travel times, the departure angles, the character of polarization, the trajectories of motion of soil particles, and other characteristics of the waves remain practically unchanged, regardless of the type of the explosion.

A short description of the records of seismic oscillations is given below. The description is more detailed for the P waves, which are most clearly recorded during underground, underwater, and contact

explosions, and also during the most powerful atmospheric explosions. As is known, P waves are of basic significance in detection and identification of all types of nuclear explosions, with the exclusion of relatively low-power atmospheric explosions, in which the P waves are of a low intensity (explosions with a power of about 15 - 20 kt), and it is not always possible to record them at considerable distances of $\Delta > 1{,}000 - 2{,}000$ km.

By means of the arrival times of the P waves, one can determine most exactly the epicenter coordinates of explosions with an accuracy of about $\pm 2 - 4$ km, and the times of the focus with an accuracy of ± 1 sec. The intensity of these waves can be used to estimate the power of the explosion [99, 110, 196, 326, etc.].

Characteristics of records of body waves. During the most powerful nuclear explosions (underground, underwater, contact, and atmospheric), type SK wide-band equipment has been used to record exactly the arrivals of the P waves, which as a rule arrive in the compression phase.. In all cases, the P waves assume the form of a short oscillation train, consisting of one, or more seldom two or three oscillations, whose period depends on the type of explosion (see Figures 3, 41, etc.). In all types of explosions, the shape of the records resemble each other.

The composite Table 25 gives data about the periods T of the waves recorded during various types of explosions and earthquakes, mainly by wide-band seismographs. The regions where they were traced are also shown.

The dependence of the periods of explosion P waves on the epicentral distance is very insignificant (Figure 43).

The periods of oscillations in the body waves in the seismograms depend on the correlation between the frequency characteristics of the receiving channel and the spectrum of the oscillation which is recorded.

TABLE 25. MEAN VALUES OF THE VISIBLE PERIODS OF THE BODY WAVES RECORDED DURING VARIOUS TYPES OF NUCLEAR EXPLOSIONS AND EARTHQUAKES

Type of source	Region of epicenter	Range of Q, km	Height or depth, m	Range of Δ, km (for P waves)	Periods of T waves, sec							Type of seismograph	Range of magnitudes	
					P	PP	PcP	PKP	S, PS	SS	SKS		M	$m_{P,S}$
Underground explosions	Nevada	1—200	300—700	1100—12000	0,7—2,0	1,0—2,0	1,0—2,0	1,4—2,0	1,2—2,0	—	—	SK, SKM, Benioff	4,0—4,4	4,6—6,2
	Alaska	80	700	4000—6000	1,0—2,0	1,0—1,5	1,0—1,5	1,2—1,6	1,5—4,0	—	—	SK, SKM	—	6,1
	Sahara	10—30	300	3000—8000	0,7—1,2	1,0—1,1	1,0—1,1	—	1,5—2,0	—	—	SKM	—	5,3—5,8
Underwater explosions	Pacific Ocean	5—30	600	5000—12000	2,5—3,0	2,5—3,5	—	3,0				SK, Benioff	—	5,5—6,5
	» »	5—10	50—150	4000—12000	1,0—1,5	1,0—1,3						SKM	—	5,5—5,8
Contact explosions	Marshall islands	10000—15000		4500—11000	4,5—5,5	1,5—5,5	4—5		7—12		7—12	SK	4,0—4,8	5,8—6,3
Atmospheric explosions	Christmas island	11000—27000		1100—10000	8—10	6—8	8—10		8—18	8—10	10—18	SK, SKD, Benioff	4,5—5,1	4,1—5,4
				8000—9000	8—10				12—15			SK, SKD	5,3	5,0
Earthquakes	From all regions		0—$7 \cdot 10^3$	3500—11000	3—5	3—15	3—10	3—16	10—16	9—16	9—16	SK, SKD	5,5—8	6—8

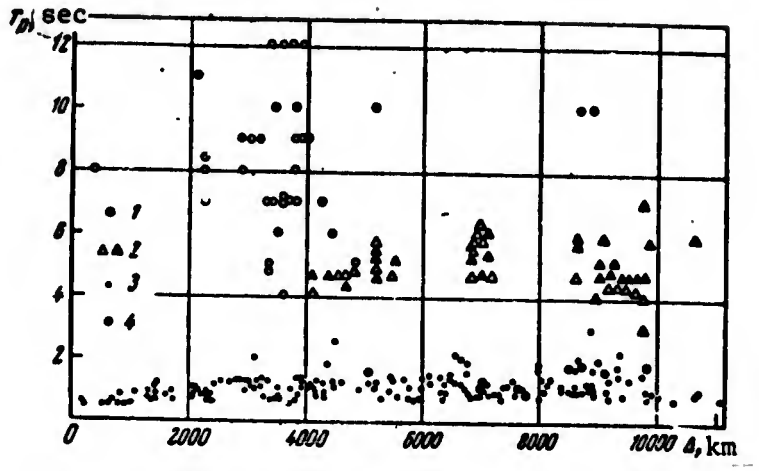

Figure 43. Dependence of periods T_p in P waves on the epicentral distance for nuclear explosions, carried out in various media. 1 - Atmospheric explosions; 2 - Contact explosions; 3, 4 - Underground and underwater explosions. Dots (3) indicate values obtained from records of seismographs with narrow passband; circles (4) indicate values obtained from records of wide-band seismographs.

The least distortions of the periods, not exceeding several percent, are attained when the body waves of all types of explosions are recorded by wide-band equipment of type SK. When equipment with a narrow passband (SKM, USF, Benioff, etc.) is used, the periods of oscillations in the records are distorted considerably when the wave spectrum maximum lies outside of the passband of the equipment.

In cases when the passband of the equipment with a narrow band does not coincide with the spectral band — for instance, when one is recording the body waves of atmospheric or contact explosions — the dominant periods of the oscillations in the records of such equipment are considerably less (by 3-4 times) than those in the records of SK seismographs.

During underground and underwater explosions, the spectral band falls within the range of the equipment passband with a narrow band, and in this case the periods in recordings from this equipment coincide

with, or are close to, the periods measured in the records of wide-band SK seismographs.

In all types of explosions we tried to use records of body waves obtained with wide-band equipment of type SK with a passband from 0.2 to 10 - 12 sec when determining the values of T in the seismograms.

During low-intensity underground explosions and shallow-water underwater explosions (with Q < 20 kt), we were unable to obtain records with type SK seismographs, particularly in zone III. In this case the periods were measured by means of records of SKM, USF, and partly Benioff seismographs with a narrow passband. Here the periods of the waves recorded by seismographs of different types were compared by the spectra, into which corrections for the irregular amplification of the equipment had been introduced previously.

It must be noted that, during powerful underground explosions, such as that of September 13, 1963, in Nevada (Q = 200 kt), that in Amchitka (Q = 80 kt), and others, the records of the body waves were simultaneously obtained in the same stations by means of both SK seismographs and SKM and USF seismographs with a narrow passband. This made it possible to compare the periods of the identical waves obtained by different types of equipment. The periods of the P waves were similar in the records of the SK seismographs and in those of the SKM seismographs. The difference in T_P usually did not exceed 40 - 50%, and only during the most powerful explosions did the periods of the P waves in the records of the SK seismographs exceed by two times the T_P in the records of the SKM seismographs.

The shortest periods of the P waves (from 0.5 to 2.0 sec) were observed in the records of underground and shallow-water underwater explosions, while during explosions carried out recently in deep holes (h > 1,000 m), the periods of the waves in the range from 2,000 to 10,000 km amounted to approximately 0.2 and 1.5 sec, respectively.

Somewhat greater values of the periods of the P waves (2.5 - 3.0 sec) were observed during deep-water underwater explosions. The values of the periods in the P waves increased to 4 - 6 sec during contact explosions, although the largest values, on the order of 8 - 10 sec, were observed during atmospheric explosions.

The periods of the body waves for each type of explosion, as a rule, depend very little on intensity. For underground explosions this question is examined in § 3 of this chapter.

The periods of P and S waves of earthquakes with $h \leq 100$ km and M of 4.5 to 6.5, recorded in the interval of Δ from 30° to 100°, depend only slightly on Δ; the average values are $T_p \approx 4.5 - 5$ sec, $T_S \approx 7.5$ sec (Figure 44). At a distance of $\Delta < 20°$, a dependence of T_p and T_S on Δ is found. In this interval of Δ, the values of T_p increase from 2.5 sec at $\Delta = 10°$ to 3.5 sec at $\Delta = 25°$, and those of T_S, respectively, from three to six sec. The growth of the periods noted in the given interval of Δ is apparently connected with the fact that, at a distance of $\Delta < 20°$, the P and S waves are generally recorded from earthquakes with $M \leq 4$. At a distance of $\Delta < 20°$ this can generally be recorded by SK instruments only in exceptional cases. The question of the dependence of T_P and T_S on M and Δ in earthquakes is studied in [90].

PP Waves. These waves are recorded during all types of explosions and have been traced during underground explosions in Nevada, during contact explosions in the Marshall Islands, and also during atmospheric and underwater explosions in the Pacific Ocean. These waves are traced in approximately the same range of epicentral distances as the corresponding waves of earthquakes. The areas in which the waves are traced during explosions are shown in Table 25.

During underground explosions and shallow-water underwater explosions, the PP waves can be traced at a distance of Δ = 5,000 6,000 km only during powerful explosions with a power of Q = 100 kt and more.

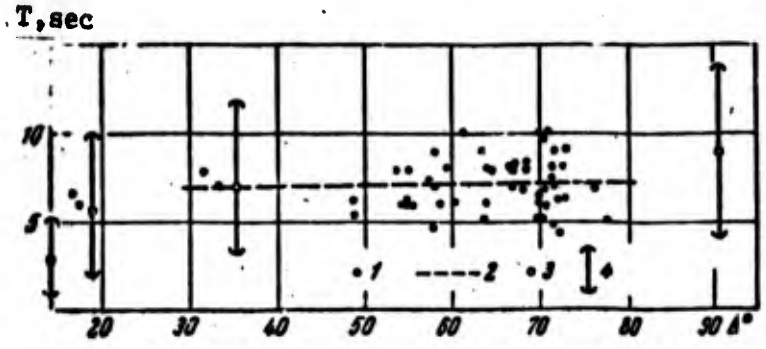

Figure 44. Dependence on epicentral distance Δ of periods T_P and T_S of dilatational P waves and transverse S waves of earthquakes with focal depth h ≥ 100 km and magnitude M = 5 - 6.5, from records of wide-band seismographs. 1 - Unit values for T_S; 2 - Averaged values of T_S; 3 - Averaged values of T_P; 4 - Maximum values of T_P.

In the records of wide-band and long-period seismographs, the records of the PP waves assume the form of short pulses consisting of 1.5 - 2 periods. During contact and atmospheric explosions in most cases the arrivals of the PP waves are not clear. However, during powerful (Q on the order of tens of megatons) atmospheric explosions, and also during underground explosions (Q > 20 kt), the arrival of PP waves is clear, especially in the records of seismographs with a narrow passband, in which it is clear that the PP waves arrive in the dilatation phase. The periods of the oscillations in the PP waves, as in the P waves, depend on the type of explosion and the parameters of the equipment adopted. However, for the type of explosion and the type of equipment in question, they are close to the periods of the P waves recorded at the same station (Figure 45). The same is observed also for earthquakes.

For PP waves, just as in the case of P waves, no noticeable dependence of the period on either the intensity of the explosion or on the epicentral distance is observed.

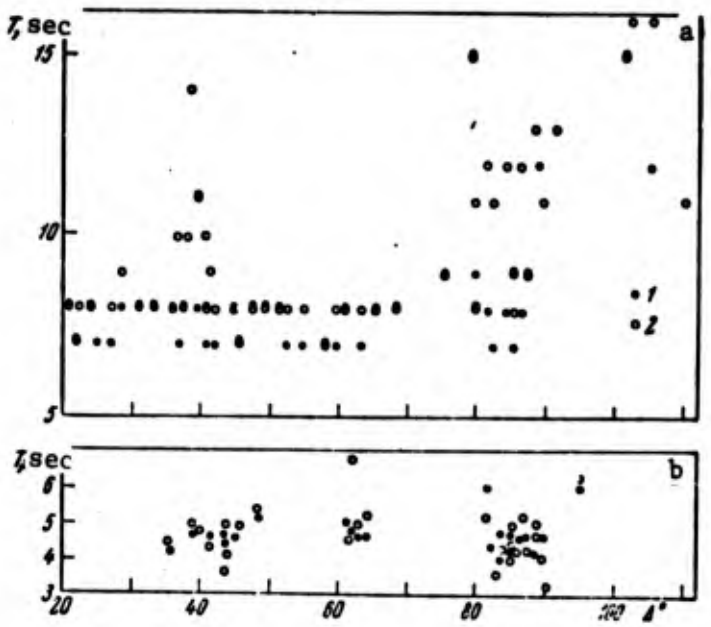

Figure 45. Comparison of periods of P waves (1) and PP waves (2) recorded on wide-band equipment. a - for earthquakes; b - for contact explosions in the Marshall Islands.

PPP Waves. These waves were observed during powerful atmospheric explosions and during contact explosions in the Marshall Islands [145, 188], as well as during underground and deep-water underwater explosions. The arrivals of these waves are usually considerably less clear than those of P and PP waves, and it is usually not possible to establish the direction of their arrival. The periods in the PPP waves are approximately the same as those for the P and PP waves. The dynamic characteristics of these waves have not been studied by us on account of the insufficient experimental data. In [188], mention is made of the fact that PPPP waves have been recorded during explosions, but they have not been observed clearly in the stations of the USSR.

PcP Waves. These waves are observed in practically all kinds of explosions. During contact and underground explosions, the PcP waves are recorded in a range of Δ values from 13 to 88° [63, 65, 166, 175, etc.], and during atmospheric explosions down to somewhat smaller values of Δ.

The shape of the oscillations in the PcP waves is quite similar to the shape of the oscillations in P waves. In most cases, it consists of one pulse oscillation (see Figure 7, g). Exactly like the P waves, the PcP waves arrive in the compression phase. Their periods are on the average 10% less than the periods of the P waves.

PKP Waves. PKP waves have been observed during contact explosions in the Marshall Islands [165, 236], underground explosions in Nevada, and underwater explosions in the Pacific Ocean. However, we have at our disposal only records of waves taken by Soviet stations during the underwater Wigwam explosion in the Pacific Ocean, and those taken by stations in Antarctica by SKM seismographs during explosions in Nevada at distances of 16,300 and 16,500 km (see also [99]). PKP_1 and PKP_2 waves have been observed; their periods fall within a range from 1.4 to 1.6 sec. The largest amplitude (about two times greater) is that of the PKP_1 waves (see Figure 41, b).

S Waves. Records of S waves have been obtained within a considerable interval of epicentral distances (up to 9,000 km) in records of SK, SKD, Golitsyn, and other seismographs during contact explosions in the Marshall Islands, atmospheric explosions at Christmas Island, and elsewhere.

During powerful underground explosions, records of S waves have been obtained in type SK and SKD equipment when Δ was at a distance of about 10,000 km.

The arrivals of S waves during contact and underground explosions are in most cases unclear. During powerful atmospheric explosions, quite clear arrivals of S waves have been observed in a number of stations of the USSR. The periods of the S waves during atmospheric explosions in the records of SK seismographs amounted to about 5 - 12 sec at distances of up to Δ=5,000 km (Figure 46). In records of Press-Ewing seismographs, they amounted to as much as 14 - 16 sec, and at larger Δ they reached 16 - 18 sec [145, 295].

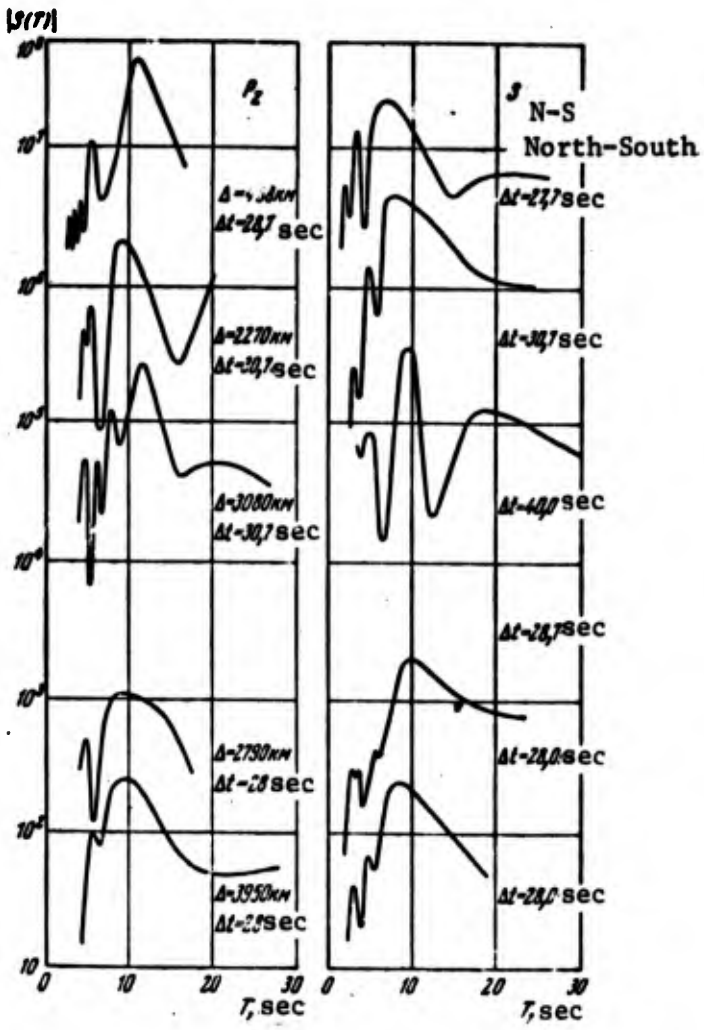

Figure 46. Spectra of dilatational P waves and transverse S waves recorded on wide-band seismographs during atmospheric explosions. The spectra were corrected for the uneven amplitude-frequency characteristics of the equipment at periods higher than 10-12 sec.

Two shapes of the oscillation train are observed in S waves. In a number of cases, the train consists of one or two oscillations. In other cases, the train consists of three or four oscillations. The periods of the first (sometimes of the first two oscillations) amount to 5 - 8 sec; in the second and third oscillations, the periods increase to 18 - 22 sec. The amplitude of the first oscillation is 2 - 3 times less than the maximum amplitude, and it is possible that the beginning of the wave recording may be distinguished somewhat later than the true arrival of the wave in some cases.

The complex character of the oscillations in S waves, as described above, is connected with the superposition of S_a waves on the S waves [339].

In the records of a number of stations, such a sharp differentiation of periods in the first and ensuing oscillations in the oscillation train is not observed. Besides, in a number of cases, the periods of the S waves only slightly exceed the periods of the P waves.

During underground explosions, the periods of S waves, recorded both by equipment with a narrow passband and by wide-band and long-period equipment, are obtained at distances of $\Delta > 4{,}000 - 5{,}000$ km

only during the most powerful explosions. They amount to approximately 2.0 - 2.5 sec. Those obtained by wide-band equipment at a distance of $\Delta \approx$ 10,000 km are approximately 6 - 8 sec.

SS Waves. These waves are recorded during powerful atmospheric and underground explosions, in the former case by wide-band and long-period equipment, and in the latter by these and also by equipment with a narrow passband. SS waves arrive against the oscillation background of the preceding waves, and the shape of their record is distorted by the superposition of other oscillations. The periods of SS waves are usually the same as the periods of S waves, but the amplitudes are 1.5 - 2 times less than the amplitudes of S waves. SS waves during explosions have thus far been very little studied.

SSS Waves. These waves have been recorded during powerful atmospheric explosions, and also during contact explosions in the Marshall Islands by seismographs of type SK and by long-period seismographs.

During other types of explosions, the waves were not clearly recorded. The character of the oscillations in SSS waves is the same as that in SS waves. The oscillation train consists of 3 - 4 oscillations with a period roughly the same as that of S waves.

SKS Waves. In stations of the USSR, these waves have been recorded during contact explosions in the Marshall Islands by SK seismographs in the range of Δ 80 to 87°. Their periods and the character of the record are the same as those in S waves [63].

ScS Waves. ScS waves have been recorded during atmospheric explosions in a number of stations in Europe, Asia, and the USA. The fact that these waves can be identified with sufficient accuracy is indicated by the agreement between the differences in the travel times of the ScS waves and the P waves — for instance, at the Palisades station (Δ = 59°, 6) and at other stations.

PcS (ScP) Waves. These waves have been traced only during powerful atmospheric and underground explosions in stations of Europe and Asia. These waves can be distinguished chiefly according to the travel times, and by the character of the polarization. Their characteristics have not been studied.

PP_k^{refl} and SS_k^{refl} Waves. During numerous atmospheric and underground explosions, each carried out in the same regions, SK, SKM, and USF instruments, as well as long-period SKD and Press-Ewing seismographs [145] have recorded seismograms in a number of cases for relatively intense waves arriving immediately 3 - 10 sec after P and S waves (Figure 47). Hereafter these waves are indicated by PP_k^{refl} and SS_k^{refl}. In the hodograph in Figure 42, the PP_k^{refl} waves are indicated by darkened circles. The arrival of SS_k waves is less clear than the arrival of the P waves, and they arrive in the dilatation phase.

These waves considerably distort the shape of the envelope of the P waves. This envelope is one of the most important criteria in identifying explosions.

For a given station, the differences in the travel times between PP_k^{refl} and P waves and between SS_k^{refl} and S waves differ little in a series of explosions carried out at the same point. For different stations they vary somewhat, depending on the thickness of the Earth's crust. For dilatational waves, they amount to 3 to 8 sec, and for transverse waves — from 6 to 9 sec. The differences in the travel times between PP_k^{refl} and P waves are given in Table 26. It is possible that the PP_k^{refl} and SS_k^{refl} waves may be waves which are reflected twice, in the region of the station, from intermediate boundaries in the Earth's crust. This is also confirmed by the fact that the difference in the travel times between PP_k^{refl} and P waves increases together with the increase in the thickness of the sedimentary layer in the region of the station (Table 26). These waves pass through the initial and basic parts of the path as forward refracted P and S waves, after which they are reflected from the Earth's surface and again reflected from the

Figure 47. Example of a record of P and PP_k^{refl} waves during an atmospheric explosion (Δ = 2,900 km).

TABLE 26. VALUE OF THE DIFFERENCE IN TRAVEL TIMES OF THE PP_k^{refl} AND P WAVES OBSERVED DURING ATMOSPHERIC EXPLOSIONS.

Epicentral distance Δ, km	PP_k^{refl} - P, sec	Approximate depths to M discontinuity, km	Approximate thickness of deposit, km	Rocks in the upper part of the section
460	8	40	3—5	Permafrost
1100	2	25—30	0	Crystalline
1760	3	30	0	"
1920	10	40—45	3	"
1960	4—5	30	0	"
2160	3	30—35	2	Sedimentary
2220	5	30	0	Crystalline
2230	4	30—35	2	Sedimentary
2300	6	40	3—4	Permafrost
2390	3	30—40	0	Crystalline
2460	4	40	2	Sedimentary
2760	7	40	2	Metamorphic
2850	3	40	0	Crystalline
2950	3	40	0	"
3080	4	40	3	Sedimentary
3340	12?	40—45	3—5	"
3840	8	45—50	10—15	"
3960	4	40	5	Crystalline
4130	4	40	0	"
5220	8	50—60		"

intermediate boundary in the Earth's crust. It is possible that the granite-basalt boundary may be such a reflecting boundary.

The author has observed PP_k^{refl} and SS_k^{refl} waves in the recordings of a number of stations of the USSR also during earthquakes.

In addition to the waves examined above, one must mention the i waves (Figure 41, a), which are connected with repeated blasts during underwater explosions and are traced clearly in a wide range of Δ [102]. These waves are of essential significance in identifying underwater explosions and in determining their depths.

No other body waves have been observed which can be traced in a broad range of Δ as clearly as those described above.

Separate observed phases, ordinarily traced in a range of Δ, have not been deciphered (see, for instance, the i_x phase in Figure 5, e), or else we do not have the pertinent data for describing them. This question still awaits investigation. For this purpose, it is possible to use the data from a number of powerful underground nuclear explosions in different regions of the globe.

Trajectories of motion in P waves. The trajectories of motion of particles of the medium in P waves have been studied for various types of explosions. The trajectories were plotted in a vertical plane passing through the epicenter of the explosion and the station, and also in a horizontal plane.

Figure 48, a-d, gives examples of trajectories of motion of medium particles in P waves of contact and underground explosions. As is clear from an examination of the trajectories given here, the motion of medium particles in the P waves during contact and underground explosions, and also during underwater and atmospheric explosions (examples of the latter are not given here), is the same as in the case of earthquakes. This is also corroborated by the determinations of the azimuths to the explosion epicenters, data on which are given in Table 27.

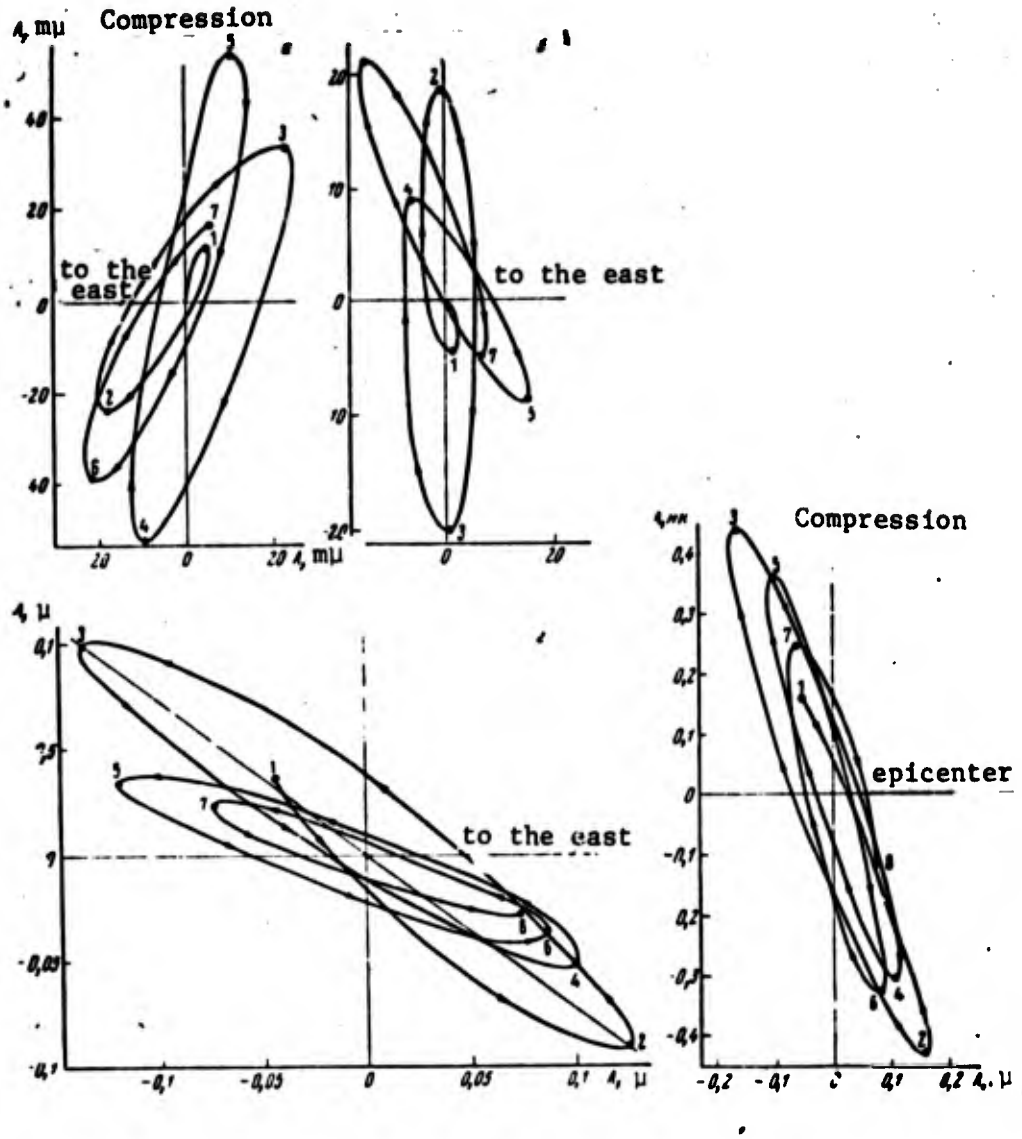

Figure 48. Trajectories of motion of medium particles in P wave, recorded: during contact nuclear explosion (Δ = 5,150 km): a - in horizontal plane; b - in vertical plane; during underground nuclear explosion (Δ = 9,946 km): c - in vertical plane; d - in horizontal plane. For ease in tracing the trajectory, characteristic numbered dots are given in the diagrams.

TABLE 27. AZIMUTHS TO EPICENTER, DETERMINED BY P WAVES OF DISTANCE CONTACT AND UNDERGROUND EXPLOSIONS, FROM DATA OF SINGLE STATIONS

Date of explosion	Type of explosion	Epicenter coordinates		Magnitude, m	W, M^m	Deviation from true azimuth, ΔAz	Type of seismo-graph	Epicentral distance Δ
		Latitude	Longitude					
May 27, 1956	On the Earth	11°29'48"N	165°22'09"E	5.62	10	-2°0'	SKM	46°52'
July 8, 1956	On a barge	11 40 17	162 12 01	5.37	10	+1.35	"	45 13
July 10, 1956	"	11 39 48	165 23 14	5.37	10	-0.31	"	46 43
July 20, 1956	"	11 40 26	165 20 22	5.55	10	-2 36	"	46 41
May 12, 1958	On the Earth	11 40 30	162 12 00	5.68	10	0 35	"	45 12
June 14, 1958	On a barge	11 39 37	162 13 31	5.36	10	-9 25	"	45 14
June 28, 1958	"	11 39 48	162 06 28	5.92	10	-1 31	SK	45 14
July 12, 1958	"	11 41 17	165 15 52	5.72*	10	-6 05	SKM	46 39
Aug 26, 1958	"	11 39 22	162 13 11	5.54	10	-3 35	"	45 14
Sept 13, 1962	Underground	37 03 38	116 01 18 W	6.2	0.200		USF	85 18
Sept 13, 1962	Underground	37 03 38	116 01 18		0.200	-2 03	"	89 37
Sept 13, 1962	Underground	37 03 38	116 01 18		0.200	+1 28	"	88 20

The differences between the true values of the azimuths, and the azimuth values calculated according to the ratio between the displacement amplitudes in P waves in the recordings of the horizontal components, fall within the range of 3-4 to 2°. The departure angles of the P waves are also very similar to the calculated values.

§ 2. Comparison of the Travel Times of Waves During Nuclear Explosions and Earthquakes

If we know precisely the epicenter coordinates of atmospheric, contact, underground, and underwater explosions with an accuracy of fractions of a second of an arc, and the times in the focus and in the epicenter, in some cases with an accuracy of up to 0.001 sec, and if the explosions are carried out repeatedly in the same region, we can determine the travel times of the body waves with a high accuracy (up to $\pm$0.1 sec) and compile more exact hodographs for them. This opens up new possibilities for using them for further study of the structure of the Earth.

For zone I, a relatively thorough comparison of the travel times of dilatational waves has been carried out for regions adjoining the test grounds of Nevada [168, 258], Alaska, Australia [192, 193], New Mexico [219, 322], the Pacific Ocean [165, 175-181, 194, 236], the Sahara [260], and other regions.

For zones II, III, and IV, the most extensive comparison of the travel times has been carried out for P waves, and somewhat less extensively for PP, PcP, PKP, S, and SKS waves, recorded during contact nuclear explosions carried out in the Marshall Islands. For the P, PP, PKP, and PcP waves, a similar comparison has been made for underground explosions carried out in Nevada, in the Marshall Islands, in Amchitka, and in other regions [168]. Comparison of the travel times has not yet been carried out for PS, PPP, SS, SSS, SSSS, ScS, and other waves during explosions or earthquakes. This is connected with the fact that it is only possible to record the arrivals of the

reflected waves, both monotypic and exchanged, less clearly than the arrivals of direct waves.

Hodographs of body waves. Below is a brief summary of the results obtained previously from a comparison of hodographs of the body waves recorded in all three zones during explosions with Jeffreys-Bullen (J.B.) hodographs for a surface focus [237].

The data on the travel times of the body waves obtained during the first powerful explosions were compared with the travel times calculated from the Jeffreys-Bullen hodograph compiled from the observations of travel times of earthquake waves. The first results revealed very good agreement between the travel times of the P waves during explosions and during earthquakes (Table 28).

P waves. The average deviations of the travel times of the P waves were 2 - 1.5 sec less than those calculated from the J.B. hodograph, and it appeared that the averaged values of the deviations depended on the region of the explosion epicenters, the epicentral distance, and the azimuth.

This decrease in the travel times of the P waves is connected by some authors with the absence of a granite layer in the region of the epicenter (oceanic type of structure of Earth's crust) and with the decrease of crust thickness to about 13 - 15 km [222]. In [236] it is stated that the decrease in the travel times t_P may be caused, not only by structural features of the crust in the epicentral region, but also by inaccuracies in the J.B. hodograph.

In [168] new tables were compiled of generalized travel times of the P, PP, PcP, and PKP waves for the surface focus according to data obtained during explosions. On their basis, tables of travel times for earthquakes with focal depths of up to 700 km were recompiled for these same waves. A new model of the mantle structure was also proposed in the same work.

TABLE 28. DEVIATIONS OF THE TRAVEL TIMES OF THE BODY WAVES DURING EXPLOSIONS FROM THE TIMES CALCULATED FROM THE JEFFREYS-BULLEN HODOGRAPH FOR THE SURFACE FOCUS (IN SEC)

Region of epicenter	Areas where recorded	Type of explosion	P	PP	PcP	PKP	S	SKS	Literature
Marshall Islands	Asia, America, Australia	Contact, on water	−2,0±0,59 (2300—10 500)	−5±1,1 (4000—9800)	−3,6 (4700—8700)	from 1.1 to 6.2 (15 200—15 600)	+4±1,0 (3900—6700)	+5±2,0 (9000—10 000)	[63, 222, 236]
Nevada	Europe, Asia, America	Contact on the Earth	−1,5 (3000—10 000)	—	−1,88±0,77	—	—	—	[166]
Amchitka Island	North America, Australia	Underground	−0,5÷2,0 (3300—11 000)	—	−3,51				[167, 175—178, 233]
Marshall Islands	America, Pacific Ocean, Australia	Contact, on the Earth	−1,2—2,0 (3500—11 000)	—	from −2 to −4 (1500—3000)	1 (16 300—16 500)	—	—	[175—186, 233]

Remark: The figures in parentheses after the deviations indicate the ranges of epicentral distances for the corresponding seismic stations (in km).

PP Waves. The deviation of the travel times of the PP waves from the times calculated according to the J.B. hodograph amounted to -5 sec. Since, in this case, PP waves with their points of reflection in the region of the Pacific Ocean were examined, the decreased travel times of the PP waves may be caused both by the features of the crust structure under the oceans and also by the inaccuracies of the J.B. hodograph for the PP waves [63].

PcP Waves. The travel times of the PcP waves were 3.6 sec less during explosions in the Marshall Islands, and 1.88 $\pm$0.77 sec less during explosions in Nevada [63, 65, 166, 175].

In the opinion of the author of references [63, 65], this may be caused by the inaccuracy of the velocity profile of the Earth, by the somewhat greater (by 10 km) radius of the Earth's core, and by a number of other causes. In [236] the possibility is mentioned that somewhat increased values of P wave velocities may exist in the lower mantle in comparison with their values calculated according to the J.B. hodograph.

PKP Waves. During explosions in the Marshall Islands [164, 165], it was established that within the range Δ = 15,200 - 15,600 km, the PKP waves arrive sooner, correspondingly, by 6.2 - 11.1 sec, than would be expected according to the J.B. hodograph. In [164, 165], this is related to the hodograph loop for these waves at a distance of Δ = 15,760 km. During underground explosions in Nevada, the travel times of PKP_1 and PKP_2 waves observed at a distance of Δ = 16,500 km coincide within an accuracy of approximately $\pm$ 1 sec with the times calculated according to the J.B. hodograph.

S Waves. The mean deviation of the observed travel times of the S waves in the given range of Δ (Table 26) from the times calculated from the J.B. hodograph amounted to +4.0 $\pm$1.0 sec during contact explosions in the Pacific Ocean, according to [65]. A possible explanation of the observed increase in the travel times according to

[63] may be a somewhat lower velocity of the transverse waves in the upper part of the mantle.

SKS Waves. The correction for the J.B. hodograph for SKS waves, according to [63], is +5.0 ±2.0 sec for contact explosions in the Pacific Ocean. During explosions emanating from other regions, the corrections for the travel times of the SKS waves have not yet been calculated.

P_n Waves. According to experimental data, the hodograph of the dilatational waves recorded as the first waves in seismograms, with Δ ranging from 200 to 1,500-2,000 km, is linear. If there is horizontal stratification of the M discontinuity, the equation for this assumes the following form:

$$t_P = a + b\Delta^\circ.$$

The values of a and b vary within the ranges shown in Table 29, depending on the region.

According to the data in [237], the coefficients a and b almost coincide during explosions and earthquakes for the identical region of Northern Europe. (When comparing values of a, the fact must be taken into account that the value a/2 has been given for earthquakes, since travel times of waves from earthquakes, with a normal focal depth of 33 km, are being considered.)

On account of the special structural features of the medium (Nevada, the Pacific Ocean), regional hodographs of explosions differ somewhat from the averaged hodograph obtained from the data on earthquakes. This also applies in equal measure to the regional hodographs of earthquakes.

Thus, a comparison of the travel times of dilatational and transverse waves caused by explosions of various types, with the travel times determined according to the J.B. hodograph, reveals that

TABLE 29. COEFFICIENTS a AND b IN HODOGRAPH EQUATION FOR P_n WAVES

Region of epicenter	Structure of medium	Type of source	a, sec	b, sec/degree	Range of Δ, km	Literature
Nevada	Continental	Underground explosions	8.6	13.73	200-1600	[141, 168]
Northern Europe	Continental	Earthquakes	$a/2 = 4.14 \pm 0.57$	13.654 ± 0.041	200-1400	[237]
Pacific Ocean (Marshall Islands)	Oceanic	Contact explosions	8.6	13.73	200-2000	[194]

there are some differences between these times.

The corrections of the J.B. hodograph for P and PcP waves for different regions amount to 1.5 - 2 sec, and to 4 sec for S waves. For PP, PPP, SS, SSS, and other waves which arrive against a background of waves arriving earlier, the corrections depend on the regional structural characteristics of the crust of the points of reflection and observation. According to preliminary data, they do not exceed $\pm$4 - 5 sec.

The travel times of P waves in zone III in continental stations in all types of explosions in general depend very little on the regional characteristics in the region of observation, but they depend to a considerable degree on these characteristics in the region of the focus [326]. Therefore, by using the travel times of the P waves and taking into account the above mentioned average corrections, one can determine by the method of successive approximations the coordinates of the explosion epicenters with the greatest accuracy (to about $\pm$15 - 10 km), even without taking into account the regional corrections in the observing stations [99, 198]. When the regional corrections were taken into consideration, the accuracy of determining the coordinates in individual cases was increased to $\pm$ 2 km with a 90% reliability level [198, 207, 279, 326].

The travel times of dilatational waves in zones I and II in a number of regions depend to a considerable degree on the regional seismogeological structure along the travel path of the waves and in the region of the observing station. Therefore, when using them to determine the epicenter coordinates, it is necessary to take into account the regional corrections of the travel times of the waves. In such cases, the accuracy in determining the epicenter coordinates is about $\pm$ 2 km, according to [198].

The travel times of other body waves — PP, PcP, PKP, and others — can also be used to determine the coordinates of the epicenters. However, the accuracy with which they are determined will

be somewhat lower than it would be if data on the travel times of the P waves were used.

When the explosion epicenters are located in oceans, one must take into consideration a correction for the regional structural features of the Earth's crust at the epicenter of the explosion.

A large amount of factual material has been collected at the present time concerning the travel times of seismic waves during explosions in different regions, and it has been published in seismic bulletins. This material makes it possible to attain a higher precision in hodographs of transverse waves in all the zones, and to make use of the more precise hodographs in studying the Earth's structure.

The connection of δt_p with the regional features in the magnitude values. A comparison was made of the deviations of the magnitudes, and the corresponding deviations in the travel times of the P waves, from the values determined according to the J.B. hodograph. The comparison was made for stations located in various regions [103]. The values of δt_p were taken from work [63], in which they were obtained from data on the travel times during nuclear explosions carried out by the USA in the Marshall Islands. In the present work, δt_p represents the difference in the average values of the observed travel times of P waves and the travel times determined by the J.B. hodograph. The values of δt_p for earthquakes were determined in [76].

The results of comparing the corrections Δm and δt_p for explosions are presented in Figure 49. It is clear from this that there is no clearly expressed dependence in the pattern of corrections Δm (graph I) and δt_p (graph I). The corrections δt_p for the majority of the stations fall within the accuracy range of δt_p of (± 0.6 sec), regardless of the regions where the stations are located. For the Δm corrections, there is a distinctly expressed tendency towards an increase of this value in the Central Asian stations located in regions with a thick layer of sedimentary rocks. The values of Δm exceed by several times the errors in calculating m, and in individual stations they reach approximately 0.4 - 0.5 units of magnitude.

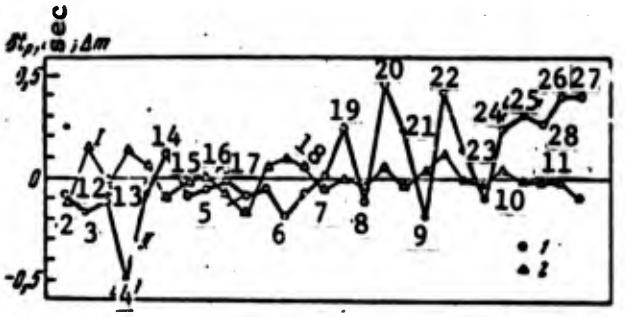

Figure 49. Comparison of averaged station corrections (II) with the corrections of δt_p in the travel times of P waves (I) for stations of the USSR. 1 - mean values of Δm; 2 - mean values of δt; 3 - for stations located in crystalline rocks, signs 1 and 2 are darkened.

1 - Kur; 2 - YU-S; 3 - Vld; 4 - Smp; 5 - Rbch; 6 - Alm II; 7 - Mg; 8 - KHrg; 9 - Sbr; 10 - Stations; 11 - Ptr; 12 - Vr. 1; 13 - Mgd; 14 - Kkht; 15 - Kb; 16 - Irk; 17 - Nr; 18 - Fr; 19 - An; 20 - Fg; 21 - Dzh; 22 - Grm; 23 - Tshk; 24 - O-Grm; 25 - Smd; 26 - Ashkh; 27 - Kub

§ 3. Dependence of the Oscillation Period of Dilatational Seismic Waves on the Power of Underground Nuclear Explosions

The dependence of the predominant periods of the oscillations of dilatational seismic waves on the TNT equivalent Q during underground nuclear explosions has been studied very little as of the present time. At the same time, this question is extremely important in detecting and identifying underground nuclear explosions. One must know the dependence of T on Q, among other things, in order to assess the possibility of applying criteria based on differences in the periods of body waves, caused by explosions and earthquakes, to the identification of underground nuclear explosions of various intensities.

On the basis of the seismic records obtained during underground nuclear explosions in a number of regions, an attempt was made to assess approximately the dependence of T on Q for dilatational waves. Records at our disposal of explosions carried out in Nevada and in other regions, whose intensities varied within the range of a factor of 10^3 (Table 30), were utilized for these purposes. The information about the TNT equivalents and about the conditions under which the explosions were carried out in the Nevada region were taken from published works (see Tables 30, 33, 34).

It must be noted that different authors give somewhat different values of the TNT equivalent for the same explosions. This indicates

TABLE 30. MEAN OSCILLATION PERIODS IN P WAVES RECORDED DURING UNDERGROUND NUCLEAR EXPLOSIONS IN NEVADA, USED IN DETERMINING THE VALUES OF a AND b IN THE FORMULA $T \approx a\sqrt[b]{Q}$

Data	Q, kt	h,m	Range of Δ, km	Number of stations	T_1, sec
13.IX 1963	200	705	6400—11000	40	1,5 ±0,01
15.X 1958	5	255	1100—8300	8	1,0 ±0,0
30.X	19	256	1100—10800	9	1,07±0,1
15.IX 1961	2,4	402	6800—10000	11	1,0 ±0,01
12.V 1962	37	438	6800—10000	44	1,21±0,01
27.VI	44—56	412	6800—10000	34	1,16±0,01
5.X	40	495	6800—11000	12	1,2 ±0,01
23.XI 1963	12,5	400—500	6800—11000	10	1,23±0,01

TABLE 31. MEAN OSCILLATION PERIODS IN BODY P_n, P^*, AND P, AND Sn WAVES RECORDED IN THE USA DURING UNDERGROUND NUCLEAR EXPLOSIONS OF DIFFERENT INTENSITIES, AND THE CORRESPONDING VALUES OF b_{mean} AND a_{mean} IN THE FORMULA $T = a\sqrt[b]{Q}$

Type of wave	Name of the explosion					
	Blanca		Logan		Rainier	
	TNT equivalent Q, kt					
	19		5		1,7	
	T*	N*	T	N	T	N
P_n	0,62±0,07	5	0,62±0,08	5	0,56±0,11	9
P_n according to [350]	0,64±0,05	5	0,68±0,04	5	—	—
P^*	0,68±0,12	4	0,70±0,10	2	0,60±0,11	7
P	0,93±0,19	3	0,75±0,15	2	0,85±0,16	8
S_n	1,07±0,11	9	0,94±0,13	8	—	—

TABLE 31 continued

Type of wave	Name of the explosion				b_{mean}	a_{mean}
	Neptune		Tamalpais			
	TNT equivalent Q, kt					
	0,09		0,072			
	T	N	T	N		
P_n	0,57	2	0,67±0,08	2	20	0,55
P_n according to [350]	0,48±0,05	—	0,5±0,05	2	20	0,55
P^*	—	—	0,6±0,05	2	20	0,65
P	—	—	—		14	0,8
S_n	—	—	—		9	0,9

*T - period in sec, N - number of observations.

that it is determined inaccurately.

The values of Q given in Tables 30 and 31 were adopted in considering the results of the seismic observations obtained during the explosions under discussion here. In [350], a special study was made of the dependence of the half-period T_{01} of the first oscillation in the P_n wave on the TNT equivalent during explosions of the Hardtack-II series. The explosions of this series were carried out in porous volcanic tuffs of Nevada under approximately identical conditions. In [350], the fact was established that there was some increase (amounting to as much as about 30%) of the half-period T_{01} of the first oscillation in the P_n wave, when the TNT equivalent of the explosion was increased by a factor of more than 10^2 (from 0.072 to 19 kt).

In the present work, the dependence of T on Q was studied for the periods of maximum oscillations in body waves of various types: P_n and S_n waves in the interval Δ = 200 - 900 km; P* waves, corresponding to the intermediate boundary in the Earth's crust (granite-basalt); and also direct refracted P waves observed at epicentral

distances from 1,200 to 11,000 km. The records obtained with seismographs with a narrow passband were studied. The average periods of oscillations in the body waves, measured on the seismograms of the above-mentioned explosions, are given in Tables 30 and 31.

In studying the dependence of T on Q, it seemed to us more advisable to examine the periods of maximum oscillations, rather than the first half-periods of the oscillations in the waves, as had been done in [350] in studying the P_n waves. The problem is that the identical maximum phases of oscillations in a train of body waves can be identified more easily in records obtained at different epicentral distances than can the first half-periods of the oscillations. In a number of cases, it was not possible to distinguish the first half-periods at all in the records, especially for waves recorded in the ensuing arrivals. This is connected with the stronger attenuation of the first oscillation due to its composition, which has a higher frequency in comparison with the frequency composition of the ensuing oscillations [100].

In studying the dependence of T on Q, both in this work, and in [350], the average periods of oscillations, measured in records obtained at various epicentral distances, were examined. Such averaging of the periods is permissible only when the oscillation period does not change with changes in the epicentral distance. For the P_n and P* waves, these requirements were satisfied within certain ranges. This fact can be verified by analyzing the periods at different epicentral distances during the identical explosions.

A constant period in the entire area of recording the P_n waves on the Earth's surface, within the measurement accuracy, was noted during nuclear explosions carried out in various regions.

Figure 43 shows the distribution of the periods of the maximum oscillations in the P_n waves at epicentral distances from 200 to 1,000 km for explosions with very similar intensities.

The periods of direct dilatational refracted P waves, recorded at the above explosions by equipment with a narrow passband, also underwent insignificant changes together with an increase in the epicentral distance. Therefore, besides comparing the T periods for P waves at identical epicentral distances during explosions of different intensities, one can also compare the average values of T. The fact must be taken into account that one is averaging data observed at the same epicentral distances at the identical number of stations.

However, it must be noted that sufficiently strong records of P waves, which were useful for determining the periods of oscillations reliably, were obtained in the USSR within the range of Δ = 2,000 - 11,000 km, and the periods of the oscillations underwent very insignificant changes with changes of Δ.

An approximate estimate of the increase in T with increase in Q was sought in the form of the following expression:

$$T = a\sqrt[b]{Q}, \qquad (17)$$

where T was expressed in seconds, and Q in kilotons.

The average value of b for P_n and P* waves is 20 (see Table 31). The average value of b for P waves is 14 $\pm$ 1.6. Taking into account the scattering of the values of T, the accuracy with which b is determined apparently does not exceed $\pm$ 20%. The value of Q in expression (17), numerically corresponding to the oscillation period during an underground nuclear explosion with a TNT equivalent of Q = 1 kt, differs somewhat for waves of different types. Its approximate value for P_0 and P_n waves is a $\approx$ 0.055; for P* waves, it is a $\approx$ 0.65. For P waves, it is a $\approx$ 0.8.

The approximate values of b, and especially of a, have a local character. In explosions in rocks which have different physical parameters (velocity, density, porosity, etc.), the values of a differ

from those found for explosions in tuffs. This is indicated particularly by the fact that the periods of P_n and P waves decrease by approximately 1.2 - 1.4 times during explosions carried out in denser crystalline rocks (for example, in Amchitka, etc.). A decline has also been noted in the period during the explosions of Gnome and Salmon, which took place in salt beds, in comparison with the periods of the same waves during explosions in Nevada, which were carried out in porous volcanic tuffs.

The variation limits of the value of b depending on local conditions will apparently not be as significant as the variation limits of a. On the basis of the small amount of data obtained during explosions in hard crystalline and metamorphic rocks, it has been shown that the value of b will vary by no more than $\pm$ 1% of its value found for P waves during explosions in tuffs.

Powerful underground explosions with a TNT equivalent on the order of several hundreds of kilotons are carried out at considerably greater depths than explosions with a power of one or tens of kilotons. The increased depth in these cases is due to the necessity of preventing ejection of soil onto the surface and pollution of the air with radioactive products.

At greater depths, the values of the density and velocity of the surrounding rocks will be greater than at lesser depths (Table 32). As has been established in deep explosions, the latter circumstance leads to a certain decrease of the period in P waves.

Consequently, in determining the dependence of T on Q, if recordings are used of explosions carried out at different depths, in particular at depths of about 300 or 700 - 1,000 m, we will obtain a value of b which is too large in formula (17). This has been actually observed. If the value of b is to be determined from the explosion data of Blanca and Logan and the data on the explosion

TABLE 32. DENSITIES AND VELOCITIES OF DILATATIONAL WAVES FOR SOME SEDIMENTARY AND CRYSTALLINE ROCKS

Rocks	Density of dry rock g/cm^2	Velocity of dilatational waves, v, km/sec	Range of fluctuations of $\rho v \cdot 10^5$ $g/cm^2 \cdot sec$	Depth h, m
Loess	0.75-1.6	0.2-0.8	0.15-1.3	10-300
Filled-up ground	0.5-0.6	0.4-0.6	0.2-0.36	10-50
Recent alluvium	1.5	0.5-2.0	0.75-3.0	50-200
Alluvium at considerable depth	2.0	3.0-3.5	6.0-7.0	300-2000
Dry sand	1.0-1.5	1.0-1.5	1.0-2.25	30-100
Water-saturated sand	1.9-2.2	1.5-2.0	1.8-4.4	10-500
Clays	1.0-1.7	1.0-2.7	1.0-4.6	30-3000
Clays	1.5-2.0	2.0-2.8	3.0-5.6	300-500
Chalk	1.5-2.2	3.5-4.0	5.25-8.8	50-500
Volcanic tuff	1.7-1.9	1.7-2.4	2.9-4.6	100-300
Glacial ice	0.8-0.9	3.4-3.6	2.7-3.1	100-2000
Hard limestone	1.9-2.5	2.8-6.4	5.3-16	50-2000
Rock salt	2.1-2.4	4.3-5.5	9.0-13.2	50-2000
Barite	4.3-4.6	4.5	19.3-20.7	
Basalt	2.4	5.0-5.6	12-13.4	50-3000
Granite	2.7	4.4-5.6	11.9-15.1	30-2000
Acmitic schists	3.0-3.5	5.0	18-21	50-300
Norite	3.0	6.2	18.6	
Magnetite schists	4.0	5.6-6.0	22.4-24	100-300
Sandstones	2.1-2.2	4.5-5.0	9.5-11.0	40-1000
Sandstones and schists in permafrost zone	2.1-2.2	5.1-5.2	10.7-11.4	150-500

of September 13, 1963, carried out at a depth of h $\approx$ 705 m, then the value obtained will be b $\approx$ 20.

It is interesting to note that, during underground TNT explosions, the period of the seismic waves depends to a greater degree on Q than in the case of nuclear explosions. Thus, for example, from the graph given in [89] for direct dilatational P_0 waves caused by underground TNT explosions in porous sedimentary deposits, one can conclude that

$$T(\text{sec}) \approx 0{,}5\sqrt[5.6]{Q(\kappa r)}. \qquad (18)$$

The fact that the dependence of T on Q is greater during underground TNT explosions than during underground nuclear explosions may be due to the fact that, on account of the necessity of increasing the dimensions of the blast chamber when the charge is increased, the focus dimensions during TNT explosions undergo considerably greater changes than the focus dimensions during a nuclear explosion.

Besides, a definite role may be played in this by the considerably shorter duration (about 10^{-7} sec) of the influence of forces in the source during nuclear explosions than during TNT explosions. It must also be kept in mind that in [4, 89] the studies pertained to waves recorded at close distances Δ, on the order of one to tens of kilometers, while in this work waves recorded at distances of Δ > 200 km are considered.

The above-mentioned weak dependence of the periods of body waves of underground nuclear explosions on the size of their TNT equivalent is utilized when distinguishing the recordings of underground nuclear explosions from recordings of earthquakes with a comparable or greater magnitude on the basis of frequency criteria.

§ 4. Dimensions of Cavities Formed During Underground Nuclear Explosions, and Their Dependence on Intensity and Explosion Conditions

In [154, 241], it was established that the dimensions of the radii of blasting cavities formed during underground nuclear explosions completely camouflaged are relatively small. For explosions of several tens of kilotons, the radii do not exceed several tens of meters (Tables 33, 34).

For camouflaged nuclear explosions carried out by the USA in four media (tuff, alluvium, granite, and rock salt), it was established in [154, 241] that the following empirical dependence holds for the radius R_k(m) of the blast cavity on the intensity of the explosion Q(kt), the depth of the explosion H(m), and the density ρ (g/cm^3):

$$R_k = (59 \div 80{,}9)\frac{Q^{1/4}}{(\rho h)^{1/4}}. \qquad (19)$$

The values of R_k calculated by formula (19) practically coincide with the observed values.

As is clear from formula (19) and Table 33, the dimensions of the blast cavities, and possibly the dimensions of the destroyed zones increase very slightly with increased explosion intensity, depth of location, and properties of the rocks surrounding the explosion during camouflaged nuclear explosions.

The radii of the blasting craters in alluvium formed during nuclear explosions are approximately the same as those during comparable TNT explosions. In [241], it is indicated that there may possibly be a decrease in the crater dimensions by 10 - 20% during an explosion in basalt involving ejection of soil, that is, in denser rocks [241, 280, 282].

TABLE 33. COMPARISON OF OBSERVED RADII OF BLAST CAVITIES IN UNDERGROUND NUCLEAR EXPLOSIONS WITH CALCULATED RADII OF CIRCLES OF FAULT PLANES IN EARTHQUAKES WITH THE SAME MAGNITUDE (THE VALUES OF Q, m, AND R_k ARE DERIVED FROM [330, 358 etc.]).

Date	Region of epicenter	Surrounding rocks	Q, kt	m	Radius of cavity during explosions R_k, m	Radius of circular fault during earthquake $d \approx (0.1\text{-}0.3) \times \sqrt[3]{E_c}$, m
Dec. 13, 1961	Nevada	Alluvium	0.43±0.04	4.3	11.3	230-700
Apr. 14, 1962		"	1.7±0.15	-	21.6	-
Feb. 8, 1962		"	2.7±0.3		24.7	-
Mar. 28, 1962		Tuff/Alluvium	3.1±0.3	4.8	25.9	580-1700
Mar. 8, 1962		"	7.8±1	4.9	27.7	740-2200
Feb. 23, 1962		"	11.2±2	5.0	32.6	860-2700
Sep. 19, 1957		Tuff	1.7	4.8	19.8	580-1700
Sep. 15, 1961		"	2.46±0.25	4.9	19.8	580-1700
Oct. 16, 1958		"	5.0±0.4	5.0	28	860-2700
Oct. 30, 1958		"	19±1.5	5.2	44.2	1260-3800
Dec. 10, 1961	New Mexico	Salt	3.1±0.5	5.0	17.4	860-3000
Oct. 22, 1964	Mississippi	"	5	5.24	18	1260-3800
Feb. 15, 1962	Nevada	Granite	5.0±1.0	5.4	19.2	1850-5650
Oct. 26, 1962		"	12.5±2.0	5.6	25.6	2740-8240
Sep. 13, 1963		Tuff	200	6.2	39	8000-24,000

TABLE 34. RELATIVE PORTION OF ENERGY OF SEISMIC WAVES E_s/E_{tot} IN PERCENTAGES, AS OBSERVED DURING UNDERGROUND NUCLEAR EXPLOSIONS, CARRIED OUT IN DIFFERENT ROCKS.

Date of Explosion	Name of Explosion	Region of Epicenter	Rocks	Depth h, m	$\rho v \cdot 10^5$, $g/cm^2 \cdot sec$
19.IX 1957	Rainier	Nevada	Volcanic tuff	274	3,8—4,8
16.X 1958	Logan	»	» »	283	4,0—5,0
30.X	Blanca	»	» »	301,1	4,0—4,6
15.IX 1961	Antler	»	» »	402	4,5
12.V 1962	Aardvark	»	» »	438	5,1
25.III	Huzik	»	Tuff/alluvium	157,4	2,9
14.IV	Pleit	»	Alluvium	191,5	2,9
13.IX 1963	Bilbee	»	»	705	5,1—5,5
31.XII 1961	Fisher	»	»	363,6	2,9
13.XII	Med	»	»	181	1,4—2,0
9.I 1962	Stoat	»	»	306,5	2,9
18.I	Agouti I	»	»	254,7	2,9
8.II	Stimuoter	»	»	181,1	1,4—2,0
9.II	Armadillo	»	»	242,8	1,4—2,0
19.II	Scintilla	»	»	153,7	2,9
23.II	Cimaron	»	Tuff/alluvium	304,8	2,9
8.III	Brazos	»	» »	256,3	2,9
5.IV	Doormouse	»	» »	261,1	2,9
27.VI	Haymaker	»	» »	412	2,9
6.VII	Sedan	»	Dry alluvium	202	1,4—2,0
15.II	Hardhat	»	Granite	286,2	12,9
26.X	Shoal	»	»	367,4	14—15
5.VII	Denny Bay	»	Basalt	33,5	8,9
1.V	Gnome	Sahara	»	200	10
10.XII 1961	Salmon	New Mexico	Salt	360,6	9—10
22.X 1964	Longshot	Mississippi	»	753	10,92
		Amchitka Is.	Andesite	700	16,5

(Table continued on next page)

TABLE 34. RELATIVE PORTION OF ENERGY OF SEISMIC WAVES E_s/E_{tot} IN PERCENTAGES, AS OBSERVED DURING UNDERGROUND NUCLEAR EXPLOSIONS, CARRIED OUT IN DIFFERENT ROCKS

Name of Explosion	ρ, g/cm^2	Q, kt	m_{mean}' in stations of USSR	$m' = 1.7+0.8\,M_L - 0.01\,M_L^2$ according to USCGS	E_s/E_{tot}, %		Radius of underground cavity R_k, m
					E_s according to formula (31) in Chapter VII	[24]	
Rainier	1,9	1,7	—	4,79	0,27	—	19,8
Logan	1,8	5,0±0,2 0,4	5,0±0,1	5,0	0,30	—	28
Blanca	1,8	19,0±1,5	5,2±0,1	5,2	0,23	—	41,2
Antler	1,9	2,46±0,25	4,9	4,9	0,34	0,20	19,8
Aardvark		37±7,0	5,4		0,30	0,31	—
Huzik	1,8	3,1±0,3	4,75	—	0,13	0,16	25,9
Pleit	2,2	1,7±0,15				0,18	21,6
Bilbee		200	6,12	5,8	0,36	0,25	—
Fisher		13,5±1,1 1,6	5,07	5,02	0,13	—	—
Med	1,8	0,43±0,04	—	4,29	0,04	0,09	11,3
Stoat		4,5	—	4,88	0,09	0,29	
Agouti I		5,9		5,1	0,22	0,09	
Stimuoter	1,8	2,7±0,3				0,28	24,7
Armadillo		6,6				0,10	
Scintilla		1,8	4,8		0,17	0,17	
Cimaron	1,8	11,2±2	5,0		0,13	0,14	32,6
Brazos	1,8	7,8±1	4,9		0,11	0,06	27,7
Doormouse		9,7		4,96	0,11	0,17	
Haymaker		56—8,0	5,36	5,3	0,17	0,07	
Sedan		100±15	4,95	5,1	0,021	0,08	Soil cast up, bound charge
Hardhat	2,7	5,0±1,0	5,4	5,4	1,5		19,2
Shoal	2,7	12,5±2,0	5,4	—	1,35	0,60	25,6
Denny Bay	2,4	0,42±0,08	4,55		0,22	0,24	Soil cast up
	2,4	16	5,4	5,4	0,74		17,4
Gnome	2,3	3,1±0,5	5,0	5,0(4,9)	0,63		
Salmon	2,4	5		5,34	0,57		18
Longshot	2,7	80	6,0±0,05		1,65		

Dimensions of destroyed zones during underground nuclear explosions. This question has been studied very little, since it entails great expenses in drilling and cutting through underground areas such as adits, drifts, etc., and also other technical difficulties. At the present time there is information about the dimensions of the destroyed zones in 35 explosions in alluvium, tuff, salt, and granites [154]. In these cases, the zone of visible disturbances in the rocks, established by the presence of cracks in them, did not exceed 2 - 3 radii of the underground cavity at the level of the explosion point, as much as 1.5 radii below and from 6 to 8 radii above along the cylindrical cavity (the duct).

However, the zone of disturbances established according to the decrease in the seismic wave velocities was considerably greater and amounted to approximately 4 - 10 radii of the underground cavity. The configuration of the disturbance zone was asymmetrical, and was elongated in the direction of the underground adit.

Comparison of radii of cavities during underground nuclear explosions and radii of circular fault during earthquakes. In [55], it was shown that for a three-dimensional model of the focus of an earthquake, the radius d of the circular fault is approximately:

$$d \approx (0{,}1 \div 0{,}3)\sqrt[3]{E_s}, \qquad (20)$$

where E_s is the seismic energy pertaining to the focus. Substituting the value of E_s [see below, formula (21)], we find for earthquakes:

$$d \approx (8{,}5 \div 25{,}5)\cdot\sqrt[3]{10^{1.4m}}. \qquad (21)$$

The values of d, calculated by formula (21), are given in Table 33.

From a comparison of the observed values of the radii R_k of cavities during underground explosions (Table 33) and the values

of d for earthquakes with the same magnitude m, it is clear that the radii of the circular ruptures exceed by 20 - 60 times (for example, for granites) the radii of cavities in explosions. These differences increase considerably with increasing m.

It is quite likely that the differences in R_k and d may be due to the fact that, in underground explosions, the dilatational waves have shorter periods than in earthquakes with the same magnitude (Figure 43). The basic factor determining the periods during explosions apparently is the shorter duration of action of the forces in the source [94].

Even when the dimensions of the destroyed or crumbling zones — constituting 2 - 3 radii of the cavity at the level of the explosion center — are taken into consideration, this will not make any practical difference in the calculation results.

§ 5. Dependence of the Seismic Effect of Underground Nuclear Explosions on the Elastic Properties of the Surrounding Rocks

It has been established experimentally that the focus-related energy E_s of seismic waves caused by underground nuclear explosions depends on the elastic and absorbing properties of the rocks surrounding the explosion, which are characterized by velocity v_p of the dilatational waves, density ρ, porosity (Table 32), and the water saturation. A role of considerable importance is played by the depth at which the charge is laid. In explosions with charges of an equal intensity, i.e., equal energy E_{tot}, placed in chambers of the identical dimensions, but in different rocks, the energy of the seismic waves will be greater, the greater the velocity of the waves and the density of the rocks surrounding the explosion, and also the greater their water saturation [331, 350]. The most significant damping of the energy of the seismic waves — up to 150 times, in comparison with the energy of explosions in granites — was observed in an explosion with ejection of soil in dry alluvium

(the Sedan explosion). The acoustic stiffness in dry alluvium is about 7 – 10 times less than in granites.

The dependence of the energy of seismic waves and their spectrum on the properties of the rocks surrounding the charge, and the influence of the depth of the charge, are well known in seismic prospecting. In order to enhance the effect of explosions and to produce seismic oscillations of a definite spectral composition, explosions during seismic prospecting are carried out in holes with a depth of up to several tens of meters, and these holes are flooded with water.

In several works [241, 229, 331, 350 etc.], an attempt was made to give a quantitative characterization of the dependence of the amplitude or the energy of the seismic waves on the properties of the rocks surrounding the explosion. However, the properties of the rocks in these cases were usually characterized only approximately, mainly by the name of the rocks only. Exceptions are the references [331 and 350], in which the properties of the rocks were characterized qualitatively. In [331], a correlation between the intensity of the seismic oscillations and the porosity of dry samples of the rocks surrounding the explosions is demonstrated.

At the present time, experimental material has been accumulated which allows us to make more valid qualitative assessments of the dependence of the relative portion of the energy of the seismic waves (not only according to P_n waves, but also according to P waves) caused by underground nuclear explosions on the properties of the surrounding rocks. As is known, the detection and identification of underground nuclear explosions by national agencies is being carried out almost exclusively by means of the P waves [182, 183, 337, 344, etc.] and the Rayleigh waves L_R.

Unfortunately, the literature gives information about the surrounding rocks, the intensities of the explosions, and the

conditions under which the explosions were carried out, only for a very few explosions: for only about 20 explosions out of a total number which exceeds 300 [241]. As for information about the dimensions of the blast chambers, which also influence the ratio E_s/E_{tot}, such information has been given only for isolated cases (for the Rainier explosion [239], the Sedan explosion [241], and some others).

Table 32 gives the velocities of dilatational waves and densities in different rocks in their natural environment at depths of from 0.001 to 1-2 km, that is, at presently accessible depths for carrying out underground nuclear explosions. The data were taken from the fundamental works [17, 19, 37, 349], and also from special determinations of the velocities and densities in blast adits and holes.

Data on the relative portion of energy E_s/E_{tot} of seismic waves caused by underground nuclear explosions carried out in various rocks (in volcanic tuffs, alluvial deposits, granites, basalts, and rock salt) are given below. The data were obtained chiefly from P waves. out of the entire combination of properties enumerated above for the surrounding rocks, which influence E_s/E_{tot}, only the influence of the acoustic stiffness of the rocks is examined.

We do not have at our disposal sufficient experimental data to estimate the influence of other factors, such as the porosity and the humidity.

Methods of studying the dependence of seismic wave energy on the acoustic stiffness of the rocks surrounding the explosion. Calculation of the seismic energy E_s released in the focus in the form of elastic seismic waves during earthquakes depends on the average values of the magnitudes m [223] and M_L [1] according to the experimentally established relations for shallow-focus earthquakes:

Footnote (1) appears on page 232

$$\lg E_c = 5{,}8 + 2{,}4m; \tag{22}$$

$$\lg E_c = 9{,}9 + 1{,}9M_L - 0{,}024M_L^2. \tag{23}$$

In this case, the values of M_L can be recalculated into the values of m' according to the following formula:

$$m' = 1{,}7 + 0{,}8M_L - 0{,}01M_L^2. \tag{24}$$

Data obtained in the range of Δ from 16 to 100° were used for determining the average values of m, calculated from the P waves. Records obtained in the USA in a range of Δ from several km to 650 km were used to calculate M_L. In practice, the seismic effect of the explosions is characterized by the seismic magnitudes m or M_L. However, one cannot use (22) or (23) to determine the E_s of explosions, based on the magnitude, in view of the fact that the mechanism of the explosion source differs from the mechanism of earthquakes. The observed connection between E_s and m and M_l differs in explosions and in earthquakes. Correlations analogous to those in (22) and (23) have not yet been established for explosion sources.

In the present study, the values of E_s for explosions were determined according to the Zoppritz-Wiechert formula. We mainly used records of P waves obtained at distances Δ from 16 to 100°.

Table 34 gives data about the intensities of underground nuclear explosions carried out by the USA and France, together with the dates when they were carried out, and the characteristics (acoustic stiffnesses) of the surrounding rocks (volcanic tuffs, alluvial deposits, rock salt, andesites, granites, basalts). The mean values of the magnitudes m_{mean}, calculated from the data of the network of USSR stations, are given, as well as the values of m', calculated from M_L by the formula (24). The values of M_L were taken from the bulletins of the USCGS and from the references [161, 163, 251, 317, 319, 322, etc.].

Discussion of the results. Table 34 gives the ratios E_s/E_{tot} for 26 explosions carried out in the USA and in other regions. These ratios, calculated from the recordings of stations in the USSR, agree well with the values given below, which were obtained in the USA [241] (see Table 35).

TABLE 35. RATIO OF ENERGY OF SEISMIC WAVES TO ENERGY OF UNDERGROUND NUCLEAR EXPLOSIONS IN DIFFERENT SURROUNDING ROCKS

Rocks	E_s/E_{tot}, %
Granite	1.0
Salt	0.8
Tuff	0.3
Alluvium	0.17
Dry alluvium	0.09

The mean value of E_s/E_{tot}, calculated for explosions carried out in crystalline rocks, is 1.0%. This value exceeds by a factor of three the mean values obtained during explosions in tuffs, is about five times greater than during explosions carried out in alluvial deposits at depths of up to 300 m, and is 11 times greater than during an explosion in dry alluvium (Sedan) [265]. Such a sharp damping of the seismic effect during the Sedan explosion is apparently connected, not with the fact that it was carried out with discharges, but most probably with the fact that the acoustic stiffness of the dry alluvium was much less than during explosions in other rocks with greater values of ρv_p.

There is a change of E_s/E_{tot} by 11 times when there is a transition from explosions in granite to explosions in dry alluvium, as is shown in Table 34. This change is apparently close to the maximum value possible change during camouflaged underground nuclear

explosions with intensities higher than 2 - 5 kt carried out in rocks in their natural setting (without concealment [247] and other special measures to reduce the seismic effect of the explosion). The data obtained agree with the data from experiments with chemical explosives [229, 231, 276].

§ 6. Changes in the Ratio of the Amplitudes to the Periods of Body Waves with Epicentral Distance

If one is to justify the use of unified magnitude scales m — elaborated in [225] for shallow-focus earthquakes — for explosions, it must be established that the changes in the ratio of the amplitudes A to the periods T in the body waves P, PP, and S as the epicentral distance is varied are identical for both explosions and earthquakes.

In the present work, the changes of the values of $(A/T)_{exp}$, together with changes of epicentral distance, are compared for P, PP, and S waves observed during underground, contact, and atmospheric explosions with the corresponding curves $(A/T)_{c.s.}$ of earthquakes, calculated from calibrated scales [225]. For the other waves, the values of A/T were obtained only at a small number of stations. These data are not sufficient to reach reliable conclusions, and therefore comparisons were not carried out for them.

Methods of comparing the experimental relationships $A/T(\Delta)$. For an experimental study of the dependence of A/T on Δ, we used data on the amplitudes and periods of P, PP, and S waves observed during underground and contact explosions, and also, to a small degree during atmospheric nuclear explosions. The recordings for the underground explosions were obtained both from wide-band equipment and from equipment with a narrow passband of the SKM, USF, and Benioff types. Those for contact and atmospheric explosions were obtained from wide-band equipment of type SK.

In order to compare and average the relationships $A/T(\Delta)$ obtained during explosions of the same type but with different intensities, carried out both in the same and in different regions, the observed values of A/T were reduced to an identical magnitude level. This was achieved in the following manner. The mean values m_{mean}

were determined from the data for individual values of m_{st}, found at stations of zone III. The amplitude dependences lg(A/T) were plotted as a function of Δ for the value of t found according to calibrated scales [225] in the [lg(A/T), Δ] system of coordinates. Then these relations for the given wave, recorded during different explosions of the same type, were combined, and the observed experimental values of $A/T(\Delta)_{exp}$ were transferred onto a single combined graph.

The graphs $A/T(\Delta)_{exp}$, plotted by the above-mentioned method, for P_Z waves for 24 underground, 11 contact, and one atmospheric explosion, are shown in Figure 50.

The A/T(Δ) graphs for the P_Z waves of underground explosions with m = 5 - 6.1 were reduced to the level m = 5.8. They are plotted in a range of Δ = 1,100 - 11,000 km. For graphs of contact explosions with m = 5.8 - 6.2, they were reduced to the level of m = 6.2 and were plotted in the range of Δ = 4,000 - 11,000 km. For the graphs of atmospheric explosions, they were reduced to the level of m = 5.1 and were plotted in the range of Δ = 1,500 - 5,200 km. The relationships of A/T(Δ) in the range of Δ = 1,100 - 1,800 km are examined only for underground explosions, since within the range of Δ mentioned, data for other types of explosions either have not been obtained (for example, for contact explosions) or are incomplete.

The values of $(A/T)_{exp}$ observed during underground explosions and reduced to a single value of m by the method mentioned above were then averaged one after another in a one-degree interval for the entire range of Δ. These averaged data for underground and contact explosions are shown in Figure 50, a, b.

Figure 51 gives the deviations of the average values of $(A/T)_{exp}$ from the values of $(A/T)_{c.s.}$ for underground explosions expressed in percentages and calculated for a one-degree interval from the scale in [225] from the relation:

$$(A/T) = \frac{(A/T)_{c.s.} - (A/T)_{exp}}{(A/T)_{c.s.}} \qquad (25)$$

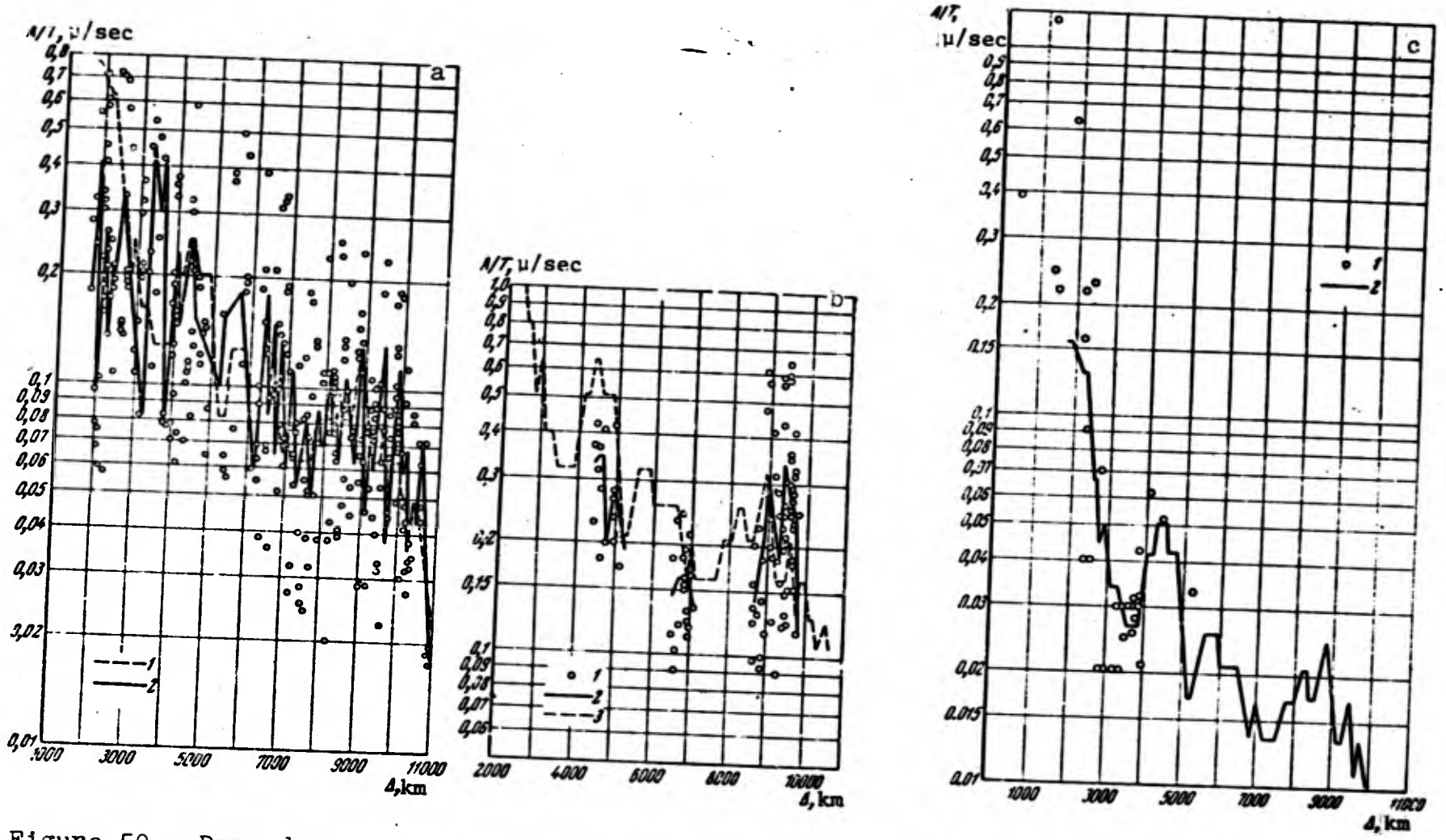

Figure 50. Dependence on epicentral distance Δ of A/T in P waves of nuclear explosions.

a - for 24 underground nuclear explosions: Circles are the experimental values; 1 - calibration curve [223] for m = 5.8; 2 - curve averaging the observed values of A/T; b - for 11 contact nuclear explosions: 1 - experimental values of A/T; 2 - calibration curve [223], m = 6.2; 3 - curve averaging the observed values of A/T; c - for atmospheric explosions: 1 - experimental values; 2 - calibration curve [223], m = 5.1.

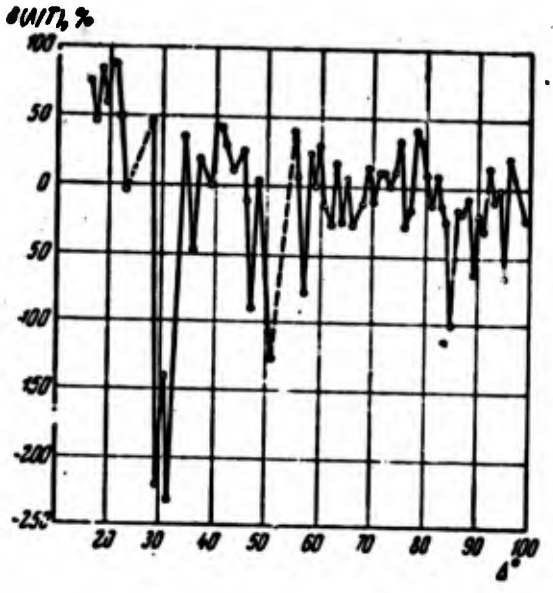

Figure 51. Mean relative deviations of the observed values of $(A/T)_{exp}$ in the P waves of underground explosions from the corresponding values of $(A/T)_{c.s.}$, calculated by the calibrated scale of [223], in relation to the epicentral distance.

Relationship of A/T(Δ) for vertical component of the P wave. Underground explosions. Regardless of the considerable scatter of individual values of $(A/T)_{exp}$, the general shape of their mean values (Figure 50, a) in zone III in the range of Δ = 4,000 - 11,000 km repeats the shape of the calibrated scale. In the given range of Δ, the differences on the average do not exceed ±20%. However, in the beginning of zone III, in the range of Δ = = 3,300 - 3,700 km, there is a local exaggeration of the values of $(A/T)_{exp}$ (up to 200%), the causes of which are as yet unclear. In this range of Δ, only a relatively small amount of data is available.

In zone II, or in the shadow zone (in the range of Δ = 1,100 - 2,500 km), the average values of $(A/T)_{exp}$ are approximately 60 - 80% too low. However, even greater deviations are observed at specific points. This shadow zone, mentioned earlier in [95, 111, 322], is apparently caused by diffraction phenomena of shorter-period oscillations (periods of about 0.5 - 1.5 seconds) in the P waves of underground explosions as compared with the periods T > 5 sec of oscillations in the P waves caused during earthquakes, contact explosions, and atmospheric explosions. The shadow zone was traced very clearly during the Gnome explosions from observations at several tens of stations [323] (Figure 52, a). We will show that considerable scatter of individual experimental values of A/T(Δ) up to 4 - 5 times their mean values was observed in [240] for the P waves of distant

(up to 10,000 km) underground nuclear explosions, and also during earthquakes in the Pacific Ocean, and for P_n waves during explosions in Nevada. In all the cases studied, the zones of elevated values of A/T in the P_n and P waves were observed in regions composed of solid crystalline rocks or a thick layer of sedimentary deposits, for which large velocities in the upper mantle are observed at the same time. The zones of reduced values of A/T are related to tectonically disturbed regions with reduced velocities in the upper mantle.

Contact explosions. The data for contact explosions were obtained in zone III in the range of Δ = 4,000 - 10,500 km (Figure 50, b). For these explosions, the mean values of $(A/T)_{exp}$ generally approach or coincide with the values of $(A/T)_{c.s.}$ calculated from the calibrated scale. However, in a relatively narrow range of values of Δ = 8,800 - 9,500 km, a zone is observed where the values of $(A/T)_{exp}$ exceed by approximately 100% the values of $(A/T)_{c.s.}$ calculated from the calibration curve. These local deviations occur mainly in the Central Asian stations, which, as was shown in [103], generally exceed the values of $(A/T)_{exp}$ in comparison with the values calculated from the calibrated scales of magnitudes [225].

Atmospheric explosions. Reliable data for $(A/T)_{exp}$ in the P_Z waves have been obtained only in the range of Δ = 1,800 - 5,200 km during the most powerful explosions (Figure 50, c). During other explosions, the values of $(A/T)_{exp}$ have been determined only for single stations. An examination of the graph in Figure 50, b reveals that the values of $(A/T)_{exp}$ in the range of Δ = 1,800 - 5,200 km are close to the calculated values of A/T (m = 5.1). For atmospheric explosions with periods T on the order of 5 - 10 sec at the end of zone II and at a distance of Δ = 1,800 - 2,000 km, the shadow zone is not observed. This corroborates the assumption of the diffractional nature of the shadow zone, which was noted in P wave recordings from underground nuclear explosions with periods of 1 - 2 seconds.

Underwater explosions. The sparse data at our disposal about the dependence of $(A/T)_{exp}$ on the epicentral distance in P_Z waves, obtained during three underwater explosions carried out by the United States in the Pacific Ocean [354], indicate that in zone III, this dependence is the same as that for P waves of shallow-focus earthquakes.

A comparison of the relationships of $(A/T)_{exp}$ and $(A/T)_{c.s.}$ in the P_Z waves reveals that in zone III for underground and contact explosions, and for atmospheric explosions in zones II and III a satisfactory similarity is observed in general. Practically the same values were obtained when a large number (15 - 20) of observations were averaged. The standard deviation of $(A/T)_{exp}$ from the average, calculated for Δ = 3,000 - 11,000 km, amounts to 12%.

Relationship A/T(Δ) for horizontal component of P wave. This relationship was studied for contact and atmospheric explosions, for which it was recorded clearly with large amplitudes of the P_H wave.

A comparison of the observed values of $(A/T)_{exp}$, in the P_H waves of contact explosions (Δ = 4,000 - 11,000 km) and of atmospheric explosions (Δ = 2,000 - 5,200 km), with the calibrated scales reveals their similarity. The magnitudes calculated from the P_Z and P_H waves ordinarily practically coincide. This indicates the usefulness of the scales of P_H waves developed for shallow-focus earthquakes in determining the magnitudes of seismic phenomena during explosions (see [103]).

Relationship A/T(Δ) for S waves. Clear S wave arrivals are observed only during the most powerful atmospheric explosions. Less clear data were obtained during contact explosions in the Marshall Islands (in the range of Δ = 4,000 - 9,000 km). The changes of $(A/T)_{exp}$ with Δ for the S waves during explosions coincide in general with the changes of the relationship $(A/T)_{c.s.}$ calculated from the calibrated scale.

The following fact also is interesting. The values of m_S for less powerful (approximately by a factor of two) explosions carried out in the same region as more powerful ones, but at a height less by a factor of 1.5, were found to have a magnitude 0.5 units greater. This may indicate that the intensity of the S waves depends on the height of the explosion. However, the dependence of A/T on Δ did not depend on h.

It should be noted that the mean magnitudes calculated from the S waves for explosions usually exceed the corresponding values of m calculated from P waves by approximately 0.2 units of magnitude.

However, due to incomplete experimental data, it was not possible to statistically study the m_P and m_S relationship during explosions.

Calculation of the dependence of A on Δ for P and S waves. The decrease of the amplitude A in P and S waves with an increase in Δ can be calculated approximately from the following formula:

$$A_{P,S}(\Delta) = \sqrt{\frac{E_c^{P,S}\left|de_0/d\Delta\right|}{8\pi R^2 \rho v_{P,S} \sin\Delta \operatorname{tg} e_0 \exp\left(kL\frac{t}{T}\right)}}, \qquad (26)$$

The above formula was obtained from the Zöppritz-Wiechert formula for the energy E_s of body waves [68]. The notation in Formula (26) is the same as that in [68].

The relationship of $A_P(\Delta)$ in P waves for oscillations with a period of 1 second is given in Figure 53 by curve 6. The curve was calculated for epicentral distances of 2,200 - 11,000 km, taking absorption in the mantle into account. The theoretical curve was not calculated at 1,100 - 2,200 km, since the value of $\left|\frac{de_0}{d\Delta}\right|$ taking into account the loop of the hodograph has not yet been found.

The values of $\left|\frac{de_0}{d\Delta}\right|$ used in the calculations were taken from the tables in [68]. The energy absorption coefficient k, in accordance with data in [227], was assumed to be $k = 1.2 \cdot 10^{-4}$ km^{-1}.

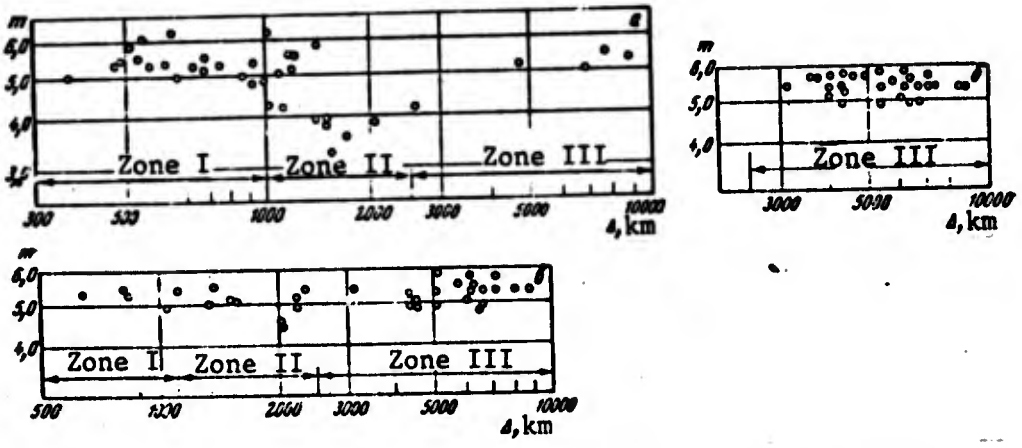

Figure 52. Dependence of m on Δ for underground explosions in zones I, II, and III.

a - for Gnome explosion in salt bed; data from [322]; b - explosion in solid rock in continental region; c - explosion in Sahara in granite.

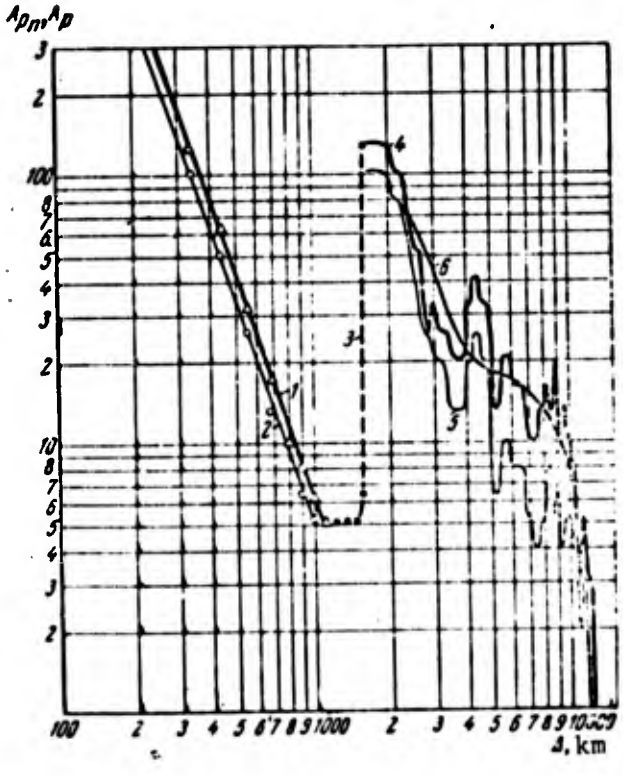

Figure 53. Amplitudes of oscillations in P_{nZ}, P_{nH}, P_Z and P_H waves with a period of 1 second, in relation to the epicentral distance

1 - 5: calculated from the calibrated scales [224];

6: calculated according to the Zöppritz-Wiechert formula taking absorption into account.

Figure 53 gives curves of $A/T(\Delta)$ calculated from the calibrated scales for earthquakes. For Δ = 1,800 - 12,00 km, they were calculated from the scale in [224] (curves 4, 5), and for Δ = 1,000 - 1,800 km — from the scale in [214, 216] (curve 3).

It is clear from a comparison of the theoretical curve $A_p(\Delta)$ with the calibration curve 4 that the decrease of A with Δ, determined by Formula (26), in general agrees satisfactorily with the shape of the calibration curve. The theoretical curve averages out the calibration curve. Analogous results were obtained also for the S waves. The observed local deviations of the experimental curve $A/T(\Delta)$ from the curve theoretically calculated by the Zöppritz-Wiechert formula indicate that there is a nonuniform structure of the mantle. In the future, as information is accumulated about the absorbing properties in separate portions of the mantle, and after more accurate relationships of $A/T = A/T(\Delta)$ have been established, it will be possible to include these deviations, along with other data, to attain increased accuracy concerning the structure of some areas of the mantle.

Dependence of A_{PP} and $(A/T)_{PP}$ on Δ during nuclear explosions. The dependence on Δ of the amplitude A_{PP} of oscillations in the PP waves and the ratio of the amplitude to the period $(A/T)_{PP}$ was studied using data obtained by wide-band SK seismographs, mainly during the most powerful contact explosions carried out by the United States in the Marshall Islands. The power of the explosions was from 10 to 15 Mt, and their unified magnitude m was 6.0 $\pm$ 0.1 to 6.2 $\pm$ 0.2 [103]. The recordings of vertical seismographs were studied.

Table 36 gives the amplitudes and periods in the PP_Z and P_Z waves recorded during the above-mentioned explosions, and also during the underwater Wigwam explosion, at stations of the USSR ESSN at Δ = 4,000 - 11,000 km.

Figure 54 gives the experimental values of A_{PP_Z} and of $(A/T)_{PP_Z}$, observed for explosions at different epicentral distances. Graphs

TABLE 36. DEPENDENCE OF A_{PP}/A_P AND $(A/T)_{PP}/(A/T)_P$ ON Δ FOR NUCLEAR EXPLOSIONS CARRIED OUT IN THE MARSHALL ISLANDS AND OFF THE COAST OF CALIFORNIA

Stations	Δ°	Date	$\frac{A}{T}$ microns/sec	A_P, microns	A_{PP}, microns	m_P	T_{PP}, sec	$\frac{A_{PP}}{T_{PP}}$
Kuril'	36°41'	26.III 1954	1,27	4,1	1,18	6,27	4,4	0,27
Yuzhno-Sakhalin	40 07	28.II	0,95	4,7	0,56	5,56	5,0	0,11
Yuzhno-Sakhalin	40 07	26.III	1,53	4,7	1,11	6,0	4,8	0,25
Petropavlov-Kamchatka	41 40	26.III	1,04	4,7	1,14	5,93	4,2	0,27
Uglegorsk	42 03	28.II	1,85	4,4	0,79	5,84	3,6	0,22
Vladivostok	42 39	28.II	0,95	4,8	0,63	5,7	5,0	0,13
Vladivostok	42 39	26.III	0,5	4,7	0,3	5,38	5.0	0,06
Vladivostok	42 39	25.IV	0,3	4,7	0,32	5,5	5,9	0,08
Magadan	49 06	4.V	0,6	5,2	0,57	5,74	5,4	0,11
Kyakhta (E-W)	61 21	28.II	0,84	5,3	0.5	6,24	4,6	0,11
Kyakhta (E-W)	61 21	26.III	0,55	5,8	0,4	6,05	6,0	0,07
Irkutsk	63 12	28.II	0,77	4,7	0,54	6,3	5,2	0,1
Irkutsk	63 12	26.III	0,71	4,7	0,5	6,3	6,0	0,11
Naryn	81 46	28.II	0,77	6,0	0,46	6,15	5,2	0,09
Frunze	82 35	28.II	1,45	4,0	0,58	6,35	4,0	0,14
Murgab	83 49	28.II	0,58	4,7	0,85	5,9	4,6	0,05
Murgab (E-W)	83 49	28.II	0,38	4,4	0,58	6,7	3,6	0,16
Frunze	82 35	26.III	0,84	4,7	0,28	6,05	4,2	0,07
Murgab (E-W)	83 49	26.III	0,75	4,4	0,75	6,73	4,4	0,17
Murgab (E-W)	83 49	25.IV	0,25	4,7	0,63	6,6	5,0	0,13
Andizhan	84 45	28.II	2,5	4,7	1,0	6,68	4,2	0,24
Fergana	85 06	28.II	1,38	4,7	0,69	6,47	4,2	0,14
Khorog	85 45	28.II	1,04	4,7	0,74	6,47	5,2	0,14
Tashkent	86 44	28.II	0,9	4,2	0,3	6,1	4,8	0,08
Tashkent	86 44	28.II	0,93	4,7	0,3	6,1	4,7	0,08
Dushanbe	87 44	28.II	0,75	4,7	0,22	5,8	5,0	0,04
Dushanbe	87 44	25.IV	0,8	4,0	0,33	6,2	5,0	0,08
Kabansk	87 48	14.V 1955	0,8	3,0	0,84	6,5	4,0	0,21
Ashkhabad	95 45	28.II 1954	0,87	6,0	1,05	6,5	6,2	0,19

(continued on next page)

TABLE 36. DEPENDENCE OF A_{PP}/A_P AND $(A/T)_{PP}/(A/T)_P$ ON Δ FOR NUCLEAR EXPLOSIONS CARRIED OUT IN THE MARSHALL ISLANDS AND OFF THE COAST OF CALIFORNIA.

Stations	A_{PP}/A_P	$\left(\frac{A}{T}\right)_{PP} / \left(\frac{A}{T}\right)_P$	Type of seismograph	Place of explosion	Conditions of explosion	Region of reflections		
						Lat.	Long.	Region
Kuril'	0,93	0,81	SVK	Marshall Islands	in water	30°C	155°E	Pacific Ocean
Yuzhno-Sakhalin	0,59	0,54	»	ditto	on earth	30	136	"
Yuzhno-Sakhalin	0,73	0,71	»	» »	in water	30	156	
Petropavlov-Kamchatka	1,1	1,05	»	» »	»	32	163	"
Uglegorsk	0,43	0,52	»	» »	on earth	32	156	"
Vladivostok	0,67	0,7	SVG	» »	»	28	151	"
Vladivostok	0,6	0,64	»	» »	in water			
Vladivostok	1,06	0,95	»	» »	on earth			
Magadan	0,95	0,82	SVK	» »	in water	28	160	"
Kyakhta (E-W)	0,6	0,69	SGK	» »	on earth	35	142	Japanese trough
Kyakhta (E-W)	0,73	0,71	»	» »	in water	35	142	"
Irkutsk	0,62	0,64	SVK	» »	on earth	36	144	Pacific Ocean
Irkutsk	0,63	0,55	»	» »	in water			"
Naryn	0,6	0,69	»	» »	on earth	32	129	East China Sea
Frunze	0,4	0,4	»	» »	»	35	129	S-E coast of Korea
Murgab	0,43	0,43	»	» »	»	34	128	Korean Straits
Murgab (E-W)	1,53	2,0	SGK	» »	»			
Frunze	0,33	0,37	SVK	» »	in water	35	129S-E	Coast of Korea
Murgab (E-W)	1,0	1,0	SGK	» »	»	34	128	Korean Straits
Murgab (E-W)	2,5	2,36	»	» »	»	35	128	So. Coast of Korea
Andizhan	0,4	0,45	SVK	» »	on earth	35		"
Fergana	0,5	0,56	»	» »	»			"
Khorog	0,71	0,64	»	» »	»	34	128	"
Tashkent	0,33	0,29	»	» »	»	37	126	Western coast of Korea
Tashkent	0,31	0,31	SGK	» »	»			
Dushanbe	0,3	0,28	SVK	» »	»	35	125	Yellow Sea
Dushanbe	0,38	0,3	»	» »	»			"
Kabansk	1,05	0,79	»	coast of Calif.	undergrd. 600 m depth	45	170	Pacific Ocean
Ashkhabad	1,2	1,16	»	Marshall Islands	in water	37	120	Shantung Peninsula

for the changes undergone by A_{PP_Z} and $(A/T)_{PP_Z}$ are shown together with changes of Δ for shallow-focus earthquakes with m = 6.2, plotted accor.ing to the Gutenberg calibration curve [225] for the PP_Z waves. Since the periods of the PP waves, for phenomena with $m \geq 6$, practically do not change with changes in Δ (see Figure 45), the shape of the graphs for A_P and $(A/T)_{PP}$ in the entire range of Δ is practically identical.

Examination of Figure 53 shows clearly that the shape of the experimental dependence of A_{PP_Z} and $(A/T)_{PP_Z}$ on Δ, observed during explosions, agrees in general with the shape of the graphs $A_{PP}(\Delta)$ and and $(A/T)(\Delta)$ for earthquakes. However, for some stations (Andizhan, Ashkhabad and others), the experimental values of A_{PP_Z} and $(A/T)_{PP_Z}$ exceed the values obtained from the calibrated scales. These deviations, as a rule, apply to those stations for which anomalously high values of A_{P_Z} and $(A/T)_{P_Z}$ (see [103]) were observed during contact explosions and other types of explosions. These overexaggerated values of A_{P_Z} and $(A/T)_{P_Z}$ are due to the seismogeological structure in the region of the stations.

It must be noted that the calibration scales [225] for PP waves were obtained for certain average conditions, without taking into account the influence of the structure of the Earth's crust, or the upper mantle in the region of reflection on the dependence $A_{PP}(\Delta)$. Gutenberg and Richter discovered this influence for the Pacific Ocean region and the continents [45]. Analogous data for the Atlantic Ocean region are given in [291]. It is possible that this may be due to a certain decrease in the amplitudes of the PP waves with the points of reflection under the oceans. This problem is examined below in greater detail.

Dependence of the ratio $A_{PP}/A_P(\Delta)$ for continental and oceanic reflections. The references [45, etc.] examine the dependence of A_{PP_Z}/A_{P_Z} on Δ for the PP waves of earthquakes reflected in the

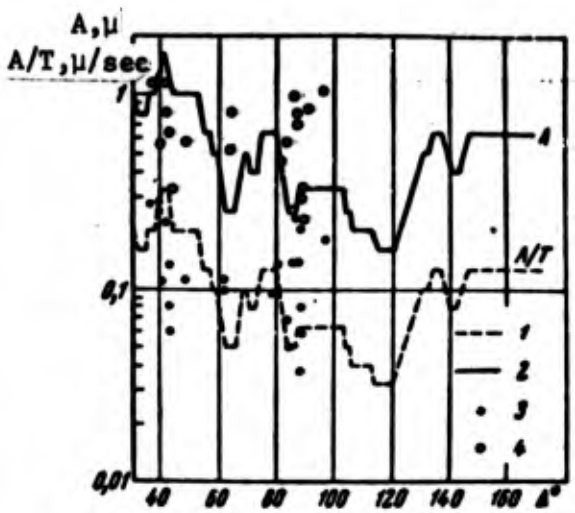

Figure 54. Amplitude A and A/T ratio for PP_Z waves of contact explosions, in relation to epicentral distance

1, 2: calibration curves, respectively, for A when T = 5 seconds and for A/T according to [223] when m = 6.2;

3, 4: observed values of A and A/T.

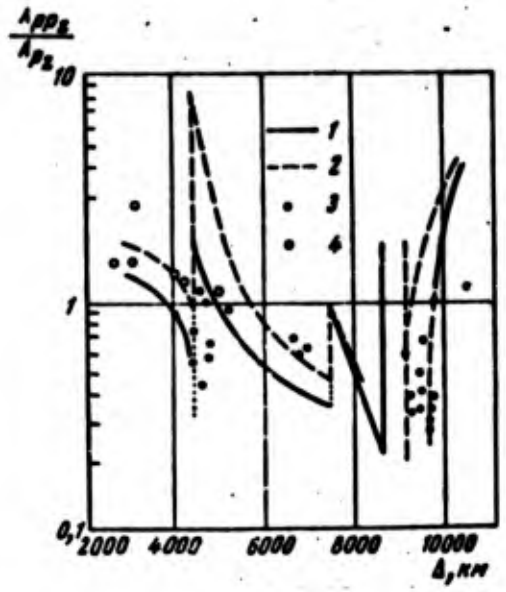

Figure 55. Dependence of A_{PP_Z}/A_{P_Z} on Δ for PP waves of contact and underwater explosions, reflected:

1: in the Pacific Ocean region;

2: from the surface of the continents (1 and 2 are from [45]);

3, 4: corresponding observed values.

continental regions and in the Pacific Ocean region. This dependence at Δ = 3,000 - 10,000 km is shown in Figure 55 according to [45].

The ratio of the PP wave amplitudes to the amplitudes of the P waves for reflection under the Pacific Ocean is 20 - 30% less than during reflection from the surface of the continents.

In this connection, it is interesting to compare the dependence of A_{PP_Z}/A_{P_Z} on Δ during earthquakes and nuclear explosions with the reflections of the PP waves in the Pacific Ocean region and reflections from the surface of continents.

Table 36 gives the values of A_{PP_Z}/A_{P_Z} according to data from stations of the USSR ESSN, as well as information on the coordinates of the wave reflection points in the Pacific Ocean during contact and underwater explosions carried out by the United States in the Marshall Islands and off the coast of California. Since periods in the P and PP waves are very similar (Table 36), the influence of the nonuniform seismogeological structure in the region of the stations on A_{PP_Z}/A_{P_Z} is practically eliminated. The values of $(A/T)_{PP_Z}/(A/T)_{P_Z}$ almost coincide with the values of A_{PP_Z}/A_{P_Z}.

Figure 55 gives the experimental values of A_{PP_Z}/A_{P_Z}, observed during explosions, for the PP_Z waves reflected in the Pacific Ocean region and from the surface of the continents.

At the present time, insufficient experimental material has been collected to study the ratio A_{PP}/A_P during explosions for the PP waves reflected from the surface of continents.

Examination of Figure 55 shows that the experimental values of A_{PP_Z}/A_{P_Z} observed during explosions with the reflection points in the Pacific Ocean can be more or less approximated by the relationship $A_{PP_Z}/A_{P_Z}(\Delta)$ established in [45] for this region from earthquake data. The values observed at the Irkutsk and Kyakhta stations (Table 36) are exceptions. The points of reflection for them are located over the deep Japanese trough. (According to the data of Gutenberg, the values of A_{PP}/A_P are large for the deep parts of the ocean than for the shallow parts.)

Thus, the decrease in the ratio A_{PP}/A_P — observed for the Pacific Ocean region from earthquake data — is in all probability also observed during nuclear explosions. Inasmuch as the influence of a nonuniform structure in the region of the station is excluded for the values of $A_{PP}/A_P(\Delta)$, the coincidence of the values of A_{PP}/A_P

during earthquakes and explosions, observed for the Pacific Ocean region, may also indicate that the dependence $A_{PP}(\Delta)$ is identical during explosions and earthquakes.

Dependence of the ratio A_{PcP}/A_P on Δ. It has been established that the experimental values of the ratio A_{PcP}/A_P during contact explosions ($T_P \approx 4 - 6$ sec, $T_{PcP} \approx 3. - 5$ sec) and during underground explosions ($T_P \approx 0.6 - 1.6$ sec, $T_{PcP} \approx 0.7 - 1.5$ sec), and even during earthquakes, are greater than the theoretically calculated values [17, 65, 166, 170]. This fact (Figure 56) indicates that the structure of the medium is more complex in the transition zone on the boundary between the mantle and the core than it is assumed to be in theoretical calculations. These calculations include the reflection phenomena on the boundary of two half spaces, with a sharp break in the values of the velocities and densities. In all probability, such a model of the medium structure is highly simplified. In [17], an attempt is made to explain this discrepancy by means of a thin layer with a high velocity on the boundary between the mantle and the core.

The dependence of A/T on Δ for the PcP waves during explosions is the same in general as for the P waves [65, 187].

Thus, there is satisfactory agreement between the dependences $A/T(\Delta)_{exp}$ and $A/T(\Delta)_{c.s.}$, calculated for the P, PP, and S waves from calibrated scales. This shows that the ratio A/T in the waves in question during explosions and earthquakes in zone III undergoes practically the same changes for all types of explosions.

Consequently, the magnitude $m_{P,PP}$ characterizes the relative seismic effect of these explosions to the same degree as it characterizes the intensity of earthquakes.

For underground explosions at the end of zone II and the beginning of zone III, unusual features of the relationship $A/T(\Delta)$ in the

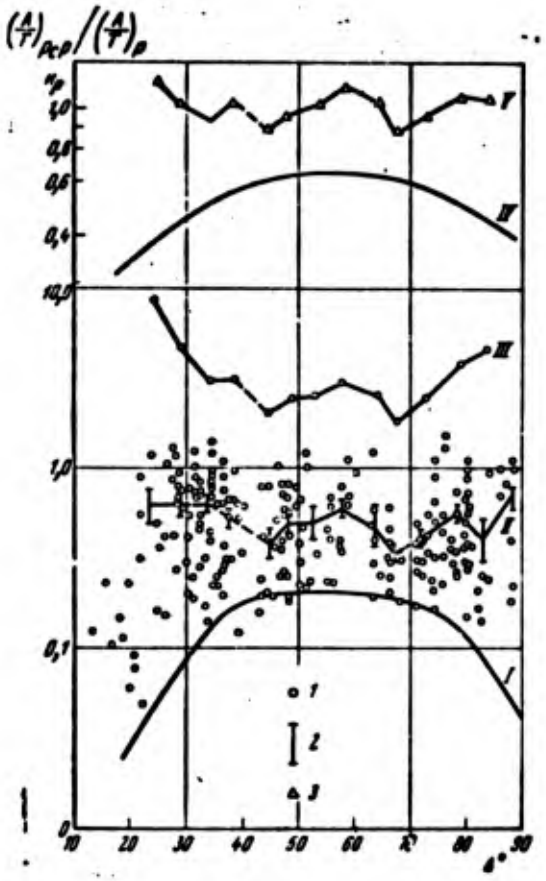

Figure 56. Comparison of experimental and theoretical reflection coefficients of PcP waves, from data in [17]

I - theoretical curve of the ratio $(A/T)_{PcP}/(A/T)_P$;

II - curve averaging the experimental values, 1 at 5-degree intervals, 2 standard deviations;

III - ratio of averaged experimental values (II) to theoretical values (I);

IV - theoretical curve of reflection coefficient k_{PcP};

V - experimental curve of reflection coefficient k_{PcP};

3 - experimental values of k_{PcP}.

P waves are observed, which are connected with the short-period composition of the oscillations. This must be taken into consideration when one is averaging the waves of m observed at a network of stations.

In conclusion, let us note that all the extrema of the A/T(Δ) curve which are observed for earthquakes are also observed on the A/T(Δ) curve obtained from data on explosions for oscillations with $T \approx 4 - 5$ sec and more. This is especially astonishing if one takes the fact into consideration that the calibration scale was plotted from data on earthquakes, for which the radiation from the focus is known to depend on the azimuth. It is obvious that, when data from many earthquakes were averaged, the influence of nonuniform radiation from the focus was excluded to a considerable degree.

§ 7. Relationship of the S Waves and P_Z Wave Amplitudes During Various Types of Explosions and Earthquakes

The mean values of the A_S/A_P ratio for shallow-focus earthquakes

in zone III (from 20° to 100°), calculated by Gutenberg's calibrated scales [225], range between 3 to 5. The corresponding values of the $(A/T)_S/(A/T)_{P_Z}$ ratio fall between 3 to 2. These ratios do not depend on the magnitude m. According to data in [90], the ratio A_S/A_P ranges between 2 to 1 in the above-mentioned range of Δ. The drop of A_S/A_P with changes in Δ is not monotonic. The areas of the largest (by 2 - 3 times) decrease of A_S/A_{P_Z} are observed for Δ from 35 to 45° and 65 - 85°. Areas of high values of A_S/A_{P_Z} (in the range of Δ = = 25 - 35°, etc.) can also be observed.

Somewhat larger A_S/A_P ratios (up to 6 - 10) are observed during deep-focus earthquakes (see the seismogram in Figure 41, c). However, this has practically no influence on the mean values of A_S/A_{P_Z}, since the annual number of deep-focus earthquakes is approximately 3% of the total annual number of all earthquakes.

Somewhat different values for the A_S/A_{P_Z} ratios were observed for waves caused by nuclear explosions (Table 37). In this case, the mean values of A_S/A_{P_Z} and the limits of their fluctuations are different for different types of explosions. Table 37 gives the results of statistical processing and evaluation of the data for A_S/A_{P_Z}.

As is clear from data in Table 37, the largest mean values of A_S/A_{P_Z} during atmospheric explosions barely differ from the corresponding values during earthquakes. During contact, underground, and underwater explosions they are smaller than during earthquakes. These differences in A_S/A_{P_Z} may be utilized in identifying the recordings of explosions.

TABLE 37. MEAN AND MAXIMUM VALUES OF THE RATIOS A_S/A_{P_Z} AND $(A/T)_S/(A/T)_{P_Z}$ FOR VARIOUS TYPES OF EXPLOSIONS AND SHALLOW-FOCUS EARTHQUAKES IN ZONE III

Type of source	Range of magnitude variations		A_S/A_{P_Z}		$(A/T)_S/(A/T)_{P_Z}$	
	M	m	Maximum values	Average	Maximum values	Average
Atmospheric explosion	4.0-5.8	4-5.1	0.5-10	1.3	1 10	3
Contact explosion	4.5-6	5.8-6.3	0.3-0.8	0.5	0.1-0.5	0.2
Underground and underwater explosion	3.5-5.9	5.3-6.5	0.05-0.2	0.1	$\leq$0.1	$\leq$0.1
Earthquakes	5.0-6.5	5.5-6.5	1-5.1	2.2	0.5-3.0	1.5

CONCLUSIONS

1. During atmospheric and contact explosions the same direct, reflected (monotypic and exchanged) body waves are recorded in zones II and III as during shallow-focus earthquakes. The areas in which the waves are traced are the same as in the case of earthquakes.

2. The periods in the body waves during atmospheric and contact explosions are close to the periods of the corresponding waves of earthquakes with a comparable magnitude. They undergo little changes when the epicentral distance changes.

3. The decrease of the oscillation amplitude ratio to the period, when the epicentral distance changes, in P and S waves of atmospheric and contact explosions is the same as in the case of corresponding earthquake waves.

4. During underground and underwater explosions, the transverse waves, as a rule, are of a low intensity, and it was not always possible to record them in the entire area in which they were present.

5. During underground and underwater explosions, the periods in the body waves are usually 2 - 3 times less than in earthquakes with a comparable magnitude. In zones III and IV they undergo practically no changes with an increase in the epicentral distance. This is connected basically with the fact that, during underground explosions, the duration of forces in the source is smaller by a factor of 10^7 than the duration of forces during earthquakes with a comparable magnitude. It is also due to the fact that the dimensions of the focus (the radius of the underground cavity formed as a result of the explosion) are approximately two orders of magnitude smaller than the corresponding radius of the circular fault during earthquakes with a comparable magnitude.

6. It was established that there is a weak dependence of the periods T_p of the oscillations in body P waves on the TNT equivalent Q of underground nuclear explosions for tuff, alluvium, and other types of rocks: $T_P \approx 0{,}9 \sqrt[11]{Q}$.

7. During underground explosions, the values of A/T in zone II for the P waves were underestimated, in comparison with the values during earthquakes — that is, a shadow zone was observed. The presence of this zone is connected with diffraction phenomena due to the shorter period of the oscillations during underground explosions.

8. The mean values of the ratio of the transverse wave amplitudes to the dilatational wave amplitudes A_S/A_{P_Z} for explosions differ from those for earthquakes. During contact, underground, and underwater explosions these ratios are smaller than during earthquakes. These differences, along with others, may be utilized in identifying the recordings of explosions.

9. The shape of the oscillations in body waves in all types of explosions is a short train, whose oscillation amplitudes on both sides of the maximum value drop off faster than in earthquakes. This is noted most clearly for P waves of underground and underwater explosions.

CHAPTER VI

CHARACTERISTICS OF SURFACE WAVES CAUSED BY VARIOUS TYPES OF EXPLOSIONS

Relatively intense Rayleigh waves (L_R) and Love (L_Q) surface waves are recorded in all types of nuclear explosions, except underwater explosions. In the continental regions, channel surface waves of types L_x, L_1, L_g, R_{g_1}, and R_{g_2} are also recorded. During explosions with intensities in the megaton class ($M \approx 4.5 - 5.5$), surface waves L_R and L_Q were recorded at epicentral distances of as much as 12,000 - 14,000 km.

During atmospheric explosions, surface waves of the Rayleigh type usually have their greatest intensity in comparison with other types of body and surface waves. In the overwhelming majority of cases, for atmospheric explosions with an intensity of several tens of kilotons, and in some cases with hundreds of kilotons, at epicentral distances of $\Delta > 2,000 - 3,000$ km only waves of this type could be recorded successfully. For this reason, it is natural that researchers should strive to use surface waves, primarily Rayleigh waves, for detecting and identifying nuclear explosions, particularly for determining the coordinates of the explosion epicenters, the

times in the epicenter, and also for the purpose of determining the explosion parameters: their TNT equivalents and the heights of atmospheric explosions.

Surface waves also yield information concerning the forces operating in the focus, i.e., the type of source and its depth. Therefore, attempts have been made in a number of works to use these waves for identifying explosions and earthquakes [55, 56, 97, 138, 150, 162, 163, 326, 345-347 etc.].

Data concerning the propagation and dispersion of surface waves caused by explosions, particularly in combination with data about body waves, open up far-reaching possibilities for studying the structure and physical properties of the Earth's crust and the upper mantle.

In this chapter, a study is made of the dynamic and kinematic characteristics of surface waves caused by atmospheric, contact, and underground explosions when the waves are propagated via continental, oceanic, and mixed paths. This is necessary in order to distinguish their differences from the corresponding characteristics of waves of earthquakes, and in order to determine the causes responsible for these differences. The discussion is also devoted to the possibility of determining the epicenters and parameters of explosions from the surface waves.

In order to clarify the differences in the dynamic characteristics of seismic waves caused by nuclear explosions in various media, the distinctive features of surface waves were studied, and their characteristics were compared with the corresponding characteristics of waves caused by earthquakes.

The following kinematic and dynamic characteristics of waves were studied: the travel times, the trajectories of motion of medium particles, the dispersion curves and other factors during explosions and earthquakes; the periods of maximum oscillations and

the spectral composition of the waves as a function of the epicentral distance; the dependence of the spectral composition of the oscillations on the type of explosions and the structure of the Earth's crust and the upper mantle on the wave propagation path; the correlation between the intensities of various types of surface and body waves, and the dependence of this correlation on Δ and on the magnitude of the phenomenon; the possibility of determining the coordinates of the epicenters and a number of other characteristics.

Data used. In this work, we used records of explosions obtained chiefly in the USSR, and partially data from stations in Europe, Asia, and America published in [145, 287-290, 292, 295, 309, 346, etc.] and in the corresponding seismic bulletins.

The clearest recordings of surface waves were obtained in recordings of long-period (DS) and ultra-long period (UDS) seismographs of the Press-Ewing design, installed in standardized stations on the territory of the USA and in the world-wide network of the USA located in various countries of the world. In the USSR, records of long-period SKD seismographs [93] were obtained at the stations of Pulkovo, Moscow, Simferopol' and others (Figure 57). Most of the records in the USSR were obtained with SK seismographs and with equipment with a narrow passband of the types SKM or USF. Since the last two types of seismographs in the range of periods now being studied had irregular amplification, it was necessary to introduce appropriate corrections. Records of seismographs with a narrow passband were used to a limited extent.

Section 1

Rayleigh Waves L_R

In the present section, we shall examine the kinematic and dynamic characteristics of L_R waves recorded in a range of Δ from several tens of km to 11,000 - 12,000 km during explosions carried

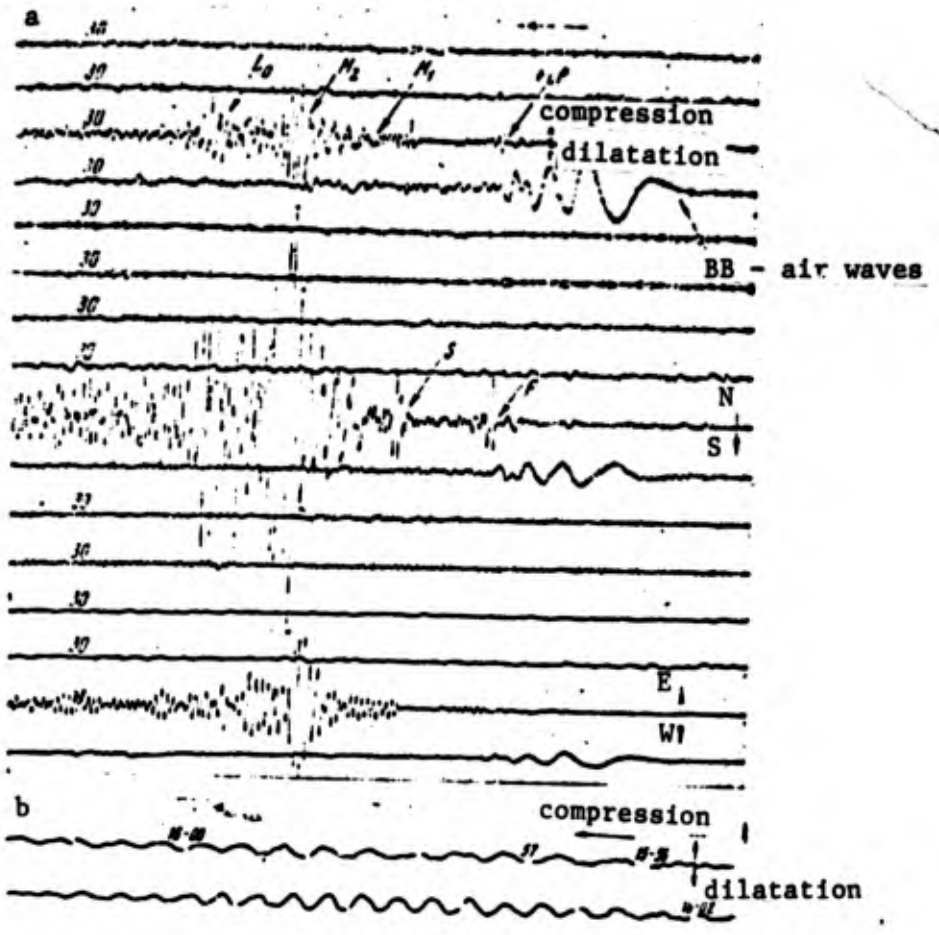

Figure 57. Example of records of surface Rayleigh L_R and Love L_Q waves from atmospheric explosions taken by SKD and SK seismographs a - Δ = 2,100 km; channels of SGKD seismograph equipped with rejection filters; BB - record of atmospheric waves by the seismographs; b - Δ = 8,880 km (explosion in Christmas Island), seismographs with no filters; wide-band SK seismographs; c - Δ = 890 km; d - Δ = 3,500 km; for underground explosions recorded by SKD seismographs with rejection filters; e - at Δ = 2,700 km; f - at Δ = 9,900 km.

(Figure continued on next page)

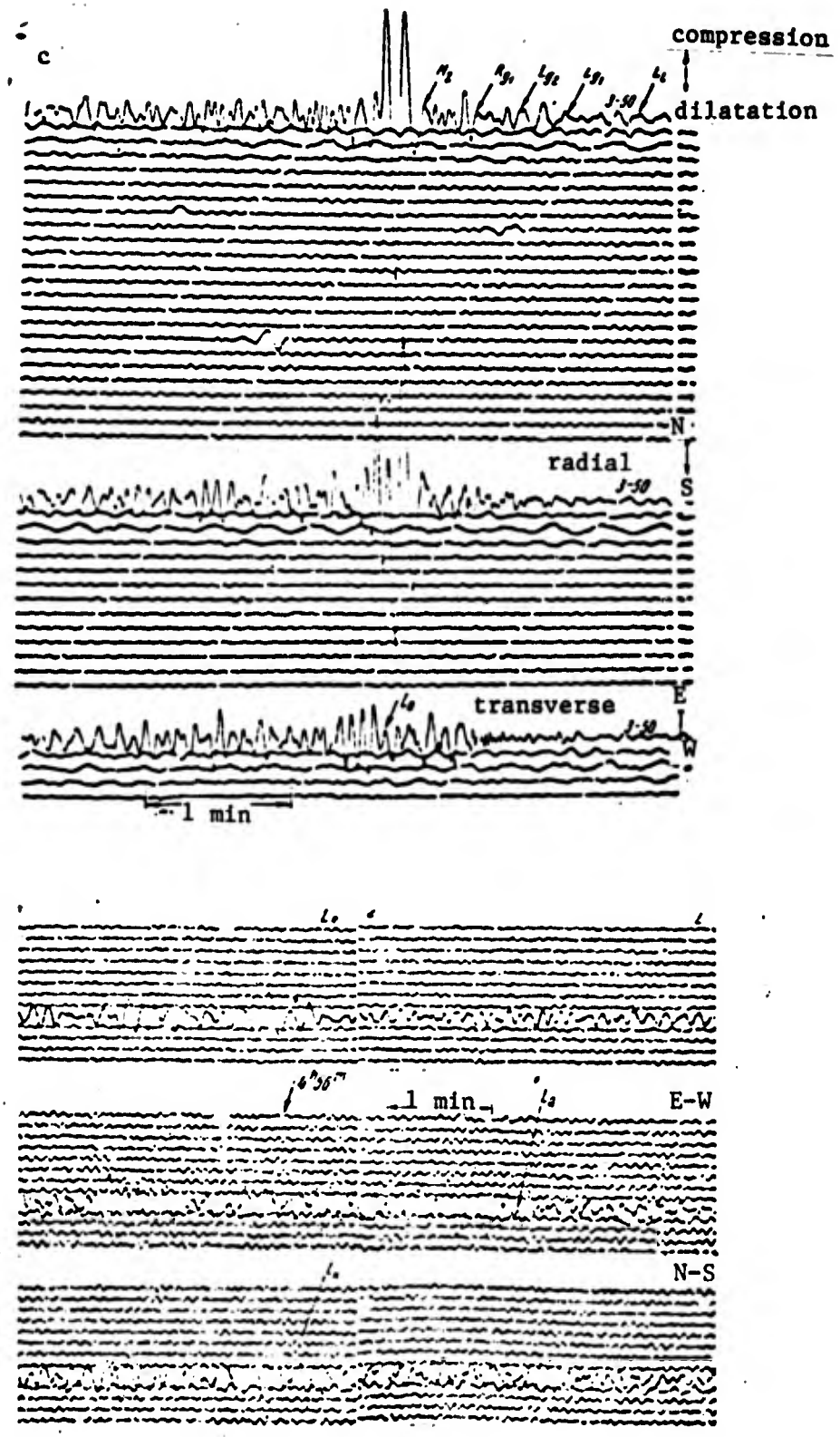

(Figure 57 continued on next page)

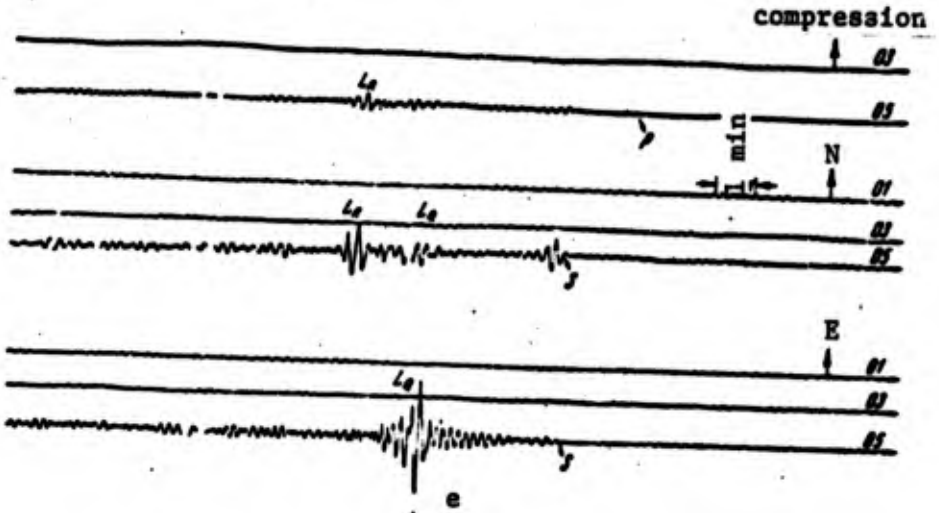

e

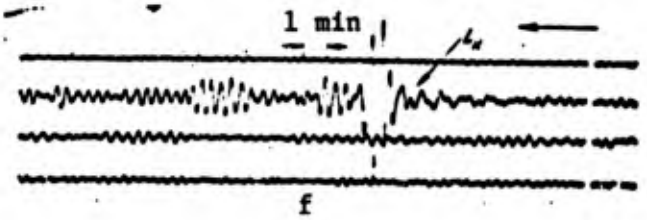

f

out in an atmospheric layer near the ground over the continents or near islands in the oceans.

§ 1. Character of the L_R Wave Records

The distinctive features of the records of an oscillation train in L_R waves during explosions, as well as during earthquakes, depend on the properties of the medium and the structure of the Earth's crust and the upper mantle along their propagation path. The wave paths, as is well known, are divided up into continental, oceanic, and mixed paths. In the last case, part of the waves advance via continental routes, and part via oceanic routes.

The records of the L_R waves, their spectral composition, the duration of the train, and a number of other characteristics depend to a considerable degree also on the type of frequency characteristics of the seismic receiving equipment. Therefore, when examining the records, the type of equipment by which they were received is indicated, and when examining their amplitude and spectral characteristics, corrections are introduced in them for irregular amplification of the seismic receiving channel.

During atmospheric, contact, and underground explosions, the records of the L_R waves propagated along similar paths are generally similar to each other when obtained by equipment of the same type, beginning at a distance of approximately $\Delta > 1{,}500 - 2{,}000$ km. High-altitude and underwater explosions are exceptions. Therefore, we shall examine the records of L_R waves with continental, oceanic, and mixed propagation paths, obtained in all types of explosions, with the exception of high-altitude and deep-water explosions.

L_R waves propagated along paths with a continental structure of the Earth's crust. During atmospheric, contact, and underground explosions, in the train of oscillations of the L_R waves recorded for $\Delta > 500 - 1{,}000$ km by long-period and wide-band equipment and in

the overwhelming majority of stations, two groups of waves are clearly distinguished, arriving successively one after the other. Following Bath [145], these waves are designated hereafter as M_1 and M_2. In the records of stations located in sedimentary or sedimentary-metamorphic rocks, a third group of oscillations is also distinguished in the train of L_R waves. This third group is designated as L_0 (Figure 57).

It must be noted that in records of wide-band SK seismographs, during atmospheric and contact explosions of small and medium intensity (up to several hundreds of kilotons), in most cases there are only two groups of waves — M_2 and L_0 — which can be clearly distinguished visually. However, in the amplitude spectra of records obtained even during these types of explosions, an extremum caused by the M_1 wave is observed (see § 7 of this chapter).

The M_1 waves are connected with the Earth's crust and the upper mantle, the M_2 waves — with the Earth's crust, and the L_0 waves — with the sedimentary or sedimentary-metamorphic layer of rocks in the region where the station is located.

M_1 waves. The first, longest-period group of oscillations with a clearly expressed normal dispersion belongs to this wave group.

The M_1 wave arrivals in the records of wide-band seismographs ordinarily are not sharp, with the waves appearing against a background of shorter-period oscillations of L_x, L_1, and other waves. However, in the records of long-period seismographs, where the oscillations with periods of up to 10 - 12 seconds have been filtered out, quite clear and sharp arrivals of the M_1 waves are observed.

The M_1 waves are polarized in the vertical plane; the motion of soil particles in the M_1 waves is retrograde and proceeds along an ellipse, whose major axis lies in the vertical plane (Figure 58). The ratio of the axes A_H/A_Z for different stations of the USSR varies from 0.7 to 1 (see Table 41).

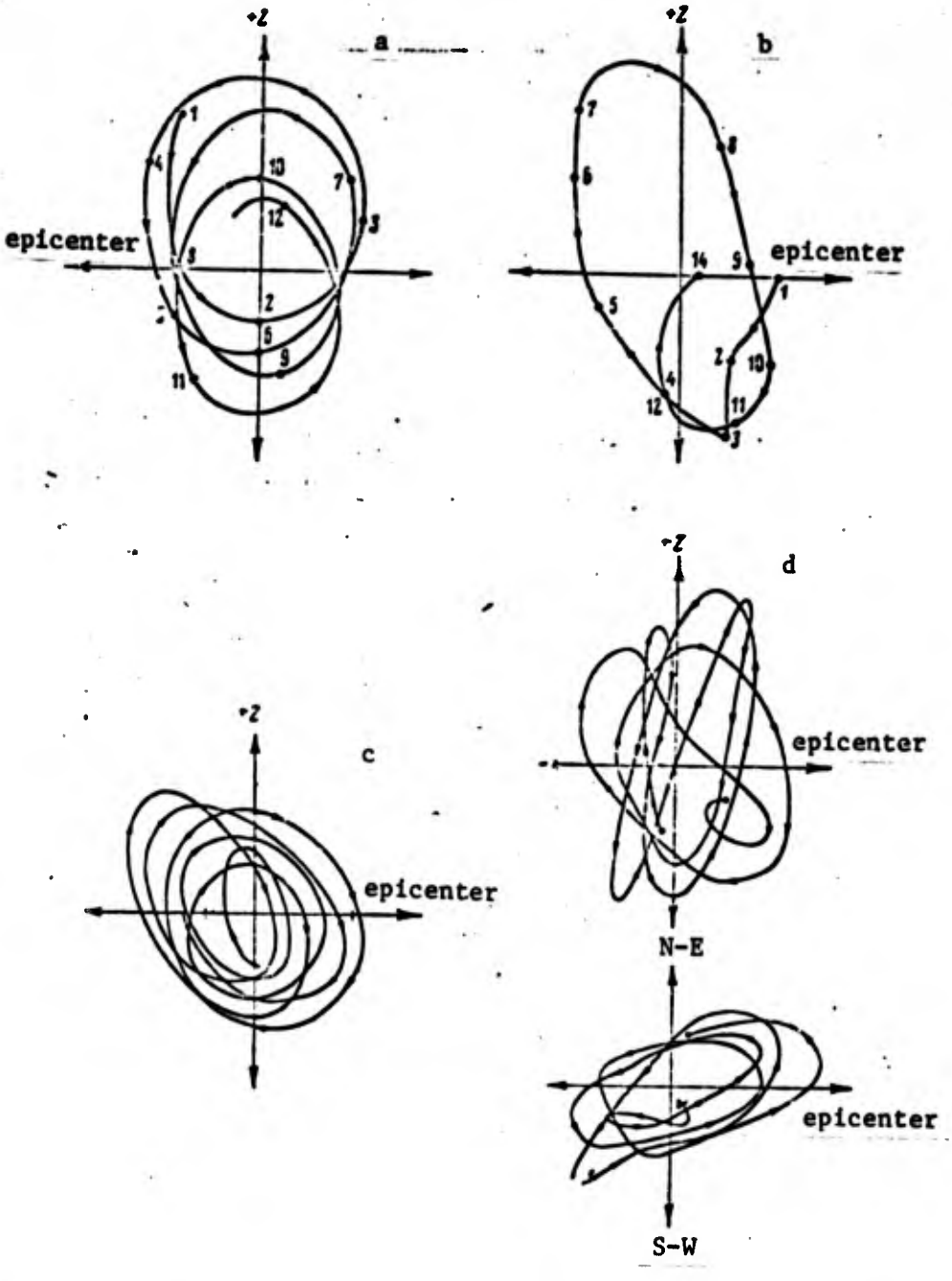

Figure 58. Trajectories of motion of particles from the medium in a vertical plane in Rayleigh waves recorded during an atmospheric explosion (Δ = 2,100 km) by SKD seismographs.

a - in M_1 waves; b - in M_2 waves recorded by wide-band equipment; c - in M_2 waves (Δ = 890 km); d - in L_0 waves (Δ = 2,080 km); the numbered points are given to simplify tracing the trajectory.

M_2 waves. The second group of shorter-period oscillations in the train of the L_R waves, which is attributed to the M_2 waves, usually arrives clearly either against a quiet background or against a background of oscillations of the M_1 waves (Figure 57, c etc.). The M_2 wave, which is known in seismology as the chief phase of the Rayleigh wave, is the most intense. In a number of cases it can be clearly distinguished from oscillations in the M_1 wave by a zone of sharp decrease of the oscillation amplitudes. A clearly expressed normal dispersion is observed (Figure 57). The M_2 wave is polarized in the vertical plane, and the motion of soil particles in it is retrograde. M_2 waves can be distinguished with exceptional clarity in the recordings of wide-band SK seismographs in any propagation paths of the L_R waves.

L_0 waves. A third group of usually regular oscillations in the train of the L_R waves belongs to the L_0 waves. This group arrives after the M_2 waves and after damping of the oscillations in them, or more frequently against their background (Figure 57, a, etc.).

L_0 waves are recorded most clearly by wide-band equipment or by equipment with a narrow passband. L_0 waves are not recorded by equipment with ultra-long periods (UDS).

The L_0 waves are weakly polarized in the vertical plane. They are characterized by a relatively weakly expressed normal dispersion and a retrograde motion of the medium particles (Figure 58,c).

In those regions where there is no layer of sedimentary-metamorphic rocks, the L_0 waves are not recorded. For instance, in records of stations located on the Baltic shield in the Scandinavian peninsula or close to it, where there are no sedimentary-metamorphic rocks, it is not possible to distinguish L_0 waves.

Hodographs. Figure 29, b and Figure 42 show the arrival times of the M_1, M_2, and L_0 waves and the time M_{max} of the maximum phase

in the M_2 waves during the most powerful atmospheric and contact explosions recorded by a network of stations in Europe and Asia — that is, in regions with a continental structure of the Earth's core. Figure 29, b and Figure 42 show the averaged hodographs for earthquakes by lines for the M_2 and M_{max} waves [112]. In the hodographs for the waves being examined, a scattering of the experimental values for the travel times of the M_1, M_2, and L_0 waves and the maximum phase of the M_2 waves can be seen. This is due to the following basic causes: (1) it was not possible to distinguish the arrivals of the waves in all the stations, and it is possible that the latest phases of the oscillations have been entered in the hodographs; (2) the propagation velocities of the waves may be different for some directions. This has been established for the M_2 waves. This is particularly important for the L_0 waves.

From a comparison of the dependence on the epicentral distance of the travel times of M_2 and M_{max} waves from explosions and earthquakes, it is obvious that this dependence is in general approximately the same for explosions as it is for earthquakes.

L_R waves moving along paths with an oceanic structure of the crust. In the USSR, M_1 and M_2 Rayleigh waves were recorded in stations equipped with long-period seismographs during the most powerful atmospheric nuclear explosions carried out by the USA in the Christmas Island region on June 10 and 27, 1962, and a number of others. When the M_1 and M_2 waves were recorded at a temporary station at Δ = 8,880 km, the waves moved practically via an oceanic path, since the length of the continental path amounted to only 1,000 km — that is, about one-ninth of the entire path length. In the cases mentioned, L_0 waves either were not observed, or were weak during atmospheric explosions, and also during contact explosions in the Marshall Islands, at the stations at Petropavlovsk-Kamchatskiy, Vladivostok, Magadan, and elsewhere. There is no layer of sedimentary rocks in the three stations mentioned.

M_1 and M_2 waves, propagated along an oceanic trajectory during contact explosions in the Marshall Islands, were recorded in the USSR only at the stations of Petropavlovsk-Kamchatskiy and Yuzhno-Sakhalinsk.

During contact and near-surface ($h \leq 2 - 3$ km) explosions, the recordings of L_R waves traveling via oceanic paths obtained both in USSR and USA stations [246, 283, 288] were similar to the recordings of the L_R waves of earthquakes with their epicenters in the same region.

A characteristic of the recordings of the waves traveling via oceanic paths is their great lifetime in the M_2 group, or in the group following immediately after the M_2 group. This is due to the presence of a layer of water along the propagation path of the waves.

The recordings of the L_R waves possessed an unusual feature during explosions carried out over Johnston Island ($h = 33$ and 70 km) [289]. There were two characteristic groups of oscillations, one with normal dispersion, and the other with anomalous dispersion. The latter waves were also polarized in the vertical plane; the motion of soil particles in them was retrograde and followed elliptical trajectories. The points of the group velocities of the given waves lie on a segment of the theoretical dispersion curve, located in the short-period part of the curve, to the left of the minimum of the group velocity in a wave with normal dispersion. The minimum is located at $T \approx 13$ seconds.

Similar surface waves with anomalous dispersion were observed earlier in U.S. stations during a deep-water nuclear explosion, the Wigwam [290]. During earthquakes, these waves have been observed by Båth in individual cases. Their existence had been predicted earlier theoretically.

Waves propagating in a layer of water with a velocity of 1.47 km/sec (phase T) have also been observed.

L_R waves propagating along mixed paths. Waves propagated along mixed paths have been recorded in the USSR in stations equipped with Golitsyn seismographs with a period of 22 seconds for the natural pendulum oscillations. Somewhat weaker records were obtained with SKD and SK seismographs. The M_1 and M_2 phases were clearly recorded.

L_0 waves can be distinguished in the records very indistinctly at distances of $\Delta > 6{,}000$ km. This may be due to the fact that the stations were at a considerable distance away from the epicenters and were located in crystalline rocks (the station of Sverdlovsk and others) or in regions with a thin layer of sedimentation (stations of Irkutsk, Tashkent, and others). In stations of the USA and Sweden, the same thing was observed in the records of the Rayleigh waves (the absence of the L_0 waves) during atmospheric and contact explosions propagated along mixed paths [145, 346].

When a considerable part of the path of the L_R waves passes along the ocean, there is an increase of the total duration of the record. This increase is conditioned by the presence of a layer of water. This same phenomenon is also characteristic for L_R waves of earthquakes, when there are mixed propagation paths [346].

During powerful high-altitude explosions carried out at elevations of more than several tens or hundreds of kilometers, two groups of intense surface Rayleigh waves are produced — one with normal dispersion, and the other with anomalous dispersion. The presence of a group of waves with anomalous dispersion is a distinctive characteristic present only in high-altitude and deep-water underwater explosions. They have a relatively greater (by 2 - 2.5 times) intensity when the explosion takes place at a height of 70 km than when it takes place at a height of 33 km. This may indicate that explosions have been carried out at elevations higher than 70 - 100 km [289].

The above-mentioned distinctive features of the record, in combination with other seismic indications (the absence or low

intensity of body waves) and also with specific electromagnetic phenomena (earth currents, radio-wave pulse, changes in the magnetic field), can be used in identifying high-altitude explosions and in tentatively estimating their height [128, 145, 342, 348].

A characteristic feature of the records of Rayleigh waves in all types of explosions, which distinguishes them from the records of earthquakes, is the considerably shorter (by 10 - 20 times) duration of the entire oscillation train.

During earthquakes with M > 4.5 - 5.5, quite lengthy oscillations in the following part of the record (after the M_1 waves) are observed, ordinarily with periods of 20 - 13 seconds. They are attributed to the Airy phase. They are followed by irregularly-shaped "Coda" oscillations with periods of about 12 - 10 seconds. However, during explosions, the record of the L_R waves is abruptly interrupted after short M_2 and L_0 phases. The records of waves proceeding along the ocean are exceptions to this (Figure 57, b).

As was shown by special model experiments and theoretical calculations for concentrated sources [213], the factors producing differences in the duration of the surface waves, in particular the Rayleigh waves, during explosions and earthquakes, are connected with the location of the source during explosions on or near the Earth's surface, and also with the direction of forces active in the source.

§ 2. Comparison of the Dispersion Curves of Group Velocities of Rayleigh Waves from Explosions and Earthquakes, Propagated along Different Paths

Below we shall examine the dispersion curves of the group velocities of L_R Rayleigh waves during nuclear explosions with continental, oceanic, and mixed paths of propagation. They are compared with the observed curves of the L_R waves excited by earthquakes and propagated along close paths.

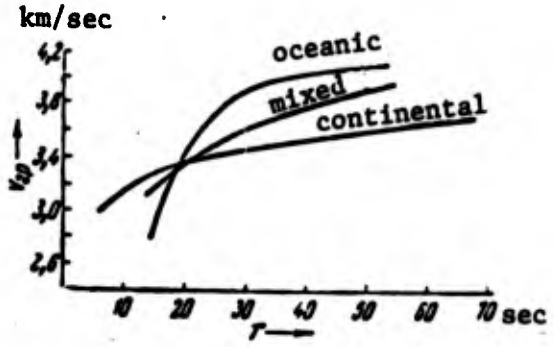

Figure 59. Dispersion curves of group velocities of Rayleigh waves recorded during atmospheric explosions with different propagation paths.

Figure 59 gives examples of the dispersion curves of L_R waves with continental, oceanic, and mixed paths of propagation, recorded in stations of Europe and Asia for atmospheric and contact nuclear explosions in the Marshall Islands and in other regions.

Figure 60 shows the distribution of the paths from the epicenters of the explosions and earthquakes to the stations.

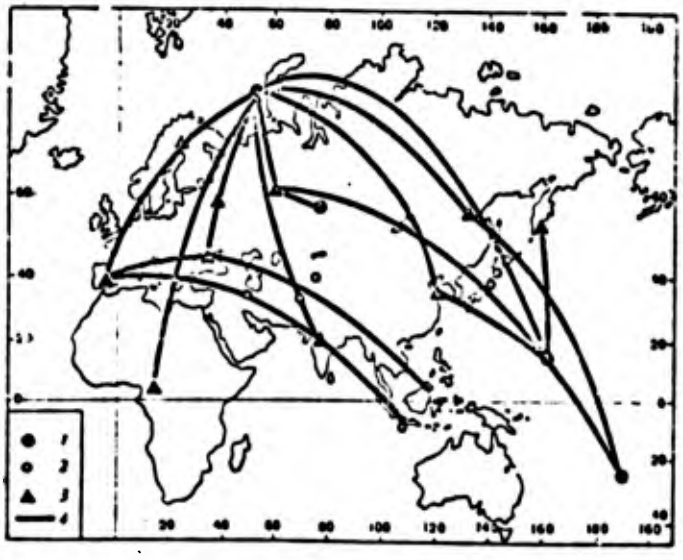

Figure 60. Distribution of paths (4) of propagation of Rayleigh waves from atmospheric explosions and earthquakes

1 - epicenters of explosions; 2 - epicenters of earthquakes; 3 - stations.

Table 38 gives the group velocities of the L_R waves for part of the paths studied. It was established that, for a given station, the dispersion curves observed during repeated explosions carried out at the same place are practically identical.

TABLE 38. GROUP VELOCITIES OF RAYLEIGH WAVES v_{gr} OBSERVED AT A NUMBER OS SEISMIC STATIONS IN EUROPE AND ASIA DURING ATMOSPHERIC AND CONTACT EXPLOSIONS.

Continental wave path propagation										Oceanic path		Mixed path					
										Explosions on Christmas Island		Explosions in the Marshall Islands				Explosion on Christmas Is.	
Δ = 1200 km		Δ = 2200 km		Δ = 1970 km		Δ = 2100 km		Δ = 5200 km		Δ = 8500 km		Δ = 8720 km		Sverdlovsk Station Δ=9970 km		Uppsala Sta. [145], Δ=13500 k 6/27/62	
T, sec	v_{gr}, km/sec	T, sec	v_{gr}, km/sec	T, sec	v_{gr}, km/sec	T, sec	v_{gr}, km/sec	T, sec	v_{gr}, km/sec	T, sec	v_{gr}, km/sec	T, sec	v_{gr}, km/sec	T, sec	v_{gr}, km/sec	T, sec	v_{gr}, km/sec
34	3,30	45	3,53	50	3,72	35	3,40	74	3,76	38	4,05	48	4,10	45	3,89	42,5	3,96
32	3,25	43	3,51	47	3,52	30	3,35	70	3,74	32	3,97	45	4,00	44	3,86	33,2	3,90
31	3,21	38	3,45	38	3,39	28	3,34	67	3,74	30	4,01	32	3,96	42	3,79	29,7	3,80
30	3,20	35	3,40	32	3,29	24	3,24	63	3,75	28	3,92	28	3,90	40	3,76	28,4	3,69
27	3,17	33	3,35	27	3,25	20	3,20	58	3,68	25	3,82	26	3,78	36	3,71	25,2	3,57
25	3,16	32	3,35	23	3,20	16	3,15	53	3,64	20	3,50	24	3,69	35	3,65	21,2	3,46
24	3,16	30	3,30	21	3,17	14	3,15	48	3,54	18	3,25	22	3,51	30	3,60	19,7	3,38
22	3,12	27	3,20	19	3,15	10	3,05	43	3,49	16	3,17	20	3,50	28	3,52		
19	3,10	25	3,20	16	3,15	8	3,00	38	3,45	15	2,95	18	3,26	25	3,44		
17	3,10	23	3,18	9	3,00	6	2,95	33	3,35			16	3,12	23	3,35		
14	3,05	20	3,18					28	3,31					20	3,22		
10	3,00	17	3,18					23	3,20					18	3,10		
8	2,95	15	3,12					18	3,15					17	3,06		
		13	3,00											16	3,04		
		11	3,07														
		9	2,94														
		7	2,88														
		6	2,88														

If the exact time and place of the explosion are known, and if it is also possible to plot the dispersion curves for many, in some cases for several tens of explosions carried out in the same place, this considerably increases the accuracy with which the group velocities can be determined.

Examples of the dispersion curves of L_R waves observed along continental, mixed, and oceanic paths, and the results of their interpretation are examined below.

Continental propagation paths. The dispersion curves with continental propagation paths for explosions and earthquakes have been compared most fully for Europe and Asia.

A comparison of the dispersion curves of L_R waves propagating along continental paths through Western and Eastern Europe, during explosions and earthquakes with their epicenters in northern Europe or northern Asia, reveals that they coincide very well.

Mixed paths. The form of the dispersion curves of L_R waves traveling along mixed paths depends to a very great degree on the character of the path. When the greater part of the path of the L_R waves goes along oceanic paths, the group velocities are greater than in those cases when the main part of the wave path goes along continents. As an example, Table 38 gives the group velocities of the L_R waves recorded in the Sverdlovsk station for an explosion in the Marshall Islands (the greater part of the path was along continents), and in the Uppsala station for an explosion on Christmas Island (the greater part of the path was along the ocean, going through the Pacific Ocean, Alaska, and the North Pole).

Oceanic paths. The network of island and coastal stations of the USA, Japan, the USSR, and other countries has established quite complete data about the dispersion of L_R waves in the Pacific Ocean, both for atmospheric explosions at Christmas Island and for contact

explosions in the Marshall Islands. Studies have also been made of the dispersion curves of the L_R waves for earthquakes coming from regions close to the epicenters of the explosions [283, 295, 346, etc.].

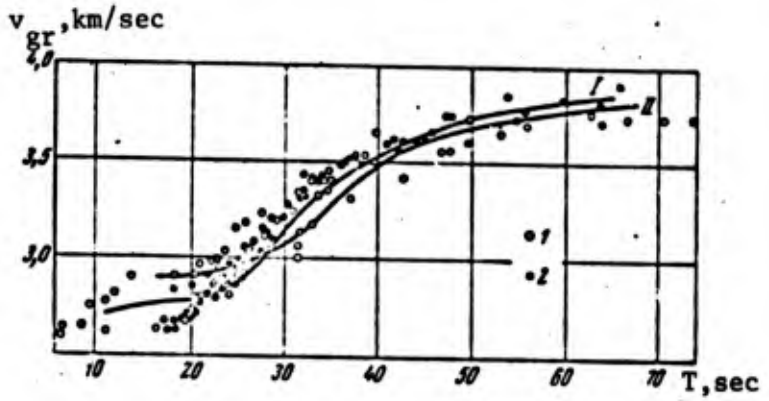

Figure 61. Dispersion curves of group velocities of Rayleigh waves propagated in Europe along mixed paths

1 - during explosions; 2 - during earthquakes, according to data in [292]; I and II - theoretical curves according to data in [292].

Figure 62 gives an example of the dispersion curves for the paths being studied. The parameters of the medium for which the dispersion curves were calculated are given in Table 39.

In this work, the thickness of the Earth's crust was determined for the north-west regions of the Pacific Ocean along the paths from the above-mentioned epicenters of explosions. The thickness of the Earth's crust in the Pacific Ocean along the path from Christmas Island to the southern tip of the Korean peninsula, and from the Marshall Islands to the stations of Hongkong, Tsukuba, and Petropavlovsk-Kamchatsky amounts on the average to about 10 - 11 km. This agrees well with the values previously determined for this region both from explosions and from earthquakes [295]. Approximately the same crust thickness has been determined also in the eastward direction from the Marshall Islands (the stations of Suva, Honolulu and others [285, 295]).

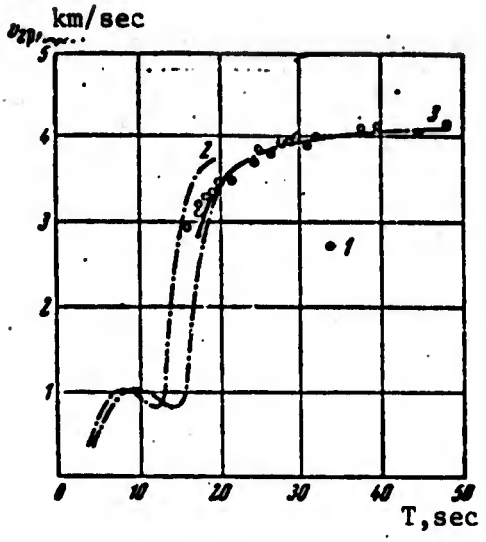

Figure 62. Dispersion curves of group velocities of Rayleigh waves with oceanic propagation paths recorded during explosions on Christmas Island

1 - experimental values at epicentral distance Δ = 8,880 km; 2,3 - theoretical curves according to [188].

TABLE 39. MEDIUM PARAMETERS ADOPTED IN CALCULATIONS OF THE DISPERSION CURVES OF GROUP VELOCITIES OF RAYLEIGH WAVES PROPAGATING ALONG OCEANIC PATHS IN THE PACIFIC OCEAN [188].

Thickness of layer, km	Velocity of dilatational waves, km/sec	Velocity of transverse waves, km/sec	Density, g/cm^2
5.545	1.52	-	1.03
0.454	1.50	0.50	1.70
0.454	2.10	1.00	1.80
5.0	6.41	3.70	2.84
	8.14	4.70	3.27

Thus, a study of the dispersion curves for the group velocities of L_R waves observed in many stations of Europe, Asia, and America during nuclear atmospheric explosions in the region of Christmas Island, and also during contact nuclear explosions in the Marshall Islands, showed that their character and the group velocities are practically the same as for waves propagated along near paths during earthquakes. Analogous data were obtained by the author during underground nuclear explosions.

The conclusion about the identical character of the dispersion of group velocities of Rayleigh waves during near-surface and surface nuclear explosions and shallow-focus earthquakes can be utilized for practical purposes. From the character of the L_R wave dispersion, it is possible to determine approximately the region and the time of the explosion [145]. This is especially important in those cases when only the surface waves and not the body waves are recorded at a single station.

§ 3. Dependence of the Oscillation Period in L_R Waves on the Epicentral Distance, the Parameters of the Explosion, and the Magnitude of the Phenomenon

In order to compare the character of $T(\Delta)$ in L_R waves caused by explosions and earthquakes, it is necessary to study the dependence of the period T of the maximum oscillations and the amplitude spectrum of the Rayleigh waves on Δ, the parameters of the explosion, Q and h, and the magnitude M of the seismic phenomenon. If these parameters were the same, this would provide experimental justification for using the M scales [24, 122] (developed for shallow-focus earthquakes) for determining the magnitudes of seismic phenomena during explosions.

In this section the results of experimental study of $T(\Delta)$ in L_R waves recorded mainly during atmospheric explosions are introduced. Data obtained during contact and underground explosions are also given. However, these data are few in number, because the number of contact explosions was relatively small, and during underground explosions, L_R waves were recorded in stations of the USSR only in some of the most powerful explosions at considerable distances Δ ($\Delta >$ 5,000 - 6,000 km).

The M_2 waves were studied most completely; records of more than 90 atmospheric explosions, five contact explosions, and five underground explosions were used. In the records of wide-band (SK) and

long-period (SKD, SG, Press-Ewing, Benioff, etc.) seismographs, when Δ ranges from 10 to 30-35°, these waves are the most intense in the group of L_R waves. The maximum amplitudes of the complete horizontal component in the M_2 waves for 10° < Δ < 30-35° both for explosions and for earthquakes are 1.7 - 1.5 times greater than the amplitudes of these components in the M_1 waves with oscillation periods of 20 - 40 seconds.

Dependence on Δ of periods of maximum oscillations in M_2 waves. The results of measuring the maximum periods of the M_1 and M_2 waves in the records of stations located at different distances Δ are shown in Figure 63 and in Table 40.

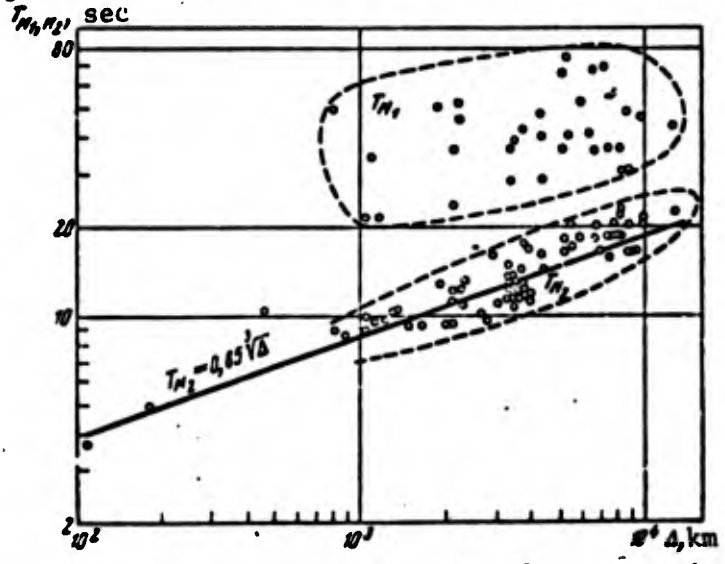

Figure 63. Averaged dependences of the period of M_1 and M_2 Rayleigh waves on the epicentral distance during atmospheric explosions. The average curve for M_2 waves of earthquakes from data in [122]; the dots are periods from different epicenters; the broken curves outline the areas containing dots pertaining to M_1 and M_2 waves.

The values of T_{M_2} in the records of vertical and horizontal instruments practically coincide when there are repeated explosions in the same region. This makes it possible to examine the total combination of data obtained by horizontal and vertical seismographs at the same time. The periods of the M_2 waves recorded for the same

TABLE 40. MEAN PERIODS T OF MAXIMUM OSCILLATIONS OF M_1 AND M_2 WAVES, AND MAXIMUM VALUES T_{max} IN M_2 WAVES, RECORDED DURING ATMOSPHERIC AND CONTACT EXPLOSIONS IN EUROPE AND ASIA

Epicentral distance		T, sec		Standard deviation, σ	T_{max} for M_2, sec	Number of observations	Type of seismograph	Type of explosion
Δ°	Δ, km	M_1	M_2					
1	2	3	4	5	6	7	8	9
				Continental path				
1—1,3	95—112		1,8	0,3	1—2,7	32	USF	
2,7—3,0	327—362		2,1	0,07	1,6—2,8	43	USF	
4,2	466		10,4	0,1	7—14,4	58	SK	
9,5	1054	17,5	9,9	0,1	9,1—12,8	48	SK	
12,2	1350	21	10,1	0,1	9—13	72	DS (P-YU)	
19,0	2110		11,5	0,5	11—12	2	SK	
19,5	2160	23	12,0	1,0	8,6—12	12	SK	
20	2230	52	12,0	0,5	10,6—12,2	54	SK	
16,8	1875	50	13,5	0,5	13—14	2	SG	
20,5	2280	45	10,7	0,1	9—12,5	94	DS (P-YU)	
20,7	2300	20,8	13	0,5	12—14	2	SK	
24,4	2710		10	0	10—10	12	SG	
26,0	2885		15,8	0,5	13—17	33	SK	
30,0	3300	22.	12,7	0,7	12—16	5	SK	
30,0	3330		11,2	0,6	10—12	8	SK	
30,0	3330		12,7	0,5	10—14	11	SK	
30,0	3330		12		12—12	1	SK	
30,3	3360		11,2	0,5	11—15	7	SK	
31,9	3440		13,6	1,0	11—15	7	SK	
31,0	3440		11,0	0,6	10—13	9	SK	
31,0	3440	20	13,4	0,5	11—14	12	SK	
31,0	3440		12,0	0,5	11—16	8	SK	
31,0	3440	22,5	14,6	0,5	12—15	33	SK	
31,5	3550	22	10,5	0,1	10—11	36	DS (P-YU)	
31,0	3440	21,5	13,0	0,1	12—16	52	DS (P-YU)	

TABLE 40. MEAN PERIODS T OF MAXIMUM OSCILLATIONS OF M_1 AND M_2 WAVES, AND MAXIMUM VALUES T_{max} IN M_2 WAVES, RECORDED DURING ATMOSPHERIC AND CONTACT EXPLOSIONS IN EUROPE AND ASIA

Epicentral distance		T, sec		Standard deviation, σ	T_{max} for M_2, sec	Number of observations	Type of seismograph	Type of explosion
Δ°	Δ, km	M_1	M_2					
1	2	3	4	5	6	7	8	9
32	3550		12,0	0,5	10—15	13	SK	
32	3550	25	11,3	0,1	10—12	48	SK	
32	3550		13,3	0,9	12—14	6	SG	
32,3	3590		13,6	0,5	11—15	7	SK	
33	3660	18	11,2	2	9—16	4	SK	
33	3660		11,6	0,5	10—14	5	SK	
33	3660		14,0	0	14—14	2	SK	
33,8	3750	26,5	12,0	1,4	10—15	6	SK	
34,0	3770	20,1	14,2	0,5	11,5—16	13	SK	
34,5	3810	20,0	17,2	0,3	14—18	28	SK	
35,0	3880		11,5	2,0	10—14	5	SK	
35,0	3880		12,0			1	SK	
34,0	3770		12,7	0,5	11—14	10	SK	
36,0	4000		14,8	1,0	10—14	9	SK	
36,0	3960	20,0	16,5	0,5	14—18	8	SK	
36,0	4000		12,0	1,0	11—13	6	SK	
36,0	4000		11,0	1,3	10—13	5	SK	
40,1	4450	28	14,2	0,5	12—14	22	SK, SKD	
48,8	5420	40	18				DS (P-YU)	
46,9	5200	72	18				DS (P-YU)	
46,9	5200	65	18			8	DS (P-YU)	
73	8114	40	20			8	DS (P-YU)	
61,2	6790	35	20			7	DS (P-YU)	
1,6	180		4,9	0,5	4—6	5	SK	
7,3	810	45		0,15	8—9,2	24	SKD	undergrd.
7,3	810		8,8	0,1	7,8—9	1	SKD	
						16		

TABLE 40. MEAN PERIODS T OF MAXIMUM OSCILLATIONS OF M_1 AND M_2 WAVES, AND MAXIMUM VALUES T_{max} IN M_2 WAVES, RECORDED DURING ATMOSPHERIC AND CONTACT EXPLOSIONS IN EUROPE AND ASIA

Epicentral distance		T, sec		Standard deviation, σ	T_{max} for M_2, sec	Number of observations	Type of seismograph	Type of explosion
Δ°	Δ, km	M_1	M_2					
1	2	3	4	5	6	7	8	9
7,9	877		8,4	0,1	8,4—11	26	SKD	
10	1111		8,8	0,1	8,4—10	16	SKD	
10,4	1154		9,4	0,1	8,6—11	16	SKD	
10,9	1210		9,5		8,6—9,1	10	SG	
13,5	1500		9	0,1	8,6—13	6	SK	
12,3	1360		10,6	0,1	8—10	10	SG	
16,6	1840		9,2	0,1	9—11	6	SG	
18,2	2020		9,2	0,02	9—11	7	SG	
18,7	2080		10,6	0,05	9—11	8	SG	
25	2780		9,5		8,6—10	10	SG	
				Mixed path				
33	3360	36	20					
63,1	7005	60	18			4	DS (P-YU)	atmosph.
57,7	6400	40				4	SK, SG	contact
62	6882		20			5	DS (P-YU)	atmosph.
63	6993		16			1	SK	undergrd.
59,9	6650	36	22			1	SK	
64	7122	88	18			8	DS (P-YU)	atmosph.
65,4	7250	35	18			4	DS (P-YU)	
66,9	7420	35	18			4	DS (P-YU)	
68,5	7603		15			4	DS (P-YU)	
68,8	7630	35	18			1	SK	undergrd.
73,8	8190	35	18			2	DS (P-YU)	atmosph.
74	8290	35	18			4	DS (P-YU)	
						6	DS (P-YU)	

TABLE 40. MEAN PERIODS T OF MAXIMUM OSCILLATIONS OF M_1 AND M_2 WAVES, AND MAXIMUM VALUES T_{max} IN M_2 WAVES, RECORDED DURING ATMOSPHERIC AND CONTACT EXPLOSIONS IN EUROPE AND ASIA

Epicentral distance		T, sec		Standard deviation, σ	T_{max} for M_2, sec	Number of observations	Type of seismograph	Type of explosion
Δ°	Δ, km	M_1	M_2					
1	2	3	4	5	6	7	8	9
80	8880		16			1	SKD	undergrd.
85	9435		16			1	SKD	undergrd.
90	9990		16			1	SKD	
90	9990		22			1	SG	
123	12500	43	22			2	DS(P-YU)	atmosph.
				Oceanic path				
31.5	3507	38					DS(P-YU)*	
33.7	3744	42	20				DS(P-YU)**	
39.3	4366	48	16				DS(P-YU)	
46.9	5215	36	20				DS(P-YU)	
41.7	4629	60	20				SK	
80	8880	48	18				SKD	

*Region of observation - Asia

**Region of observation - Pacific Ocean

Δ by equipment of the same type from two regions with similar seismogeological structure have similar values. Therefore, the entire set of data about the periods of the M_2 waves produced in regions with a continental structure of the Earth's crust during atmospheric explosions is examined at the same time. The greatest epicentral distance for a continental path was 73°.

It is remarkable that in the same stations, the periods were very similar in the records of different types of seismographs. This phenomenon is explained by the relatively narrow amplitude spectrum of the M_2 waves (see § 6 of this chapter).

As a result of analyzing numerous records of Rayleigh waves, it was established that in all types of nuclear explosions, together with the increase of Δ, an increase in the period of the maximum oscillations in the M_2 waves is observed. The dependence on Δ of the average periods in the M_2 waves (Figure 63) may be approximated by a curve of the type $T(\Delta) \approx 0.85 \sqrt[3]{\Delta}$, which was established in [122] for the corresponding waves of shallow-focus earthquakes. The deviation of the average values of T_{M_2} from the approximate dependence does not exceed 10 - 15% for most of the stations, and only individual stations give deviations of up to 25%. The deviations mentioned fall within the range of values established for earthquake waves.

According to the data from stations in the USSR, obtained during a rather small number of underground explosions, the dependence of T_{M_2} on Δ in the range from 300 - 500 to 10,000 km is generally the same as during atmospheric explosions and earthquakes. The most complete data were obtained for continental propagation paths of the M_2 waves of atmospheric explosions. The changes undergone by $T(\Delta)$ in mixed and oceanic propagation paths of the waves from the explosions mentioned at 3,000 km < Δ < 13,500 km agree satisfactorily with the corresponding dependence $T(\Delta)$ for the continental propagation paths during earthquakes.

It is clear from an analysis of the experimental data that the character of the changes undergone by the periods T_{M_2} together with changes of Δ, as well as the values themselves of T_{M_2} at the same distances Δ for the maximum oscillations in the M_2 waves during atmospheric, contact, and underground explosions carried out in different regions, are the same as those during shallow-focus earthquakes. The changes in $T = T(\Delta)$ do not depend on the intensity of the explosion, nor on its height or magnitude of the phenomenon. This shows that the period of the maximum oscillations in the M_2 waves depends very little, or not at all, on the type of source (earthquake or explosion).

Character of the changes of $T(\Delta)$ in the M_1 waves. The changes in the maximum values of the periods in the train of M_1 waves, together with the epicentral distance during atmospheric and contact explosions with $4.5 < M < 5.5$, was studied from the records obtained by long-period seismographs. The results of the measurements are given in Table 40 and shown in Figure 63. In the records of SK seismographs, it was usually not possible to distinguish the first, longest-period oscillations due to the low amplification of the equipment in the range $T > 20 - 25$ seconds. The values of T given in Table 40 for stations equipped with SK seismographs evidently refer to the ensuing oscillations in the train of M_1 waves. This observation refers to some of the records of SD seismographs — in particular, to records obtained during explosions with M on the order of 4.5 or less.

An examination of the dependence $T(\Delta)$ for the M_1 waves (Figure 63) reveals clearly that, as Δ increases, the maximum periods of oscillations in the M_1 waves increase relatively little. In most cases, the maximum periods in the M_1 waves are about 40 - 50 seconds in all types of explosions, and only in individual stations did they reach values of 60 - 75 seconds. Just as for $T(\Delta)$, no dependence of the period in the M_1 waves on the height and intensity of the explosions was observed for the M_2 waves.

The dependence $T(\Delta)$ in the M_1 waves in all types of explosions is practically identical, and it is approximately the same as in earthquakes with comparable magnitudes. The latter follows as a result of the fact that the dispersion curves of the group velocities of L_R waves are of the same type during explosions and earthquakes with similar propagation paths (see § 2 of this chapter). It must be noted that the dependence $T(\Delta)$ for the M_1 waves was studied from considerably less complete data than the corresponding dependence for the M_2 waves.

The uniform dependence of $T(\Delta)$ in the M_1 waves and their uniform dispersion curves during explosions and earthquakes with comparable magnitudes indicates that they are determined chiefly by the structure of the crust and the upper mantle along the propagation path of the surface waves, and hardly depend, or depend to a very small degree, on the type of source.

Dependence $T(\Delta)$ in the L_0 waves. It has been established that the periods, both of the maximum oscillations in the train of L_0 waves, and the oscillations with the largest periods (the latter oscillations are confined to the beginning of the train), depend basically on the seismogeological structure in the region of the station, and depend to a relatively insignificant degree on the epicentral distance. At a distance of $\Delta > 1{,}500 - 2{,}000$ km, there is no dependence of the periods on the type of explosions and their parameters. For stations located in regions with a thick (approximately 5 - 10 km) layer of sedimentary or sedimentary-metamorphic rocks, the periods in the L_0 waves underwent approximately identical changes — from 10 - 8 seconds at the beginning of the train to 6 - 5 seconds at the end of the train when there was a change in Δ from 2,000 to 10,000 km. The above-mentioned changes of T in the L_0 waves were observed, for instance, at the Ashkhabad station during explosions in the Marshall Islands (Δ = 10,660 km). In stations located in metamorphic rocks, the periods in the train of L_0 waves changed from 6 - 5 to 4 - 3 seconds.

Because of the considerable dependence of T in L_0 waves on the seismogeological structure in the regions where the stations were located, it was not possible to establish an average dependence $T(\Delta)$ for these waves.

§4. Spectra of L_R Waves from Explosions and Earthquakes

The study of the amplitude spectra of the L_R waves of explosions and earthquakes was aimed at a solution of the following basic problems:

1. Selection of the optimum parameters of the receiving equipment for recording L_R waves (these questions are dealt with in § 5 of Chapter III).

2. Clarification of possible differences in the spectra of the L_R waves during distant (Δ > 1,000 - 1,500 km) explosions of different types and during earthquakes.

3. Establishing the differences in the seismogeological structure along the propagation path of the waves and in the focus region.

In order to solve these problems, spectra of the L_R waves recorded during various types of explosions and during earthquakes in a range of Δ from several hundreds km to 10,000 - 12,000 km, were studied. The magnitudes of the explosions and earthquakes fell within a range of M from 4 to 6.

Studies were made of the spectra of waves traveling via continental, oceanic, and mixed paths. Most widely used in these studies were the records obtained in the USSR with wide-band equipment of types SK and SKD, and those obtaired in foreign stations by selective long-period and ultra-long period equipment (long-period seismographs

of the Benioff and Press-Ewing types). The maximum amplification occurred at T = 25 seconds and larger values.

Since in many cases the M_1, M_2 and L_0 waves cannot be distinguished from each other, the spectrograms of the entire record of the L_R waves are examined. It should be mentioned that the spectra of the entire record of the L_R waves are also examined in [346].

The durations of the records of the L_R waves vary during earthquakes, depending on the epicentral distance and the magnitude of the phenomenon. In connection with this, the duration of the analyzed sections of the record also underwent changes. The durations of the analyzed sections Δt are indicated on the corresponding spectra. As a result, the spectra which are examined are those of the records of the L_R waves obtained by vertical seismographs and not complicated by superposition of other waves. In those cases when spectra of records obtained by horizontal instruments were examined, those selected for analysis were the seismograms of radially installed horizontal seismographs, not complicated by superposition of Love waves.

Under the above-mentioned conditions, the spectra of the records of the L_R waves obtained by horizontal and vertical seismographs of the same type were practically identical (Figure 64).

In the study of the basic characteristics of the spectra of the L_R waves, of the periods T_{max} of their basic maxima, and also of the boundary periods T_{left} and T_{right}, taken at a level of 0.5 of the value of the maximum amplitude of the maximum under examination, corrections were introduced into the spectra for the irregular amplification of the equipment. Corrections for the irregular amplification of the equipment were not introduced when comparing the spectra of L_R waves recorded at the same station by equipment of the same type during different types of explosions and during earthquakes.

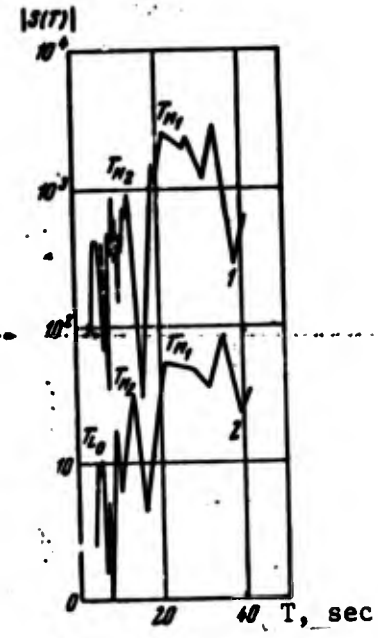

Figure 64. Amplitude spectra of Rayleigh waves from an atmospheric explosion recorded by wide-band seismographs (Δ = 700 km)

1 - vertical component; 2 - horizontal component, Δt = 237 seconds; here and below the scale on the vertical axis is arbitrary.

Character of the spectra of the L_R waves. During explosions, and also during earthquakes, the M_1, M_2, L_0 and some other aves in many cases have no time separation in the recordings, and the train of oscillations in the L_R waves appears to be a result of interference. This, together with other factors, determines the presence of a number of extrema in the spectra of the L_R waves. The maxima which are dominant in the amplitude are connected with the M_1 and M_2 waves. They can be seen in spectra of L_R waves recorded at a Δ from 800-1,000 to 10,000 - 12,000 km in all types of explosions and during earthquakes traveling via continental, oceanic, and mixed paths (Figures 65 - 68). The maximum amplitudes in both maxima are commensurable. Their periods, hereafter designated as T_{M_1} and T_{M_2}, in most cases are close to the periods of the maximum oscillations in the recording of the M_1 and M_2 waves, respectively (see § 3), and are also close to the periods of the maxima in the spectra of the recordings which are visually related to the M_1 and M_2 waves.

In most cases, the periods of the maxima T_{M_1} and T_{M_2} during explosions and earthquakes recorded in a range Δ = 1,000 - 10,000 km fall within the ranges: T_{M_1} - from 20-30 to 30-40 seconds; T_{M_2} - from 10-12 to 18-22 seconds.

In the spectra of many records, extrema in periods of 40-50 seconds and more can also be distinguished, having in a number of

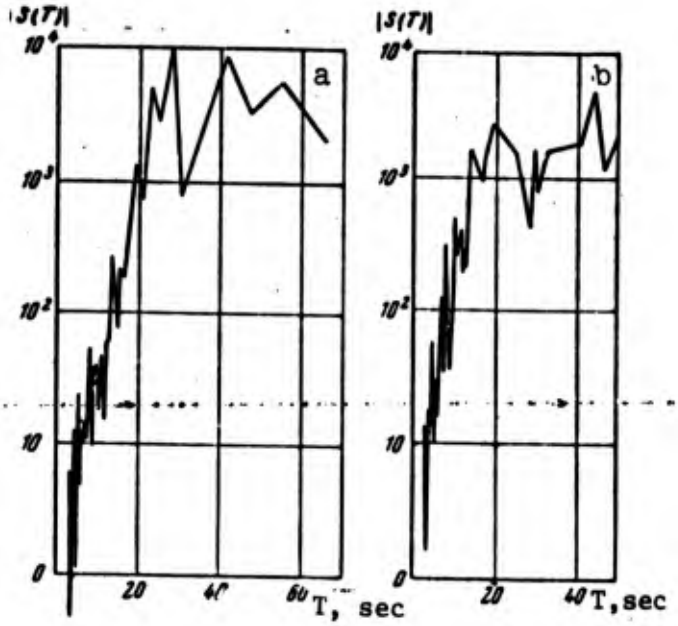

Figure 65. Spectra of Rayleigh waves from atmospheric explosions recorded by wide-band spectrographs along close continental paths

a - Δ = 2,110 km, Δt = 406 sec;
b - Δ = 3,840 km, Δt = 363 sec

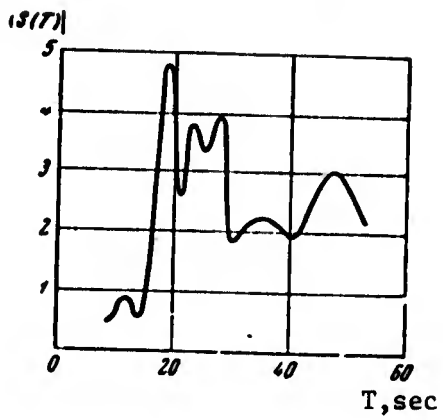

Figure 66. Example of amplitude spectrum of Rayleigh waves from an atmospheric explosion moving along an oceanic path.

(Δ = 8,800 km, Δt = 600 sec)

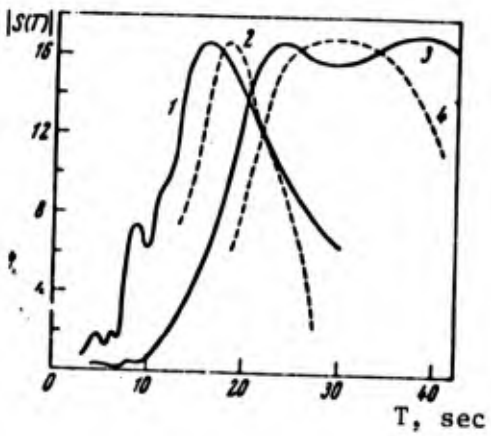

Figure 67. Spectra of surface waves recorded at the same station (Δ = 3,500 - 8,000 km) from different sources in a continental region, corrected for irregular amplification of the equipment.

1,2 - underground explosions;
3,4 - earthquakes

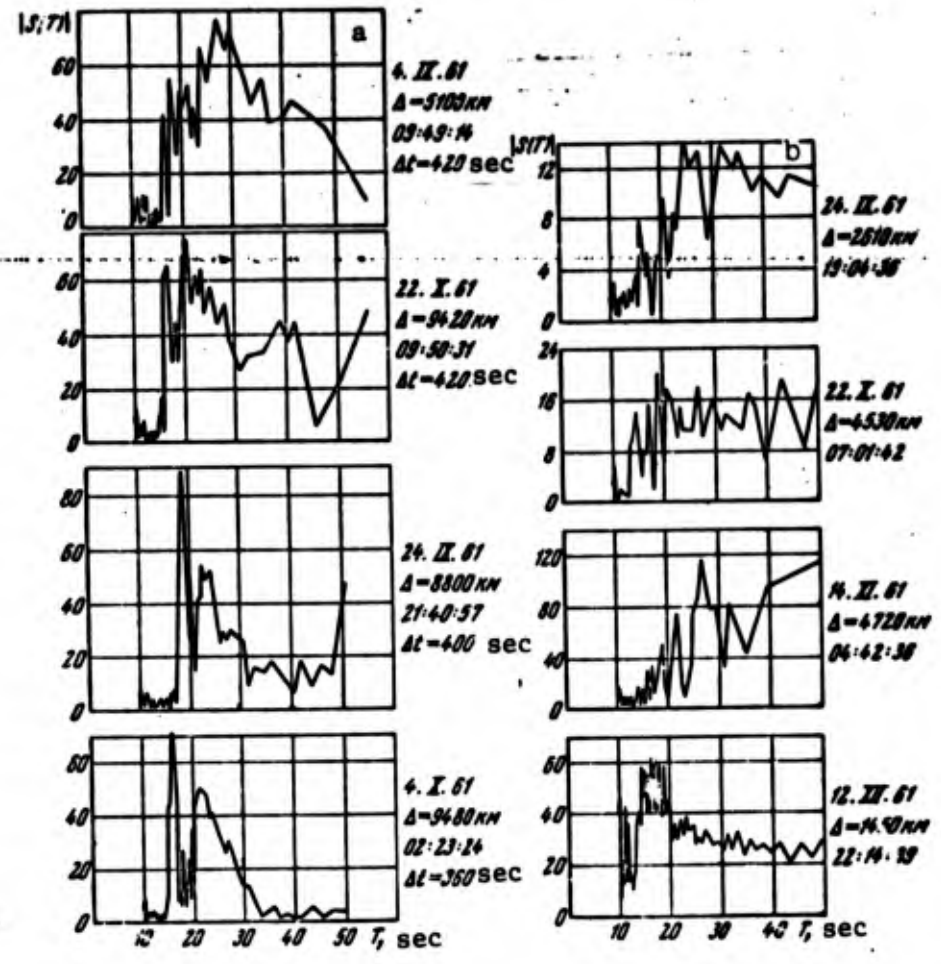

Figure 68. Spectra of Rayleigh waves from earthquakes with epicenters in various regions of the Pacific Ocean belt, recorded by the Pasadena station

a - oceanic paths; b - continental paths (from [346])

cases either the greatest amplitudes, or amplitudes of the spectral components which are commensurate with the corresponding amplitudes in the extrema with periods T_{M_1} and T_{M_2} (Figures 64, 65 etc.). However, the sections of the spectrum with T > 45 - 50 seconds were not studied in detail due to the small amplification of the equipment in the given range of periods.

In those cases when in the region of the station there is a thick layer of sedimentary or sedimentary-metamorphic rocks, with which the L_0 waves are usually connected in the recordings, there is also a supplementary maximum in the spectrum. The period of this maximum is usually close to the period of the maximum oscillation in the train of L_0 waves (approximately 6 - 10 seconds). The amplitudes of the maxima with T_{L_0} are comparable with the corresponding values for the maxima with T_{M_1} and T_{M_2} only at $\Delta < 2,000 - 3,000$ km, and this occurs to a greater degree during underground explosions and earthquakes than during atmospheric explosions (Figures 68 and 69). At a distance of $\Delta > 5,000 - 6,000$ km, the amplitudes of the maxima with periods of T_{L_0} during explosions and earthquakes with $M < 4.5 - 5.5$ usually do not exceed 5 - 10% of the amplitudes of the maxima with T_{M_1} and T_{M_2} (Figure 67 etc.).

Examples of numerous spectra of L_R waves from different types of explosions and earthquakes have established that, together with the increase in Δ, there is a considerable decrease in the relative contribution of the short-period components with periods of less than 10 seconds (Figure 67) to the spectra of the waves being studied. As a result of this, in all types of explosions and earthquakes with similar paths, the basic features of the L_R wave spectra become similar at a distance of $\Delta > 4,000 - 5,000$ km (Figure 66). An increase of T_{M_1} and T_{M_2} with the increase of Δ is also observed.

Since, with comparable values of M and Δ, the duration of the train of L_R waves during atmospheric, contact, and underground explosions is considerably shorter than during earthquakes, the width of the spectrum during explosions should be somewhat broader than during earthquakes. However, this can be clearly seen only at relatively short Δ (up to 2,000 - 3,000 km) (Figure 69). At a distance of $\Delta > 4,000$ km, it is not possible to detect this feature of the spectra of the L_R waves from atmospheric explosions, chiefly due to the strong dependence of the spectrum on the structure of the

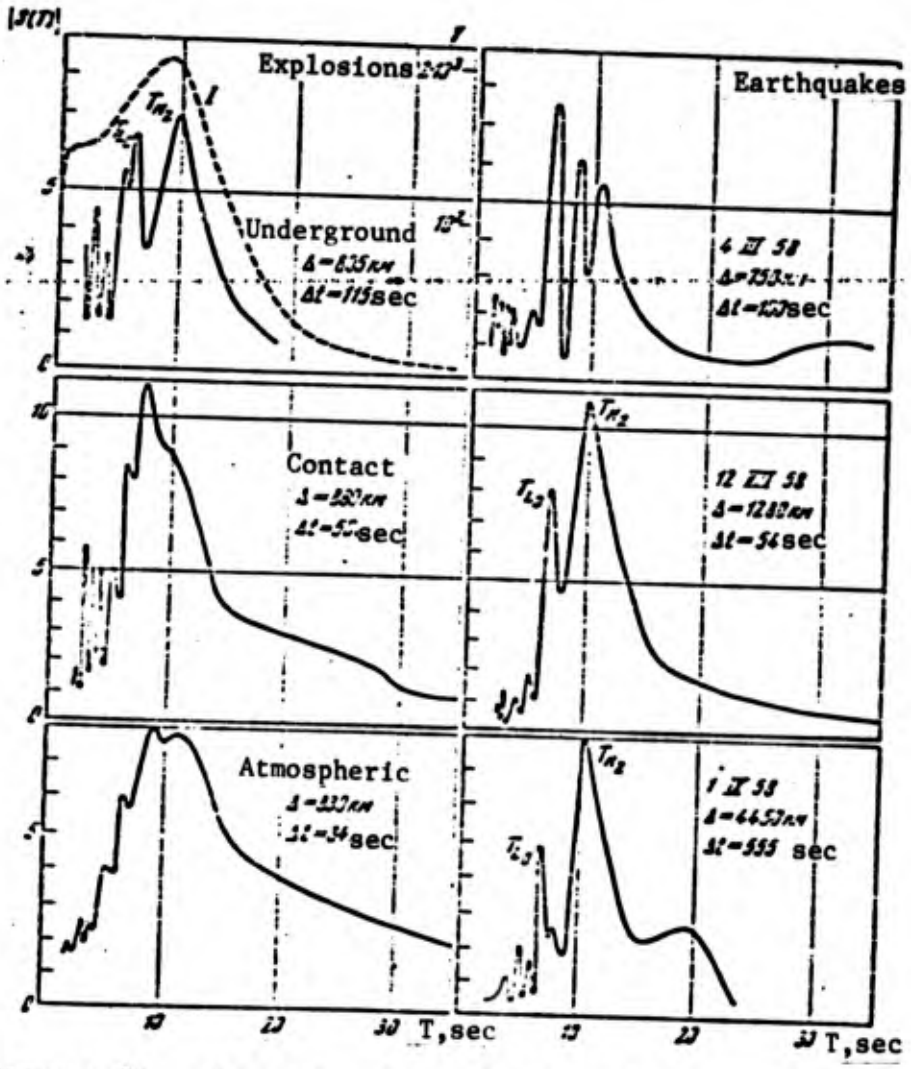

Figure 69. Spectra of surface waves recorded by wide-band seismographs at different Δ from different explosions and earthquakes, and the amplification curve of the seismograph (I).

medium along the propagation path of the waves and due to the considerable attenuation of the short-period components with an increase in Δ. It must be noted that the width of the spectral band is determined very approximately, and the methods of determining it have not yet been formalized.

A comparison of the spectra of explosions and earthquakes traveling along the same paths is given below. It should be noted

that the shape of the spectra can be compared in a range of periods in which the amplitudes of the spectral components are not less than 10 - 15% of the maximum amplitudes in the spectrum being studied. This is connected with the fact that the accuracy with which the spectra are calculated in different computers with different programs does not exceed 5 - 10%.

Shape of L_R wave spectra during atmospheric explosions from the same epicenter. The spectra of the L_R waves recorded at the same station, at a distance of $\Delta > 1{,}000 - 1{,}500$ km, during atmospheric explosions of the same type with very similar intensities and heights and from the same epicenter, are very similar. In these cases the L_R wave spectra are similar in their basic qualitative features. The distribution of the extrema is approximately retained — that is, the values of T_{M_1}, T_{M_2}, and T_{L_0} do not change. However, the ratios between the amplitudes of the corresponding spectral components depend on the period when the intensity of the explosion changes.

Quantitative studies have not yet been made of the ratios for the spectral component amplitudes as a function of the intensity of the explosion for contact and underground explosions. However, it is apparently not as significant as in the case of atmospheric explosions.

Dependence of the shape of the L_R wave spectra on the seismo-geological structure along their propagation path. As was shown above, the spectra of the L_R waves from explosions and earthquakes, recorded at distances of $\Delta > 2{,}000 - 3{,}000$ km in different stations with Δ close to each other, are qualitatively similar in their basic features when they follow continental, oceanic, or mixed paths of propagation of the same types. But the spectra of the L_R waves differ very noticeably when the propagation paths are of different types, both during explosions and during earthquakes (Figures 65 - 69). These differences appear in changes in the shape of the basic maxima, the values of their periods, the width of the bands, their amplitude ratios, and also in the somewhat different dependence of

the above-mentioned spectral characteristics on Δ.

A characteristic feature of the L_R wave spectra with oceanic propagation paths for explosions and earthquakes are two, most distinct maxima, whose amplitudes are commensurate. These maxima are connected with the M_1 and M_2 waves (Figure 67 etc.). A characteristic feature for the spectra of the M_2 waves recorded at distances of $\Delta > 4{,}000$ km is the sharp drop of the spectral component amplitudes from the maximum towards the shorter periods, beginning with T = 16 - 18 seconds (Figure 66). There is also a considerable narrowing of the band in the section of the spectrum with maximum T_{M_2} in comparison with the band of the same section when a continental path is followed. This is caused by the increase in the duration of the recording of oscillations in M_2 waves, due to the presence of a thick (5 km) layer of water along the propagation path of the L_R waves.

When spectra of the L_R waves of contact and atmospheric explosions, and also of earthquakes with oceanic propagation paths are compared (Figures 66 and 67), it is obvious that at distances of $\Delta > 3{,}000$ km, they are almost identical to each other, both at a single station and in different stations. This similarity in the character of the spectra is caused by the relative similarity of the seismogeological structure of the oceanic crust and the upper mantle underlying it.

When they travel via mixed paths, the spectra of the L_R waves recorded in adjacent stations usually differ considerably from each other, both for the same explosion or earthquake and for different explosions and earthquakes. The difference in the form of the spectra in this case is connected with the great changes in the seismogeological structure along the wave propagation path, and not with the type of the source.

It must be observed that in the spectra of L_R waves, recorded during powerful underground explosions, some differences from the

spectra of the waves from other sources are apparent. The width of these spectra, as a rule, is somewhat narrower, and the maximum of the basic extremum is shifted toward shorter periods.

The similarity of spectra of the L_R waves moving along the same paths, or along paths whose structure is very similar (this similarity is observed in various types of explosions except underground ones, and also in earthquakes) reveals that the Rayleigh wave recordings depend very little on the type of source and are determined by the structure of the medium on the propagation path of the waves. The strong dependence of the amplitude spectra on the structure of the medium on the wave propagation path conceals to a significant degree the distinctive features of the spectra, which are determined by the differences in the type of sources in the case of explosions and of earthquakes.

The analysis of the spectra of Rayleigh waves has led to the following conclusions:

1. At a distance of $\Delta > 3{,}000 - 4{,}000$ km, the basic features of the spectrum of L_R waves in all types of explosions and during earthquakes are determined mainly by the seismogeological structure along the propagation path of the waves.

2. The non-uniformities in the seismogeological structure along the propagation path of L_R waves influence their spectra so greatly that, in the range of periods from 5-8 to 40-50 seconds, which has been studied at a distance of $\Delta > 1{,}000 - 1{,}500$ km, it is not possible at the present time to distinguish between explosions and earthquakes based on the character of the spectrum. Statistical calculations have not yet substantiated consistent differences in the spectra of L_R waves from underground explosions and earthquakes at a distance of $\Delta > 2{,}000 - 2{,}500$ km. This question requires further clarification.

the above-mentioned spectral characteristics on Δ.

A characteristic feature of the L_R wave spectra with oceanic propagation paths for explosions and earthquakes are two, most distinct maxima, whose amplitudes are commensurate. These maxima are connected with the M_1 and M_2 waves (Figure 67 etc.). A characteristic feature for the spectra of the M_2 waves recorded at distances of $\Delta > 4{,}000$ km is the sharp drop of the spectral component amplitudes from the maximum towards the shorter periods, beginning with $T = 16 - 18$ seconds (Figure 66). There is also a considerable narrowing of the band in the section of the spectrum with maximum T_{M_2} in comparison with the band of the same section when a continental path is followed. This is caused by the increase in the duration of the recording of oscillations in M_2 waves, due to the presence of a thick (5 km) layer of water along the propagation path of the L_R waves.

When spectra of the L_R waves of contact and atmospheric explosions, and also of earthquakes with oceanic propagation paths are compared (Figures 66 and 67), it is obvious that at distances of $\Delta > 3{,}000$ km, they are almost identical to each other, both at a single station and in different stations. This similarity in the character of the spectra is caused by the relative similarity of the seismogeological structure of the oceanic crust and the upper mantle underlying it.

When they travel via mixed paths, the spectra of the L_R waves recorded in adjacent stations usually differ considerably from each other, both for the same explosion or earthquake and for different explosions and earthquakes. The difference in the form of the spectra in this case is connected with the great changes in the seismogeological structure along the wave propagation path, and not with the type of the source.

It must be observed that in the spectra of L_R waves, recorded during powerful underground explosions, some differences from the

3. The analysis of L_R wave spectra is qualitative, especially in the range of periods T > 30 - 40 seconds, since the equipment in the above-mentioned range of periods has a relatively small amplification.

§ 5. Ratios of Amplitudes of Horizontal and Vertical Components in Rayleigh Waves During Contact and Atmospheric Explosions

During earthquakes, Rayleigh waves are polarized in a vertical plane, and particles from the medium move along an ellipse in the direction from the station towards the epicenter. The ratio of the complete horizontal component of soil displacement A_H in Rayleigh waves to the vertical component A_Z is close to the theoretical value, which is 0.68 [112] for a Poisson ratio of $\sigma = 0.25$.

Taking into account what has already been said, the magnitudes of earthquakes may be determined not only by means of horizontal seismographs, for which calibration scales have been worked out, but also by vertical seismographs. However, in this case, the values of M will be 0.18 magnitude units too large.

M can be determined from the recordings of the vertical components of Rayleigh waves more reliably in many cases, inasmuch as the recordings of vertical instruments are not complicated by the superposition of Love waves.

In this section, we will study the A_H/A_Z ratio in Rayleigh waves caused by nuclear explosions.

A_H/A_Z ratio for M_1 and M_2 waves propagated along continental paths during atmospheric and contact explosions. The A_H/A_Z ratio for Rayleigh waves caused by atmospheric and contact explosions was studied by means of the recordings obtained by SK and SKD seismographs. The ratios of the maximum amplitudes A_H/A_Z in the M_2 waves were

primarily studied. The character of the changes in A_H/A_Z in the M_2 waves for various stations in the USSR is seen clearly from the data given in Table 41.

It is clear from Table 41 that for a number of stations — both those at small distances such as Δ = 180 km, as well as those at considerable distances such as Δ = 5,217 km — the mean values of the A_H/A_Z ratio in the M_2 waves are close to the theoretical value, which is 0.68. Close agreement between the experimental and the theoretical values is observed more often in stations located in crystalline or metamorphic rocks, for which the Poisson ratio is close to 0.25.

The value of A_H/A_Z in stations located in a thick layer of sedimentation in some cases surpasses by 1.5 - 2 times the value of 0.68. The mean value of A_H/A_Z in all stations amounts to 0.94 $\pm$ 0.24 in explosions in one region, and to 0.86 $\pm$ 0.25 in explosions in another region. It must be noted that the values of A_H/A_Z found by means of the M_1 waves from the scale in [214], and by means of the M_2 waves from the scale in [122], practically coincide.

A comparison of A_H/A_Z for M_2 waves determined in the same stations during explosions in various regions revealed that in some stations these values were very similar, while in others they differed considerably (up to 1.5 - 2 times).

§ 6. Dependence of A/T on Δ in M_2 Waves

In this section, on the basis of experimental data obtained chiefly during atmospheric explosions, the dependence of A/T on Δ in M_2 waves during explosions is compared with the corresponding dependence for earthquakes. The average values of $A/T(\Delta)$, calculated from the calibration curves of the M scales [24, 122], were examined for the earthquakes.

TABLE 41. VALUES OF A_H/A_Z RATIO IN RAYLEIGH WAVES RECORDED DURING ATMOSPHERIC EXPLOSIONS.

Epicentral distance Δ, km	Number of determinations	A_H/A_Z	Epicentral distance Δ, km	Number of determinations	A_H/A_Z	Type of seismograph	Type of wave	Rocks in region of station	Thickness of deposits km
180	16	0,61±0,10	2390	2	0,73±0,06	SK	M_3	metamorphic	0,5—1,0
180	4	0,60±0,2	—	—	—	BEGIK-M	»	»	0
805	5	1,71±0,09	3550	2	1,50±0,12	SK	»	sedimentary	5—6
880	5	1,12±0,05	3500	1	0,9	"	»	»	2—3
1105	5	0,91±0,09	—	—	—	"	»	»	2
1160	5	1,18±0,11	3820	2	1,47±0,50	"	»	»	5
1210	3	1,18±0,32	—	—	—	"	»	»	2
1360	5	0,77±0,10	—	—	—	SG	»	»	2
1850	3	0,74±0,09	—	—	—	SK	»	»	2
—	—	—	1993	21	0,97±0,09	DS, P-YU	M_1, M_3	crystalline	2
2017	4	0,58±0,11	3440	3	0,91±0,09	SK	M_3	sedimentary	2
2080	4	0,70±0,25	4020	2	1,86±0,20	"	»	»	10—15
2785	5	1,25±0,17	2116	3	0,79±0,27	"	»	»	1,8
			544	27	0,66±0,04	"	»	»	2—2,5
			1034	15	0,71±0,04	"	»	crystalline	0
			1332	10	1,26±0,12	P-YU	M_1	»	0
			1332	10	0,97±0,10	SG	M_3	»	0
			2160	13	0,71	SKD	M_1	sedimentary	1,8
			2160	12	0,81±0,03	SK	M_3	»	—
			3340	3	1,39±0,14	"	»	»	8—10
			3340	3	0,68±0,40	"	»	»	2—3
			3660	2	1,42±0,27	"	»	»	5—8
			3870	3	1,61±0,28	"	»	»	15
			4440	2	0,56±0,11	"	»	crystalline	0
			5217	15	0,65±0,00	P-YU	»	»	0
			3600	3	0,95±0,04	SK	»	sedimentary	2—3
			8800	2	0,80	SKD	M_3	crystalline	0

The dependence $A(\Delta)$ for M_2 waves as found from the explosion data shows a large scatter in comparison with the values calculated from the calibration curve. This is due to differences in the geological structure in the region where the station is located, which leads to a certain difference in the value of T_{M_2} for the same Δ.

The attenuation of the maximum oscillation amplitudes in the M_1 and M_2 waves recorded during explosions has generally the same character as during earthquakes [5, 114] (see § 2 of this chapter). Therefore, the dependence $A(\Delta)$ is not examined.

Methods of plotting average dependence $A/T(\Delta)$ in M_2 waves. It was necessary to first normalize the observed values of $A/T(\Delta)$ in order to process statistically the entire set of data of $A/T(\Delta)$ obtained during various explosions differing both in intensity and height, and consequently, also in magnitude. This normalization was carried out by the following two methods:

1. The experimental values of $A/T(\Delta)$ were plotted in the system of coordinates $\lg A/T;\lg\Delta$ for the given explosion. The dependence $A/T(\Delta)$ calculated from the calibration scale or from the following equation, derived from [24], was plotted on this same graph with respect to the average magnitude M for the given explosion:

$$M = \lg(A/T) - 1{,}66\lg\Delta^\circ + 3{,}3, \qquad (27)$$

This equation closely approximates the tabular values of the calibrated scale [122]. Then, by successive superposition of the curves calculated by the calibrated scale for the given M_{mean}, we transferred onto the same graph the experimental values of $A/T(\Delta)$ observed for explosions, both with the same and different values of Q and h. The same procedure was followed separately both for the complete horizontal and for the vertical components.

The normalization method described above was used when plotting the composite graph for A/T = A/T(Δ) for explosions in different regions, including those in the Marshall Islands.

The composite dependences of A/T(Δ) plotted by the method described above for the complete horizontal and vertical components observed in the range of Δ = 180 - 3,500 km during atmospheric explosions and from 4,000 to 9,000 km during contact explosions in the Marshall Islands are shown in Figure 70. The magnitudes of the explosions fluctuated from 3.5 to 6.0.

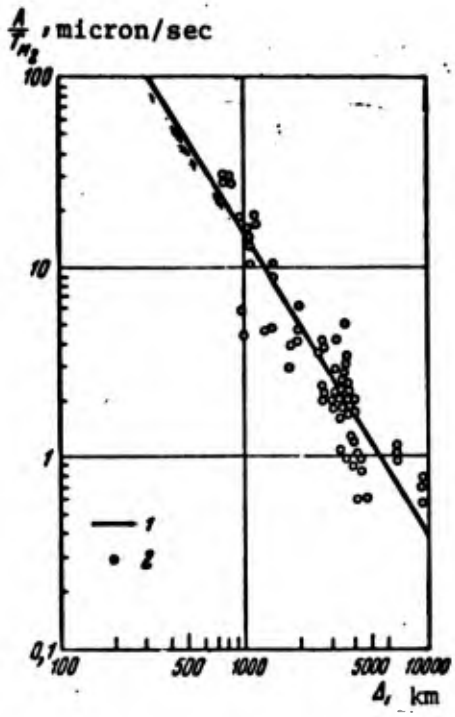

Figure 70. Dependence of A/T on Δ for horizontal component of M_2 Rayleigh waves during atmospheric and contact explosions

1 - calibration curve from data in [122]; 2 - experimental values.

2. A somewhat different method of normalizing the experimental values of A/T(Δ) was selected for averaging the data obtained only during atmospheric explosions. In this case, the lg(A/T) curves plotted as a function of lgΔ for different explosions were normalized by superimposing the values of lg(A/T) on the same station. This method was selected because the epicenters of the explosions remained practically unchanged.

Composite graphs showing the dependence of lg(A/T) on lgΔ for the complete horizontal and vertical components are shown in Figure 71, and the values of A/T, averaged for a 100-kilometer range, are given in Table 42. The magnitudes of the explosions amounted to 3.6 to 5.8.

TABLE 42. AVERAGE VALUES OF A/T FOR M_2 WAVES FROM ATMOSPHERIC EXPLOSIONS RECORDED AT DIFFERENT DISTANCES Δ.

Epicentral distance Δ, km	Horizontal component				Vertical component			
	A/T, micron/sec	Deviations: Arithmetic mean $\pm\delta$	Deviations: Mean square $\bar{\sigma}$	No. of determinations	A/T, micron/sec	Deviations: Arithmetic mean $\pm\delta$	Deviations: Mean square $\bar{\sigma}$	No. of determinations
94—140	23,0	4	—	5	20,0	3,5	—	6
200—300	7,7	1,84	—	5	4,8	1,5	—	4
360	6,7	1,16	—	6	4,2	1,23	0,53	8
460	2,98	1,22	0,38	27	3,47	0,56	0,15	25
1000—1100	1,54	0,14	0,03	23	2,06	0,38	0,09	24
1300—1400	0,70	0,16	0,06	26	0,76	0,22	0,04	22
2080	1,10	0,00	0,00	27	1,05	0,00	0,00	27
2100—2200	0,43	0,15	--	3	0,61	0,26	—	5
2200—2300	0,34	0,08	0,03	25	0,34	0,11	0,04	27
2800—2900	1,14	0,31	0,10	16	0,36	0,21	0,07	17
3200—3400	0,45	0,10	0,10	26	0,27	0,08	0,03	27
3400—3600	0,42	0,19	0,09	80	0,35	0,11	0,02	78
3600—3800	0,63	0,18	0,06	16	0,28	0,08	0,04	15
3800—4000	1,08	0,31	0,10	16	0,35	0,08	0,03	15
4450	0,36	0,11	0,06	10	0,43	0,16	0,08	11
5220	0,21	0,03	0,01	10	0,29	0,07	0,02	10

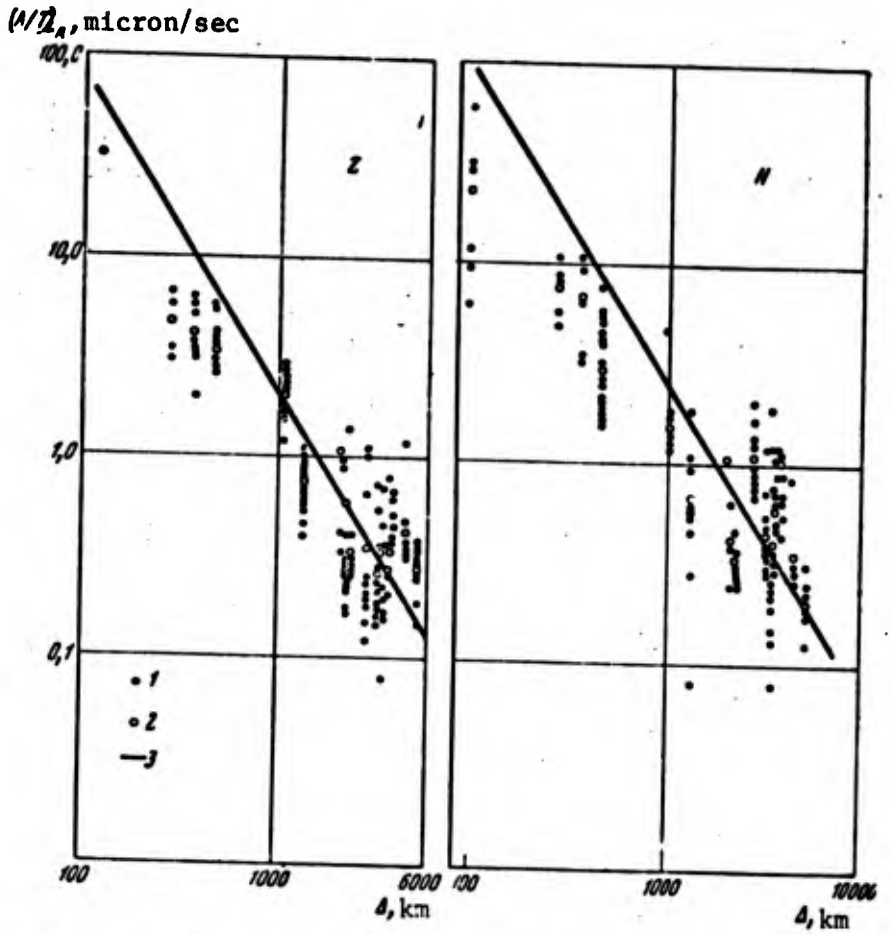

Figure 71. Dependence of A/T on Δ in M_2 waves during atmospheric explosions in the same region

1 - observed values; 2 - average values; 3 - calibration curves from data in [122].

Discussion of results. An examination of the averaged data given in Figure 71 and in Table 42 reveals that, for the explosions being studied, the general shape of the dependences A/T(Δ) in the interval Δ = 1,000 - 10,000 km for the complete horizontal and the vertical components can be approximated with some accuracy by an equation like (27), which was established for the M_2 waves of shallow-focus earthquakes.

In order to estimate the scatter of the experimental values of A/T(Δ), calculations were made to determine the mean arithmetic deviations δ and the mean square deviations $\bar{\sigma}$ of a single measurement from its mean arithmetical value A/T_{mean} determined in a one-degree

interval (Table 42). For most of the stations, $\bar{\sigma}$ varies from 5 to 10%.

The differences in the values of $\bar{\sigma}$ for different stations are due to a number of causes, the ratio of the signal level to the microseism level, the intensity and height of the explosion, the azimuth towards the epicenter, etc., which, naturally, varied from explosion to explosion at the individual stations. However, it is very difficult to take these factors into consideration.

Estimates were also made of the deviation of $(A/T)_{mean}$ from the calibrated curve approximating them. In the range of Δ under consideration, the mean-square relative deviation of a single measurement from the calibrated curve is on the order of 5 - 7%.

The values of $\bar{\sigma}$ obtained in determinations of $A/T(\Delta)$ show that the magnitudes of explosions can be determined by the calibrated scale in [122] with an accuracy of $\delta = \pm 0.2$ magnitude units from the data of 10 - 12 stations without taking into account station corrections. This is a relatively high accuracy, which has been attained in a number of cases in practice when determining the M of earthquakes. By introducing station corrections, this accuracy can be further increased by at least a factor of two λ — that is, errors in M can be reduced to $\pm$ 0.1 magnitude units.

It is especially necessary to distinguish the area of Δ up to 500 - 600 km, in which values of A/T which are too low are observed for the horizontal and vertical components, and consequently magnitudes M_{st} at the given stations which are too low in comparison with their mean values M_{mean}. It has been established that the deviations $\Delta M = M_{mean} - M_{st}$ increase with an increase in M. The cause for this may be that the more powerful explosions — that is, the explosions with greater values of M — are carried out as a rule at greater altitudes than the less powerful explosions. This influences the spectral composition of the oscillations in the M_2

waves recorded at distances Δ of up to 500 km. At distances of $\Delta \geq 800 - 1{,}000$ km, the spectral composition of the oscillations in the M_2 waves depends to a larger extent on the character of the path than is the case with smaller values of Δ. The influence of the spectral composition of the oscillations in the source is greatly concealed by the influence of the medium.

It must not be ruled out that the calibration values of $\lg A/T$ for $\Delta < 500$ km have been determined with insufficient accuracy.

Thus, the analysis of numerous experimental data shows that the relationship $A/T(\Delta)$ in the M_2 waves from atmospheric and contact explosions carried out in different regions in a range of epicentral distances from 1,000 to 10,000 km is close to the analogous relationship established in [24, 120-126, 215] for shallow-focus earthquakes. In the above-mentioned range of Δ, its character does not depend on M. This indicates that the calibrated scales worked out for earthquakes may possibly be used during explosions.

In the range of $\Delta < 500$ km, a dependence of $A/T(\Delta)$ on the magnitude is observed. When M changes from 3.5 to 5.7, ΔM reaches a value of approximately 0.5 - 0.9 magnitude units. Therefore, when using the M scales for $\Delta < 500 - 600$ km, the corresponding corrections must be taken into consideration.

Section 2

Love Waves and Channel Waves

§ 7. Love Waves

Love waves L_Q have been recorded only during atmospheric and underground nuclear explosions. During atmospheric explosions, it was not possible to record them from all regions. During underground explosions, it was not possible to record them during all the explosions carried out in a given region. In atmospheric explosions, L_Q waves were observed in those cases when a part of their path went across seas or oceans.

In cases when L_Q waves were recorded, it was usually possible to distinguish them quite reliably in the recordings. In this case, the following distinctive features of the recordings are the criteria for the L_Q waves. The same also applies to L_Q waves in earthquakes:

1) The L_Q waves propagate with faster velocities than the L_R waves, and therefore they first appear in the group of long-period oscillations (see Figure 27, d, Figure 57, d, Figure 72, Figure 73, b).

2) Vertical instruments do not record these waves.

3) When the horizontal instruments are oriented exactly towards the epicenter, the waves are observed only in the transverse component.

4) In cases when the horizontal instruments are arbitrarily oriented, the motion of medium particles in the L_Q waves proceeds along an ellipse lying in the horizontal plane; the major axis of the ellipse is perpendicular to the epicenter-station line.

5) The periods of the T_{L_Q} waves increase with changes in Δ according to the same laws as for earthquakes (Figure 74).

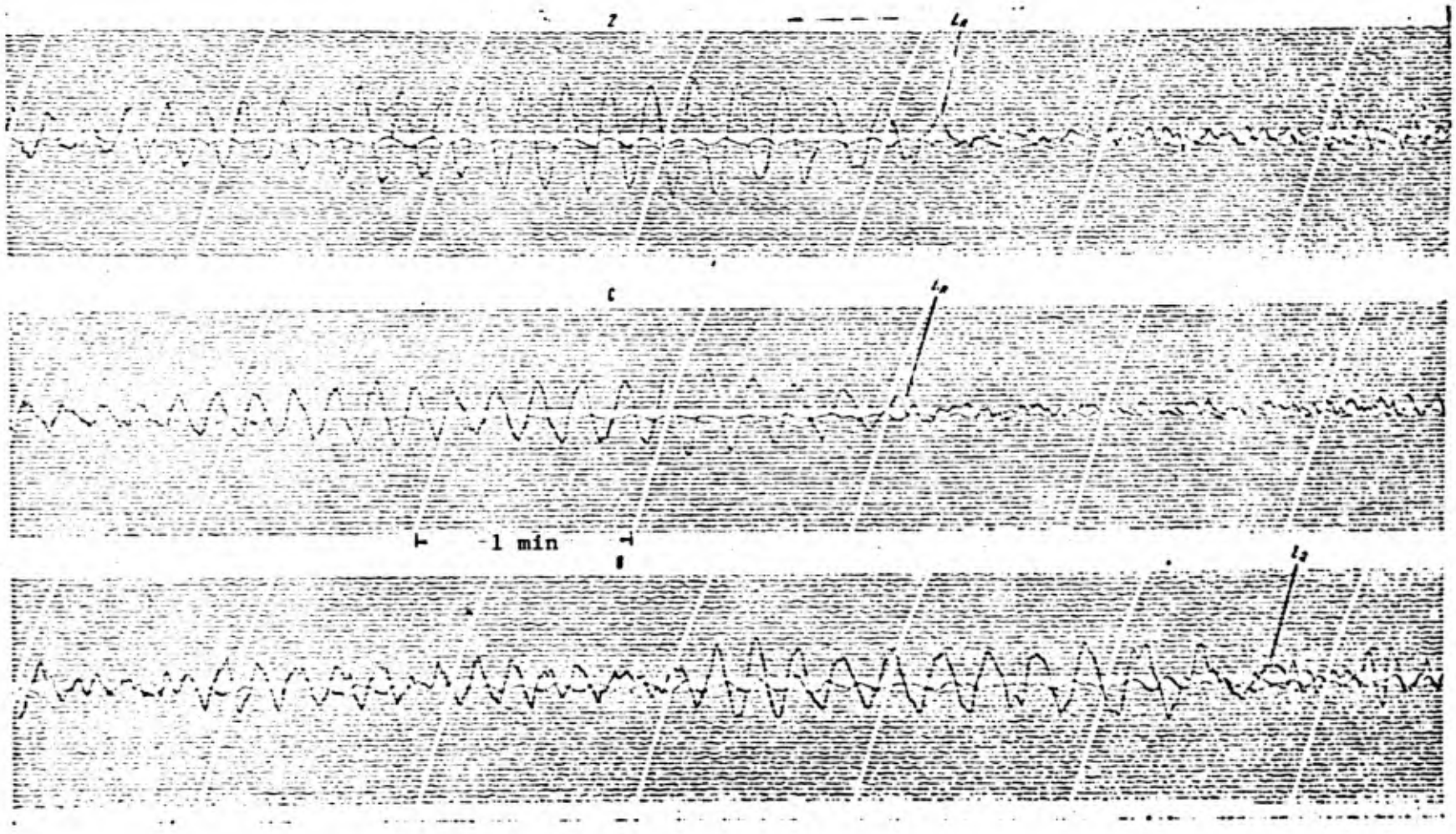

Figure 72. Recording of Love waves L_Q and Rayleigh waves L_R during the earthquake of January 31, 1960 at 18 hours 51 minutes, h = 100 km; m = 4.5; Δ = 3,800 km.

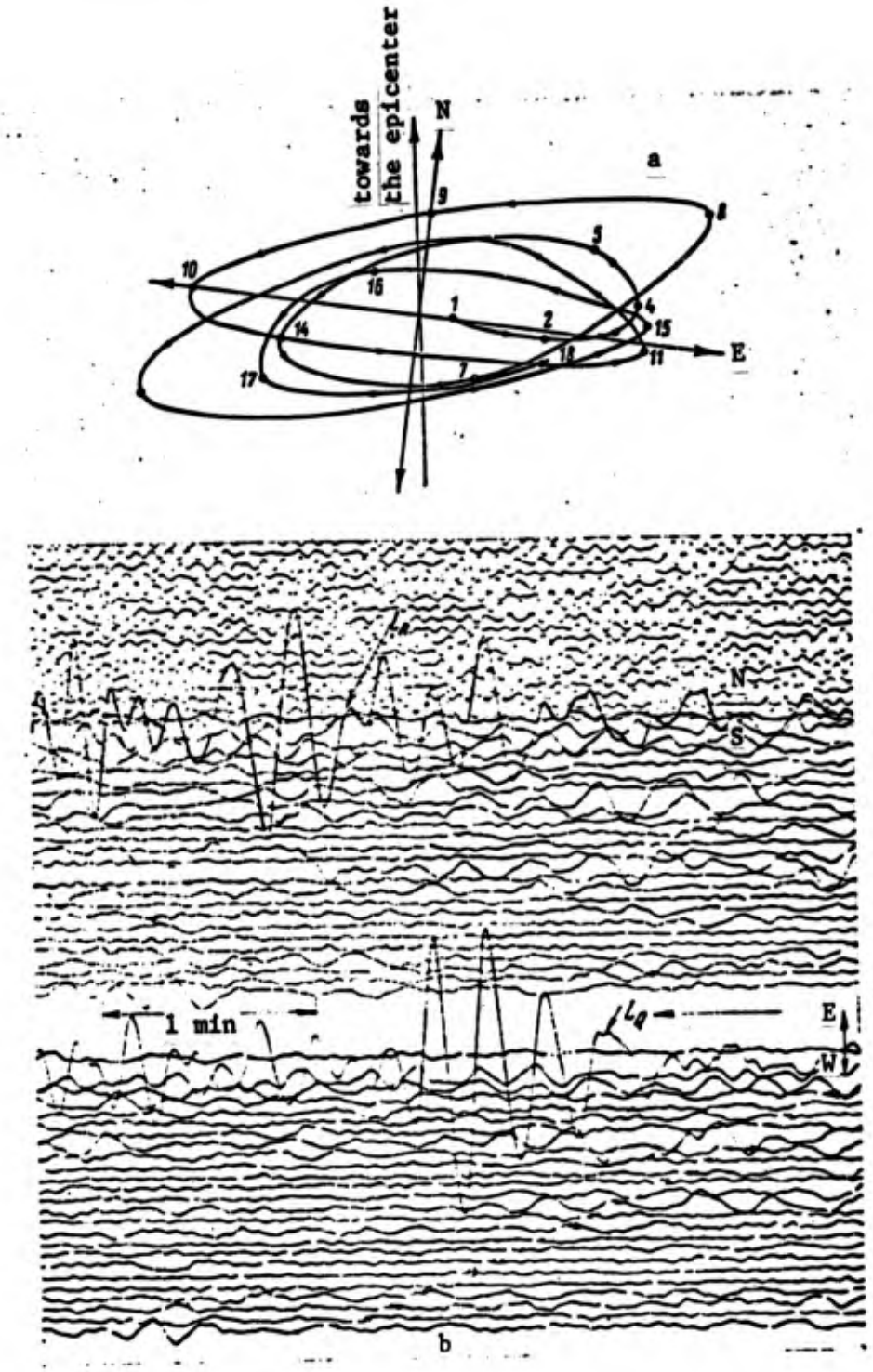

Figure 73. Motion trajectory of particles in the medium for Love waves (a), and recording of these waves taken by wide-band seismographs (b) during an atmospheric explosion (Δ = 3,660 km).

The numbered points are given to facilitate tracing of the trajectory.

6) A normal dispersion of group velocities is characteristic for L_Q waves.

7) Changes in the amplitude A and in the A/T ratio with changes in Δ following practically the same laws as those which apply to the L_R waves.

The recordings of the L_Q waves during atmospheric and underground explosions are briefly characterized below.

Atmospheric explosions. The L_Q waves have the appearance of a short oscillation train with normal dispersion of the group velocities. At distances of $\Delta > 2{,}000 - 3{,}000$ km, the train usually consists of 4 - 5 oscillations with clearly expressed leading and trailing fronts.

The periods of the L_Q waves in the initial part of the recording increase with increases in Δ in accordance with approximately the same laws as those which apply to the periods of the M_2 waves of explosions and earthquakes (Figure 74). At distances of $\Delta \gtrsim 1{,}000$ km, in the recordings of wide-band seismographs, the periods amount to about 10 sec, and at a distance of $\Delta \sim 4{,}000$ km they amount to 13 - 15 seconds. At the end of the train, the periods amount to about 5 - 8 seconds. In the recordings of long-period seismographs, the periods of the L_Q waves at a distance of $\Delta \gtrsim 2{,}000 - 3{,}000$ km amount to 30 - 40 seconds. The number of oscillations in a train, in recordings of ultra-long period equipment, is somewhat less (usually 2 - 3) than in the recordings of wide-band seismographs. The periods in the L_Q waves at a distance of $\Delta > 2{,}000 - 3{,}000$ km in the recordings of this type of seismographs practically do not depend on the intensity of the explosion.

The trajectory of motion of the medium particles in the L_Q waves assumes the shape of an ellipse in the horizontal plane (Figure 73, a). The ellipse major axis is perpendicular to the line going through the epicenter and the station.

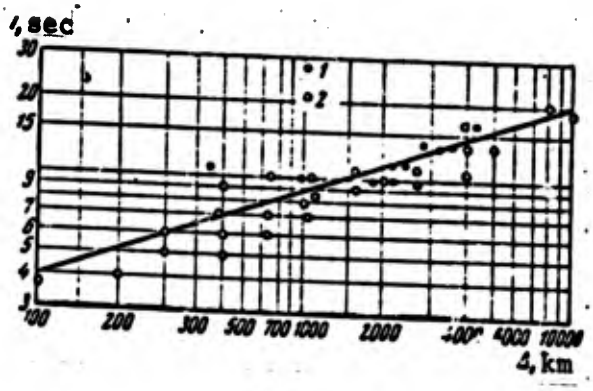

Figure 74. Averaged dependences of the period in Love waves on Δ:

1 - for atmospheric explosions;
2 - for earthquakes.

The dispersion curves of the group velocities for the L_Q waves observed in the Russian platform are very close to the corresponding dispersion curves for earthquakes in nearby regions. In the cases under study here, the group velocities of the L_Q waves amount to v_{gr} = 3.8 km/sec at T = 48 sec, and v_{gr} = 3.2 km/sec at T = 15 sec. The propagation velocity of the maximum phase of the oscillations in the L_Q waves exceeds the propagation velocity of the M_2 waves (see the hodographs of the M_2 and L_Q waves in Figure 42). The intensity of the maximum oscillations in the L_Q waves at short distances of $\Delta \approx$ 500 - 1,000 km in a number of cases is somewhat smaller than for the Rayleigh M_2 waves (Figure 27, d). However, at greater distances of Δ > 1,500 - 2,000 km, this intensity becomes approximately the same as for M_2 waves (see Figure 57, d and Figure 73, b).

In a number of stations, L_Q waves were not recorded during powerful atmospheric explosions. In this connection, in [145] and in other studies, it was proposed that the fact that L_Q waves were absent during atmospheric explosions be used in order to distinguish waves caused by explosions from waves caused by earthquakes. However, the experience of stations in the USSR and other nations [295] in recording Love waves during the same atmospheric explosions, in which some seismic stations did not record these waves, indicates at any rate that this criterion is ambiguous and of little effect.

Underground explosions. The recordings of L_Q waves obtained during underground explosions are just as clear as those obtained during atmospheric explosions (see Figure 57, d). All the kinematic and

dynamic characteristics of the L_Q waves during underground explosions are no different from the characteristics of L_Q waves recorded during atmospheric explosions.

The mechanism by which the L_Q waves are excited during underground explosions is as yet unclear. A number of hypotheses have been advanced on this question, including one which attributes the excitation of L_Q waves to the nonuniform structure of the medium in the horizontal direction near the focus [358] and on the propagation path of the waves, because of faults, asymmetry of the source, and other factors.

The intensity of the full horizontal components of the L_Q waves, both during atmospheric explosions and during underground explosions, is comparable with the intensity of the M_2 waves. Therefore, when the magnitudes M are determined according to the L_Q waves with respect to the scale for M_2 waves [122], values are obtained which practically coincide with the values of M determined according to the M_2 waves.

A comparison of the recordings of the L_Q waves during explosions and during earthquakes (see Figure 57, d and Figure 72) reveals that there is a considerably shorter (ten times or more) duration of the wave train and a greater steepness of the leading and trailing fronts of the oscillation train during explosions, in comparison with those during earthquakes. This characteristic feature, together with others, can apparently be utilized in distinguishing the recordings of explosions from those of earthquakes. However, thus far no statistical assessments of the effectiveness of the above-mentioned parameters of the waves have been made.

For purpose of identifying explosions, L_Q waves are of less universal significance than the dilatational and Rayleigh waves, on account of the fact that they are not excited in all explosions and apparently do not propagate in all directions.

§ 8. Type L_x, L_1, L_g and R_g Waves

During many atmospheric, contact, underground, and also shallow-water underwater nuclear explosions carried out in regions with a continental structure of the Earth's crust and along continental propagation paths, relatively intense groups of oscillations have been observed which, on the basis of their kinematic and dynamic characteristics, are attributable to surface channel waves of the L_x, L_1, L_{g1}, L_{g2}, R_{g1}, and R_{g2} types (Figures 29 - 31, 42, etc.). These waves propagate with the same velocities that are characteristic for the corresponding waves of earthquakes (see Table 43 and the hodographs in Figures 29 - 31, 42).

There are various points of view concerning the nature of these waves. Some authors (Gutenberg, Båth) [45, 228] consider the L_{g1} waves to be channel waves, and connect their propagation mechanism with the presence of a zone with a lowered velocity in the granite layer of the Earth's crust. Press [298] is inclined to consider only the L_{g2} waves as channel waves, and he considers the L_{g1} waves as waves repeatedly reflected from a discontinuity in the Earth's crust (like reflections in whispering galleries). Ye. F. Savarenskiy [113] and Oliver [287] regard these waves as higher harmonics of Love and Rayleigh waves. They connect the L_x and L_1 waves with the presence of wave guides in the astenosphere. A number of authors regard the R_g waves as higher harmonics of Rayleigh waves.

Type L_x, L_1, L_{g1}, L_{g2}, R_{g1} and R_{g2} waves caused by explosions are characterized by the following kinematic and dynamic features.

1. The propagation velocities of these waves (see Table 43, and also the hodographs in Figures 29 - 31 and 42) do not change together with an increase in the epicentral distance throughout the entire area in which they are traced, from tens of km to 5,000 -

TABLE 43. COMPILATION OF VELOCITIES AND PERIODS OF TYPE L_g AND R_g SURFACE WAVES DURING DIFFERENT TYPES OF EXPLOSIONS AND DURING EARTHQUAKES, RECORDED BY SK, SKM, USF, PRESS-EWING AND OTHER TYPES OF SEISMOGRAPHS

Type of source	Region of observation and range of recording	Number of observations used	Type of waves												Literature
			L_x		L_1		L_{g1}		L_{g2}		R_{g1}		R_{g2}		
			v, km/sec	T, sec	v	T	v	T	v	T	v	T	v	T	
Atmospheric explosions	Europe and Asia, 6,000 km	15—37	4,0	4—8	3,78	7—12	3,53	4—11	3,38	7—12	3,23	8—9	3,02	7—9	Author [145]
	USSR 3,500 km	4—10	4,01	1—5	3,8	1—5	3,55	1—4	3,4	1—4	3,2	2—4	—	—	Author
Underground explosions	USSR 5,000 km	1—3	4,0	1,5—2,5	3,8	1,5—2,5	—	1,5—2,5	—	1,5—2,5	—	—	—	—	Author
	North America 1,000 km	more than 30	—	—	—	—	3,55	0,89 to 1,4—2	3,36	0,8—2,0	—	—	—	—	Author [317, 320
	Central Asia 2,500 km	2	—	—	—	—	3,55	0,2—2,0	—	0,5—2,0	—	—	—	—	[10,77]
Earthquakes	USSR 9,000 km	20—70	4,0	1—5	3,8±0,09	4—7	3,51±0,06	1—6	3,34±0,04	2—11	3,29	4,5—8	3,09±0,08	1—14	[10,77]
	Europe	—	—	—	3,8	4—12	—	3—8	3,37	4—10	—	—	3,0—3,1	3—14	[113]
	United States	—	—	—	3,8±0,1	0,5—6	3,55±0,1	0,5	3,1±0,1	0,5—6	—	—	3,05	8—12	[45]

6,000 km. This, together with the other data given below, indicates that the waves under study here have a surface or channel character.

2. The waves are traced only if there is a continental type crust in the region of the epicenter and along their propagation path. Along oceanic paths, these waves have not been recorded at considerable epicentral distances, neither during contact (on the ground or on the water) nor during underwater or atmospheric nuclear explosions carried out by the United States in the region of the Marshall Islands, over Johnston Island, or along the coast of the Pacific Ocean (the Wigwam explosion, etc.).

3. The oscillation periods in the waves being investigated depend to a considerable degree on the type of explosion when they are recorded at the same Δ and at the same point. The waves with the shortest periods (0.2 - 2.0 seconds) were recorded in shallow-water underwater and underground nuclear explosions. Those with the longest periods (up to 6 - 10 seconds) (at $\Delta \approx$ 3,000 - 5,000 km) were recorded during powerful atmospheric explosions (see Table 42 and Figure 75).

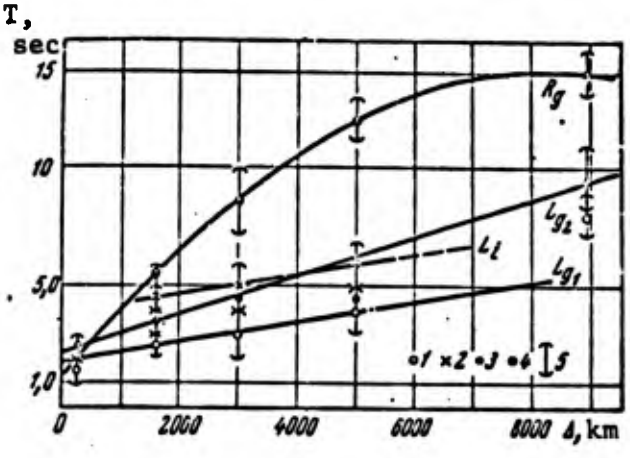

Figure 75. Dependence of period in channel waves on epicentral distance.

1 - 4 - experimental values;
5 - standard deviations.

For type L_g and L_i waves, an insignificant increase in the period is observed together with an increase of Δ. The periods increase according to approximately the same law as that which applies for these waves during earthquakes with foci in the Earth's crust and $M \approx 5 - 6$. However, the dispersion of the waves is expressed only very slightly. The periods of the L_x, L_i, L_{g1} and L_{g2} waves differ only slightly. The smallest periods are those of the type L_{g1} and L_{g2} waves. Somewhat larger periods are characteristic for the R_g waves.

In the range of $\Delta \approx 2{,}000 - 5{,}000$ km, the periods of waves such as those being considered exceed the periods of the body waves by no more than 1.5 times, while the periods of the Love and Rayleigh waves in all cases exceed the periods of the body waves considerably, by 2 - 3 times or more.

4. Studies have been made of polarization in the L_x, L_i, L_g and R_g waves and their dispersion during atmospheric explosions in a region with a continental structure. It has been established that the L_x, L_i, L_g and R_g waves are polarized elliptically in a vertical plane. The motion of particles in the waves is retrograde. The dispersion in these waves is normal, but is expressed to a considerably lesser degree than in the case of L_Q and L_R waves. Analogous polarization and dispersion are also observed for the waves being investigated during contact and underground explosions.

5. The intensity of the L_x, L_i, L_{g1}, L_{g2} and R_g waves depends on the type of explosion and its intensity. During underground explosions and shallow-water underwater explosions, the most intense waves are the L_{g1} and L_{g2} waves. During atmospheric explosions the most intense groups of waves are the L_x, L_i, and R_g waves. The decrease in the amplitudes of the types of waves being examined together with the increase in distance has not yet been studied fully.

6. The decrease in the oscillation amplitudes with increasing distance for L_{g1} waves during underground explosions has been most fully studied. During explosions, the amplitude in the L_{g1} waves with a period of 1.5 - 2.5 seconds decreases in the range of Δ = = 150 - 2,700 km in inverse proportion to the epicentral distance with an exponent of 2.8. In this case, if we assume that the divergence of the L_{g1} waves is proportional to $\Delta^{-1/2}$, then

$$(A/T)_{L_{g_1}} = \frac{A\sqrt{T}}{\Delta^{1/2}} e^{-0.0065\Delta}. \qquad (28)$$

7. Inasmuch as the L_{gl} waves can be rigorously traced both in explosions (especially underground ones) and in earthquakes, an attempt was made to plot a calibrated scale $m_{L_{gl}}$ for these waves corresponding to the unified m scale of Gutenberg. A calibrated scale for the amplitudes of the complete horizontal component was compiled from the data of underground explosions. Since the ratio of the horizontal component amplitudes to the vertical component amplitudes in the L_{gl} waves is 1.4 ± 0.15, this same scale can be used for recordings of vertical instruments. The difference in the values $\Delta m = m_Z - m_H$ in this case will not exceed 0.15 magnitude units.

8. Attempts were made to apply the scale for $m_{L_{gl}}$ to determine the magnitudes of shallow-focus earthquakes with epicenters from the same region in which explosions were carried out. These attempts showed that the correlation of the intensities of the dilatational waves and the L_{gl} waves was different for explosions and earthquakes from the same region (Table 44). As is clear from Table 44, the difference of magnitudes determined from the L_{gl} waves and from the dilatational waves amounts to 0.5 magnitude units.

Thus, according to preliminary data, during underground TNT explosions relatively more intense (by 3 - 4 times) channel surface waves of type L_{gl} are excited compared with shallow-focus earthquakes with comparable magnitudes.

§ 9. Determining the Seismic Elements from L_R and L_Q Waves

Just as in earthquakes, it is possible to determine from the L_R and L_Q waves the azimuth Az towards the epicenter, as well as to estimate approximately the epicentral distance Δ, the time at the focus, and the location of the explosion epicenter. These elements can be determined most effectively from the M_2 waves of atmospheric and contact explosions, during which these waves are the most intensive.

TABLE 44. DIFFERENCES IN MAGNITUDES CALCULATED BY MEANS OF THE P_n, P* and L_{g1} WAVES DURING UNDERGROUND EXPLOSIONS AND EARTHQUAKES (NUMBERING OF EARTHQUAKES CORRESPONDS TO NUMBERING IN FIGURE 32)

Type of source	No. in Fig. 32	m_{P_n}	m_{P^*}	$m_{L_{g_1}}$	$m_{P_n}-m_{P^*}$	$m_{L_{g_1}}-m_{P^*}$
Underground explosion	1	4,4	4,4	4,4	0	0
	2	4,8	4,8	4,8	0	0
Earthquake	1	—	4,0	4,7	---	0,7
	2	4,7	4,2	4,8	0,5	0,6
	3	5,6	5,1	5,6	0,5	0,5
	4	4,5	4,0	4,5	0,5	0,5
	5	4,5	4,0	4,6	0,5	0,6
	6	4,5	3,8	4,2	0,7	0,4

Determining the azimuth towards the epicenter. The azimuth is determined according to the correlation of the maximum oscillation amplitudes in the M_2, M_1 and L_Q waves in the recordings of horizontal instruments from the following relationship:

$$\operatorname{tg} Az = A_{E-W}/A_{N-S} \quad . \tag{29}$$

Here A_{E-W} and A_{N-S} are the maximum amplitudes of the corresponding oscillations in the recording of the east-west and north-south components in the M_2, M_1 or L_Q waves. The value of Az can also be determined from the ratio of the ellipse axes of the medium particle trajectories of motion in the above-mentioned waves.

From a comparison of the true values Az_{true} with the values Az_{calc} calculated from the M_2, M_1 and L_Q waves, we learn that the accuracy of determining Az does not exceed 3 - 5°. The value of Az can be determined more accurately by the M_2 waves than by the M_1 waves. In explosions, the azimuthal variations of A_Z, which are observed for earthquakes, do not appear [270].

Determining Δ. When only the L_R waves are recorded, approximate estimates of Δ can be made from the periods of the maximum oscillations in the M_2 waves from (27), from the difference in the travel times of the M_2 and L_Q waves, from the dispersion curves, and by other methods applied in seismology.

If the azimuths are determined from the surface waves in a number of stations, then it is possible to determine the location of the explosion epicenter by corresponding graphic or analytical methods, and then to calculate the Δ to each station and the mean time at the focus. However, the accuracy with which the location of the epicenter can be determined in such cases is small (on the order of 100 km), and the accuracy with which one can determine the time at the focus is approximately 10 - 15 seconds.

§ 10. Atmospheric Waves Recorded by Seismographs

A feature of the seismic recordings of powerful atmospheric and contact explosions is the presence in the seismograms of vertical and horizontal long-period seismographs of intense long-period oscillations which appear at the moment subsonic air waves arrive at a given point [95, 101, 242, 348] (see Figure 57). The periods of the initial oscillations in the recordings of the seismographs amount to from several hundredths to several tens of seconds, depending on the intensity of the explosion and on the epicentral distance. The shape of the atmospheric waves recorded by the seismographs coincides with the shape of the corresponding recordings of microbarographs (see Figure 57, a and 76, a), especially in the initial part of the recording. Short-period oscillations with periods of less than 40 - 30 seconds, which complicate the recordings of atmospheric waves in microbarograms [102], are usually not recorded by seismographs.

The mechanism by which atmospheric waves affect seismographs is not yet completely clear. However, there is no doubt that the atmospheric waves affect the seismographs at the moment of arrival at

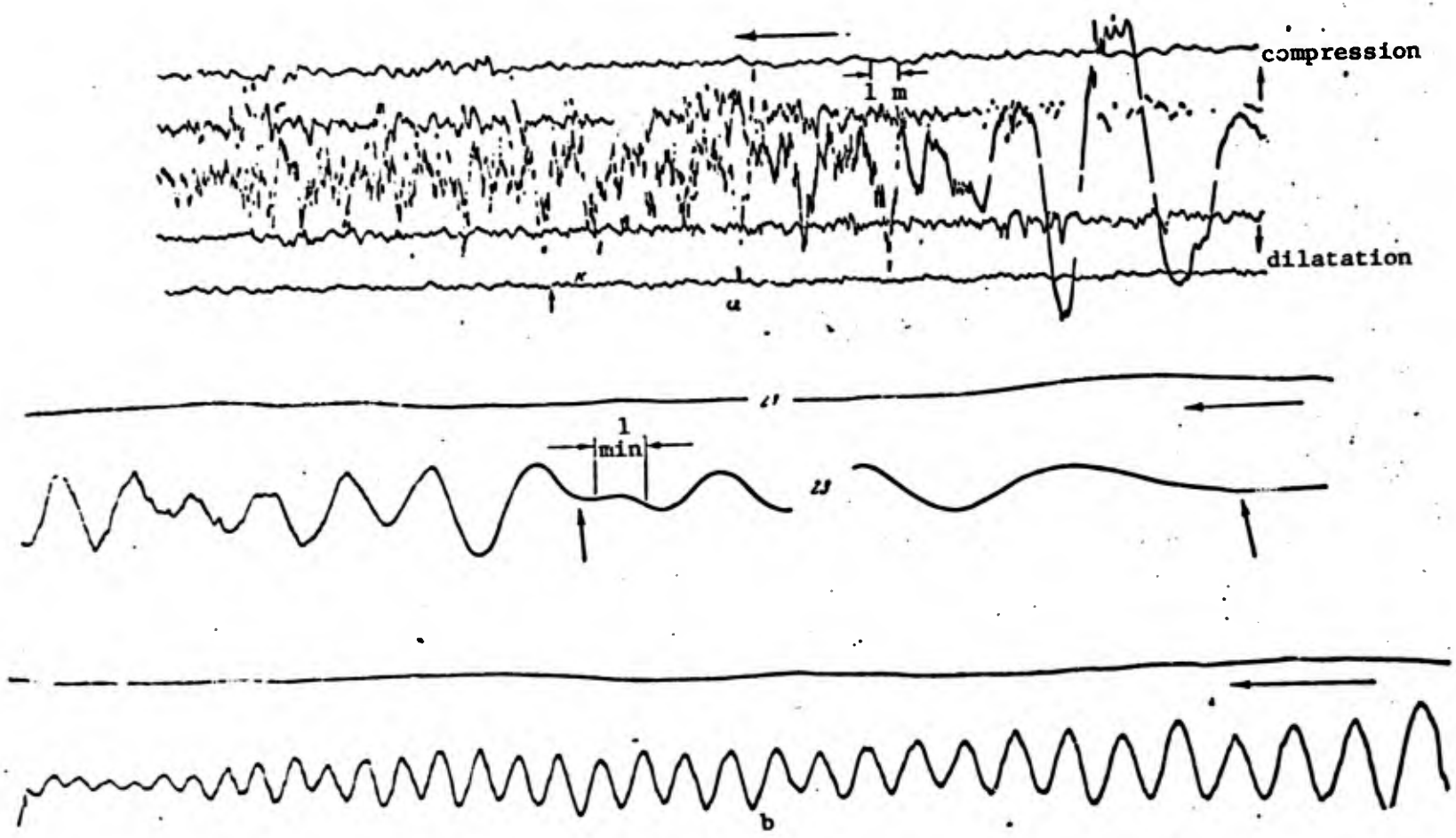

Figure 76. Recording by EDMB-I microbarograph [96] of atmospheric waves from atmospheric explosions.

a - Δ = 2,100 km;

b - Δ = 8,880 km (explosion over Christmas Island).

the observation point. Recordings of seismic waves in the seismogram, at the same time as a normally dispersed oscillation train (with a characteristic shape caused by the action of atmospheric waves on the seismographs), unequivocally indicate that atmospheric or contact nuclear explosions have occurred.

CONCLUSION

1. In all types of nuclear explosions the same types of surface seismic waves are recorded — Love waves, Rayleigh waves, L_x waves, L_i waves, L_g waves, and R_g waves — which are usually observed in shallow-focus earthquakes. For explosions in the water, on the water, or over the surface of the water, waves propagating in the water with a velocity of 1.47 km/sec (phase T) are observed by coastal stations.

2. New types of seismic surface waves have not been observed in nuclear explosions. For atmospheric and contact explosions, a characteristic feature is the presence of subsonic wave recordings in the seismograms.

3. All the above-mentioned waves cannot always be recorded at the same time in all types of explosions. The most intense Rayleigh waves usually are encountered most frequently. These waves are recorded in practically all types of explosions. Therefore, the Rayleigh waves, like the body waves, are the most important in detecting and identifying all types of nuclear explosions.

4. In all types of explosions, three groups of oscillations can be distinguished in the recordings of the Rayleigh waves: 1) the longest-period oscillations, propagating in the Earth's crust and the upper mantle — M_1 waves; 2) a shorter-period train of intense oscillations, propagating in the Earth's crust — M_2 waves; 3) a train of oscillations connected with a sedimentary or sedimentary-metamorphic layer of rocks in the region of the station — L_0 waves.

5. The ratio of the amplitudes in Rayleigh waves L_R to the amplitudes of the dilatational P and transverse S waves depends on the type of explosions. The greatest ratios L_R/S and L_R/P, sometimes exceeding the corresponding ratios in earthquakes, are observed during atmospheric explosions, and the smallest ratios — during underground explosions.

6. During underground explosions and collapse of the rocks from the vaults of the chambers formed as a result of the explosion, the shape of the train of the Rayleigh wave recording is the same (except for the arrival direction). This may indicate that the recording of Rayleigh waves is determined, not by the type of source, but basically by the properties of the medium along the propagation path of the waves.

7. Unlike Rayleigh waves, Love waves do not occur in all types of explosions. In particular, they are not recorded during underwater and contact explosions, and they are not always observed in atmospheric explosions. In a number of cases, these waves cannot be recorded for all azimuths, and their intensity in underground explosions varies greatly when there is a slight shift in the epicenter. This instability of the characteristics of Love waves can be connected with the secondary nature of their excitation in a number of cases — that is, they do not originate immediately in the vicinity of the source, but in the irregularities in the structure of the medium along the propagation path of the waves.

The channel waves L_g are recorded along continental propagation paths in all types of explosions.

8. It has been established that the kinematic characteristics of surface waves during explosions are the same as those for corresponding earthquake waves. Also the characteristics of some of the dynamic characteristics of the waves are similar, such as the motion trajectory of particles in the medium, the dependence of the amplitude and the period of oscillations on the epicentral distance, etc. This

permits us to use the methods and scales developed in seismology — for use with earthquakes — when determining seismic elements and the magnitudes of seismic phenomena, that is, explosions.

9. Together with this, some of the dynamic characteristics of surface waves — the duration of the train, the shape of the envelope, the ratio of the intensities of the Rayleigh waves and the body waves, and others — are different, both in different types of explosions, and in explosions and earthquakes. The differences which have been observed are used for identifying explosions, either independently or in combination with other recording characteristics.

CHAPTER VII

ENERGY OF SEISMIC WAVES DURING VARIOUS TYPES OF EXPLOSIONS

The portion of the energy from an explosion used in the formation of seismic waves, and also the energy ratios between dilatational, transverse, and surface waves during explosions and earthquakes, together with other parameters of the waves, characterize the mechanism in the foci of seismic phenomena. A knowledge of their values enables us to solve a number of fundamental problems, such as working out methods for estimating the TNT equivalents of explosions, providing the foundation of criteria for distinguishing seismic recordings from explosions of different types from those of earthquakes — in particular, the magnitude criterion (M, m) for underground explosions, and others.

A study of this problem for explosions may help in organizing research on the character of the energy release in the foci of earthquakes.

A calculation of the portion E_s of the total energy of an explosion E_{tot} which goes into the formation of seismic waves during various types of explosions is given below.

§ 1. Methods of Calculating the Energy of Seismic Waves

The E_s of explosions was calculated as the sum of the energy of the forward dilatational waves E_s^P, of the transverse waves E_s^S, and of the surface Rayleigh waves E_s^L:

$$E_s = E_s^P + E_s^S + E_s^L \tag{30}$$

E_s^P and E_s^S were calculated in the range of epicentral distances higher than 20°, and E_s^L in the range from 4 to 50°. The Zöppritz-Wiechert formula was used to calculate $E_s^{P,S}$ [68, 69]:

$$E_s^{P,S} = 8\pi^2 R^2 V\rho \frac{\sin\Delta \sin e_0}{|de_0/d\Delta|} e^{-kL} \int_0^{t_0} \dot{X}^2 dt. \tag{31}$$

Here, $\dot{X}$ is the displacement velocity in the incident body wave; e_0 is the departure angle of seismic radiation; L is the length of the ray path; and k is the energy absorption coefficient.

The value of

$$\frac{\sin\Delta \sin e_0}{|de_0/d\Delta|}$$

on the upper boundary of the mantle is given in [68]. R is the Earth's radius, which is 6,370 km. The remaining notations are the same as in [68]. When calculating E, the integral in (31) was replaced by the sum.

The values of $k_p = 2\alpha_p$ were calculated by formulas taken from [105] for waves propagating in the upper mantle up to $\Delta \leq 4{,}000$ km:

$$\alpha_P = 2{,}8 \cdot 10^{-4} \cdot \frac{1}{T} k_M^{-1}, \tag{32}$$

and for the lower mantle ($\Delta > 4{,}000$ km):

$$\alpha_P = 1{,}8 \cdot 10^{-4} \cdot \frac{1}{T} k_M^{-1}. \tag{33}$$

In calculating E_s^L, a formula proposed by S. Ya. Kogan was applied [69]:

$$E_c^L = 2\pi R\rho v_L^2 a_1 e^{k_L \Delta} \sin \Delta \int_0^\tau U_X(t,0)\, U_Z(t,0)\, dt, \qquad (34)$$

where U_X is the amplitude of the complete horizontal component of soil displacement; U_Z is the amplitude of the vertical component; a_1 is a constant equal to 4.704, for the Poisson coefficient, which is equal to 1/4; v_L is the velocity of the Rayleigh surface waves $\approx$ 3.16 km/sec (in the range $1{,}000 < \Delta < 5{,}000$ km); k_L is the energy absorption coefficient, assumed to be $6 \cdot 10^{-4}$ km^{-1}; τ is the recording train duration in the seismogram. If U_{Z_i} and U_{H_i} designate the amplitudes of the vertical and horizontal components of soil displacements, then, as is shown in [73, 81 - 83], Formula (34) can be reduced to the following:

$$E_c^L = 0{,}85\pi^2 R\rho\, a_1 e^{k_L \Delta} \sin \Delta \sum_{i=1}^{n} U_{H_i} U_{Z_i}. \qquad (35)$$

In the calculations, all the values were given in a CGS system, and the initial values of E_s were obtained in ergs. When calculating the portion of the energy used for the formation of the seismic waves E_s/E_{tot}, it was assumed that the energy of a nuclear explosion with a TNT equivalent of 1 kt is equal to $4.25 \cdot 10^{19}$ erg. Table 45 gives information about the data used in making calculations of E_s according to the Zöppritz-Wiechert and the S. Ya. Kogan formulas. The TNT equivalent was known for the explosions indicated here.

Calculations of E_s from the body waves of atmospheric explosions were made only for four of the most powerful explosions (Table 45); in the other explosions, the S waves were not recorded with a sufficient intensity at large distances from the epicenter (above 50°). During underground explosions in Nevada, the E_s was calculated from the surface waves only in the most powerful explosions. During underground explosions in Nevada, the transverse waves were recorded at stations of the USSR only in some cases and only at a small number of

TABLE 45. DATA USED TO CALCULATE E_s FROM THE FORMULAS OF ZÖPPRITZ-WIECHERT AND S. YA. KOGAN

Type of explosion	Region of epicenter	Number of explosions used to determine E_s from the waves		
		P	S	L
Atmospheric	Continental	4	3	8
Contact	Marshall Islands, continental	-	-	8
		7	3	3
		-	-	8
Underground	Nevada, continental	12	-	3
		5	3	5
Underwater	Pacific Ocean	3	-	-

stations. During underwater explosions in the Pacific Ocean, the transverse and surface waves were not observed in the USSR with a sufficient intensity.

§ 2. Energy Ratios of Body and Surface Waves During Various Types of Explosions and During Earthquakes

Table 46 gives the results of calculating the portion of energy from an explosion used for the formation of seismic waves during various types of explosions, E_s/E_{tot}, and also the ratios of E_s calculated from the Zöppritz-Wiechert and S. Ya. Kogan formulas [see Formulas (31) and (35)].

The results of calculations by the Zöppritz-Wiechert Formula (31) showed that, in the case of atmospheric explosions carried out over

TABLE 46. PORTION OF EXPLOSION ENERGY USED FOR FORMATION OF SEISMIC WAVES DURING VARIOUS TYPES OF NUCLEAR EXPLOSIONS

Type of explosion	Height or depth of explosion, km	Ratio E_s/E_{tot} of seismic energy E_s calculated by the Zöppritz-Wiechert and S. Ya. Kogan formulas, to total energy of explosion E_{tot}	
		by Zöppritz-Wiechert formula for body waves	by S. Ya. Kogan formula for Rayleigh waves
Atmospheric	In layer of atmosphere near the ground	$1.3 \cdot 10^{-7}$	$4 \cdot 10^{-8}$
Contact, on earth and on water	0	$1.3 \cdot 10^{-5}$	$1.5 \cdot 10^{-7}$
Underground, in tuff and in granite	0.3 - 0.7	$1.10 \cdot 10^{-3}$	10^{-6}
Underwater (in Pacific Ocean)	0.15	-	-
	0.60	4.10^{-2}	-

oceanic islands and continents, the seismic energy of the body waves is 10^{-7} of the total explosion energy. In the case of contact explosions, it is about 10^{-5}; in the case of underground explosions, it is $(1 - 3)\cdot 10^{-3}$. In the case of underwater explosions, it is $(1 - 4)\cdot \cdot 10^{-2}$.

The portion of the energy of the surface waves out of the total explosion energy is approximately 10^{-8} in the case of atmospheric explosions, 10^{-7} in the case of contact explosions, and 10^{-6} in the case of underground explosions. During shallow-focus earthquakes,

the energy of the surface waves is usually about 1% of the energy of the body waves.

It must be noted that the values of E_s^L are too low, since the energy of the surface waves was calculated not only from recordings of SKD instruments, but also from those of SK instruments with a pass-band from 0.1 to 8 - 12 seconds. The long-wave (with periods higher than 20 - 25 seconds) portion of the oscillation train in the surface waves was barely recorded by these seismographs.

The energy ratios between the body and surface waves obtained in this way for different types of explosions agree with the data on the recording ranges (see Table 4), and also with the data given in [58, 209, 295]. However, for atmospheric and contact explosions, there is a certain divergence from the results of [209]. The latter may be caused by the fact that, in [209], seismographs with longer periods than those used in this book were employed.

The calculations showed that the experimental ratios, established for earthquakes for calculating the energy of seismic waves according to the m and M magnitudes, are inapplicable for calculations in the case of explosions. As was already mentioned in the preceding chapters, this is due to the fact that there are differences between explosions and earthquakes in the intensity ratio of body and surface waves. It is also due to the distinctive features of the focus during explosions.

Analogous results were obtained by Gutenberg in calculations of seismic wave energy for underwater explosions [218]. The same thing was observed for underground explosions in [175] and others.

Thus, the ratio of surface wave energy to the body wave energy amounts to approximately 0.1 for atmospheric explosions, 0.01 for contact explosions, 0.001 for underground explosions, and 0.01 for shallow-focus earthquakes.

The differences in the energy ratios between surface and body waves during underground explosions and earthquakes, or the differences in the corresponding values of A/T, are used in identifying the seismic recordings of underground explosions according to the magnitude criterion M = M(m) [97, 326].

The following correlation, connecting M with m, was established experimentally from observational data at seismic stations of the USSR. It is valid for shallow-focus earthquakes in a range of magnitude values from M = 3 to 6.5.

$$M = (0{,}69 \pm 0{,}10)m + (1{,}16 \pm 0{,}06). \qquad (36)$$

The corresponding relation for underground nuclear explosions is:

$$M = (0{,}89 \pm 0{,}21)m - (0{,}55 \pm 0{,}12). \qquad (37)$$

Analogous relations for earthquakes and explosions have been determined from observational data in the United States, England, and Canada [97, 326].

It is obvious from the relations mentioned above that, in the range of M under study, its value for underground explosions is less by one or two units of magnitude M than for earthquakes of the same magnitude m determined by the dilatational waves. This makes it possible to identify unequivocally the recordings of underground explosions recorded at distances of $\Delta \geq 3{,}000$ km.

BASIC CONCLUSIONS AND DIRECTIONS OF FURTHER RESEARCH

1. The wave field was studied during various types of explosions and earthquakes. Hodographs and curves showing the dependence of the A/T ratio on the epicentral distance were plotted for the most stable recorded waves. Primarily, dilatational waves prevail during underground, underwater, and contact nuclear explosions, which are traced at epicentral distances up to 17,000 - 18,000 km. For atmospheric explosions, surface Rayliegh waves prevail.

No new types of waves were discovered, except atmospheric waves, recorded by seismographs during atmospheric and contact explosions.

2. The differences in the dynamic characteristics of the same types of waves caused by different types of explosions and by earthquakes, as well as differences in the dynamic ratios of waves of different classes, were established. The criteria for identifying explosions are based on these differences. The basic criteria are the differences in the intensity ratios between different classes of dilatational and surface waves, in the shape of the envelope of the oscillation trains of individual body and surface waves and of the entire recording, as well as differences in the spectral composition of the oscillations in the body waves.

3. On the basis of a study of the spectra of the useful waves and microseisms, methods of increasing the effective sensitivity of the seismic receiving equipment were examined. The optimum passbands of the equipment were indicated. The minimum signal levels which can be registered by single seismographs at stations with a low microseismic level were estimated.

Further research on seismic wave fields occurring during explosions and earthquakes should be pursued primarily in the following directions:

1. Study of the structure of the wave field, especially the intensity ratios between waves of different types and classes, including those in the low-frequency spectral region. On this basis, new criteria for distinguishing between explosions and earthquakes can be developed.

2. Increasing the effective sensitivity of short-period and long-period equipment, by: 1) improving their installation conditions; 2) adopting more refined systems for grouping a relatively small number of seismographs in an array of several tens of stations; 3) grouping short-period seismographs in arrays installed in holes at different depths, and subsequent electronic grouping with computers, in which digital filtration, variable time delays, and other procedures have been incorporated.

3. Automation of the analysis processes, both at the point of observation, and at the central point. To do this, it is necessary, in particular, to change over to reproducible magnetic recording.

4. Development of new, more refined methods of determining the mechanism and focal depth of the seismic phenomena.

In some of the areas enumerated above, research is already being carried out, and in others the necessary equipment is now being developed.

REFERENCES

1. Анализ сейсмических наблюдений на электронных машинах.— Вычислительная сейсмология, вып. 1. Изд-во «Наука», 1966.
2. Андрианова З. С., Кейлис-Борок В. И., Левшин А. Л., Нейгауз М. Р. Поверхностные волны Лява. Изд-во «Наука», 1965.
3. Ан В. А., Баканновский В. Л., Зеликман Э. И., Кабыченко Н. В., Осадчий А. П., Сорохтин О. Г. Многоканальный аналого-цифровой преобразователь.—Передовой научно-технический и производственный опыт, № 5—64—677/20,1964.
4. Аптикаев Ф. Ф. Сейсмические колебания при землетрясениях и взрывах. Изд-во «Наука», 1969.
5. Архангельская В. М., Федоров С. А. Некоторые результаты изучения затухания поверхностных волн Релея.— Изв. АН СССР, серия геофиз., № 8, 1961.
6. Архангельский В. Т. и др. Руководство по производству и обработке наблюдений на сейсмических станциях СССР. Ч. I и II. Изд-во АН СССР, 1952 и 1954 гг.
7. Архангельский В. Т., Введенская Н. А., Гайский В. Н. и др. Руководство по производству и обработке наблюдений на сейсмических станциях СССР. Ч. 2. Руководство по обработке группы сейсмических станций. Изд-во АН СССР, 1954.
8. Архангельский В. Т. Вопросы теории длиннопериодного вертикального сейсмографа.—Изв. АН СССР, серия геофиз., № 10, 1960.
9. Архангельский В. Т. Метод изменения увеличения электродинамического сейсмографа при сохранении вида его частотной характеристики.—Труды ИФЗ АН СССР. № 19 (186), 1961.
10. Архангельская В. М. Исследования короткопериодных волн Релея. Ч. I и II.— Изв. АН СССР, серия геофиз., № 8, 1961; № 9, 1964.
11. Архангельская В. М. Определение направления на эпицентр землетрясения по записям поверхностных волн при удаленных землетрясениях.—Труды ГеоФИАН СССР, № 30, (157), 1955.
12. Архангельский В. Т., Киприос Д. П., Москвина А. Г., Соловьев В. Н., Федосеенко Н. Е., Фремд В. М., Шебалин Н. В. Аппаратура и методика наблюдений на сейсмических станциях СССР. Изд-во АН СССР, 1962.
13. Буне В. И. и др. Методы детального изучения сейсмичности. Под ред. Ю. В. Ризниченко. Изд-во АН СССР, 1960.
14. Белотелов В. Л., Кондорская Н. В. Спектры объемных волн камчатских землетрясений.—Изв. АН СССР, серия геофиз., № 4, 1964.
15. Белотелов В. Л., Рыкунов Л. Н. Устройство для цифрования сейсмограмм.—Изв. АН СССР, серия геофиз., № 3, 1963.
16. Берзон И. С. Об определении показателя степени функции расхождения для преломленных волн по экспериментальным данным.—Изв. АН СССР, серия геофиз., № 4, 1951.
17. Берзон И. С., Коган С. Д., Пасечник И. П. О возможности построения тонкослоистой модели области перехода от оболочки к ядру Земли.—Докл. АН СССР, т. 178, № 1, 1968.
18. Берзон И. С., Епинатьева А. М., Парийская Г. Н., Стародубровская С. П. Динамические характеристики сейсмических волн в реальных средах. Изд-во АН СССР, 1962.
19. Берч Фр., Шерер Дж., Спайер Г. Справочник для геологов по физическим константам. ИЛ, 1949.
20. Борисевич Е. С. (Ред.). Новые приборы для регистрации сейсмических явлений.—Труды ИФЗ АН СССР, № 3, 1964.
21. Борисевич Е. С., Катюшкин В. Ф. Гальванометры типа ГБ к сейсмическим осциллографам.—Труды ИФЗ АН СССР, № 19 (186), 1961.

22. Борисевич Е. С., Касторский С. А., Мосягина М. С. Осциллограф сейсмический типа ОСБ-V.—Труды ИФЗ АН СССР, № 19 (186), 1961.
23. Бюллетени сети сейсмических станций СССР за 1952—1965 гг. Изд-во АН СССР, 1953—1967 гг.
24. Ванек И., Затопек А., Карник В., Кондорская Н. В., Ризниченко Ю. В. и др. Стандартизация шкал магнитуд.—Изв. АН СССР, серия геофиз., № 2, 1962.
25. Виник Л. П. Пространственно-временная фильтрация сейсмического сигнала.—Изв. АН СССР, серия геофиз., № 6, 1963.
26. Виник Л. П. Структура 4—6-секундных микросейсм. Докл. АН СССР, т. 162, №5, 1965.
27. Виник Л. П. О группировании низкочастотных сейсмографов.— Изв. АН СССР, серия геофиз., № 5, 1961.
28. Виник Л. П., Пручкина Н. М. Исследование структуры коротко-периодных микросейсм.—Изв. АН СССР, серия геофиз., № 5, 1964.
29. Виник Л. П., Денисков А. С., Коньков Г. О. Структура микросейсм в области частот около 1 *гц*. II. Результаты наблюдений.— Изв. АН СССР, серия физики Земли, № 8, 1967.
30. Виник Л. П. Структура микросейсм в области частот около 1 *гц*. I. Методика анализа.— Изв. АН СССР, серия физики Земли, № 8, 1967.
31. Воюцкий В. С. Обнаружение слабых сейсмических сигналов способом накапливания.—Прикл. геофизика, вып. 15. М., 1955.
32. Воюцкий В. С. Метод накапливания как средство увеличения эффективной чувствительности аппаратуры. В сб. «ГСЗ земной коры в СССР». Л., Гостоптехиздат, 1962.
33. Воюцкий В. С., Гродзенский В. А. Способ определения и идентификации удаленных взрывов. Сб. «Разведочная и промысловая геофизика», вып. 47. Гостоптехиздат, 1963.
34. Воюцкий В. С. Способ регистрации сейсмических колебаний с накапливанием сигналов.—Прикл. геофизика, вып. 33. М., 1963.
35. Воюцкий В. С. Метод и аппаратура для асинхронного накапливания сигналов.—Изв. АН СССР, серия геофиз., № 11, 1964.
36. Гальванометры зеркальные постоянного тока типа М-17 завода «Вибратор». Упр. агрегатостроения и приборостроения ЛСНХ. Л., 1962.
37. Гамбурцев Г. А. Основы сейсморазведки. ГНТИН и ГТЛ, 1959.
38. Гамбурцев Г. А. Избранные труды. Изд-во АН СССР, 1960.
39. Гамбурцев Г. А., Ризниченко Ю. В., Берзон И. С., Епинатьева А. М., Пасечник И. П., Косминская И. П., Карус Е. Е. Корреляционный метод преломленных волн. Изд-во АН СССР, 1952.
40. Голицын Б. Б. Избранные труды. Т. II. Сейсмология. Изд-во АН СССР, 1960.
41. Гоцадзе О. Д., Кейлис-Борок В. И., Кириллова И. В., Коган С. Д. и др. Исследование механизма землетрясений.— Труды ГеоФИАН, СССР, № 40 (166), 1957.
42. Грошевой Г. В., Федосеенко Н. Е. Способ контроля чувствительности и определения частотных характеристик сейсмоприемных каналов при помощи магнитоэлектрического генератора.— Изв. АН СССР, серия геофиз., № 5, 1953.
43. Гурвич И. И. К теории сферического излучателя сейсмических волн.— Изв. АН СССР, серия физики Земли, № 10, 1965.
44. Гольцман Ф. М. Основы теории интерференционного приема регулярных волн. Изд-во АН СССР, 1962.
45. Гутенберг Б. Физика земных недр. ИЛ, 1963.
46. Дараган С. К. К вопросу о коррекции частотной характеристики сейсмического тракта.—Изв. АН СССР, серия физики Земли, № 3, 1967.
47. Дашков Г. Г. Опыт использования электромеханических фильтров. В сб. «Аппаратура и методика сейсмических наблюдений». Изд-во «Наука», 1966.
48. Джонсон Г. В., Хиггинс Г. Х., Вайолет К. И. Подземные ядерные взрывы. ИЛ, 1962.
49. Запольский К. К. Измерения уровня и спектрального состава коротко-периодных микросейсм.—Труды ИФЗ АН СССР, № 10, 1960.
50. Запольский К. К., Халтурин В. И. Аппаратура и методика исследования физических характеристик сейсмических волн в реальной среде.—Труды ИФЗ АН СССР, №10, 1960.
51. Исаев В. С. О зависимости преобладающей частоты спектра колебания от числа видимых периодов импульса. В сб. «Сейсмическая разведка».—Труды ИФЗ АН СССР, № 6 (173), 1959.
52. Кейлис-Борок В. И., Малиновская Л. Н. К вопросу о распознавании взрывов по вступлениям объемных волн.—Труды ИФЗ АН СССР, № 20, 1962.
53. Кейлис-Борок В. И. Об оценке размеров очага землетрясений и величины подвижки в нем. Ann. Geofis, Roma, 12, № 2, 1959.

54. Кейлис-Борок В. И. Интерференционные поверхностные волны. Изд-во АН СССР, 1960.
55. Кейлис-Борок В. И. Различие спектра поверхностных волн при землетрясениях и взрывах.—Труды ИФЗ АН СССР, № 15 (182), 1960.
56. Кейлис-Борок В. И., Яновская Т. Б. О зависимости спектра поверхностных волн от глубины источника в пределах земной коры.—Изв. АН СССР, серия геофиз., № 11, 1962.
57. Кейлис-Борок В. И., Азбель И. Я., Яновская Т. Б. Методика совместной интерпретации годографов и амплитудных кривых при изучении верхней мантии. В сб. «Вычислительная сейсмология», вып. 1, 1966.
58. Кирнос Ф. А. О доле энергии, идущей на образование сейсмических волн при взрывах ВВ.— Труды СИ АН СССР, № 121, 1947.
59. Кирнос Д. П. Некоторые вопросы инструментальной сейсмологии.— Труды ГЕОФИАН СССР, № 27 (154), 1958.
60. Кирнос Д. П., Кондорская Н. В. О вычислении истинного значения первой амплитуды движения почвы при вступлении сейсмической волны.—Изв. АН СССР, серия геофиз., №12, 1958.
61. Кирнос Д. П., Колесников Ю. А., Рыков А. В. Об инструментальном анализе сейсмограмм.—Труды ИФЗ АН СССР, № 2 (193), 1963.
62. Кирнос Д. П., Колесников Ю. А., Коган Л. А. К инструментальному определению инженерных спектров.—Труды ИФЗ АН СССР, № 28 (195), 1963.
63. Коган С. Д. Времена пробега продольных и поперечных волн, вычисленные по данным ядерных взрывов, произведенных в районе Маршалловых островов.—Изв. АН СССР, серия геофиз., № 3, 1960.
64. Коган С. Д., Пасечник И. П., Султанов Д. Д. Различие в периодах сейсмических волн, возбуждаемых при подземных взрывах и землетрясениях.—Докл. АН СССР, т. 128, № 6, 1959.
65. Коган С. Д. Времена пробега и амплитуды волн *PcP* при поверхностных источниках.—Изв. АН СССР, серия физики Земли, № 3, 1963.
66. Коган С. Д., Пасечник И. П., Султанов Д. Д. Сейсмические наблюдения советских сейсмических станций в Антарктике.—Анналы МГГ. М., 1959.
67. Коган С. Д., Пасечник И. П., Султанов Д. Д. Сейсмические наблюдения в Антарктике.—Изв. АН СССР, серия геофиз., № 2, 1961.
68. Коган С. Я. Определение энергии объемных сейсмических волн.— Изв. АН СССР, серия геофиз., № 10, 1959.
69. Коган С. Я. Об определении энергии сейсмических волн произвольной формы.—Изв. АН СССР, серия геофиз., № 5, 1960.
70. Коган С. Я. К вопросу о связи параметров воздушного взрыва с сейсмической энергией.—Изв. АН СССР, серия физики Земли, № 4, 1965.
71. Коган С. Я. О влиянии поглощения на форму сейсмического импульса.— Изв. АН СССР, серия геофиз., № 9, 1961.
72. Коган С. Я. Об определении коэффициентов поглощения сейсмических волн.—Изв. АН СССР, серия геофиз., № 12, 1961.
73. Коган С. Я. Обзор теорий поглощения сейсмических волн.— Изв. АН СССР, серия физики Земли, № 11, 1966.
74. Коган С. Я. О сейсмической энергии, возбуждаемой источником, находящимся на поверхности.—Изв. АН СССР, серия геофиз., № 7, 1963.
75. Колесников Ю. А., Соловьев В. И. Установка для цифрования сейсмограмм.—Труды ИФЗ АН СССР, № 55, 1964.
76. Кондорская Н. В. По поводу региональных особенностей времен пробега сейсмических волн.—Изв. АН СССР, серия геофиз., № 7, 1957.
77. Корндалин Е. А. Некоторые характеристики волн типа L_g и R_g и региональные особенности их распространения.—Изв. АН СССР, серия геофиз., № 9, 1961.
78. Коул Р. Подводные взрывы. ИЛ, 1950.
79. Кузьмина И. В., Ромашов А. М., Рузев Б. Б., Харин Д. А., Шемякин Е. И. Сейсмический эффект взрывов на выброс в нескальных связанных грунтах.—Труды ИФЗ АН СССР, № 21, 1962.
80. Кухтикова Т. И., Французова В. И., Ефремова Г. П. и др. О преобладающих периодах поверхностных волн.—Докл. АН Тадж. ССР, т. 6, № 3, 1963.
81. Люкэ Е. И. Об экспериментальной зависимости энергии сейсмических волн от условий взрыва.—Изв. АН СССР, серия геофиз., № 12, 1960.
82. Люкэ Е. И. Зависимость энергии поверхностной волны от параметров воздушного взрыва.— Изв. АН СССР, серия физики Земли, № 4, 1967.
83. Люкэ Е. И. Экспериментальное изучение зависимости волн Релея от мощности и высоты взрыва в воздухе.—Изв. АН СССР, серия физики Земли, № 2, 1967.
84. Магницкий В. А., Хорошева В. А. К вопросу о волноводе в оболочке Земли и его физической природе.—Докл. АН СССР, т. 135, № 2, 1960.

85. Методы и программы для анализа сейсмических наблюдений. Сб. «Вычислительная сейсмология», вып. 3. Изд-во «Наука», 1967.
86. Машинная интерпретация сейсмических волн. Сб. «Вычислительная сейсмология», вып. 2. Изд-во «Наука», 1966.
87. Монахов Ф. И., Пасечник И. П., Шебалин Н. В. Сейсмические станции СССР, работавшие по программе МГГ. Изд-во АН СССР, 1959.
88. Нифонтов Б. Н., Протопопов Д. Д., Ситников Н. Е., Куликов А. В. Подземные ядерные взрывы. Атомиздат, 1969.
89. Нерсесов И. Л., Николаев А. Б. К вопросу о зависимости преобладающих частот при взрывах от величины заряда.—Труды ИФЗ АН СССР, № 25 (192), 1962.
90. Нерсесов И. Л. (ред.). Основные экспериментальные закономерности динамики сейсмических волн. Изд-во «Наука», 1968.
91. Обнаружение ядерных испытаний.— Труды инженеров по электротехнике и радиоэлектронике. Тематический выпуск, т. 12, 1965. Русский перевод. Изд-во «Мир», 1966.
92. Осадчий А. П., Дараган С. К. Аппаратура КОД для многоканальной цифровой регистрации сейсмических сигналов. Машинная интерпретация сейсмических волн. В сб. «Вычислительная сейсмология», вып. 2. Изд-во «Наука», 1966.
93. Параметры и амплитудно-частотные характеристики приборов сейсмических станций СССР. ИФЗ АН СССР, 1963—1965.
94. Парийский Б. С., Радченко В. П., Кейлис-Борок В. И. Продольные волны, возникающие при разрыве. В сб. «Вычислительная сейсмология», вып. 1. Изд-во «Наука», 1966.
95. Подземные ядерные взрывы. ИЛ, 1962.
96. Пасечник И. П., Федосеенко Н. Е. Электродинамический микробарограф с гальванометрической регистрацией.— Изв. АН СССР, серия геофиз., № 1, 1958.
97. Пасечник И. П. Идентификация подземных ядерных взрывов. Вестник АН СССР, № 11, 1968.
98. Пасечник И. П., Федосеенко Н. Е. Опыт модернизации сейсмографов типа СВК и СГК.—Изв. АН СССР, серия геофиз., № 12, 1959.
99. Пасечник И. П., Коган С. Д., Султанов Д. Д., Цибульский В. И. Результаты сейсмических наблюдений при подземных ядерных и тротиловых взрывах.—Труды ИФЗ АН СССР, № 15, 1960.
100. Пасечник И. П. К определению параметров затухания волн P_n и P^*.— Изв. АН СССР, серия геофиз., № 12, 1960.
101. Пасечник И. П. Сейсмический метод обнаружения и идентификации ядерных взрывов.—Изв. АН СССР, серия геофиз., № 6, 1961.
102. Пасечник И. П. Наука доказала: Ядерные взрывы можно обнаружить, где бы они ни производились.—Ж. «Природа», № 7, 1962.
103. Пасечник И. П. Зависимость сейсмической магнитуды от особенностей сейсмогеологического строения в пункте наблюдения.—Изв. АН СССР, № 11, 1962.
104. Пасечник К. П. Аномалии во временах пробега продольных волн на восточном склоне Среднего Урала.—Изв. АН СССР, серия геофиз., № 4, 1964.
105. Пасечник И. П. К определению зависимости от частоты коэффициента поглощения продольных сейсмических волн, распространяющихся в мантии Земли.— Докл. АН СССР, т. 166, № 6, 1966.
106. Пятецкий-Шапиро И. И., Желанкина Т. С., Кейлис-Борок В. И. и др. Определение эпицентров на электронной цифровой вычислительной машине.—Докл. АН СССР, т. 151, № 2, 1968.
107. Раутиан Т. Г. Затухание сейсмических волн и энергия землетрясений.— Труды ТИССС АН ТаджССР, вып. 7, 1960.
108. Ризниченко Ю. В. О расхождении и поглощении сейсмических волн.— Труды ГЕОФИАН СССР, № 35, (162), 1956.
109. Ризниченко Ю. В. Методы массового определения координат очагов близких землетрясений и скоростей сейсмических волн в области расположения очагов.—Изв. АН СССР, серия геофиз., № 4, 1958.
110. Ризниченко Ю. В. О сейсмических магнитудах подземных ядерных взрывов.—Труды ИФЗ АН СССР, № 15, 1960.
111. Ризниченко Ю. В., Шамина О. Г. Сопоставление амплитудных кривых, полученных на волноводной модели мантии, с сейсмическими данными.—Изв. АН СССР, серия геофиз., № 8, 1964.
112. Саваренский Е. Ф., Кирнос Д. П. Элементы сейсмологии и сейсмометрии. Изд. ГТТИ, М.—Л., 1949; 2-е изд., ГТТЛ, 1955.
113. Саваренский Е. Ф., Вальднер Н. Г. Волны L_g и R_g от землетрясений Черноморского бассейна и некоторые соображения об их природе. В сб. «Сейсмические исследования». Изд-во АН СССР, 1960.
114. Саваренский Е. Ф., Соловьева О. Н., Лазарева А. П. Дисперсия волн Релея и строение земной коры на севере Евразии и в Атлантическом океане.—Бюлл. Совета по сейсмологии, № 11, 1960.

115. Саваренский Е. Ф., Федоров С. А., Гогичайшвили Б. В. Определение истинного движения почвы и его спектра по сейсмограммам.—Изв. АН СССР, серия геофиз., № 9,1963.
116. Садовский М. А. Оценка сейсмических опасных зон при взрывах.— Труды СИ АН СССР, № 106,1941.
117. Садовский М. А. Опытные исследования механического действия ударной волны взрыва.—Труды СИ АН СССР, № 116, 1945.
118. Садовский М. А. Механическое действие воздушных ударных волн по данным экспериментальных исследований.В сб. «Физика взрыва», № 1. Изд-во АН СССР,1952.
119. Седов Л. И. Методы подобия и размерности в механике. ГИТТЛ, 1954.
120. Соловьев С. Л. К вопросу о соотношении между энергией объемных волн и интенсивностью землетрясений.— Бюлл. Совета по сейсмологии, № 6, 1957.
121. Соловьев С. Л. О соотношении между энергией объемных волн и интенсивностью землетрясений.—Бюлл. Совета по сейсмологии, № 6, 1956.
122. Соловьев С. Л., Шебалин Н. В. Определение интенсивности землетрясения по смещению почвы в поверхностных волнах.—Изв. АН СССР, серия геофиз., № 7, 1957.
123. Соловьев С. Л. Об изменении с расстоянием амплитуды колебаний почвы в поверхностных волнах Курило-Камчатских землетрясений.—Изв. АН СССР, серия геофиз., № 11, 1958.
124. Соловьев С. Л. Некоторые результаты применения шкалы интенсивности на сейсмических станциях СССР.—Studia Geophys. et geod., v. 2, 1958.
125. Соловьев С. Л., Шенин В. Б. Интенсивность землетрясений по данным дальневосточных и континентальных станций СССР.—Изв. АН СССР, серия геофизич., № 9, 1959.
126. Соловьев С. Л., Минин А. П. Соотношение между амплитудами и периодами продольных волн от землетрясений.—Изв. АН СССР, серия физики Земли, № 10, 1965.
127. Сытинский А. Д. Гидрометеорологические условия генерации микросейсм. Сб. статей, № 6. Изд-во «Наука», 1964.
128. Троицкая В. А. Эффекты в земных токах, вызванные высотными атомными взрывами.— Изв. АН СССР, серия геофиз., № 9, 1960.
129—130. Федотов С. А. О поглощении поперечных волн в верхней мантии.— Изв. АН СССР, серия геофиз., № 6, 1963.
131. Федоров Е. К., Тамм И. Е., Семенов Н. И., Садовский М. А., Пасечник И. П. и др. Доклад совещания экспертов по изучению методов обнаружения нарушений возможного соглашения о приостановке ядерных испытаний.—Атомная энергия, 5, вып. 4, 1958.
132. Халтурин В. И., Урусов Н. Б. Оценка поглощения продольных волн в земной коре по наблюдениям над местными землетрясениями.—Труды ИФЗ АН СССР, № 25 (192), 1962.
133. Халтурин В. И. Методика оценки спектрального состава сейсмических колебаний по записям частотно-избирательной станции ЧИСС.—Труды ИФЗ АН СССР, № 25, 1963.
134. Хорошева В. В. Некоторые результаты исследования волн P_a и S_a по сейсмограммам станций СССР.—Изв. АН СССР, серия геофиз., № 11, 1960.
135. Харкевич А. А. Спектры и анализ. ГИТТЛ, 1957.

136. Adams J. B. Some engineering problems of the CERN proton synchrotron. Discovery, July,1957.
137. Adams W. M. a. o. Report of the studies of underground nuclear explosions.— J. Geophys. Res., v. 66, No 3, 1961.
138. Aki Keyti. A note on surface waves from the Hardtack nuclear explosion. J. Geophys., Res., v. 69, No 6, 1964.
139. Anderson D. L. a. Kovach R. L. Attenuation in the mantle and rigidity of the core from multiply reflected core phases.—Proc. Natl. Acad. Sci. US., v. 51, No 2, 1964.
140. Anderson D. L. a. o. Attenuation of seismic energy in the upper mantle. Geophys., Res.,v. 70, No 6, 1965.
141. Bailey L. E., Romney C. F. Seismic waves from the Nevada underground explosion of September 19, 1957.—Bull. Geol. Soc. Am., 69, No 12, 1958.
142. Bates C. C. Vela Uniform, the nations quest for better detection of underground nuclear explosions.—Geophysics, v. 26, No 4, 1960.
143. Bates C. C. Detection and identification of nuclear explosions underground (Project VELA Uniform).—Proc. IRE, 50, No 11, 1962.
144. Bates C. C., George T. E. On site inspection of nuclear tests.— IRE Trans. Nucl. Sci., v. 10, No 1,1963.
145. Bäth M. Seismic records of Explosions especially Nuclear Explosions. Part III, Försvarets forskingsanstalt Avdeling 4, Stockholm, 1962.

146. Båth M. a. o. Amplitudes of explosion generated seismic waves.— Geofis. pura e appl., v. 51, 1962.
147. Birtill J. W., Whiteway F. E. The application of phased arrays to the analysis of seismic body waves.—Philos. Trans. Roy. Soc. London, v. 258, No 1091, 1965.
148. Backus M. M. Teleseismic signal extraction.— Proc. of the Roy. Soc., v. 290, No 1422,1966.
149. Benioff H., Gutenberg B., Richter C. F. Progress report seismological lab., California Inst. of Technol., 1954.—Trans. Amer. Geophys. Union, v. 36, No 4, 1956.
150. Ben-Menahem A. a. Toksöz M. N. Source mechanism from spectra of long-period seismic surface waves. The Mongolian earthquake of December 4, 1957. J. Geophys. Res., v. 67, No 5, 1962.
151. Berg J. W. a. o. Elastic displacement of primary waves from explosive sources.— Bull. Seism. Soc. America, v. 54, No 3, 1964.
152. Berg J. N. a. Long L. T. Characteristics of refracted arrivals seismic waves.— J. Geophys. Res., v. 71, No 10, 1966.
153. Berg J. W., Trembly L. D., Laun P. R. Primary ground displacements and seismic energy near the Gnome explosion.—Bull. Seismol. Soc. America, 54, No 4, 1964.
154. Boardman C.,R. a. o. Responses of four rock mediums to contained nuclear explosions.—J. Geophys. Res., v. 69, No 16, 1964.
155. Bolt B. A., Sutton D. Y. Seismic observations from the 1956 atomic explosions in Australia.The Geophysica Journal of the R. A. Soc., v. 1, No 2, 1958.
156. Booker Aaron, Mitronovas Walter. An application of statistical discrimination to classify seismic events.— Bull. Seismol. Soc. America, v. 54, No 3, 1964.
157. Bradner H. and Dodds J. Comparative seismic noise on the ocean bottom and on land. J. Geophys Res., v. 69, No 20, 1964.
158. Broding R. A., Bentley N. J., Hearn D. P. A study of a three-dimensional seismic detection system.— J. Geophysics Res., v. 29, No 2, 1964.
159. Brune J. N. and Oliver J. The seismic noise of the earth's surface.— Bull. Seismol. Soc. Am., v. 49, No 4, 1959.
160. Brune J., Oliver J., Nafe J.— A simplified method for the analysis and synthesis of dispersed wave trains.— J. Geophys. Res., v. 65, No 1, 1960.
161. Brune J., Espinosa A. a. Oliver. J. Relative excitation of surface waves by earthquakes and underground explosions in California—Nevada region.— J. Geophys. Res., v. 68, No 11, 1963.
162. Brune J. A. a. Pomeroy P. W. Surface wave radiation patterns for underground nuclear explosions and small magnitude earthquakes.— J. Geophys. Res., v. 68, No 17, 1963.
163. Brune J. N., Pomeroy P. W. Radiation patterns of surface waves from underground nuclear explosions in Nevada.—Trans. Am. Geophys. Union, v. 44, No 1, 1963.
164. Burg J. P. Three-dimensional filtering with an array of seismometers.— Geophysics, v. 29, No 5, 1964.
165. Burke-Geffney T. N. a. Bullen K. On the seismological aspects of the 1954 hydrogen bomb.—Austral. J. Phys., v. 11, No 3, 1958.
166. Buchbinder Goetz G. R. PcP from the nuclear explosion Bilby of September 13, 1963.— Bull. Seism. Soc. Am., v. 55, No 2, 1965; PcP travel times from Longshot and the density ratio of the mantle-core boundary.—Trans. Amer. Geophys. Union, 47, No 1,1966.
167. Bulletin of the International Seismol. Centr. Edinburg, 1964—1966, продолжающий The International Seismol. Summary, Oxford 1954—1963.
168. Bulletin of the Seismol. Soc. Am., v. 58, No 4, 1968. Special number — 1968 seismological tables for P phases.
169. Carder D. S. The Seismograph and the Seismograph station. Washington, 1956.
170. Carder D. S. a. Bailey L. F. Seismic wave travel times from nuclear explosions — Bull. Seism. Soc. Am., v. 48, No 4, 1958.
171. Carder D. S. a. o. Surface Motion from large explosions.— J. Geophys. Res., v. 64, No 10, 1959.
172. Carder D. S., Cloud W. K. Surface Motion from a series of underground nuclear tests.—GTR-1705, 1959.
173. Carder D. S., Mickey W. V. Ground effects from underground explosions.—Bull. Seismol. Soc. Am., v. 52, No 1, 1962.
174. Carder D. S. Ground effects from the Gnome and Logan explosions.—Bull. Seism. Soc. Am., v. 52, No 5, 1962.
175. Carder D. S. a. o. Seismic waves arrivals from Longshot, 0° to 27°.— Bull. Seismol. Soc. Am., v. 57, No 4, 1967.
176. Carder D. S., Gordon D. W. a. Jordan J. N. Analysis of surface focus travel times.— Bull. Seismol. Soc. Am., v. 56, No 4, 1966.

177. Cleary J. a. Hales A. L. An analysis of the travel times of P waves to North American Stations, in the distance range 32° to 100°.— Bull. Seismol. Soc. Am., 56, No 2, 1966.
178. Cleary J. P times to Australian Station from nuclear explosions.— Bull. Seismol. Soc. Am., v. 57, No 4, 1967.
179. Cleary J. Azimuth variation of the Longshot source terms.—Earth and Planet Sci. Letters, v. 3, No 1, 1967.
180. Carder D. S. Mantle structure an infared from seismic waves travel times from nuclear explosions in the Central Pacific.—Geol. Soc. Am. Spec. Paper, No 73, 1963.
181. Carder D. S. Travel times from Central Pacific nus clear explosionsand inferred mantle structure.—Bull. Seismol. Soc. Am., v. 54, No 5, 1964.
182. Carpenter E. W., Savill R. A., Whright G. K. The Dependence of seismic signal amplitudes on the size of the undergound exrplosi ons.—Geophys. J. Roy. Astron. Soc., v. 6, No 4, 1962.
183. Carpenter E. W. Explosion seismology. Science, v. 147, No3656, 1965.
184. Claerbout J. F. Detection of P-waves from weak sources atgreat distances.— Geophysics, v. 29, No 2, 1964.
185. Carpenter E. W. Teleseismic signals calculated for underground, underwater and atmospheric explosions.—Geophysics, v. 32, No 1, 1967.
186. Control and reduction of armaments. Detection of and inspection for underground nuclear explosions. Staff Study No 10 Subcommittee on Foreign Relation, US Senate, June 23,1958.
187. Dana S. W. The amplitudes of seismic waves reflected and refracted at the Earth's core.—Bull. Seism. Soc. Am., v. 35, No 1, 1945.
188. Davidson D. Nuclear Burst Effects on long-distance high-frequency circuits.— J. Geophys. Res., v. 68, No 1, 1963.
189. De Noyer J., Willis D. E., Wilson J. T. Observed asymmetry of amplitudes from a high explosive source.—BSSA 52, No 1, 1962.
190. Don Leet L. The Detection of Underground Explosions.— Scientific American, June, 206, No 6, 1962.
191. Station detects underground nuclear blasts. Electronics, 49, 1960.
192. Doyle H. A. Seismic recordings of atomic explosions in Australia. Nature, v. 180, No 4577, 1957.
193. Doyle H. A., Everingham I. B., Hogan T. K. Seismic recordings of large explosions in South Eastern Australia.—Austral. J. Phys., v. 12, No 3, 1959.
194. Doyle H. A. Travel times to Australian Stations from Pacific Nuclear explosions in 1958.—J. Geophys. Res., 68, No 4, 1963.
195. Epstein H. M. a. Klingensmith R. W. Detection and Identification of Nuclear Burst.— Batelle Techn. Rev., 13, No 8, 1965.
196. Flinn E. A. Local earthquakes location with an electronic computer.— Bull. Seismol. Soc. Am., v. 50, No 3, 1960.
197. Flinn E. A., Romney C. F., Rugg A. M., Woolson J. Analitical results from low-frequency seismic measurements in a Deep Well.—Geol. Soc. Am. Spec. Paper, N 68, 1962.
198. Flinn E. A. Confidence regions and error determinations for seismic event location.—Revs. Geophys., v. 3, No 1, 1965.
199. Fogelson D. E., Duvall W. G., Atdison T. C. Strain energy in explosion generated near explosions.— Geophysics, v. 11, No 3, 1959; v. 30, No 3, 34. Proceedings of the IEEE, v. 53, No 12, December, 1965.
200. Fuchs K. On the properties of deep crustal reflectors. Zeitschrift für Geophysik, v. 35, H. 2, 1969.
201. Frantti G. E., Willis D. E., Wilson J. T. The spectrum of seismic noise.—Bull. Seismol. Soc. Am., v. 52, No 1, 1962.
202. Frantti G. E. The nature of high-frequency Earth noise spectra.— Geophysics, v. 28, No 4,1963.
203. Frantti G. E. Spectra underground explosions and earthquakes.— Bull. Seismol. Soc. Am., 53, No 5, 1963.
204. Frantti G. E., Levereault L. A. Auditory discriminations of seismic signals from earthquakes and explosions.—Bull. Seismol.Soc. Am., v. 55, No 1, 1965.
205. Frantti G. E. Attenuation of P from offshore Maine explosions.— Bull. Seismol. Soc. Am., v. 55, No 2, 1965.
206. Glasston S. The effects of nuclear weapons U.S. Atomic energy commission. Washington D.C.,1962.
207. Freedman M. G. A statistical discussion of residuals from explosions.— Bull. Seismol. Soc. Am., v. 56, No 3, 1966.
208. Glen C., Herbst R. F., Springer D. L. Amplitudes of seismic arrivals from M discontinuity.—J. Geophys. Res., v. 67, No 4, 1962.
209. Griggs D. T., Press F. Probing the earth with nuclear explosions.— Bull. Seismol. Soc. Am., v. 60, No 1, 1960.
210. Grossling B. F. Seismic from underground atomic explosion in Nevada.— Bull. Seismic. Soc. Am., v. 49, 1959.

211. Gudzin M. G., Hamilton J. H. White Mountains seismological observatory.—Geophysics, v. 26, No 3, 1961.
212. Gudsin M. G., Holle E. G. Seismological observatories Proc. IRE, v. 50, No 11, 1962.
213. Gupta J. E., Kisslinger C. Model study of explosion-generated Rayleigh waves in a half space.— Bull. Seism. Soc. Am., 54, No 2, 1964.
214. Gutenberg B., Richter C. F. Earthquake magnitude, intensity, energy and acceleration.—Bull. Seism. Soc. Am., v. 32, 1942.
215. Gutenberg B. Amplitudes of surface waves and magnitudes of shallow earthquakes.— Bull. Seism. Soc. Am., 35, No 2, 1945.
216. Gutenberg B. Amplitudes of P, PP and S and magnitude of shallow earthquakes.— Bull. Seism. Soc. Am., v. 35, No 2, 1945.
217. Gutenberg B. Magnitude determination for deep focus earthquakes.— Bull. Seism. Soc. Am., v. 35, No 3, 1945.
218. Gutenberg B. Seismic Waves from the atomic bomb tests. - Trans. Am. Geophys. Union, v. 27, No 6, 1946.
219. Gutenberg B. Interpretation of records obtained from the New Mexico atomic bomb test, July 16, 1945.—Bull. Seism. Soc. Am., v. 36, No 4, 1946.
220. Gutenberg B. Travel times from blasts in Southern California.— Bull. Seism. Soc. Am., v. 41, No 1, 1951.
221. Gutenberg B. Waves from blasts recorded in Southern California.— Trans. Am. Geophys. Union, 33, No 3, 1952.
222. Gutenberg B. Travel times of longitudinal waves from surface foci.— Proc. Sci. Un. States, v.39, No 8, 1953.
223. Gutenberg B. Magnitude and energy of earthquakes.— Annali di Geofisica, Rome, v. 9, No 1, Gennaio, 1956.
224. Gutenberg B., Richter C. F. Earthquake magnitude, intensity, energy and acceleration (Second Paper).—Bull. Seism. Soc. Am., v. 46, No 2, 1956.
225. Gutenberg B. The Energy of earthquakes.— The Quarterly Journal of the Geological Society, v. 112, No 4, 1956.
226. Gutenberg B. Spectrum of P and S in records of distant earthquakes.— Zeitschr. f. Geophys., 23,1957.
227. Gutenberg B. Attenuation of seismic waves in the earth's mantle.—Bull. Seism. Soc. Am., v. 48, No 3, July 1958.
228. Gutenberg B. Low-velocity layers in the earth's ocean and atmosphere.— Science, v. 131,405, 1960.
229. Haas C. J., Rinehart J. S. Some aspects of coupling between explosives and rocks.—Naval Ordinance Test Stat. China Lake, Calif., 18, 1962.
230. Hankins D. M. Observations from some Gnome seismograms.— Bull. Seism. Soc. Am., v. 52, No 5, 1962.
231. Haskell N. A. A static theory of the seismic coupling of a contained underground explosion.—J. Geophys. Res., No 9, 66, 1961.
232. Herrin E. a. Taggarty J. Epicenter locations of the Salmon event.— J. Geophys. Res., v. 71, No 14,1966.
233. Helterbran W. a. Jordan. J. Teleseismic data from Longshot. Abstract. Trans. Am. Geophys. Union, v. 64, No 2,1966.
234. Haskell N. A. Analytical approximation for the elastic radiation from a contained underground nuclear explosion.— J. Geophys. Res., v. 72, No 10, 1967.
235. Holzer F. Measurements and calculations of peak shock waves parameters from underground nuclear detonations.—J. Geophys. Res., v. 70, No 4, 1965.
236. Jeffreys H. Travel times for pacific explosions.— Geophys. J. Roy. Astron. Soc., No 2, 1962.
237. Jeffreys H., Bullen K. E. Seismological tables. 1940.
238. Jordan J. N., Mickey W. V., Helterman W., Clark D. N. Travel times and amplitudes from Salmon explosion.—J. Geophys. Res., v. 71, No 4, 1966.
239. Johnson G. W., Higgins G. H., Violet C. E. Underground nuclear detonations.—J. Geophys. Res., v. 64, No 10, 1959.
240. Jordan J., Black R. a. Bates C. C. Patterns of Maximum amplitudes of P_n and P waves over regional and continental areas.—Bull. Seism. Soc. Am., No 4, 55, 1965.
241. Johnson G. W., Higgins G. H. Engineering applications of nuclear explosions: Project Plowshar. Revs. Geophys., No 3, 1965.
242. Kavabata Y. Geophysical effects associated with the high altitude nuclear explosion. Part V, Acoustic and seismic waves.— J. Geomag. and Geoelectric, VII, No 2, 1959.
243. Knopoff L., MacDonald G. F. Attenuation of small amplitude stress waves in solids.—Revs. Modern Phys., 30, 1958.
244. Knopoff L. Attenuation of elastic waves in the earth.— Rev. Geophys., v. 2. No 4, 1964.
245. Kovach R. L., Lehner F. and Miller Ray. Experimental ground amplitudes from small surface explosions.—Geophysics, v. 28, No 1, 1963.

246. Kuo J., Brune J. a. Major M. Rayleigh waves dispersion in the Pacific Ocean for the period range 20 to 40 seconds.— Bull. Seism. Soc. Am., v. 30, 1962.
247. Latter A. L., Lelevier R. E., Martinelli E. A., McMillan W. G. A method of concealing underground nuclear detonations.— J. Geophys. Res., v. 66, No 3, 1961.
248. Lehmann I. On the travel times of P as determined from nuclear explosions.— Bull. Seismol. Soc. Am., v. 54, No 1, 1959.
249. Lehmann I. The travel times of the longitudinal waves of the Logan and Blanca atomic explosions and their velocities in the upper mantle.—Bull. Seismol. Soc. Am., v. 52, No 3, 1962.
250. Lynn R. D. A low-frequency geophone for borehole use.— Geophysics, v. 28, No 1, 1963.
251. Marshal P. D., Carpenter E. W., Donylas A., Jonng J. B. Some seismic results of the Longshot explosions.— Atomic Weapons. Res. Establ. U. K. Atomic Author. Rept. 15, 1966.
252. Mathey R. Problème de la detection et de l'identification des explosions souterraines à l'aide de seismographes. Les chroniques de l'âge Nucleaire, No 2, Sept.—Oct. 1958.
253. Mathey R., Rocard J. Performans de certains seismographes a courte periode.—Cr. Acad. Sci., 298, No 24, 1959.
254. Mathey R. et Rocard J. Performances de seismographes a forte amplification.— Comptes Rendus de l'Académie des Sci., T. 242, No 20, 1958.
255. Mateker E. J., Kisslinger C., McEvilly T. V. SH motion from explosions in soil.—J. Geophys. Res., v. 66, No 10, 1961.
256. McEvilly V., Rodgers P. N. A parametrically excitel seismometer with improved long period response.—Trans. Am. Geophys. Union, v. 47, No 1, 1966.
257. Menard J. Z., Bogert B. P., Walker R. A. Real-time, high resolution spectroscopy of seismic background noise.—Bull. Seism. Soc. Am., v. 54, No 1, 1964.
258. Mickey W. V., Jordan J., Helterbran N., Clarkdon M. Travel times and amplitudes from the Salmon explosion.—J. Geophys. Res., v. 71, No 14, 1966.
259. Meren R. F. A study of apparent angles of emergence at Marathon Ontario from the lake superior data.—Bull. Seismol. Soc. Am., v. 55, No 2, 1965.
260. Merlet Y. Note Relative aux phases sismiques observees entre 100 et 200 km dans le Massif du Hoggar.— Comptes Rendus Academie des Sciences, v. 255, No 25, 1962.
261. Miller W. E. The Caltech digital Seismograph.— J. Geophys. Res., v. 68, No 3, 1963.
262. Milne A. R. Comparison of spectra of an earthquake T-phase with similar signals from nuclear explosions.—Bull. Seismol. Soc. Am., v. 49, No 4, 1959.
263. Mitronovas W., Sutton G. H. a. Pomeroy P. W. Short-period seismic energy radiation patterns from underground nuclear explosions and small magnitude earthquakes.— Bull. Seismol. Soc. Am., v. 57, No 4, 1967.
264. Moltshan G. M., Pissarenko V. F. a. Smirnova N. A. Some statistical methods of detecting signals in noise.—J. Geophys. Royal Astronom. Soc., v. 8, No 3, 1964.
265. More Data on Sedan. Wash. Atomic Energy Report, v. 8, 10, 1962.
266. Murphy L. M. Seismological program of the U. S. Coast and Geodetic Survey. Trans. Am. Geophys. Union, v. 42, No 2, 1961.
267. Murphy L. M. World-wide network of standartized seismographs.— Trans. Amer. Geophys. Union., v. 42, No 2, 1961.
268. Murpheý B. F. Particle motion near explosions in halite.— J. Geophys. Res., v. 66, No 3, 1961.
269. Nafi M., Ben-Menahem Ari, Toksõz M. N. Comparative study of source mechanism from surface waves of nuclear explosions and earthquakes.—Geol. Soc. Am., Spec. Paper., 73, No 24, 1963.
270. Nagamune T. On the azimuthal deviation of earthquake magnitude.— Zisin J. Seismol. Soc. Jap., No 4, 1958.
271. Nagumo S. a. o. Construction of ocean bottom seismograph.— Bull. Earthquake Res. Inst. Univ. Tokyo, 43, Part 4, 1965.
272. Naimark B. M. Algorithm for automatic recognition of a seismic signal by a computer.— Rev. Geophys., v. 3, No 1, 1965.
273. Nakamura Y., Howell B. F. Maine seismic experiment: frequency spectra of refraction arrivals and the nature of Mohorovicic discontinuity.—Bull. Seism. Soc. Am., v. 54, No 1, 1964.
274. Nalecz M., Zawicki J. A hall-effect seismograph.— Bull. Seism. Soc. Am., v. 52, No 2, 1962.
275. Nation J. B., Hales A. L., Dowling J. J. Some logistics of the east coast on-shore of-shore experiment (ECOOE) earthquake notes.— Earth. Notes. Soc. Am., v. 37, No 1, 1966.
276. Nicholls H. R. Coupling explosive energy to rock.— Geophysics, v. 27, No 3, 1962.

277. Norden Y. A. E. Tectonic leads in the coseismal line spread at the Nevada underground nuclear detonation «Blanco».—Oklahoma Geol. Notes, v. 21, No 9, 1961.
278. Norden Y. A. E. Intercontinental detection of underground nuclear explosions in Oklahoma.—Oklahoma Geol. Notes, v. 21, No 10, 1961.
279. Nordquist J. M. Special-purpose program for earthquake location with an electronic computer.— Bull. Seism. Soc. Am., v. 52, No 2, 1962.
280. Nordyke M. D. a. Ray W. Cratering and a radioactivity results from a nuclear cratering detonation in basalt — Geophys. Res., v. 69, No 4, 1964.
281. Nuclear blast detectors ring nation's capital.— Science News Letter, Dec. 28, 1963.
282. O'Brien P. N. S. Seismic energy from explosions.— Geophys. J. Roy. Astr. Soc., 3, No 1, 1960.
283. Oliver J., Ewing M., Short-period oceanic surface waves of the Rayleigh and first shear modes.—Trans. Am. Geophys. Union, 39, 1958.
284. Oliver J., Ellis R. M., Russell R. D. Analysis of Canadian Longshot data.— Earth and Planet. Sci. Letters. v. 1, No 4, 1966.
285. Oliver J., Ewing M., Press F. Crustal structure and surface waves dispersion. Part IV. Atlantic and Pacific Ocean Basin.— Bull. Geolog. Soc. Am., v. 66, 1955.
286. Oliver J. On the long period character of shear waves.— Bull. Seism. Soc. Am., v. 51, No 1, 1961.
287. Oliver J. Long period waves and the Lg phases.— Ann. IGY, v. 30, 1965.
288. Oliver J., Ewing M. Seismic surface waves at Palisades from explosions in Nevada and Marshall Islands.—Proc. Nat. Acad. Sci., USA, v. 44, No 8, 1958.
289. Oliver J., Pomeroy P. Seismic waves from high-altitude nuclear explosions.— J. Geophys. Res., v. 65, No 10, 1960.
290. Oliver J., Pomeroy P., Ewing M. Long-period seismic waves from nuclear explosions in various environments.—Science, v. 181, 3416, 1960.
291. Papazachos B. Angle of incidence and amplitudes ratio of *P* and *PP* waves.— Bull. Seismol. Soc. Am., v. 54, No 1, 1964.
292. Payo G. Dispersion of Rayleigh waves produced by nuclear explosions. Crustal Structure of Western Europe.—Ann. Geophys., v. 17, No 2, 1964.
293. Phinney R. A. a. o. Processing of seismic data from an automatic digital recorder.— Bull. Seismol. Soc. Am., v. 53, No 3, 1963.
294. Pomeroy P., Sutton G. The use of galvanometers as band rejection filters in electromagnetic seismographs.—Bull. Seism. Soc. Am., 50, 1960.
295. Pomeroy P. W. Long period seismic waves from large near-surface nuclear explosions.—Bull. Seism. Soc. Am., v. 53, No 1, 1963.
296. Press F., Ewing M. Crustal structure and surface wave dispersion.— Bull. Seism. Soc. Am., v. 40, 241, 1950; v. 42, 315, 1952; v. 43, 137, 1953.
297. Press F., Ewing M. Waves with P_n and S_n velocity at great distances.— The Proc. of the National Acad. of Science, v. 41, No 1, 1955.
298. Press F. Velocity of Lg waves in California.— Trans. Am. Geophys. Union, 37, No 5, 1956.
299. Press F. The need for fundamental research in seismology.—Trans. Am. Geophys. Un., v. 40, No 3, Sept., 1959.
300. Press F. Crustal structure in the California — Nevada Region.— J. Geophys. Res., 65, 1960.
301. Press F., Archambeau C. Release of tectonic strain by underground nuclear explosions.— J. Geophys. Res., v. 67, No 1, 1962.
302. Press F., Dewart G. a. Gilman R. A study of diagnostic techniques for identifying earthquakes.—J. Geophys. Res., v. 68, No 10, 1963.
303. Press F. Diagnostic aids for distinguishing explosions and earthquakes.— Geolog. Soc. Am., Spec. Paper, No 73, 1963.
304. Press F. Seismic waves attenuation in the crust.—J. Geophys., Res., v. 69, No 20, 1964.
305. Puraglove S. D. The riddle of the black boxes.— Popul. Mech., 120, No 2, 1963.
306. Randall M. J. Generation of horizontally polarized shear waves by undergound explosions.—J. Geophys. Res., v. 67, No 12, 1962.
307. Rawson D. E. Review and summary of some project Gnome results.— Trans. Am. Geophys. Un., v. 44, No 1, 1963.
308. Results of Gnome peaceful nuclear detonation in New-Mexico.— Engineer, 215, No 5592.
309. Report on observations made at Kiruna geophysical observatory during the series of nuclear weapon tests carried out at Novaya Zemlya between 10 Sept. and 4 Nov. 1961. Kiruna, Geophysical Observatory.
310. Riihimaa J. Timing equipment for explosion seismology.— Geophysica, v. 7, No 2, 1959.
311. Ritsema A. R. On the seismic records of nuclear test explosion.— Madjalah ilmn alamutuk Indonesia, 113, 1957.

312. Robinson E. A. Mathematical development of discrete filters for the detection of nuclear explosions.—Geophys. Res., v. 68, No 19, 1963.
313. Rocard I. Sur les Signaux seismiques de longe periode obtenus lors du test nucleaire de Reggeni de 13 fevrier 1960.—C. R. Acad. Sci., v. 250, No 12, 1960.
314. Rocard I. Sur les inegualites de la propagation sismique des ondes de volume a longue distance.—C. R. Acad. Sci., v. 254, No 7, 1962.
315. Rocard I. Sur les signaux seismiques de courte period obtenus lors du text nucleaire de Reggane le fevrier 1960.— C. R. Acad. Sci., v. 250, No 11, 1960.
316. Rocard I. Effect de la profondeur ou de l'altitude d'une explosion sur ses signaux sismiques.— C. R. Acad. Sci., v. 254, 13, 1962.
317. Romney C. F. Amplitudes of seismic body waves from underground nuclear explosions.—J. Geophys. Res., v. 64, No 10, 1959.
318. Romney C. Short period shear waves and their application to discriminating between earthquakes and explosions in the need for fundamental research in seismology. Report of the Panel on Seismic Improvement, US Department of State, Appendix, 2, 1959.
319. Romney C. Seismic detection methods for underground explosions.— IEEE Trans. on Nuclear Science, 10, No 1, 1963.
320. Romney C. F. Earthquakes in the USSR. Before the Joint Committee on atomic energy, 5—7, March, 1963.
321. Romney C. F., Batus C. C. Status of the Seismic research program recommended by the Panel on Seismic Improvement.—Trans. Am. Geophys. Un. 42, No 2, 1961.
322. Romney C., Brooks B. G., Mansfield R., Carder D. S., Gordan J. N., Gardon D.W. Travel times and amplitudes of principal body phases recorded from Gnome.— Bull. Seism. Soc. Am., v. 52, No 5, 1962.
323. Romney C. F. a. o. Principles of an experimental large aperture seismic array (LASA).— Proceedings of the JEEE, v. 12, December 1965.
324. Ryall A. Improvement of array seismic recordings by Digital Processing.— Bull. Seism. Soc. Am., 1964, v. 54, No 1.
325. Ryall A., Stuart D. J. Travel times and amplitudes from nuclear explosions, Nevada Test Site to Ordway, Colorado.— J. Geophys. Res., v. 68, No 20, 1963.
326. Seismic methods for monitoring underground explosions.— SIPRI, Stockholm, 1968.
327. Shimshoni M., Smith S. W. Seismic signal enhancement with three-component detectors.—Geophysics, v. 34, No 5, 1964.
328. Schwind J. J. a. o. PS converted waves from large explosions.— J. Geophys. Res., v. 65, No 11, 1960.
329. Simpson S. M. Ir. Studies on underground nuclear detection and further digitized seismic data.—US. Govt. Res. Repts., v. 38, No 14, 1963.
330. Smith S. W. Generation of seismic waves by underground explosions and the collapse of cavities.—J. Geophys. Res., v. 68, No 5, 1963.
331. Springer D. L. P wave coupling of underground nuclear explosions.— Bull. Seismol. Soc. Am., v. 56, No 4, 1961.
332. Stewart S. W. A reinterpretation of phase velocity data based on the Gnome travel time curves.—Bull. Seism. Soc. Am., 52, No 5, 1962.
333. Stewart S. W., Diment. Frequency content of seismograms of nuclear explosions and aftershocks.— Geol. Surv. Pr. Paper, No 242, 1961.
334. Stewart S. W. Pakiser L. C. Crustal structure in eastern New Mexico interpreted from the Gnome explosions.— Bull. Seism. Soc. Am., v. 52, No 5, 1962.
335. Stubbs P. Simpler detection of underground bomb tests.— New Scientist, No 297, 26 july, 1962.
336. Stubbs P. The New Seismology.— New Scientist, v. 25, No 429, 1965.
337. Sutton G. H. Note on long period noise in seismographs.— J. Geophys. Res., v. 67, No 5, 1962.
338. Sutton G. H., Pomeroy P. W. Analog analysis of seismograms recorded on magnetic tape.—J. Geophys. Res., v. 68, No 9, 1963.
339. Tandon A. N., Claudhury H. M. Seismic waves from hign yield atmospheric explosions.—Indian J. Meteorol. and Geophys., v. 14, No 3, 1963.
340. Tatel H. E., Adams L. H., Tatel M. A. Studies of the earth's crust using waves from explosions.—Am. Phil. Soc. Proc., v. 97, 1953.
341. Technical aspects of the detection and inspection controls of a nuclear weapons test ban., Summary —analysis of hearing, April 19, 20 21 and 22, 1960. Joint Committee on atomic energy congress of the US Government Printing Office, Washington, 1960.
342. The effect of nuclear weapons. US. Department of Defence, June 1957.
343. The detection and recognition of underground explosions. A special report of the united Kingdom atomic energy authority. Published by the United Kindom atomic energy authority. 11, Charles II Street, London, S. W. 1. December 1965.
344. Thirlaway H. I. Earthquake or explosion. New Scientist, v. 18, No 338, 1963. Interpreting array records: explosion and earthquake P wave trains which have traversed the deep mantle.—Proc. of the Roy. Soc., v. 290, No 1422, 1966.

345. Toksöz M. N., Ben-Menahem A., Harkrider D. G. Determination of source parameters of explosions and earthquakes by amplitude equalization of seismic surface waves. I. Underground nuclear explosions.—Geophys. Res., v. 69, No 20, 1964.
346. Toksöz M. N., Ben-Menahem A. Excitation of seismic surface waves by atmospheric nuclear explosions.—Geophys. Res., v. 69, No 8, 1964.
347. Toksöz M. N., Harkrider D. G., Ben-Menahem A. Determination of source parameters by amplitude equalization of seismic surface waves. II. Release of tectonic strain underground nuclear explosions and mechanisms of earthquakes.—Geophys. Res., v. 70, No 4, 1965.
348. Uyeda H., Maeda H., Kimpara A., Obayashi T., Ishikawa S., Kawabata G. Geophysical effects associated with high-altitude nuclear explosion., J. G. E. XI, No 2, 195, 1959.
349. Warner S. E., Violet C. E. Properties of the environment of underground nuclear detonation of the Nevada test site. UCRL-5542 Rev., April 1959.
350. Werth G. C., Herbst R. R. Comparison of amplitudes of seismic waves from nuclear explosions in four media.— J. Geophys. Res., v. 68, No 5, 1963.
351. Weston D. E. The low frequency scaling laws and source levels for underground explosions and other disturbances.— Geophys. J., 3, No 2, 1969.
352. Willis D. F., DeNoyer J., Wilson J. T. Differentiation of earthquakes and underground nuclear explosions on the basis of amplitude characteristics.—Bull. Seismol. Soc. Am., v. 53, No 5, 1963.
353. Willis D. E. Comparison of seismic waves generated by different types of source.— Bull. Seismol. Soc. Am., v. 53, No 5, 1963.
354. Willis D. E. Seismic measurements of large underwater shots.— Bull. Seismol. Soc. Am., v. 53, No 4, 1963.
355. Willis D. E. Variations in compressional waves at teleseismic distances. J. Geophys. Res. v. 70, No 8, 1965.
356. Wilson J. T., Cales T. W. VELA uniform and seismology.— Trans. Am. Geophys. Union, v. 44, No 2, 1963.
357. Wright J. K., Carpenter E. W., Savill R. A. Some studies of the P waves from underground nuclear explosions.— J. Geophys. Res., v. 67, No 3, 1962.
358. Wright J. K., Carpenter E. W. The generation of horisontally polarized shear waves by underground explosions.— J. Geophys. Res., v. 67, No 5, 1962.
359. Whiteway F. E. The use of arrays for earthquake seismology. — Proceedings of the Roy. Soc., v. 290, No 1422, 1966.
360. Wiechert D. H. Computer hardware and Programming requirements for the delay-sum-and-correlate method of proccssing seismic array data.—Seismological Series of the Dominion observatory, 1967.

SYMBOL LIST

Russian	Typed	Meaning
СК	SK	not defined
СКМ	SKM	not defined
Б	B	not defined
УСФ	USF	not defined
ПР	ind	industrial
Я	nuc	nuclear
ЛеВ	left	left
ПР	right	right
П.С.	u.s.	useful signal
ПОМ	int	interference
ПР	dom	dominant
СТ	st	stations
ТХ	qu	quiet
СР	med	medium
Ш	noi	noise
СП	sp	spectrum
МР	max	maximum
ОТР	refl	reflection
КМ	kt	kilotons
С	s	seismic
ОБЩ	tot	total
ЭКСП	exp	explosion
КШ	c.s.	calibrated scales
ГР	gr	group
З	w	west
С	n	north
Ю	s	south
ИСТ	true	true
ВЫЧ	calc	calculated
В	e	east